

Mars Reconnaissance Orbiter

# **CRISM DATA PRODUCT SOFTWARE INTERFACE SPECIFICATION**

## **Version 1.3.7.6**

Prepared by:

**Scott Murchie**  
JHU/APL

**Edward Guinness and Susan Slavney**  
PDS Geosciences Node  
Washington University

Approved by:

---

Scott Murchie  
Principal Investigator, CRISM

---

Richard Zurek  
Project Scientist, MRO

---

Raymond E. Arvidson  
Director, PDS Geosciences Node

---

Steve Noland  
MRO Science Operations System  
Engineer, MRO

June 22 , 2022

## DOCUMENT CHANGE LOG

Date	Description	Sections affected
12/15/03	Initial Draft	All
11/22/04	Calibration data records redefined based on instrument calibration results; data processing details (App. I) added; descriptions of macros updated; EDR and TRDR labels updated based on needs of data processing; housekeeping file updated for consistency with flight software	All
3/2/2005	Rewritten upon recommendation of reviewers	All
9/14/2005	<p>Added distinguishing features of wavelength filters, exp, and frame rates for level 4 CDRs</p> <p>Distinguished MRO:WAV file for CDR and RDR</p> <p>Added metakernel list files, wavelength files to MRDRs and MTRDRs in figures and text</p> <p>Updated alarm limits</p> <p>Added 12 to 8 bit inverse table to level 6 CDRs</p> <p>Updated labels for level 4 and level 6 CDRs</p> <p>Updated summary parameters</p> <p>Added wavelength filter as keyword and included in EDRs and CDRs</p> <p>Added functional test to cases where macro ≠ EDR</p> <p>Added image source to variable settings</p> <p>Fixed sphere lamp 1 and 2 confusion</p> <p>Changed gain_offset to pixel_proc fin CDR filename</p> <p>Added compression_type = none, 8_bit to EDR labels</p> <p>Added MRO:SPHERE_TEMPERATURE to CDR labels</p> <p>Added MRO:FRAME_RATE to LDD list for EDR</p> <p>Added exp time parameter to CDR file name</p> <p>Added MRO:WAVELENGTH_FILTER to LDD for EDRs</p> <p>Made underscores in file names and product IDs consistent</p> <p>Renamed MTRDRs using convention for MRDRs; add required layers (observation ID, counter, column)</p> <p>Added column(s) to MRDR geometry image</p> <p>Made observation ID hexadecimal, and corrected its length in all example labels</p> <p>Reformatted MTRDR sample label to parallel MRDR</p> <p>Added SUBTYPE of product to MRDR and MTRDR name</p> <p>Updated graphics</p> <p>Made 1 label per image file</p> <p>Redefined MTRDRs along line of data archive SIS</p> <p>Added MRO:EXPOSURE_PARAMETER to LDD list, to CDR name, EDR and CDR labels</p> <p>Added correction for shutter position to sphere radiance</p>	All
5/3/2006	<p>split TP into different test patterns</p> <p>add VNIR and IR FPU electronics temperatures as keywords and included in CDR labels and table of CRISM-specific keywords</p> <p>added prefix bytes to TRDR label</p> <p>copy applicable changes to Data Archive SIS</p> <p>specify which value is used for sphere, spec housing temp, detector temp, FPE temp</p> <p>add VL (valid limit) 14-bit DN level 6 CDR</p> <p>revise MRO:activity CAT file</p> <p>add event log, instrument settings and data compressibility level 6 CDRs</p> <p>revise observation description</p> <p>make heater zone definitions consistent</p> <p>update definition of how bad pixels are filled</p> <p>update macros</p>	All

	<p>add example labels for MRDR, MTRDR wavelength files</p> <p>add section on SPICE files</p> <p>add section on browse files</p> <p>add section on extras; move target list stuff to extras</p> <p>update description of observation ID files</p> <p>removed specific values of alarm limits and referenced appropriate CDR6</p> <p>update calibration appendix</p> <p>add compression_type = none, 8_bit to EDR keyword list</p> <p>made observation_id and observation_number hexadecimal</p> <p>update parameter formulations</p> <p>create LDD keywords INVALID_PIXEL_COORDINATES, REPLACED_PIXEL_COORDINATES and corresponding CAT file</p> <p>modify SC CDR4 for sphere correction; add VNIR image in units of 14-bit DN to use as a reference for the correction</p> <p>add CDR6 BS for bias step</p> <p>modify descriptions of DB, EB, and GH CDR6's</p> <p>fixed CDR4 sample label sphere nomenclature</p> <p>specify DDR geometry to 610, 2300 nm</p> <p>add CDR for daily housekeeping</p> <p>changed format of CDR4 images from IEEE_REAL to PC_REAL</p> <p>defined 000 as inapplicable exposure time parameter</p> <p>rename WV to WA for level-4 CDR</p> <p>rename SR to SS for sphere radiance model</p> <p>updated EDR, TRDR, DDR sample labels</p> <p>deleted appendix a</p> <p>added sample ADR label</p> <p>Redefined definition of nonuniformity files</p> <p>Eliminated CDR6 tables of CDR4s created inflight</p> <p>Added ST CDR6s</p> <p>Added ACT and PRE CDR6s and defined their distinct nomenclature</p> <p>Refined definition of AS CDR6</p> <p>Added BW CDR6</p> <p>Added HV CDR6</p> <p>Added PS CDR4</p> <p>Added RW CDR4</p> <p>Added RF CDR4</p> <p>Renamed WV CDR4 to WA CDR4, to eliminate confusion with the WV CDR6</p> <p>Added SH CDR4</p> <p>Added SL and VL CDR6s</p> <p>Renamed SR CDR4 to SS</p> <p>Added SW CDR6</p> <p>Made the counter in the EDR or TRDR file name hexadecimal</p> <p>Updated nomenclature of CDR4s to include additional identifiers</p> <p>Added resampled TRDR, filetype "RTR"</p> <p>Refined ADR definitions</p> <p>Made the counter in the EDR or TR</p> <p>DR file name hexadecimal</p> <p>Updated nomenclature of CDR4s to include additional identifiers</p> <p>Added resampled TRDR, filetype "RTR"</p> <p>Added ADR directory</p> <p>Made DDRs band sequential</p>	
7/10/2006	<p>Renamed ACT and PRE CDR6s to BTF and ATF</p> <p>Updated calibration description in Appendix I</p> <p>Redefined last 3 layers of a DDR to exclude CRISM-derived data</p> <p>Added missing commas in sample DDR label</p> <p>Changed units of radiance to W/(m**2 micrometer sr)</p>	All

	Replaced local data dictionary keyword MRO:FPE_ELECTRONICS_TEMPERATURE with MRO:FPE_TEMPERATURE	
10/1/2006	<p>Added INVALID_PIXEL_LOCATION or to TRDR labels</p> <p>Added keywords specific to resampling and atmospheric corrections to TRDR label</p> <p>Added keywords specific to resampling and atmospheric corrections to LDD, and tables of CRISM-specific keywords</p> <p>Updated list of summary products</p> <p>Added keywords specific to resampling and atmospheric corrections to tables of CRISM-specific keywords</p> <p>Added definitions of RTRs</p> <p>Described and differentiated version 0 and 1 DDR</p> <p>Added EDR, TRDR, and MRDR browse product labels to appendix</p> <p>Describe SPICE kernels generated by CRISM</p> <p>Updated definition of DDR browse products</p> <p>Added DDR browse product labels to appendix</p>	All
2/7/2007	<p>Added AT and RT CDR4s and CT CDR6 describing wavelength-dependent atmospheric transmission, for post-calibration data processing</p> <p>Changed primary source of MRO:DETECTOR_TEMPERATURE from IR temperature sensor 2 to IR temperature sensor 1</p> <p>Change of definition of wavelength filters on 11 Dec 2006 noted</p> <p>Changed units of elevation layer in DDR to kilometers</p> <p>Changed latitude range separating MRDR map tiles projected equirectangularly and polar stereographically</p> <p>Redefined calibrated data layer of MRDRs and MTRDRs to be I/F instead of radiance</p> <p>Redefined 'HYD' IR browse product into three separate products based on first results from Mars</p>	All
5/16/2007	<p>Changed units of MOLA elevation in DDR description</p> <p>Fixed nomenclature of OTT tables in EXTRAS directory</p> <p>Updated descriptions of SB and NU CDRs</p>	All
8/23/2007	<p>Corrected character string in file names to designate EPFs</p> <p>Added definition of TOD observing mode</p> <p>Updated descriptions of SPICE kernels</p> <p>Added information on number of wavelengths to descriptions of EDRs generated by each observation type</p> <p>Defined separate backplane files for I/F and Lambert albedo versions of MRDR and MTRDR because they may not be filled identically</p> <p>Updated definitions of summary products, including replace D2400 with SINDEX and add BD920</p> <p>Updated nomenclature of MRDRs to include tile number</p> <p>Deleted UR CDR6 and RA CDR4 which aren't being generated</p>	All
11/29/2010	<p>Added description of LDR data set</p> <p>Added descriptions of limb scans and hyperspectral survey</p> <p>Updated definition of MTRDRs and associated browse products</p> <p>Updated archive data volume estimates</p> <p>Updated descriptions of procedures to represent actual flight processes</p> <p>Updated calibration summary in Appendix</p> <p>Replaced sample labels with current formats</p> <p>Updated description of summary products to include OLINDEX2</p>	All
2/29/2012	Added description of TRR3 data filtering	All
03/13/2014	TERs and MTRDRs	All
04/10/2014	TERs and MTRDRs – PDS peer review liens	All
08/10/2015	TERs and MTRDRs – post-PDS review modifications	All
2/29/2016	TERs and MTRDRs – additional post-PDS review modifications	All

4/15/2022	<p>Added description of changes to MRDRs with version number</p> <p>Add information to all sections regarding class types and the activities that were added / retired over the course of the MRO mission</p> <p>Updated description of radiometric calibration in Appendix L</p> <p>Updated description of TER and MTRDR processing in Appendix P1</p> <p>Added Appendix P3 to describe history and current status of MRDR processing</p> <p>Added information on history of gimbal angle range and on how that affected the evolution of observation classes and the structure of activities within observation classes</p> <p>Updated and added applicable documents and references</p> <p>Removed information on resampled TRDRs which is not a data product type that will be delivered</p> <p>Added JCAT to applicable software</p> <p>Cleaned up and completed TER/MTRDR sample labels</p> <p>Corrected numerous random errors</p> <p>Deleted STO class type which was never acquired</p> <p>Deleted table of expected data volume in section 2 which was overtaken by events</p>	All
6/22/2022	<p>Expanded description of how DISORT is used in the MRDR data processing workflow</p> <p>Clarified the calculation and interpretation of spectral summary parameters</p>	<p>2.2.8</p> <p>3.4.1</p>

## CONTENTS

<b>1. INTRODUCTION .....</b>	<b>12</b>
<b>1.1 Purpose and Scope.....</b>	<b>12</b>
<b>1.2 Contents.....</b>	<b>13</b>
<b>1.3 Applicable Documents and Constraints.....</b>	<b>13</b>
<b>1.4 Relationships with Other Interfaces.....</b>	<b>14</b>
<b>2. DATA PRODUCT CHARACTERISTICS AND ENVIRONMENT .....</b>	<b>14</b>
<b>2.1 Instrument Overview.....</b>	<b>14</b>
2.1.1 Hardware overview .....	15
2.1.2 Key variables in observing modes.....	17
2.1.3 Summary of orbital observing modes .....	19
2.1.4 Details of observing modes .....	22
<b>2.2 Data Product Overview.....</b>	<b>30</b>
2.2.1 EDRs .....	31
2.2.2 CDRs .....	31
2.2.3 ADRs .....	32
2.2.4 TRDRs .....	32
2.2.5 DDRs .....	32
2.2.6 LDRs.....	32
2.2.7 TERs and MTRDRs .....	32
2.2.8 MRDRs .....	33
2.2.9 SPICE Files .....	34
2.2.10 Browse Products.....	34
2.2.11 Extra Products .....	34
<b>2.3 Data Processing .....</b>	<b>39</b>
2.3.1 Data Processing Level.....	39
2.3.2 Data Product Generation .....	40
2.3.3 Data Flow and Delivery .....	42
2.3.4 Labeling and Identification .....	42
<b>2.4 Standards Used in Generating Data Products .....</b>	<b>58</b>
2.4.1 PDS Standards .....	58
2.4.2 Time Standards .....	58
2.4.3 Coordinate Systems .....	59
<b>2.5 Data Validation .....</b>	<b>59</b>
2.5.1 EDR level.....	59
2.5.2 EDR to RDR level .....	59
2.5.3 RDR level.....	60
<b>3. DETAILED DATA PRODUCT SPECIFICATIONS.....</b>	<b>61</b>
<b>3.1 EDR.....</b>	<b>61</b>
3.1.1 Data Product Structure and Organization .....	61
3.1.2 Label Description .....	79
<b>3.2 DDR.....</b>	<b>81</b>
3.2.1 Data Product Structure and Organization .....	81
3.2.2 Label Description .....	83
<b>3.3 LDR .....</b>	<b>84</b>
3.3.1 Data Product Structure and Organization .....	84
3.3.2 Label Description .....	85
<b>3.4 Targeted RDR .....</b>	<b>86</b>
3.4.1 Data Product Structure and Organization .....	86
3.4.2 Label Description .....	95

<b>3.5 Map-Projected Multispectral RDR .....</b>	<b>100</b>
3.5.1 Data Product Structure and Organization .....	100
3.5.2 Map projection standards .....	101
3.5.3 Label Description .....	102
<b>3.6 Targeted Empirical Record and Map-projected Targeted Reduced Data Record .....</b>	<b>103</b>
3.6.1 Data Product Structure and Organization .....	103
3.6.2 Label Description .....	105
<b>3.7 Level-6 CDR .....</b>	<b>106</b>
3.7.1 Data Product Structure and Organization .....	106
3.7.2 Label Description .....	106
<b>3.8 Level-4 CDR .....</b>	<b>109</b>
3.8.1 Data Product Structure and Organization .....	109
3.8.2 Label Description .....	109
<b>3.9 ADR.....</b>	<b>113</b>
<b>3.10 CRISM-Generated SPICE Files .....</b>	<b>115</b>
<b>3.11 Browse Products.....</b>	<b>116</b>
3.11.1 EDR Browse Products .....	116
3.11.2 TRDR Browse Products .....	117
3.11.3 MRDR, TER, and MTRDR Browse Products .....	118
<b>3.12 Extra Products.....</b>	<b>123</b>
3.12.1 EDR Extras Products .....	123
3.12.2 TRDR Extras Products .....	126
3.12.3 TER/MTRDR Extras Products .....	126
<b>4. APPLICABLE SOFTWARE.....</b>	<b>126</b>
<b>4.1 Utility Programs .....</b>	<b>126</b>
<b>4.2 Applicable PDS Software Tools.....</b>	<b>127</b>
<b>APPENDIX A. EDR LABEL.....</b>	<b>128</b>
<b>APPENDIX B. DDR LABEL.....</b>	<b>131</b>
<b>APPENDIX C1. TRDR LABEL (RADIANCE IMAGE + LISTFILE) .....</b>	<b>133</b>
<b>APPENDIX C2. TRDR LABEL (I/F IMAGE) .....</b>	<b>137</b>
<b>APPENDIX D1. MRDR LABEL (I/F IMAGE) .....</b>	<b>141</b>
<b>APPENDIX D2. MRDR LABEL (DERIVED DATA IMAGE).....</b>	<b>143</b>
<b>APPENDIX D3. MRDR LABEL (SUMMARY PRODUCT IMAGE).....</b>	<b>145</b>
<b>APPENDIX D4. MRDR LABEL (WAVELENGTH FILE) .....</b>	<b>148</b>
<b>APPENDIX E1. TER LABEL (CORRECTED I/F FILE).....</b>	<b>150</b>
<b>APPENDIX E2. TER LABEL (DATA PROCESSING INFORMATION FILE) .....</b>	<b>152</b>
<b>APPENDIX E3. TER LABEL (REFINED SUMMARY PRODUCT FILE).....</b>	<b>154</b>
<b>APPENDIX E4. TER LABEL (SUMMARY PRODUCT FILE) .....</b>	<b>157</b>
<b>APPENDIX E5. TER LABEL (WAVELENGTH FILE) .....</b>	<b>160</b>
<b>APPENDIX E6. MTRDR LABEL (CORRECTED I/F FILE).....</b>	<b>162</b>
<b>APPENDIX E7. MTRDR LABEL (DATA PROCESSING INFORMATION FILE).....</b>	<b>165</b>
<b>APPENDIX E8. MTRDR LABEL (DERIVED INFORMATION FILE).....</b>	<b>168</b>
<b>APPENDIX E9. MTRDR LABEL (REFINED SUMMARY PRODUCT FILE).....</b>	<b>171</b>
<b>APPENDIX E10. MTRDR LABEL (SUMMARY PRODUCT FILE).....</b>	<b>175</b>

APPENDIX E11. MTRDR LABEL (WAVELENGTH FILE) .....	179
APPENDIX F. LEVEL 6 CDR LABEL.....	181
APPENDIX G. LEVEL 4 CDR LABEL .....	183
APPENDIX H. LDR LABEL .....	186
APPENDIX I1. EDR BROWSE PRODUCT HTML FILE LABEL .....	188
APPENDIX I2. EDR BROWSE PRODUCT PNG FILE LABEL .....	189
APPENDIX J1. TER ‘TAN’ BROWSE PRODUCT LABELS .....	191
APPENDIX J1. MTRDR ‘TAN’ BROWSE PRODUCT LABELS.....	194
APPENDIX K. MRDR BROWSE PRODUCT 'TRU' PNG FILE LABEL .....	197
APPENDIX L. RADIOMETRIC CALIBRATION DETAILS.....	199
APPENDIX M. TEMPERATURE SENSOR AND HEATER LOCATIONS .....	249
APPENDIX N. DESCRIPTION OF TRR3 FILTERING .....	255
APPENDIX O. DESCRIPTION AND USAGE OF ADRS .....	266
APPENDIX P1. TER/MTRDR DATA PROCESSING & PRODUCT DESCRIPTION ..	267
APPENDIX P2. TER/MTRDR EXTRAS DOCUMENTATION .....	276
APPENDIX P3. MRDR DATA PROCESSING AND PRODUCT DESCRIPTION .....	280

## FIGURES AND TABLES

DOCUMENT CHANGE LOG .....	2
CONTENTS .....	6
FIGURES AND TABLES.....	9
ACRONYMS .....	10
Table 2-1 CRISM Investigation Objectives and Implementation .....	14
Figure 2-2a. Photographs of CRISM OSU, DPU, GME.....	16
Figure 2-2b. CRISM block diagram.....	16
Figure 2-2c. CRISM Optical Sensor Unit (OSU) configuration.....	16
Figure 2-2d. CRISM optical diagram.....	17
Figure 2-3. Sample VNIR and IR image frames (viewing internal integrating sphere). ....	17
Table 2-4. CRISM Observing Modes .....	21
Figure 2-5. Elements to a CRISM targeted observation. ....	22
Table 2-6. Translation of different observation classes into EDRs. ....	27
Figure 2-7. Translation of 12-bit DNs into 8-bit DNs using LUTs.....	30
Table 2-8. Definitions of CRISM data products.....	35
Figure 2-9. Sequential processing of EDRs to yield RDRs showing roles of CDRs & ADRs .....	36
Figure 2-9a. Sequential processing of DDRs and TRDRs to create TERs and MTRDRs. ....	37
Figure 2-9b. Sequential processing of DDRs and TRDRs to create MRDRs.....	38
Figure 2-10. Tiling scheme for the map-projected multispectral survey .....	39
Table 2-11. Processing Levels for Science Data Sets.....	39
Table 2-12. Contents of each type of CRISM observation .....	41
Table 2-13. Nomenclature of Observation Tracking Tables .....	58
Figure 3-1. Contents of a CRISM Experiment Data Record (EDR). ....	62
Table 3-2. Items in housekeeping list file.....	63
Table 3-3. Bit mapping of scan motor status word .....	76
Table 3-4. Bit mapping of scan motor control word .....	76
Table 3-5. Alarms coded in housekeeping.....	77
Table 3-6. Alarms for monitored housekeeping and responses to out-of-limits conditions .....	78
Table 3-7. CRISM-specific values for EDR label keywords.....	79
Figure 3-8. Contents of a CRISM Derived Data Record (DDR). ....	83
Table 3-9. CRISM-specific values for DDR label keywords.....	84
Table 3-10. CRISM-specific values for LDR label keywords .....	86
Figure 3-11. Contents of a CRISM Reduced Data Record for a single observation (TRDR). ....	87
Table 3-12. Formulation of parameters for summary products.....	89
Table 3-13. CRISM-specific values for TRDR label keywords .....	95
Figure 3-14. Contents of a CRISM Reduced Data Record for a multispectral map tile (MRDR). ....	102
Table 3-15. CRISM-specific values for MRDR label keywords.....	103
Figure 3-16. Contents of a CRISM Map-projected Targeted Reduced Data Record (MTRDR).....	104
Table 3-17. CRISM-specific values for TER/MTRDR label keywords .....	105
Figure 3-18. Contents of a CRISM Calibration Data Record (CDR). ....	106
Table 3-19. Descriptions of calibration-related level-6 CDRs .....	107
Table 3-20. Descriptions of operational level-6 CDRs.....	108
Table 3-21. Descriptions of level-4 CDRs.....	110
Table 3-22. CRISM-specific values for CDR label keywords.....	112
Table 3-23. LUT for atmospheric opacity (ADR type = CL) .....	114
Table 3-24. LUT for predicted atmospheric / photometric / thermal correction (ADR type = AC) .....	114
Table 3-25. LUT for local surface temperature (ADR type = TE) .....	114
Figure 3-26. Example EDR browse product .....	117
Table 3-27. Contents of OBS_ID Table. ....	123

## ACRONYMS

A/D	Analog to Digital Converter
ADC	Analog to Digital Converter
ADR	Ancillary Data Record
APL	The Johns Hopkins University Applied Physics Laboratory
CAT	CRISM Analysis Tool
CRISM	Compact Reconnaissance Imaging Spectrometer for Mars
CDR	Calibration Data Record
CSV	Comma-Separated Value (a format for organizing tabular data in ASCII format)
CTX	Context Imager (on Mars Reconnaissance Orbiter)
DAC	Digital to Analog Converter
DDR	Derived Data Record
DPCM	Differential Pulse-Code Modulation (compression)
DPU	CRISM Data Processing Unit
EDR	Experiment Data Record
EPF	Emission Phase Function
FOV	Field-of-View
FPU	Focal Plane Unit
Gb	Gigabit ( $10^9$ bits)
GME	CRISM Gimbal Motor Electronics
HIRISE	High-Resolution Imaging Science Experiment (on Mars Reconnaissance Orbiter)
HOP	High-output Paraffin actuator; on CRISM a HOP deploys the cover
I/F	Intensity divided by flux, or the ratio of radiance to incident solar radiation
IR	Infrared
JHU/APL	The Johns Hopkins University Applied Physics Laboratory
JPL	Jet Propulsion Laboratory
LDR	Limb Data Record
LED	Light-emitting diode
LOS	Line-of Sight
Ls	Solar longitude; a measure of Mars' motion in its orbit, in degrees, since northern hemisphere vernal equinox
LUT	Look-up Table
LVDS	Low-Voltage Differential Signal
MOC	Mars Orbiter Camera (on Mars Global Surveyor)
MOLA	Mars Orbiter Laser Altimeter (on Mars Global Surveyor)
MRDR	Map-projected Multispectral Reduced Data Record
MRO	Mars Reconnaissance Orbiter
MTRDR	Map-projected Targeted Reduced Data Record
MUX	Multiplexed or multiplexer
OMEGA	Observatoire pour la Minéralogie, l'Eau, les Glaces et l'Activité (on Mars Express)
OSU	CRISM Optical Sensor Unit
PDS	Planetary Data System
RDR	Reduced Data Record
SIS	Software Interface Specification
SOC	Science Operations Center

SNR	Signal-to-noise ratio
SPICE	SPacecraft, Instrument, Camera, and Events; a set of data formats for spacecraft ephemeris, attitude, and instrument pointing
Tb	Terabit ( $10^{12}$ bits)
TBD	To Be Determined
TER	Targeted Empirical Record
TES	Thermal Emission Spectrometer (on Mars Global Surveyor)
THEMIS	Thermal Emission Imaging System (on Mars Odyssey)
TRDR	Targeted Reduced Data Record
VNIR	Visible / near-infrared

# **1. INTRODUCTION**

## **1.1 Purpose and Scope**

The purpose of this Data Product Software Interface Specification (SIS) is to provide users of the data products from the Compact Reconnaissance Imaging Spectrometer for Mars (CRISM) with:

- A detailed description of the products
- A guide to interpreting and using their contents
- A description of how they were generated, including data sources and destinations
- A description of how raw data can be calibrated, including what archived data products are necessary and the procedures to use

Although this is beyond the scope of the strictest definition of the contents of a Planetary Data System (PDS) SIS, this approach is adopted because CRISM is a complicated instrument which has generated an extremely large data set that include multiple observing modes. The authors believe that detailed information is required for users to correctly utilize the data products described herein.

There are eleven CRISM data products defined in this SIS document. These include:

- 1) Experiment Data Record (EDR) consisting of raw, uncalibrated CRISM spectra;
- 2) Derived Data Record (DDR) containing pointing and other ancillary information for observations pointed at Mars' surface;
- 3) Limb Data Record (LDR) containing pointing and other ancillary information for observations pointed at Mars' limb;
- 4) Targeted Reduced Data Record (TRDR), which is a radiometrically calibrated EDR;
- 5 and 6) two types of Calibration Data Records (CDRs), which are files used to generate radiance or radiance/solar irradiance (I/F) values in a TRDR from an EDR;
- 7) Ancillary Data Records (ADRs), which are files used to correct I/F values for atmospheric, photometric, or thermal effects, and which document the data set;
- 8) Map-Projected Multispectral Reduced Data Record (MRDR);
- 9) Targeted Empirical Record (TER) and
- 10) Map-projected Targeted Reduced Data Record (MTRDR) which are paired product types;
- 11) Browse products for EDRs, TRDRs, TERs, MTRDRs, and MRDRs.

This SIS is intended to provide enough information to enable users to read and understand the data products. The users for whom this SIS is intended are the scientists who will analyze the data, including those associated with the Mars Reconnaissance Orbiter Project and those in the general planetary science community.

## **1.2 Contents**

This Data Product SIS describes how data products generated by the CRISM are processed, formatted, labeled, and uniquely identified. The document details standards used in generating the products and software that may be used to access the product. Data product structure and organization is described in sufficient detail to enable a user to read and understand the product. Finally, an example of each product label is provided.

The CRISM investigation team has also delivered, in parallel with flight data, a spectral library of analog materials that is useful to interpreting flight data. That is described in:

1. CRISM Spectral Library Software Interface Specification, S. Slavney and S. Murchie, Mar. 10, 2006.

## **1.3 Applicable Documents and Constraints**

This Data Product SIS is responsive to the following Mars Reconnaissance Orbiter documents:

2. Mars Exploration Program Data Management Plan, R. E. Arvidson and S. Slavney, Rev. 2, Nov. 2, 2000.
3. Mars Reconnaissance Orbiter Project Data Archive Generation, Validation and Transfer Plan, R. E. Arvidson, S. Noland and S. Slavney, Jan. 26, 2006.
4. Mars Reconnaissance Orbiter (MRO) Compact Reconnaissance Imager and Spectrometer for Mars (CRISM) Experiment Operations Plan, S. L Murchie, version 1.7, June 2005.
5. CRISM Archive Volume Software Interface Specification, S. L Murchie, E. Guinness, and S. Slavney, version 1.2.7.4, April 15,, 2022.

This SIS is also consistent with the following Planetary Data System documents:

6. Planetary Data System Data Preparation Workbook, Version 3.1, Jet Propulsion Laboratory (JPL) D-7669, Part 1, February 1, 1995.
7. Planetary Data System Data Standards Reference, Version 3.6, JPL D-7669, Part 2, August 1, 2003.
8. Planetary Science Data Dictionary Document, JPL D-7116, Rev. E, August 28, 2002.

The reader is referred to the following documents for additional information:

9. Seidelmann, P. K., et al., Report of the IAU/IAG working group on cartographic coordinates and rotational elements of the planets and satellites: 2000, Celestial Mechanics and Dynamical Astronomy, 82, 83-111, 2002.
10. Murchie, S.L, et al. (2009) The CRISM investigation and data set from the Mars Reconnaissance Orbiter's Primary Science Phase, J. Geophys. Res., 114, E00D07.
11. Viviano-Beck, C. E., et al. (2014) Revised CRISM spectral parameters and summary products based on the currently detected mineral diversity on Mars, J. Geophys. Res. Planets, 119, 1403–1431;  
[https://pds-geosciences.wustl.edu/missions/mro/spectral\\_library.htm](https://pds-geosciences.wustl.edu/missions/mro/spectral_library.htm)
12. <https://crismtypespectra.rsl.wustl.edu>

Finally, this SIS is meant to be consistent with the contract negotiated between the Mars Reconnaissance Orbiter Project and the CRISM Principal Investigator (PI) in which reduced data records and documentation are explicitly defined as deliverable products.

## 1.4 Relationships with Other Interfaces

Data products described in this SIS are produced by the CRISM Science Operations Center (SOC). Changes to the SOC processing algorithms may cause changes to the data products and, thus, this SIS. The RDR products are dependent on the CRISM EDR products. As such, changes to the EDR product may affect the RDR products.

Changes in CRISM data products or this SIS may affect the design of the CRISM archive volumes.

# 2. DATA PRODUCT CHARACTERISTICS AND ENVIRONMENT

## 2.1 Instrument Overview

CRISM addresses the objectives of characterizing Martian aqueous mineralogy and crustal composition, seasonal variation in the surface and atmosphere, and identifying new targets of scientific interest using the three-pronged strategy described in Table 2-1. Murchs11

**Table 2-1 CRISM Investigation Objectives and Implementation**

Objective	Implementation / Measurement Strategy	Observation / Planning Design
Find new targets of interest: aqueous deposits, crustal composition	Target observations using previous geologic studies and results from the Thermal Emission Spectrometer (TES), Thermal Emission Imaging System (THEMIS), Mars Orbiter Camera (MOC), etc.	Target list assembled from previous studies Screened / added to using targeting basemap
	Use Mars Express OMEGA data to find new targets lacking morphologic or thermal IR signatures	Derived products from OMEGA included in targeting basemap
	Find targets below OMEGA's resolution using near-global mapping at key wavelengths (IR through 2017)	72-channel, ~200-m/pixel VNIR+IR multispectral survey 262-channel, ~200 m/pixel VNIR+IR hyperspectral survey 107-channel, ~200 m/pixel VNIR hyperspectral mapping 92-channel, ~100 m/pixel VNIR hyperspectral mapping
Separate the surface and atmosphere	Observe emission phase function (EPF) at each targeted observation to quantify atmospheric effects (through 2012)	±60° or -60° to +30° EPF inherent to full and half resolution targeted observations through 2012
Provide information on spatial/ seasonal variations in aerosols, H <sub>2</sub> O, CO <sub>2</sub> , and ices	Regularly acquire global grids of EPFs to monitor seasonal variations in surface and atmospheric properties (through 2012)	High time-resolution (atmospheric monitoring campaign) High spatial-resolution (seasonal change campaign)
	Sample compositional layering and seasonal change of polar ices	Key areas targeted with full and half resolution Monitor seasonal cap with multispectral observations
Measure surface targets with high spatial and spectral resolutions and high signal-to-noise ratio (SNR)	Measure thousands of targets at full spectral resolution and high spatial resolution	Full and half resolution targeted observations provide coverage at 6.55 nm/channel, 15-40 m/pixel (at nadir) Multispectral windows or trips of multispectral survey provide coverage of key regions of the planet at ~100 m/pixel, including seasonal polar caps to track seasonal changes
	Measure key regions of the surface at key wavelengths at higher resolutions than multispectral survey	Radiometric calibration using integrating sphere Background calibrations using shutter are integrated with each observation
	Conduct inflight calibration of background and responsivity to provide radiometric accuracy	

### **2.1.1 Hardware overview.**

The CRISM system, design, and function are illustrated in Figure 2-2. CRISM consists of three boxes: the Optical Sensor Unit (OSU) which includes the optics, gimbal, focal planes, cryocoolers and radiators, and focal plane electronics; the Gimbal Motor Electronics (GME), which commands and powers the gimbal motor and encoder and analyzes data from the encoder in a feedback loop; and the Data Processing Unit (DPU), which accepts and processes commands from the spacecraft and accepts and processes data from the OSU and communicates it to the spacecraft. The CRISM OSU has a one-time deployable cover that protects the instrument optics from contamination. The cover was opened in September 2006 following MRO's aerobraking into its science orbit.

The optical and sensor assembly in the OSU consists of a visible/near-infrared (VNIR) focal plane covering 362-1053 nm at 6.55 nm/channel and a cryogenically cooled infrared (IR) focal plane covering 1002-3920 nm at 6.55 nm/channel. Each field-of-view (FOV) is approximately 605 61.5- $\mu$ rad pixels wide. On each side of the VNIR FOV and one side of the IR FOV there are detector elements not illuminated through the spectrometer slit, that measure instrument background and scattered light in the spectrometer cavity simultaneously with each scene measurement (Figure 2-3). A shutter can block the FOV to interleave full-field background measurements. The shutter can also be positioned to view a closed-loop controlled integrating sphere simultaneously by each focal plane, providing radiometric response and flat-field calibration. In addition, either of two redundant lamps can illuminate each focal plane directly to measure detector non-uniformity. Each focal plane has a dedicated electronics board that provides the required clock signals and bias voltages, and digitizes the video data from the focal plane. The digitized data is transmitted through the twist capsule to the DPU. The infrared focal plane is cooled to  $\leq 125\text{K}$  by one of three cryocoolers (selectable by the DPU).

The scanning subsystem consists of the Gimbal Motor Electronics (GME), a high-resolution angular encoder, and the gimbal drive motor. The GME contains the motor driver circuitry, and responds to a commanded profile from the DPU. Software in the DPU implements a control algorithm, utilizing feedback information from the 20-bit encoder to maintain closed-looped control. The system accurately follows a programmed scan pattern that is carefully designed to compensate for orbital motion and to accomplish the desired scan pattern across the Martian surface.

The DPU receives unregulated 28-32 volt power from MRO and provides regulated secondary power to CRISM, receives and processes commands from the MRO, controls the CRISM subsystems, and acquires and formats CRISM science and housekeeping data that is then sent to the spacecraft solid state recorder for downlink to earth.

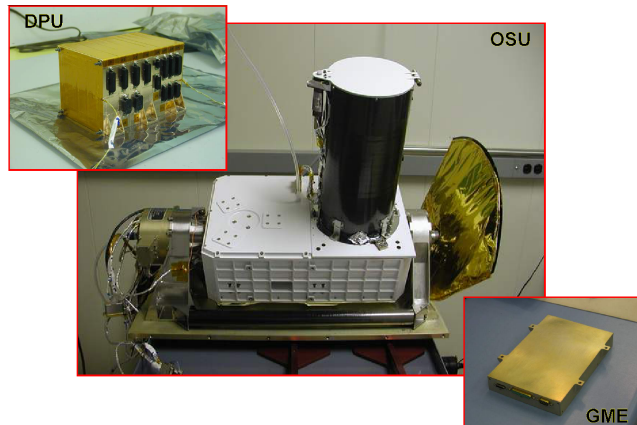


**Figure 2-2a.**  
**Photographs**  
**of CRISM OSU,**  
**DPU, GME.**

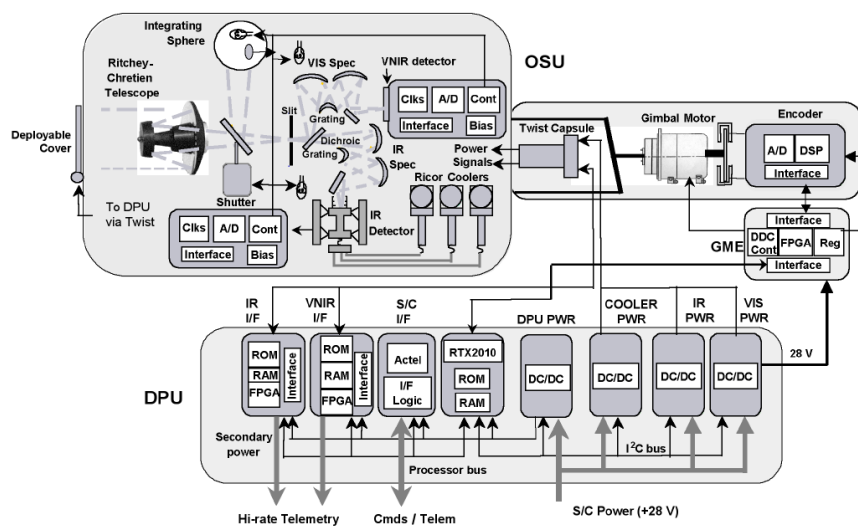


**Figure 2-2b.**  
**CRISM block**  
**diagram.**

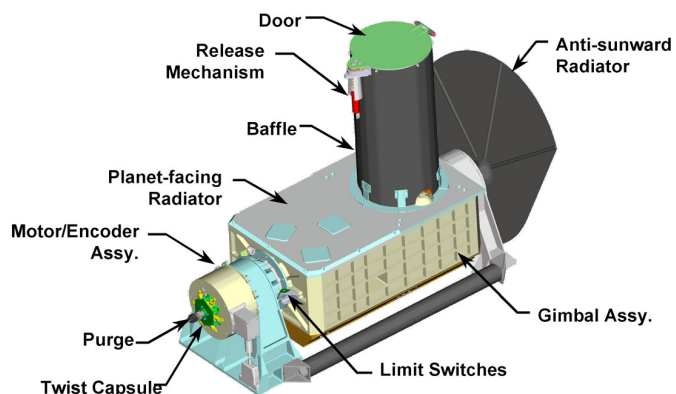


**Figure 2-2c.**  
**CRISM Optical**  
**Sensor Unit**  
**(OSU)**  
**configuration.**

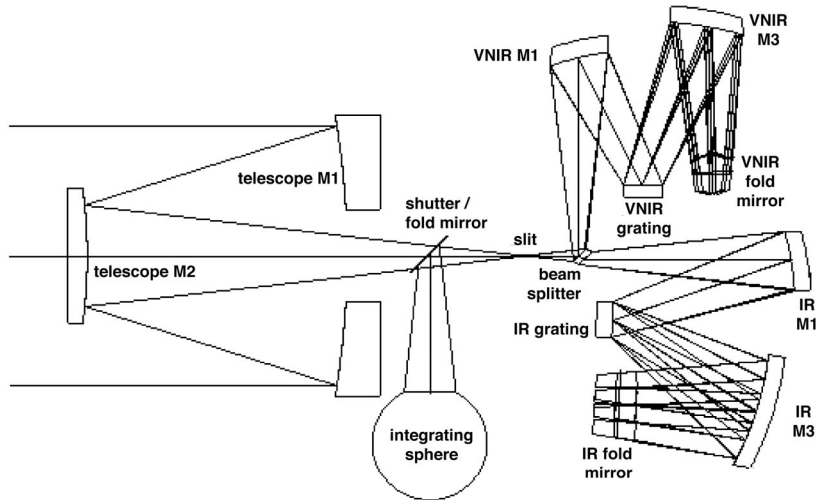


**Figure 2-2d.**  
**CRISM optical diagram.**

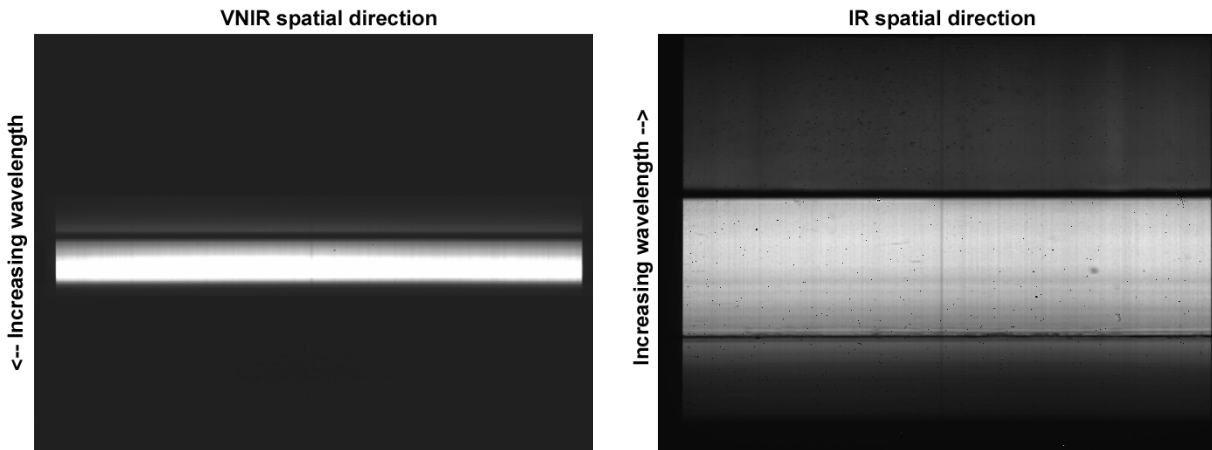


**Figure 2-3. Sample VNIR and IR image frames (viewing internal integrating sphere).**

### 2.1.2 Key variables in observing modes

Key variables ("configurations") in constructing observing scenarios include the following. All are selectable separately for the VNIR and IR detectors.

- Image source. Image data may be generated using digitized output from the detector, or using one of up to seven test patterns.
- Detector row selection. All detector rows, sampling different wavelengths, having useful signal can be saved. Alternatively an arbitrary, commandable subset of rows can be saved. The number of rows with useful signal is 545, 107 in the VNIR and 438 in the IR, and these subsets of VNIR and IR detector rows are used for hyperspectral observing. Prior to 10 Dec 2006 the nominal number of rows for multispectral mode was 73, 18 in the VNIR and 55 in the IR. On 10 Dec 2006 an extra channel was added to the VNIR for calibration purposes, for a total of 19. For each detector, there are four options of channel selection to choose from rapidly by command: hyperspectral (545 total channels), multispectral (73 total channels prior to 10 Dec 2006, 74 total

channels on and after 10 Dec 2006), and two sets of expanded multispectral (84 and 92 channels prior to 10 Dec 2006, 85 and 93 channels on and after 10 Dec 2006). New options are set by uploading a data structure to the DPU. In 2010, the smaller of the two expanded multispectral channel selections was replaced with the largest value supportable at a 15 Hz frame rate, all 107 VNIR channels and 155 IR channels; most of the IR channels are contiguous from 1.8-2.55  $\mu$ m to cover key mineral absorptions. In 2012, the other expanded multispectral channel selection was replaced with the largest value of VNIR channels supportable at a 30 Hz frame rate, 92 channels.

- Pixel binning. Pixels can be saved unbinned or binned 2x, 5x, or 10x in the spatial direction. No pixel binning in the spectral direction is supported.
- Compression. All CRISM data are read off the detector in 14-bit format and are compressed real-time in hardware. Compression options, in succession, are:
  - Subtraction of an offset, on a line by line basis. Offsets are set by uploading a data structure to the DPU.
  - Multiplication by a gain, on a line by line basis, with the output in 12-bit format. Gains are set by uploading a data structure to the DPU. (Raw 12-bit data are stored onground in data products as 16-bit numbers.)
  - Optionally, conversion from 12 to 8 bits using one of eight look-up tables (LUTs) specified on a line by line basis. These choices are set by uploading a data structure to the DPU. This option is not used in flight.
  - Optionally, lossless Fast + differential pulse-code modulation (DPCM) compression. This option is used for all data in flight.
- Pointing. CRISM has two basic gimbal pointing configurations and two basic superimposed scan patterns. Pointing can be (1) fixed (nadir-pointed in the primary science orbit) or (2) dynamic, tracking a target point on the surface of Mars and taking out ground track motion. Two types of superimposed scans are supported: (1) a short, 4-second duration fixed-rate ("EPF-type") scan which superimposes a constant angular velocity scan on either of the basic pointing profiles, or (2) a long, minutes-duration fixed-rate ("target swath-type") scan.
- Frame rate. Frame rates of 1, 3.75, 5, 15, and 30 Hz are supported. The 1 Hz frame rate is used for hyperspectral measurements of the onboard integrating sphere, because the long exposures possible at 1 Hz are needed for appreciable SNR at the shortest wavelengths. 3.75 Hz is used for targeted hyperspectral measurements of Mars; this is the highest frame rate at which the DPU electronics support onboard compression options over the range of wavelengths imaged onto the detectors with useful SNR. 15 and 30 Hz frame rates are used for nadir-pointed multispectral and hyperspectral mapping measurements that return selected wavelengths. The 5 Hz frame rate is not used in flight, because at that rate the electronics do not support compression of a hyperspectral wavelength selection, and it would produce excessive along-track smear in a nadir-pointed observation.
- Integration time. Integration times are in increments of 1/480th of the inverse of the frame rate. At 1 Hz, for example, available integration times are 1/480th sec, 2/480th sec...480/480th , and at 15 Hz, 1/7200th sec, 2/7200th sec...480/7200th sec.
- Calibration lamps. Radiometric calibration is provided inflight by either of a pair of lamps that directly illuminates each focal plane with "white" light, and by either of two lamps in the

integrating sphere. All focal plane lamp settings are open-loop with 4095 possible levels, meaning that current is commanded directly. For the integrating sphere, closed loop control is available at 4095 levels. For closed loop control, the setting refers to output from a photodiode viewing the interior of the integrating sphere; current is adjusted dynamically to attain the commanded photodiode output. In flight, all regular radiometric calibrations have used the integrating sphere running under closed-loop control, and specifically the IR-controlled lamp which provides more uniform illumination. The focal plane lamps were used for restricted cruise tests of linearity of the detectors' response.

- Shutter position. Open, closed, or viewing the integrating sphere. The shutter is actually commandable directly to position 0 through 32. In software, open=3, sphere=17, closed=32. NOTE: during integration and testing, it was discovered that at positions  $\leq 2$  the hinge end of the shutter is directly illuminated and creates scattered light. Position 3 does not cause this effect, but the other end of the shutter slightly vignettes incoming light.

### **2.1.3 Summary of orbital observing modes**

During the orbital mission, CRISM uses combinations of instrument settings to acquire several basic types of observations as described in Table 2-4. Targeted mode (original configuration shown in Figure 2-5) provides high-resolution hyperspectral measurements of the surface, (through 2012) with accompanying measurements of atmospheric opacity and trace gases. As a target is over flown it is covered by a slow, continuous scan of the field-of-view, taking out most ground track motion. During this operation, the instrument gimbal covers angles  $\pm 35^\circ$ . This central scan is bracketed by five incoming and five outgoing  $\pm 0.3^\circ$  scans centered on the center point of the target, at  $5^\circ$  increments in gimbal position over the range of  $40^\circ$ - $60^\circ$  in gimbal angle. The total of eleven scans provides an 11-angle emission phase function<sup>1</sup> (EPF) that contains information needed for photometric and atmospheric correction of the central targeted scan. Beginning in August 2010, aging of the gimbal led to restriction of the range of gimbal motion, eliminating the 5 incoming  $\pm 0.3^\circ$  scans. Beginning in October 2012, further restriction of gimbal motion to  $\sim 0^\circ$  to  $+30^\circ$  led to cessation of EPF measurements, and reductions in the along-track dimension of the central scan.

In atmospheric EPF mode, the central scan is replaced by 1 or 3  $\pm 0.3^\circ$  scans covering a geographically restricted region. The main purpose is recovery of an 11- or 13-position EPF to estimate atmospheric opacity and collect additional hyperspectral measurements of trace gases. Atmospheric EPF mode is used every  $\sim 9^\circ$  of solar longitude (Ls; a measure of Marian season, where  $0^\circ$  is northern hemisphere vernal equinox) to acquire a low spatial density global grid of EPFs to track seasonal variations in surface and atmospheric properties. The grid is covered in 1 solar day. Every  $\sim 36^\circ$  of Ls, a cluster of grids is taken on non-contiguous days to provide a higher spatial density grid to monitor seasonal change in surface material spectral properties. The grids are overlain on a best-effort basis; repeat coverage to  $\pm 25$  km can be accomplished from careful

---

<sup>1</sup> An emission phase function is a set of observations of a location on the Martian surface at near-constant solar incidence angle but variable emission angle (and thus phase angle). Because the atmospheric path length varies while illumination is held constant, an EPF enables simultaneous solution for atmospheric and surface components to radiance using estimated surface and atmospheric wavelength-dependent scattering functions. The EPF geometries envelope that of the central scan, so the estimated atmospheric and surface components of its measured radiance can be separated.

selection of the orbits along which the EPFs are taken. Restrictions on gimbal motion beginning in August 2010 leave an 8-position EPF measurement in this type of observation.

Beginning in late 2008, approximately every 2 months the grids of EPFs have been supplemented with a cluster of two or more orbits of limb-scan measurements, located at longitudes nearest to Nili Fossae and Ascraeus Mons. In this type of observation the spacecraft is pitched to allow the gimbal access to the limb, and gimbal motion is used to scan the field-of-view (FOV) from below the horizon to at least 120 km above it. Over each orbit ~15 scans are collected over the day side of Mars, and several additional scans past the ascending and descending terminators look for airglow over the polar regions.

In each of several mapping modes, the instrument is fixed pointing at nadir, and selected wavelengths are measured at spatial resolution that is reduced by binning pixels in the spatial direction, to manage data volume. This mode of operation is intended to search for new targets of interest and to provide moderate spatial and spectral resolution contextual mapping of surface composition. Two modes of multispectral operation were used initially: ~200 m/pixel "multispectral survey" mode which is designed to accomplish coverage rapidly, and ~100 m/pixel "multispectral window" mode which is intended for higher spatial resolution in key areas. Multispectral windows were discontinued in March 2008 due to interference of 30 Hz operating mode with closed loop control of cryocoolers.

Aging on coolers led to collection of their operation into 1 of every 4 MRO 2-week planning periods, beginning in 2009. In June 2009, during periods of time where the cryocoolers were off, a new mode of mapping hyperspectrally using all 107 VNIR wavelengths was initiated. This was augmented to 100 m/pixel (using 92 channels with useful signal) beginning in January 2012.

Beginning in January 2010, ~200 m/pixel "hyperspectral survey" mode using all VNIR wavelengths and an expanded set of IR detector rows was initiated, to provide a contextual hyperspectral (at 0.4-1.0, 1.3-1.5, and 1.9-2.5  $\mu\text{m}$ ) mapping mode for target-rich regions of the planet. Acquisition of these large data products was restricted to periods when a cryocooler was on.

In optical depth tracking mode, the instrument is fixed pointing at nadir, and a short burst of data is taken periodically with CRISM's full wavelength selection, but at spatial resolution that is reduced by binning pixels in the spatial direction to manage data volume. This mode of operation is intended to supplement EPFs with high spatial density measurements with full hyperspectral capability, to provide additional monitoring of trace gases.

In addition, radiometric calibrations using the onboard integrated sphere and measurements of detector bias are taken at least daily. Background measurements are integrated with each type of observation.

On a monthly basis, the flat-field response is assessed by imaging bland regions of Mars.

**Table 2-4. CRISM Observing Modes**

Mode	Pointing	Description and Observation Type Acronym	Coverage, YEAR_DOF Used
Targeted (hyperspectral)	Tracking as shown, once per target	Full resolution (FRT) Spatial pixels unbinned for target - 18 m/pixel @300 km, 10x binned for EPF	
		Half resolution short (HRS) Spatial pixels 2x binned for target - 36 m/pixel @300 km, 10x binned for EPF; same swath length as above	~6500 per Mars year 2006_270 thru 2012_146 (1-sided EPF after 2010_080)
		Half resolution long (HRL) Spatial pixels 2x binned for target - 36 m/pixel @300 km, 10x binned for EPF; twice swath length as above	
Spatially oversampled for on-ground rendering at $\leq 12$ m/pixel		Along-track oversampled (ATO) With 1-sided EPF thru 2012_142; subsequently without, and with shorter central scan	2011_079 thru 2012_142 2012_293 thru present
Reduced-length targeted (hyperspectral)	Central swath only, scanned at $0^{\circ}$ - $30^{\circ}$ gimbal angle	Full resolution short (FRS) Spatial pixels unbinned for target - 18 m/pixel	
		Along-track undersampled (ATU) Spatial pixels unbinned, smeared – 18x36 m/pixel	2012_275 thru present
		Tracking as shown but only center of target measured	Emission phase function (EPF) Spatial pixels 10x binned (~200 m/pixel @300 km)
Atmospheric (hyperspectral)	Nadir-pointed	Tracking Optical Depth (TOD) Spatial pixels 10x binned (~200 m/pixel @300 km)	Lat./lon. grids every ~9° of Ls 2006_270 thru 2012_146 (1-sided after 2010_280)
	Limb scans w/ special S/C pointing	Limb scan measurements (LMB) Spatial pixels 10x binned; ~200 m vertical sampling	Between other scheduled observations 2007_217 thru 2017_112
		VNIR +IR Multispectral survey (MSP) 73/74 or 94/95 selected channels, spatial pixels 10x binned (~200 m/pixel @300 km)	2 orbits every 2 months 2009_192 thru 2017_119
Mapping (selected wavelengths)	Nadir-pointed	VNIR+IR Multispectral windows (MSW) 73/74 or 94/95 selected channels, spatial pixels 5x binned (~100 m/pixel @300 km)	~85% of Mars 2006_270 thru 2018_046
		VNIR+IR Hyperspectral survey (HSP) 262 channels, spatial pixels 10x binned (~200 m/pixel @300 km)	Selected targets 2006_270 thru 2008_072
		VNIR-only Hyperspectral map (HSV) 107 channels, spatial pixels 10x binned (~200 m/pixel @300 km)	39% of Mars, focused on selected areas 2010_001 thru 2018_046
		VNIR-only Hyperspectral map (MSV) 92 channels, spatial pixels 5x binned (~100 m/pixel @300 km)	2009_174 thru present
			2012_013 thru present
Radiometric Calibration	-	Observations of onboard integrating sphere	Daily
Bias Calibration	-	Dark observations at multiple exposure times	Daily
Flat-Field Calibration	Nadir-pointed	Observations of bland regions of Mars (FFC) Spatial pixels unbinned, 18x800 m/pixel	2006_270 thru present

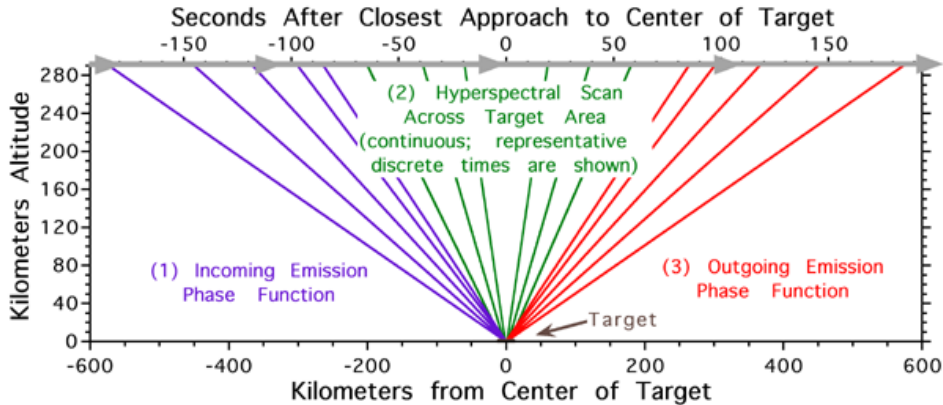


**Figure 2-5. Elements to a CRISM targeted observation.**

#### 2.1.4 Details of observing modes

Commanding of CRISM uses onboard macros, sequences of commands that configure the instrument for a particular operation, acquire data, and then return the instrument to a reference configuration. Up to 255 macros are stored onboard, and the data acquired by part or all of one macro is the fundamental data unit that populates a single EDR. Several macro updates occurred during orbital operations, to reconfigure operations for aging of hardware.

CRISM science observations have used 17 basic sequences of macros that translate into different sequences of EDRs (Table 2-6). All of the sequences use an onboard MRO target list for autonomous pointing and time of observations by the spacecraft guidance and controls system. A target ID<sup>2</sup> is used to uniquely identify a target on this list.

##### 2.1.4.1 Gimbaled Observations: Targeted, EPF, and limb scan measurements

Five of the macro sequences were intended for execution while the gimbal is tracking a target, and superimposing slow scans for a central swath and EPF measurements, through May 2012 while the gimbal retained most of its range of motion: Full resolution targeted observation, half resolution (long or short) targeted observation, atmospheric survey EPF, and along-track oversampled observation. All followed the same basic outline. The gimbal is first set to +60° to begin the scan (+30° beginning in August 2010), which then starts at the commanded time. During approach to the target, the scan profile is designed to slowly sweep the optical line-of-sight (LOS) back and forth across the target. Thus, instead of holding the target still within the FOV, short ±0.3° scans are superimposed (part 1 in Figure 2-5, only prior to August 2010). These short scans are called EPF scans. During target over-flight (+35° to -35° gimbal angle through August 2010; +30° through -35° through May 2012; part 2 in Figure 2-5), the gimbal takes a much longer sweep across the target. It is this long central scan that differentiates the classes of observations. The incoming EPF sequence is repeated outgoing, except in reverse order (part 3 in Figure 2-5). Four

<sup>2</sup> MRO autonomously determines spacecraft attitude and time to execute a CRISM observation. The inputs include latitude, longitude, and elevation of the target and the command macro sequence and gimbal profile to signal to CRISM to execute. Each observation is given a unique tag or "target ID" to identify it. On MRO this nomenclature is diagnostic of a particular mode of targeting so it is preserved in this SIS. However in PDS data product labels it is replaced by the term "observation ID" and is equivalent to it.

"dark" measurements of instrument background are taken, marking the start and end of EPF scans and bracketing the central scan.

After restriction of gimbal motion to  $0^\circ$  through  $+30^\circ$ , two new targeted observation types were defined (full resolution short and along-track undersampled), and along-track oversampled observations were truncated to a shortened central scan with bracketing dark measurements.

A full resolution targeted measurement (FRT) utilizes CRISM's full resolution capabilities, at the expense of a relatively large data volume. The gimbal is first moved to the starting position of the central scan, which depends on the scan's length, scans at a rate of 1 pixel (approximated as 60  $\mu\text{rad}$ ) per integration time, and crosses the target at mid-scan. The number of integrations is selected to mostly occupy the range of gimbal angles between  $\pm 35^\circ$  (through August 2010) or  $+30^\circ$  through  $-35^\circ$  (August 2010 through May 2012). Depending on the altitude above a particular target, one of several choices of macros is used to mostly occupy but not overfill this gimbal range, and a corresponding gimbal setup macro is used. The data are taken without spatial pixel binning, and accompanying dark data are correspondingly taken without pixel binning. However to conserve data volume, the EPF scans where present are taken with 10x pixel binning; the gimbal scan rate for the EPFs yields approximately square pixels projected onto the surface.

A half resolution long targeted measurement (HRL) covers a larger area, but at half the spatial resolution. It is intended for targets for which areal coverage is more important than the highest possible resolution. The LOS is scanned at a rate of 2 pixels (120  $\mu\text{rad}$ ) per integration time, and sufficient integrations are executed to mostly occupy the range of gimbal angles between  $\pm 35^\circ$ . Depending on the altitude above a particular target, one of several choices of macros is used to mostly occupy but not overfill this gimbal range, and the corresponding gimbal setup macro is used. The duration of the scan is the same as for a full resolution targeted measurement taken from the same altitude. The data are taken with 2x spatial pixel binning; the higher scan rate yields approximately square pixel footprints projected onto the planet surface. The area covered by the central scan is approximately twice that as for a full resolution targeted measurement. The dark data are correspondingly taken with 2x pixel binning. However to conserve data volume, the EPF scans (one-sided from August 2010 through May 2012, absent thereafter) are taken with 10x pixel binning; the gimbal scan rate yields approximately square pixels projected onto the surface.

A half resolution short targeted measurement (HRS) is a lower data volume alternative to the two types of targeted observations just described, intended to provide flexibility in covering more targets. The LOS is scanned at a rate of 2 pixels (120  $\mu\text{rad}$ ) per integration time, and sufficient integrations are executed to occupy approximately half the range of gimbal angles between  $\pm 35^\circ$ . Depending on the altitude above a particular target, one of several choices of macros is used, and the corresponding gimbal setup macro is used. The duration of data collection over the central scan is half that of a full resolution targeted measurement taken from the same altitude. The data are taken with 2x spatial pixel binning; the higher scan rate yields approximately square pixel footprints projected onto the planet surface. The area covered by the central scan is approximately the same as that as for a full resolution targeted measurement. The dark data are correspondingly taken with 2x pixel binning. However to conserve data volume, the EPF scans are taken with 10x pixel binning; the gimbal scan rate yield approximately square pixels projected onto the surface.

An along-track oversampled measurement (ATO) is analogous to a full resolution targeted measurement, except that the gimbal is scanned over the central swath at approximately a three-times slower rate, yielding a high degree of pixel overlap in the along-track direction. On ground,

the spatially oversampled measurement is rendered at a higher spatial resolution of  $\leq 12$  m/pixel. At the time this observation type was initiated, the gimbal range had already been restricted to  $+30^\circ$  to  $-60^\circ$ , so only the outgoing EPF measurements were made. The data are taken without spatial pixel binning, and accompanying dark data are correspondingly taken without pixel binning. However to conserve data volume, the EPF scans where present are taken with 10x pixel binning.

In an EPF measurement, the central scan is replaced with 1 or 3 EPF scans. The EPFs and dark data are all taken with 10x pixel binning. An EPF measurement is intended to characterize the atmosphere or the average surface properties of a kilometers-sized area, as a part of tracking seasonal changes. The gimbal angle range used was  $+60^\circ$  through  $-60^\circ$  through August 2010, and  $+30^\circ$  through  $-60^\circ$  from August 2010 through May 2012.

A full resolution short targeted measurement (FRS) is the counterpart to a full-resolution targeted measurement once the scan range of the gimbal was reduced to  $0^\circ$  to  $+30^\circ$ . An abbreviated central scan is bracketed by dark measurements. The gimbal is first moved to the starting position at  $+30^\circ$ , scans at a rate of 1 pixel (approximated as 60  $\mu\text{rad}$ ) per integration time, and finishes the central scan when the gimbal reaches nadir. The data are taken without spatial pixel binning, and accompanying dark data are correspondingly taken without pixel binning.

An along-track undersampled targeted measurement (ATU) is the counterpart to a half resolution long targeted measurement once the scan range of the gimbal was reduced to  $0^\circ$  to  $+30^\circ$ . An abbreviated central scan is bracketed by dark measurements. The gimbal is first moved to the starting position at  $+30^\circ$ , scans at a rate of 2 pixels (approximated as 120  $\mu\text{rad}$ ) per integration time, and finishes the central scan when the gimbal reaches nadir. The data are taken without spatial pixel binning, and accompanying dark data are correspondingly taken without pixel binning. Spatially, the pixels have a rectangular footprint twice as long in the along-track direction, restoring the length of the central scan to almost that of the original full resolution targeted observation.

In a limb scan measurement (LMB), a spacecraft pitch puts the limb just inside the gimbal range. Images are binned spatially as with EPF measurements, but the FOV is scanned across the limb at a rate of 1 pixel per integration time to maximize vertical sampling. Dark measurements are located between each measurement of the limb.

For all gimbaled observations except limb scan measurements, during the period from 2008 through 2017 when cryocooler operation was concentrated into 1 of every 4 planning periods, VNIR+IR data were taken while the cooler was operational, and VNIR-only data were taken when the cooler was not operating. Targets were sorted accordingly by the mineral phase of interest at the target. Mineral targets with absorptions at 0.9–1  $\mu\text{m}$  (low-Ca pyroxene, olivine, and ferric minerals) were targeted with VNIR-only observations. Mineral targets expected to have hydroxysilicates, carbonates, and non-ferric sulfates were targeted with VNIR+IR measurements.

Acquisition of IR data ceased on 2018 DOY 046 after apparent failure of the last functional cryocooler in December 2017 and unsuccessful attempts to use the coolers over the next weeks.

#### **2.1.4.2 Nadir observations: Multispectral and hyperspectral survey, multispectral windows, hyperspectral mapping, and TODs**

The VNIR+IR multispectral survey was CRISM's original mapping mode, intended to map large areas at Mars Odyssey/THEMIS-IR scale of resolution, for two purposes: (a) to find sites for

targeted measurements, or (b) to characterize composition over large, contiguous areas. This type of observation does not use a scan profile, but is nadir-pointed and measures selected wavelengths at elevated frame rates. The basic configuration is a repeating sequence of alternating Mars-viewing and background measurement macros. The Mars-viewing periods are constrained to be in blocks of 3 minutes so that adequate interpolation of background is possible. CRISM spent most of its observing time in this mode or its derivatives while cryocooling of the IR detector remained an option.

There are two versions of multispectral survey, one in which data are retained in 12-bit form (MSP), and one in which the data are converted from 12 to 8 bits using a variety of LUTs that can be specified by detector row to provide a least-information-loss choice for any given wavelength (MSS). In Mars orbit only the 12-bit version has been used.

Multispectral survey data and accompanying background calibrations are taken in 10x pixel binning mode, with 73/74 or 94/95 channels selected (before or after 6 Dec 2006). Dark and Mars data are all taken at 15 Hz, yielding 200-m effective pixels.

The hyperspectral survey (HSP) is an augmentation of the multispectral survey, with the increased density of wavelength sampling providing capability to separate subtly different spectral signatures and to provide improved capability to detect and map carbonate absorptions. It is intended to map regions rich in mineral diversity where contiguous coverage by targeted observations is impractical over the lifetime of MRO. As with multispectral survey, the basic configuration is a repeating sequence of alternating Mars-viewing and background measurement macros. The data are always taken in 12-bit format. Scene data and accompanying background calibrations are taken in 10x pixel binning mode at 15 Hz frame rate, yielding 200-m effective pixels.

Multispectral windows resemble the above multispectral survey, except that they are taken at 30 Hz with 5x pixel binning, yielding 100-m effective pixels projected on Mars. In practice they were used mainly as "ride-along" observations: if a High-Resolution Imaging Science Experiment (HiRISE) or Context Imager (CTX) measurement was not coordinated with a CRISM targeted measurement, then a 15-second duration multispectral window measurement was commonly executed, with the window centered on the center of the HiRISE or CTX target. This assured that observations by either of those instruments are accompanied by at least a minimal CRISM observation. The data were always taken in 12-bit format. Multispectral windows were discontinued in 2008; subsequently strips of multispectral or hyperspectral survey data have been used for the same purpose.

Tracking optical depth measurements (TOD) resemble the multispectral survey, except that they are taken with all wavelengths at 3.75 Hz in brief bursts every approximately 48 seconds, yielding 10 x 10 km footprints every 2° of latitude. These data are always taken in 12-bit format. TODs are designed to fill time between other observations to maintain a high spatial density of sampling of atmospheric properties.

VNIR-only hyperspectral mapping has been performed while coolers have been off beginning in 2009. There are two variants. HSV observations are analogous to the hyperspectral survey except with all 107 VNIR wavelengths only. Mars data and accompanying background calibrations are taken in 10x pixel binning mode at 15 Hz, yielding 200-m effective pixels. MSV observations are analogous to multispectral windows except with the 92 VNIR wavelengths having useful signals. Mars data and accompanying background calibrations are taken in 5x pixel binning mode at 30 Hz, yielding 100-m effective pixels.

#### ***2.1.4.3 Calibrations (CAL and ICL observations)***

Radiometric calibration is performed at least daily. A radiometric calibration consists of a set of sphere measurements (with the sphere operated closed-loop) with bracketing measurements of the ambient background with the shutter viewing the darkened sphere. These data are used to recover radiometric responsivity. Although data can be taken using the bulbs controlled by each of the VNIR and IR focal plane electronics, the flight calibration and ground calibration pipeline use the IR-controlled bulb because of its better along-slit uniformity.

Bias calibration is performed at least daily. A bias calibration consists of a set of shutter-closed measurements at each frame rate, at 4-5 integration times per frame rate. These data are used to recover detector bias, i.e., the offset image with zero scene radiance or thermal background.

Flat-field calibration is performed at monthly or comparable intervals. A flat-field calibration consists of a set of a bland region of Mars with bracketing background measurements. These data are used to recover non-uniformity of the VNIR detector. (The integrating sphere provides sufficient signal for this to be measured in the IR, but in the VNIR, at wavelengths <600 nm there is insufficient signal at a single detector element to determine non-uniformity at the desired accuracy of 0.001.)

**Table 2-6. Translation of different observation classes into EDRs  
(med. gray through August 2010, lt. gray through May 2012).**

Full resolution targeted observation (FRT; 3.75 Hz)	Half resolution (long or short) targeted observation (HRL, HRS; 3.75 Hz)	Atmospheric survey EPF (3.75 Hz)
full spatial resolution background measurement with shutter closed	half spatial resolution background measurement with shutter closed	reduced spatial resolution (10x-pixel-binned) background measurement with shutter closed
reduced spatial resolution (10x-pixel-binned) measurement of Mars for EPF (5 times)	reduced spatial resolution (10x-pixel-binned) measurement of Mars for EPF (5 times)	reduced spatial resolution (10x-pixel-binned) measurement of Mars for EPF (5 times)
full spatial resolution background measurement with shutter closed	half spatial resolution background measurement with shutter closed	reduced spatial resolution (10x-pixel-binned) background measurement with shutter closed
full spatial resolution measurement of Mars	half spatial resolution measurement of Mars	reduced spatial resolution (10x-pixel-binned) measurement of Mars for EPF
full spatial resolution background measurement with shutter closed	half spatial resolution background measurement with shutter closed	reduced spatial resolution (10x-pixel-binned) background measurement with shutter closed
reduced spatial resolution (10x-pixel-binned) measurement of Mars for EPF (5 times)	reduced spatial resolution (10x-pixel-binned) measurement of Mars for EPF (5 times)	reduced spatial resolution (10x-pixel-binned) measurement of Mars for EPF (5 times)
full spatial resolution background measurement with shutter closed	half spatial resolution background measurement with shutter closed	reduced spatial resolution (10x-pixel-binned) background measurement with shutter closed

Along-track oversampled targeted observation (ATO; 3.75 Hz)	Full resolution short targeted observation (FRS; 3.75 Hz)	Along-track undersampled targed observation (ATU'3.75 Hz)
full spatial resolution background measurement with shutter closed	full spatial resolution background measurement with shutter closed	full spatial resolution background measurement with shutter closed
full spatial resolution measurement of Mars	full spatial resolution measurement of Mars	full spatial resolution measurement of Mars (pixels smeared 2x in along-track direction)
full spatial resolution background measurement with shutter closed	full spatial resolution background measurement with shutter closed	full spatial resolution background measurement with shutter closed
reduced spatial resolution (10x-pixel-binned) measurement of Mars for EPF (5 times)		
full spatial resolution background measurement with shutter closed		

Tracking optical depth observation (TOD; 3.75 Hz)	Limb scan observation (LMB; 3.75)
reduced spatial resolution (10x-pixel-binned) background measurement with shutter closed	reduced spatial resolution (10x-pixel-binned) background measurement with shutter closed
reduced spatial resolution (10x-pixel-binned) measurement of Mars (4 times)	reduced spatial resolution (10x-pixel-binned) measurement of Mars
(repeat last 2 sequences n times)	(repeat last 2 sequences n times)
reduced spatial resolution (10x-pixel-binned) background measurement with shutter closed	reduced spatial resolution (10x-pixel-binned) background measurement with shutter closed

<b>Multispectral or hyperspectral survey (MSP, HSP; 15 Hz)</b>	<b>Multispectral window (MSW; 30 Hz)</b>
reduced spatial resolution (10x-pixel-binned) VNIR+IR background measurement with shutter closed	reduced spatial resolution (5x-pixel-binned) VNIR+IR background measurement, shutter closed
reduced spatial resolution (10x-pixel-binned) VNIR+IR measurement of Mars	reduced spatial resolution (5x-pixel-binned) VNIR+IR measurement of Mars
(repeat last 2 sequences $n$ times)	(repeat last 2 sequences $n$ times)
reduced spatial resolution (10x-pixel-binned) VNIR+IR background measurement with shutter closed	reduced spatial resolution (5x-pixel-binned) VNIR+IR background measurement, shutter closed

<b>VNIR-only hyperspectral mapping (HSV; 15 Hz)</b>	<b>VNIR-only hyperspectral mapping (MSV; 30 Hz)</b>
reduced spatial resolution (10x-pixel-binned) background measurement with shutter closed	reduced spatial resolution (5x-pixel-binned) background measurement, shutter closed
reduced spatial resolution (10x-pixel-binned) measurement of Mars	reduced spatial resolution (5x-pixel-binned) measurement of Mars
(repeat last 2 sequences $n$ times)	(repeat last 2 sequences $n$ times)
reduced spatial resolution (10x-pixel-binned) background measurement with shutter closed	reduced spatial resolution (5x-pixel-binned) background measurement, shutter closed

<b>Radiometric Calibration (observing sphere)</b>		<b>Flat-field Calibration</b>	
full spatial resolution background measurement of the internal integrating sphere before it is powered on (VNIR 1 Hz, IR 1 Hz)	reduced spatial resolution (10x-binned) background measurement of the internal integrating sphere before it is powered on (VNIR 1 Hz, IR 15 Hz)	full spatial resolution background measurement with shutter closed, 1 Hz	reduced spatial resolution (10x-binned) background measurement with shutter closed, 15 Hz
full spatial resolution measurement of the internal integrating sphere illuminated under closed-loop control using primary lamp (VNIR 1 Hz, IR 1 Hz)	reduced spatial resolution (10x-binned) measurement of the internal integrating sphere illuminated under closed-loop control using primary lamp (VNIR 1 Hz, IR 15 Hz)	full spatial resolution measurement of bland scene on Mars, 1 Hz	reduced spatial resolution (10x-binned) measurement of bland scene on Mars, 15 Hz
full spatial resolution background measurement of the internal integrating sphere after it is powered on (VNIR 1 Hz, IR 1 Hz)	reduced spatial resolution (10x-binned) background measurement of the internal integrating sphere after it is powered on (VNIR 1 Hz, IR 15 Hz)	full spatial resolution background measurement with shutter closed, 1 Hz	reduced spatial resolution (10x-binned) background measurement with shutter closed, 15 Hz
full spatial resolution background measurement of the internal integrating sphere before it is powered on (VNIR 1 Hz, IR 3.75 Hz)	reduced spatial resolution (5x-binned) background measurement of the internal integrating sphere before it is powered on (VNIR 1 Hz, IR 30 Hz)	full spatial resolution background measurement with shutter closed, 3.75 Hz	reduced spatial resolution (5x-binned) background measurement with shutter closed, 30 Hz
full spatial resolution measurement of the internal integrating sphere illuminated under closed-loop control using primary lamp (VNIR 1 Hz, IR 3.75 Hz)	reduced spatial resolution (5x-binned) measurement of the internal integrating sphere illuminated under closed-loop control using primary lamp (VNIR 1 Hz, IR 30 Hz)	full spatial resolution measurement of bland scene on Mars, 3.75 Hz	reduced spatial resolution (5x-binned) measurement of bland scene on Mars, 30 Hz
full spatial resolution background measurement of the internal integrating sphere after it is powered on (VNIR 1 Hz, IR 3.75 Hz)	reduced spatial resolution (5x-binned) background measurement of the internal integrating sphere after it is powered on (VNIR 1 Hz, IR 30 Hz)	full spatial resolution background measurement with shutter closed, 3.75 Hz	reduced spatial resolution (5x-binned) background measurement with shutter closed, 30 Hz
<b>Bias Calibration (IR only)</b>			
full spatial resolution background measurement with shutter closed, series of integration times, 1 Hz			
full spatial resolution background measurement with shutter closed, series of integration times, 3.75 Hz			
reduced spatial resolution (10x-binned) background measurement with shutter closed, series of integration times, 15 Hz			
reduced spatial resolution (5x-binned) background measurement with shutter closed, series of integration times, 30 Hz			

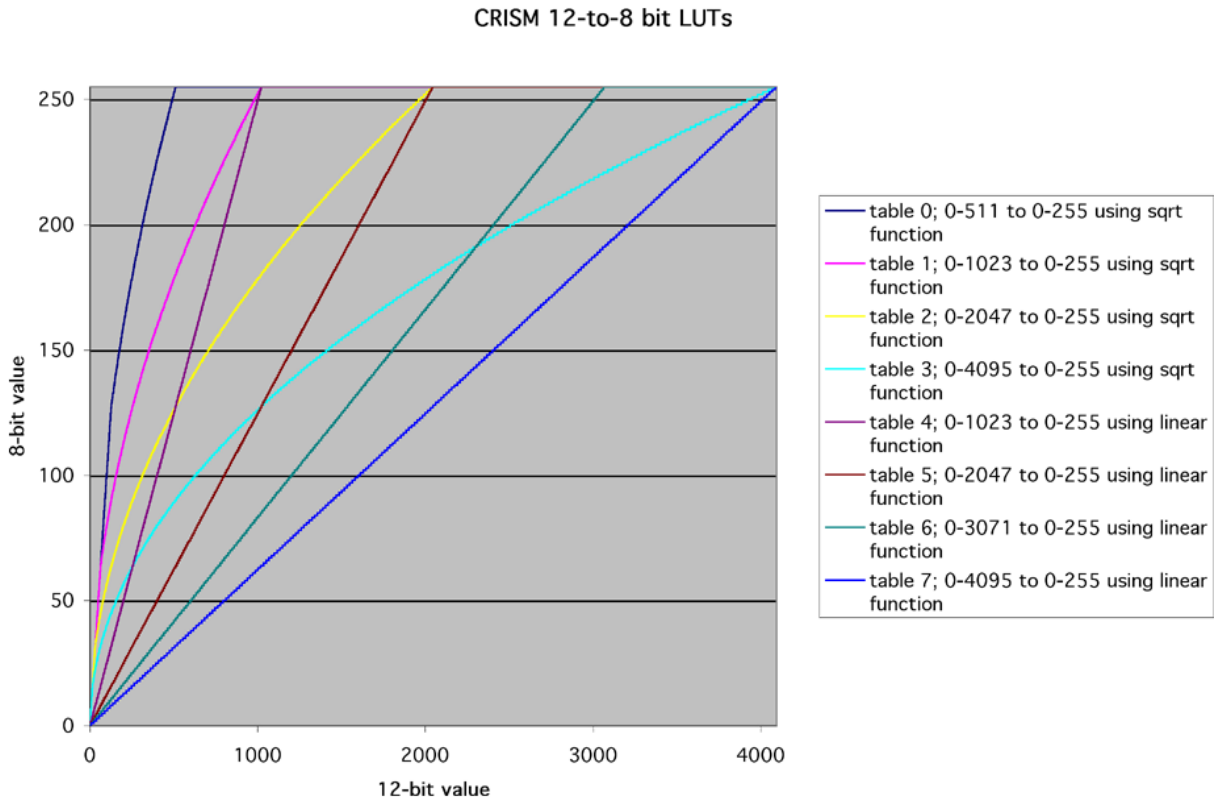


**Figure 2-7. Translation of 12-bit DNs into 8-bit DNs using LUTs.**

## 2.2 Data Product Overview

The CRISM data stream downlinked by the spacecraft unpacks into a succession of compressed image frames with binary headers containing housekeeping. In each image, one direction is spatial and one is spectral. There is one image for the VNIR focal plane and one image for the IR focal plane. The image from each focal plane has a header with 220 housekeeping items that contain full status of the instrument hardware, including data configuration, lamp and shutter status, gimbal position, a time stamp, and the target ID and macro within which the frame of data was taken. A number of the housekeeping items are particular to the image frame to which they are attached; others represent instrument hardware or software status and are identically represented in the header from each focal plane.

CRISM standard data products (Table 2-8) and the supplementary browse products represent rearranged values from the data stream, or corresponding derived products, with the basic unit of organization being that portion of the output from one macro which has a consistent instrument configuration (shutter position, frame rate, pixel binning, compression, exposure time, on/off status and setting of different lamps). The flow of data processing and the relationship of data products is shown in Figure 2-9. The data processing flow for the TER/MTRDR product suite is shown in Figure 2-9a.

### **2.2.1 EDRs**

In an EDR (Figure 3-1) the values are unmodified but are rearranged: the headers are stripped off and placed into a text list file, and the frames are merged into a multiple-band image. The multiple-band image consists of 12-bit data, stored as 16-bit values. There is one EDR per focal plane.

The list file is based on the 220 housekeeping items. 5 of the items are composite in that each bit of a 32-bit word encodes particular information on gimbal status or control. These separate items are not broken out, except for the gimbal status at the beginning, middle, and end of each exposure, from which gimbal position is broken out (3 additional items). The housekeeping is pre-pended with spaces for 10 additional frame-specific items useful in data validation, processing, and sorting, for a total of 233 items per frame:

- A data quality parameter produced during data validation, as discussed in section 2.5
- $L_s$ , degrees
- Solar distance, km
- Time of day at center of FOV, hhmm.ss with 1 Mars solar day = 2400.00
- Preliminary latitude, longitude at center and edges of FOV, degrees
- Preliminary  $i$  (incidence angle) at center of FOV, degrees
- Preliminary  $e$  (emission angle) at center of FOV, degrees
- Preliminary  $g$  (phase angle) at center of FOV, degrees
- Predicted dust opacity, unitless

For the most part, the output from one macro from one focal plane equals an EDR. However there are only 255 available macro slots, so to best utilize available macro space, three types of complex inflight calibrations are lumped into one macro from which several EDRs are generated:

- At times when the focal plane lamps were used, output from a focal plane lamp macro consists of sequential frames taken at different focal plane lamp settings. These different settings are NOT distinguished by a separate macro ID, but they are stored in separate EDRs.
- The output from a bias calibration macro consists of sequential frames taken at different exposure times with the shutter closed. These different exposures are NOT distinguished by a separate macro ID, but they are stored in separate EDRs.
- Onboard functional test macros cycle the instrument through different frame rate, binning, and compression configurations. These different configurations are NOT distinguished by a separate macro ID, but they are stored in separate EDRs.

In the data archive, EDRs are grouped into the outputs from one observation. For each observation, there is also a text report on data validation for the EDRs generated by each detector.

### **2.2.2 CDRs**

EDRs containing bias measurements or measurements of background, bias, or the internal integrating sphere are processed into level-4 CDRs. A level-4 CDR contains derived values needed to convert a scene-viewing EDR into units of radiance. These are in image format, with multiple

versions corresponding to different pixel binning states. Other level 4 CDRs are derived from ground measurements. A level-6 CDR contains tabulated information, for example for correcting for detector non-linearity, converting housekeeping to physical units, or converting EDRs from 12 to the original at-sensor 14 bits prior to calibration.

### **2.2.3 ADRs**

An Ancillary Data Record (ADR) is used to correct scene measurements calibrated to units of radiance for photometric, thermal emission, or atmospheric effects. An ADR is a hyperdimensional binary table or cube containing reference information used by algorithms that correct at-sensor radiance to the reflected solar component of I/F with thermal and atmospheric effects removed.

### **2.2.4 TRDRs**

A Targeted Reduced Data Record or TRDR (Figure 3-4) is comparable to a scene-viewing EDR except that image data has been converted to units of radiance using level-4 and level-6 CDRs, and the list file is converted into physical units using a level-6 CDR. A TRDR may also contain I/F, in a separate file.

### **2.2.5 DDRs**

A Derived Data Record (DDR, Figure 3-3) accompanies each observation pointed at Mars' surface, and includes information needed to map project data calibrated to units of radiance or I/F, or to process them further to Lambert albedo corrected for photometric, atmospheric, and thermal effects.

There are two types of information in DDRs: geometric information (latitude, longitude, incidence, emission and phase angles) and information on surface physical properties (slope magnitude and azimuth, thermal inertia). The physical information is derived by retrieving information from other data sets for the latitudes and longitudes corresponding to each detector element, and thus is in non-resampled sensor space.

### **2.2.6 LDRs**

A Limb Data Record (LDR) accompanies each observation scanned across Mars' limb, and includes information on the tangent height of each pixel above Mars' surface and photometric angles to analyze the measured radiances.

### **2.2.7 TERs and MTRDRs**

A Map-projected Targeted Reduced Data Record (MTRDR, Figure 3-16) is similar in concept to an MRDR map tile in that the observed spectral radiance data have been transformed to corrected I/F and map projected, though MTRDRs are derived from hyperspectral targeted observations (e.g. FRT, HRL, HRS class types) rather than push-broom mapping observations (e.g. MSP, HSP, MSW, HVS, or MSV class types). The MTRDR data processing flow is illustrated in Figure 2-9a and integrates a series of standard and empirical spectral corrections, spatial transforms, parameter calculations, and renderings in the generation of a high-level analysis and visualization data product suite. The MTRDR data processing pipeline is described in detail in Appendix P1. A Targeted Empirical Record (TER) is the immediate precursor to an MTRDR, with the TER consisting of fully corrected, full spectral range data in the IR detector sensor space, while the

MTRDR has been map projected according to MRO project standards and spectral channels with questionable radiometry (“bad bands”) have been removed from the image cube.

### 2.2.8 MRDRs

A map-projected multispectral RDR (MRDR, Figure 3-6) consists of several or more strips of multispectral survey data (or hyperspectral survey data downsampled to multispectral survey wavelengths) mosaicked into a map tile. Thus a map tile is constructed from a large number of TRDRs. The mosaic is uncontrolled (accepting existing pointing data with image mismatch at seams generally less than one ~180-m pixel). A global pattern of 1964 such tiles (Figure 2-10) has been developed, forming a major data product for multispectral survey observations. Each tile contains data in units of I/F extracted from a TRDR, plus Lambert albedo, summary products, and the DDR data used to generate them. So, for every latitude or longitude in an MRDR, there is both an I/F and all the information providing traceability to a companion I/F corrected for atmospheric and photometric effects (Lambert albedo). The MRDRs also include text files having information on the wavelength of the layers of the Lambert albedo and I/F multiband images.

The MRDR data processing flow for versions 1 and 3 is shown in Fig. 2-9. The flow for version 4 is illustrated in Figure 2-9b. Similar to the MTRDR flow it includes a series of standard and empirical corrections for spectral artifacts, spatial transforms to register VNIR to IR data, summary parameter calculations, and renderings in the generation of a high-level analysis and visualization data product suite. These steps occupy part of the segment of the flow In Fig. 2-9b entitled “Image Processing”. In addition, the image processing flow contains steps to normalize the spectral content of mapping strips to an atmosphere lacking  $H_2O$ ,  $CO_2$  and  $CO$  absorptions with a dust opacity  $\tau_{dust}$  of 0.2 and water-ice  $\tau_{ice}$  opacity of 0.0. This normalization is done in two parallel steps. For the mapping strips acquired while CRISM was still collecting EPFs, it is accomplished with the DISORT radiative transfer model applied to I/F spectra from component mapping strip TRDRs, using pixel coordinates, elevation, and solar longitude from TRDRs headers and DDRs, and latitude-longitude-time dependent opacities of dust from CRISM EPF measurements and water-ice from MARCI measurements from ADRs. In application, the CRISM MRDR DISORT modeling consists of a dense collection of forward RT models that span the operational (e.g. wavelength range, spectral sampling) and observational circumstances (e.g. observation geometry, atmospheric state) of the CRISM MPS/HSP data set that collectively form a look up table that relates the observed radiance (or reflectance) at the top of the atmosphere in a given mapping observation sample to the model surface reflectance, assuming a Lambert surface (McGuire et al. [2013]). For I/F spectra from mapping strips acquired subsequently to EPF measurements, atmospheric gas absorptions are normalized out using the volcano scan correction and a photometric correction is performed using a Lambert function; strip-dependent differences in dust and water-ice opacities remain.

In v4, strip-dependent differences are normalized out using the segment of the work flow entitled “Optimization”. Using DISORT-corrected, map-projected mapping strips acquired under clear atmospheric conditions during periods of good cryocooler performance as a reference, additional DISORT- and volcano scan-corrected mapping strips are spectrally normalized to the reference strips using gains and offsets derived in areas of overlap or proximity (O1). A second round of optimization is performed (O2) on summary parameters calculated from the corrected I/F.

Finally, tiles of the input and output I/F, summary parameters, and DDR information are assembled from map-projected strips, with the stacking order designed to put data acquired at lowest solar

incidence angles “on top”. To minimize inclusion of data acquired during atmospheric dust events, specific time periods are excluded from the whole MRDR workflow.

For additional details and definitions of terms, see Applicable Document [10].

The MRDR data processing pipeline is described in more detail in Appendix P3.

### **2.2.9 SPICE Files**

Four types of SPICE kernels are needed to calculate CRISM's pointing:

- Frames kernel (FK). This file defines the relationships of the of CRISM's field of view to the spacecraft, with the gimbal at "nadir".
- Instrument kernel (IK). This file describes the relationship of position of each detector element (at a row or wavelength and spatial or column position) to a zero position within the field of view.
- Gimbal C kernel. This file gives a time history of the angle of the gimbal within the gimbal plane, relative to its commanded nadir.
- Metakernel. This file gives, for any time span covered by a gimbal C kernel, the MRO and CRISM SPICE kernels used to create DDRs for observations occurring during that time period.

### **2.2.10 Browse Products**

Browse products are PNG files that show a summary of EDR, TRDR, TER, MTRDR, or MRDR data characteristics in the spatial plane of the data. For the EDRs, the PNG files show median values from a selected wavelength range. For TRDRS, TERs, MTRDRs, or MRDRs, the PNG files show scaled values of key layers derived from the spectral data. Accompanying labels describe the scaling to the 8-bit PNG files. The PNG files may be accompanied by an HTML file that describes the EDR browse products for one observation, or the MRDR browse products for one map tile.

TRDR, TER, and MTRDR browse products also include the scaled data values of the PNG file in a PDS3 image file (IMG) and have an associated ENVI header file (HDR), allowing the user to load the PDS image file into the ENVI software application. The PNG, HDR and IMG files are described by a detached PDS label file.

### **2.2.11 Extra Products**

The EDR EXTRAS directory contains ASCII text files having a time ordered history of observations and the characteristics of the sites observed, as well as the history of the hardware and software state of the CRISM instrument.

Several engineering-related files, which have a format and nomenclature like that of level 6 CDRs, include a history of alarms settings and software control parameters that are uploaded as binary tables ("data structures"), and events log, heater settings, and the model of data compressibility that is used in observation sequence planning. These cover only the early part of the MRO mission.

Other files document the characteristics of flight macros that were active during different periods of the MRO mission. There are three files for each macro load: the macro dictionary itself, a summary of each macro's function, and a description of the image data generated by each macro.

A table connects specific observations with regions of interest on Mars, science objectives, and specific observation conditions.

The TRDR EXTRAS directory contains visualizations of the observation geometry, content, and structure for hyperspectral targeted observation class types.

The TER EXTRAS directory contains a series of data processing visualizations for each CRISM hyperspectral targeted observation that has been processed through the MTRDR pipeline. The MTRDR EXTRAS directory contains one visualization of the primary MTRDR spectral data product for each processed hyperspectral targeted observation. Every TER/MTRDR data product set that is released to the PDS has been reviewed and approved by members of the CRISM SOC. The information generated by this release review process is included in a Microsoft Excel format spreadsheet that is stored in the top level TER/MTRDR EXTRAS directories. A detailed description of the TER and MTRDR EXTRAS products is provided in Appendix P2.

**Table 2-8. Definitions of CRISM data products.**

Data Product	PDS Data Set ID	Data Processing Level	Example PDS Labels
Experiment Data Record (EDR)	MRO-M-CRISM-2-EDR-V1.0	2	Figure 3-1; Appendix A
Calibration Data Record (CDR)	MRO-M-CRISM-4/6-CDR-V1.0	4, 6	Appendices F,G
Derived Data Record (DDR)	MRO-M-CRISM-6-DDR-V1.0	6	Figure 3-8; Appendix B
Limb Data Record (LDR)	MRO-M-CRISM-6-LDR-V1.0	6	Appendix H
Targeted RDR (TRDR)	MRO-M-CRISM-3-RDR-TARGETED-V1.0	3	Figure 3-11; Appendix C
Multispectral RDR (MRDR)	MRO-M-CRISM-5-RDR-MULTISPECTRAL-V1.0	5	Figure 3-14; Appendix D
Targeted Empirical Record (TER)	MRO-M-CRISM-4-RDR-TARGETED-V1.0	4	Appendix E
Map-Projected TRDR (MTRDR)	MRO-M-CRISM-5-RDR-MPTARGETED-V1.0	5	Figure 3-16; Appendix E

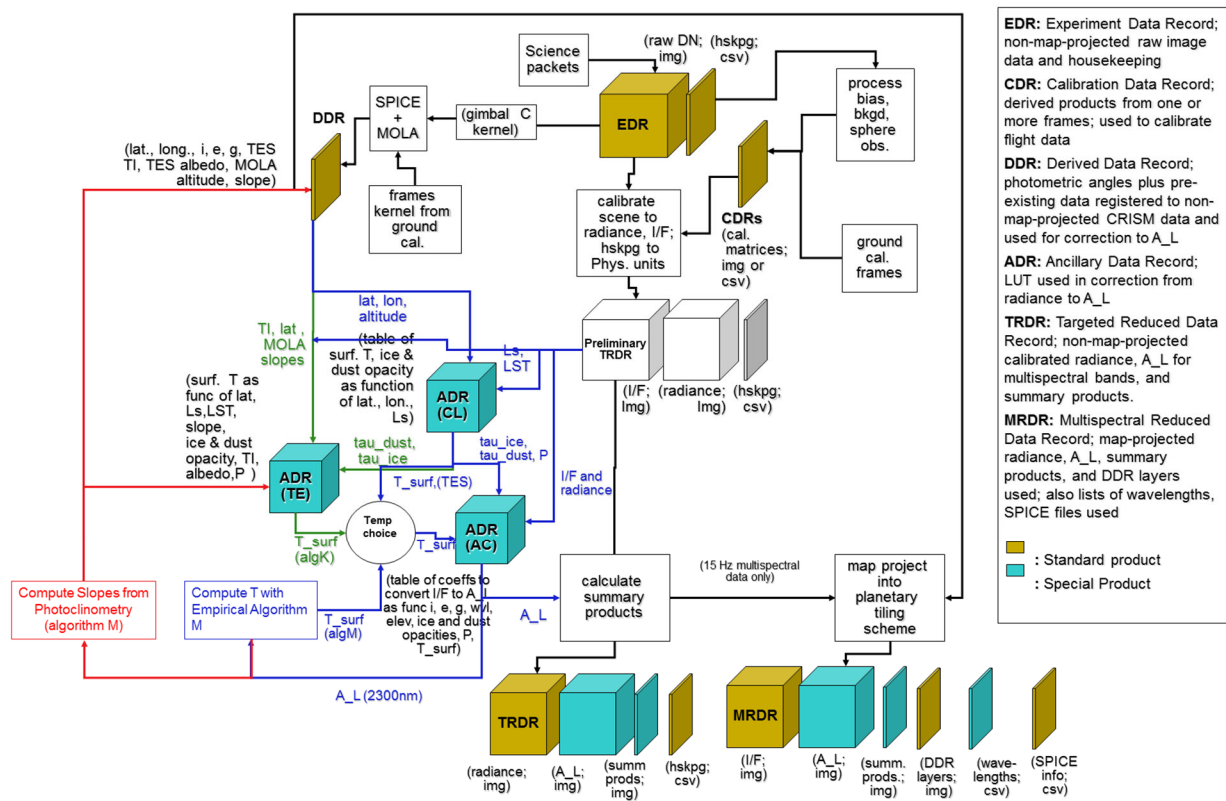


**Figure 2-9. Sequential processing of EDRs to yield RDRs of Mars data, showing the roles of CDRs and ADRs.**

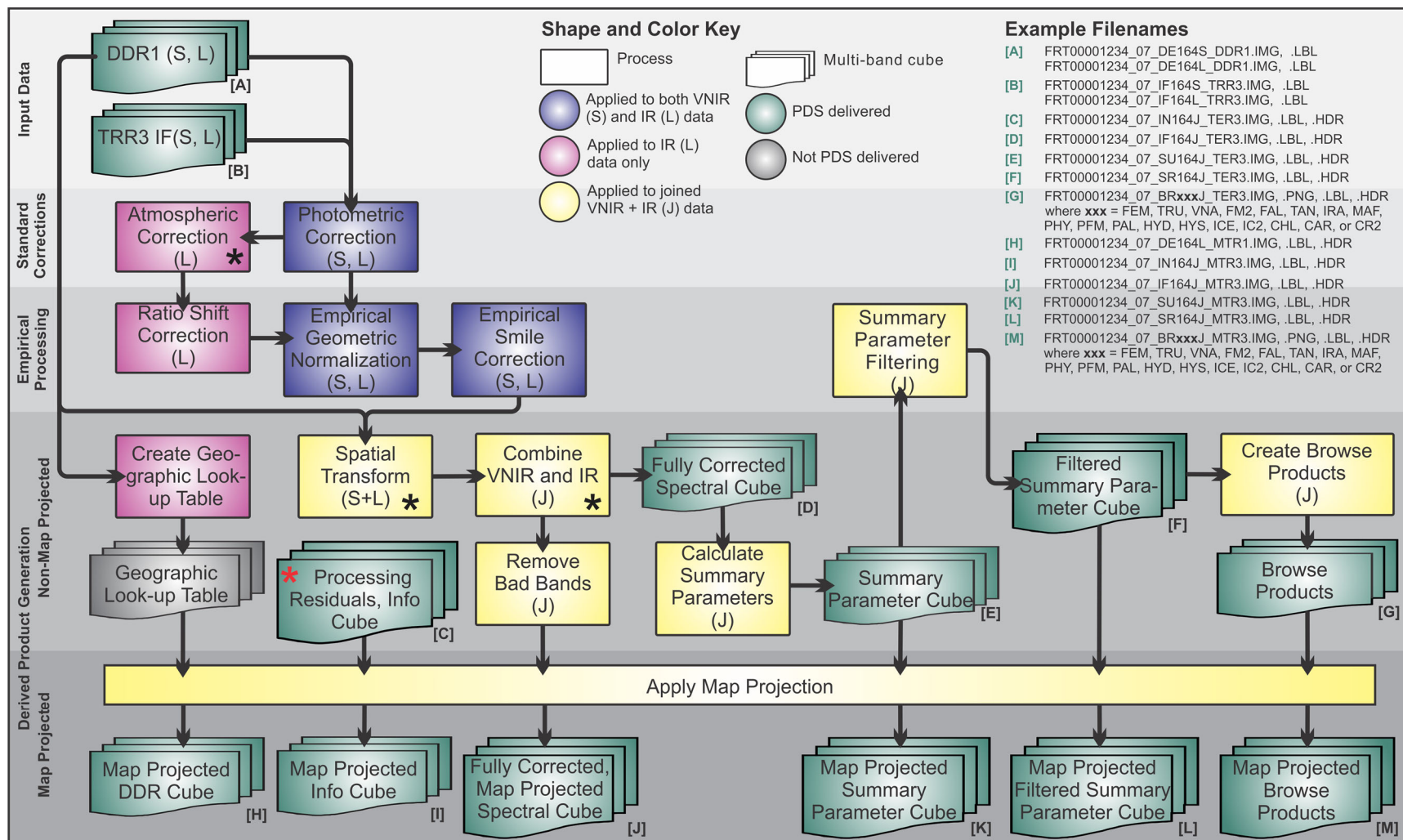


**Figure 2-9a. Sequential processing of DDRs and TRDRs to create TERs and MTRDRs.**

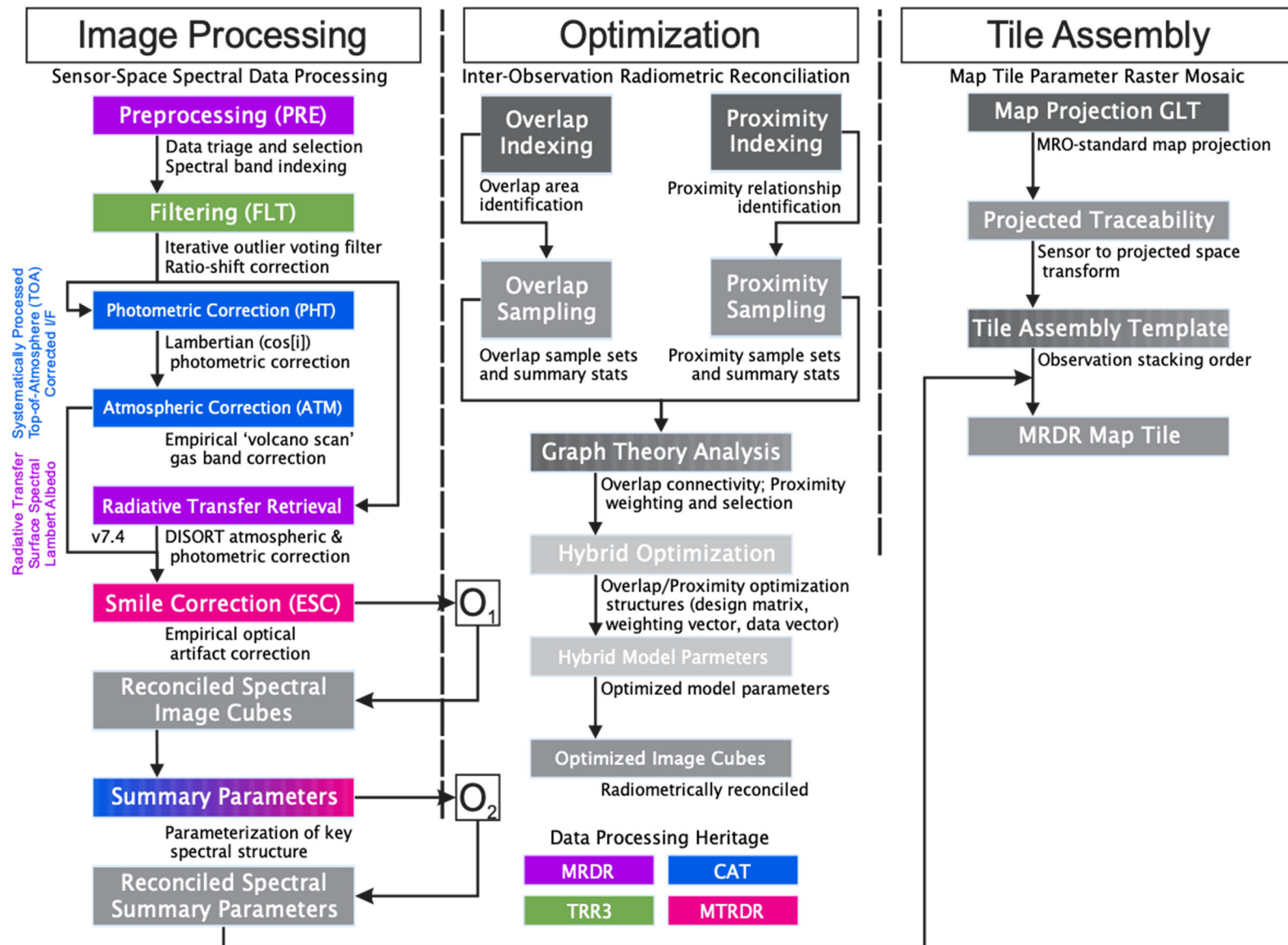
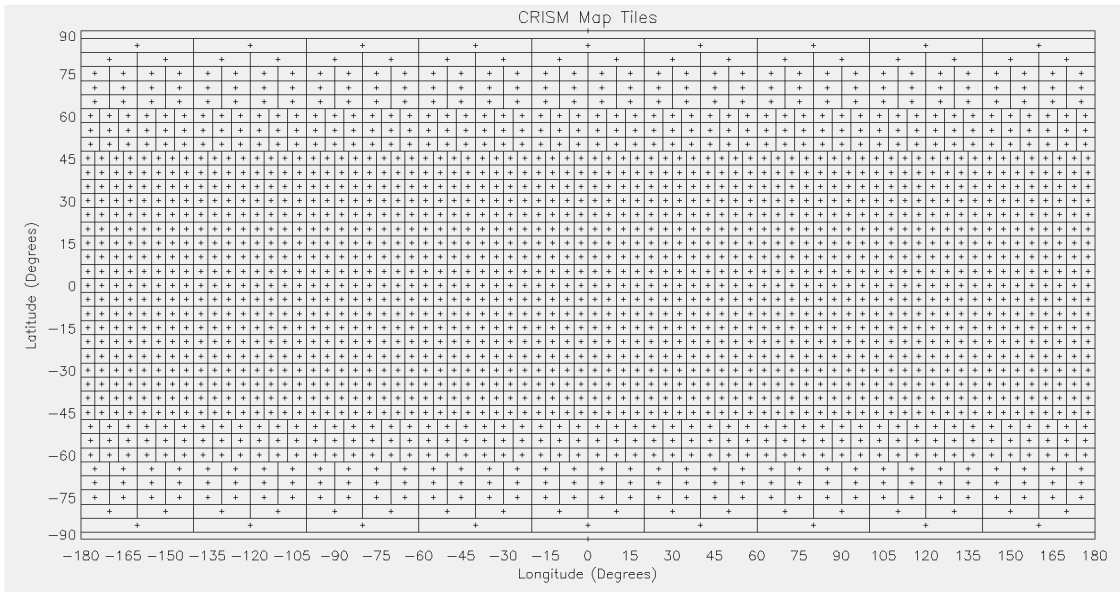


Figure 2-9b Sequential processing of DDRs and TRDRs to create v4 MRDRs.



**Figure 2-10. Tiling scheme for the map-projected multispectral survey, shown in global, EQUIRECTANGULAR map form.**

## 2.3 Data Processing

### 2.3.1 Data Processing Level

This SIS uses the Committee On Data Management And Computation (CODMAC) data level numbering system to describe the processing level of the CRISM data products. Table 2-11 shows the description of the CODMAC data processing levels and the correlation with the NASA processing levels. The CODMAC system is used here because it is the standard used by the PDS. CODMAC data processing levels for CRISM data products are listed in Table 2-8.

**Table 2-11. Processing Levels for Science Data Sets**

NASA	CODMAC	Description
Packet data	Raw - Level 1	Telemetry data stream as received at the ground station, with science and engineering data embedded.
Level-0	Edited - Level 2	Instrument science data (e.g., raw voltages, counts) at full resolution, time ordered, with duplicates and transmission errors removed.
Level 1-A	Calibrated - Level 3	Level 0 data that have been located in space and may have been transformed (e.g., calibrated, rearranged) in a reversible manner and packaged with needed ancillary and auxiliary data (e.g., radiances with the calibration equations applied).
Level 1-B	Resampled - Level 4	Irreversibly transformed (e.g., resampled, remapped, calibrated) values of the instrument measurements (e.g., radiances, magnetic field strength).

NASA	CODMAC	Description
Level 1-C	Derived - Level 5	Level 1A or 1B data that have been resampled and mapped onto uniform space-time grids. The data are calibrated (i.e., radiometrically corrected) and may have additional corrections applied (e.g., terrain correction).
Level 2	Derived - Level 5	Geophysical parameters, generally derived from Level 1 data, and located in space and time commensurate with instrument location, pointing, and sampling.
Level 3	Derived - Level 5	Geophysical parameters mapped onto uniform space-time grids.
	Ancillary – Level 6	Data needed to generate calibrated or resampled data sets.

### 2.3.2 Data Product Generation

#### 2.3.2.1 Data acquisition

The high-level observation plan in Table 2-4 has been translated into a preliminary timeline for a number of types of targets. This has involved internal planning of CRISM observations as described above, as well as coordination with MRO Project objectives and spacecraft resource constraints.

- First, based on the data expected from the sequence of macros executed for each type of observations, a predicted data volume for each type of observation is calculated. This is summarized in Table 2-12 for different configurations of VNIR ± IR data and structure of component images as gimbal angle range became constricted and cryocooler usage became segmented in time..
- Second, the MRO project has allocated CRISM and other instruments a fraction of spacecraft resources, downlink and spacecraft pointing.
- Third, based on coverage goals summarized in Table 2-4, observing opportunities are identified that both address the science objectives and fit within allocated downlink.

During the first 6 months of the mission, approximately half of the orbits were devoted to nadir pointing for multispectral survey observations, with off-nadir observations requiring spacecraft pointing mostly on remaining orbits. After that 6-month period, multispectral survey and other types of mapping data were collected between off-nadir observations requiring spacecraft pointing. The off-nadir opportunities are of 3 types: (a) Mars Exploration Program (MEP)-selected targets, the highest priority, for which all instruments observe the same target at high spatial resolution; (b) coordinated targets, observed in the same way, of which each instrument chooses a fraction; and (c) single-instrument targets for which other instruments may or may not operate at high spatial resolution. Remaining downlink allocation is filled with targets that are observed at high spatial resolution but without off-nadir pointing. In addition, some non-coordinated HiRISE or CTX observations are be accompanied by a short, reduced-resolution CRISM observation (a ridealong, typically and MSW or MSP strip).

**Table 2-12. Contents of each type of CRISM observation**

Class of observation	Frame rate, Hz	Activity	Pixel binning	#	Wave-lengths	Frames (typical)
Full resolution targeted (FRT) or along-track oversampled (ATO)	3.75	central scan	1	1	107 or 545	390
	3.75	EPF scans	10	0,5 or 10	107 or 545	15
	3.75	dark sets	1	3 or 4	107 or 545	12
Half resolution short or long targeted (HRS, HRL)	3.75	central scan	2	1	107 or 545	243, 320
	3.75	EPF scans	10	0,5 or 10	107 or 545	15
	3.75	dark sets	2	4	107 or 545	12
Full resolution short or along track undersampled targeted (FRS, ATU)	3.75	central scan	1	1	107 or 545	174
	3.75	dark sets	1	2	107 or 545	12
	3.75	EPF scans	10	8, 11 or 13	545	15
Limb scan (LMB)	3.75	dark sets	10	3 or 4	545	12
	3.75	Individual scans	10	variable	545	540
TOD	3.75	dark sets	10	same	545	12
	3.75	3-second segments	10	12	545	12
Multispectral survey (MSP)	15	dark sets	10	4	545	12
	15	3-minute segments	10	8	73/74 or 94/95	2700
Hyperspectral survey (HSP)	15	dark sets	10	9	73/74 or 94/95	12
	15	3-minute segments	10	8	262	2700
Multispectral window (MSW)	30	dark sets	10	9	262	12
	30	1 3-minute segment	5	1	73/74 or 94/95	5400
VNIR hyperspectral mapping, 200 m/pixel (HSV)	15	dark sets	10	8	107	2700
VNIR hyperspectral mapping, 100 m/pixel (MSV)	15	3-minute segments	10	9	107	12
Radiometric calibration	30	dark sets	5	8	92	5400
	30	dark sets	5	9	92	12
	1 (VNIR), 1 (IR)	sphere background	1	2	545	12
	1 (VNIR), 1 (IR)	sphere frames	1	1	545	32
	1 (VNIR), 3.75 (IR)	sphere background	1	2	545	12
	1 (VNIR), 3.75 (IR)	sphere frames	1	1	545	32
	1 (VNIR), 15 (IR)	sphere background	10	2	73	12
	1 (VNIR), 15 (IR)	sphere frames	10	1	73	32
Bias calibration (IR only)	1 (VNIR), 30 (IR)	sphere background	5	2	73	12
	1 (VNIR), 30 (IR)	sphere frames	5	1	73	32
	1	dark frames, several integration times	1	4	438	10
	3.75	dark frames, several integration times	1	5	438	10
Flat-field calibration (only 1 frame rate at a time)	15	dark frames, several integration times	10	4	55/56 or 155	10
	30	dark frames, several integration times	5	4	55/56	10
	1	dark sets	1	2	545	12
	1	3-minute segments	1	1	545	180
Flat-field calibration (only 1 frame rate at a time)	3.75	dark sets	1	2	545	12
	3.75	3-minute segments	1	1	545	675
	15	dark sets	10	2	73	12
	15	3-minute segments	10	1	73	2700
	30	dark sets	5	2	73	12
	30	3-minute segments	5	1	73	5400

### 2.3.2.2 Data processing overview

Data processing to standard products for delivery to the PDS (EDRs, CDRs, TRDRs, DDRs) occurs in the CRISM Science Operations Center (SOC). ADRs are created by the science team and delivered to the SOC for application to the data. Additional processing to special products (LDRs, MRDRs, TERs, MTRDRs) also occurs in the SOC.

The sequence of processing used to create deliverable data products is discussed in section 2.2 and shown graphically in Figures 2-9, 2-9a, and 2-9b. Appendix L provides detailed mathematical formations of CDRs, and of the derivation of radiance in TRDRs using the CDRs. Appendix P provides a detailed description of the TER/MTRDR data processing pipeline.

### **2.3.3 Data Flow and Delivery**

Downlinked CRISM data are forwarded with spacecraft housekeeping and pointing information from JPL to the CRISM Science Operations Center (SOC) at The Johns Hopkins University Applied Physics Laboratory (APL), where they are processed to EDRs in near-real time. DDRs and LDRs are generated at the SOC using SPacecraft, Instrument, Camera, and Events (SPICE) and other data sources. TRDRs are also generated at the SOC from EDR products, and for multispectral survey data, MRDRs are generated from TRDR mapping strips. After validation CRISM data products are transferred to the PDS Geosciences Node for archiving and distribution.

CRISM data archiving is overseen by Co-I Arvidson, manager of the PDS Geosciences Node. The approach outlined above is consistent with the MRO Data Archive Plan (R. Arvidson, author). Ground data including calibration files and the spectral library were delivered at various times through Mars orbit insertion. For flight data, delivery of EDRs, DDRs, LDRs, TRDRs, and CDRs occurs at 3-month intervals following 6 months of validation, on hard drives and deep-archive media to be determined by the PDS. Additionally, at selected delivery times MRDRs covering selected tiles of the global maps and TERs and MTRDRs derived from selected targeted observations are delivered.

When upgrades occur to data calibration, TRDRs, MRDRs and/or TERs and MTRDRs are redelivered with an increment to version numbers. The current v3 radiometric calibration was implemented in February, 2010.

### **2.3.4 Labeling and Identification**

#### **2.3.4.1 EDR, DDR, LDR, and TRDR**

EDRs, DDRs, LDRs, and TRDRs are CRISM products representing raw and calibrated data with geometric and timing information necessary for map projection and various post-processing correction. In summary:

- a) EDRs represent raw data and TRDRs represent calibrated data. Both are in units of sensor space. They contain the optical and spatial distortions present at the sensor.
- b) DDRs represent geometric information for observations pointed at Mars' surface, indexed to the wavelength bands of EDRs and TRDRs that are closest to 610 nm (VNIR) and 2300 nm (IR).
- c) LDRs represent geometric information for observations pointed at Mars' limb, indexed to the wavelength bands of EDRs and TRDRs that are closest to 610 nm (VNIR) and 2300 nm (IR).

The file naming convention for EDR, DDR, LDR, and TRDR products is as follows.

(ClassType)(ObsID)\_(Counter)\_(Activity)(SensorID)\_(Filetype)(version).(Ext)

where:

ClassType =

FRT (Full Resolution Targeted Observation; discontinued 2012)  
HRL (Half Resolution Long Targeted Observation; discontinued 2012)  
HRS (Half Resolution Short Targeted Observation; discontinued 2012)  
FRS (Full Resolution Short Targeted Observation; initiated 2012)  
ATO (Along-Track Oversampled Targeted Observation; initiated 2011)  
ATU (Along-Track Oversampled Targeted Observation; initiated 2012)  
EPF (Atmospheric Survey EPF; discontinued 2012)  
LMB (Limb Scan Observation; initiated 2009, discontinued 2017)  
TOD (Tracking Optical Depth Observation; initiated 2007, discontinued 2017)  
MSP (Multispectral Survey; discontinued 2018)  
HSP (Hyperspectral Survey; initiated 2010, discontinued 2018)  
HSV (Hyperspectral Survey - VNIR only, pixels 10x-binned; initiated 2010)  
MSV (Hyperspectral Survey - VNIR only, pixels 5x-binned; initiated 2012)  
MSW (Multispectral Window; discontinued 2008)  
FFC (Flat Field Calibration)  
CAL (Radiometric Calibration)  
ICL (Calibration source intercalibration)  
FUN (Functional test)  
UNK (no valid EDRs within observation that indicate class type)

ObsID = nnnnnnnn, Observation ID, unique for the whole CRISM mission, expressed as a hexadecimal number

Counter= nn, a monotonically increasing ordinal counter of EDRs from one Observation ID, expressed as a hexadecimal number

Activity = for an EDR, type of observation, e.g.

BI### – Bias measurements / Macro#  
DF### – Dark field measurements / Macro#  
LP### – Lamp measurements / Macro #  
SP### – Sphere measurements / Macro #  
SC### – Scene measurements / Macro #  
T1### – Focal plane electronics test pattern 1 / Macro #  
T2### – Focal plane electronics test pattern 2 / Macro #  
T3### – Focal plane electronics test pattern 3 / Macro #

T4### – Focal plane electronics test pattern 4 / Macro #  
T5### – Focal plane electronics test pattern 5 / Macro #  
T6### – Focal plane electronics test pattern 6 / Macro #  
T7### – Focal plane electronics test pattern 7 / Macro #  
UN### – Instrument configuration does not match macro library / Macro #

for a TRDR, type of product, e.g.

RA### – Radiance / Macro#  
IF### – I/F / Macro #

for a DDR or LDR, type of product, e.g.

DE### – Derived product / Macro#

SensorID = S or L for VNIR or IR

Filetype = EDR, DDR, LDR, or "TRR" for TRDR

version = 0, 1,...,9, a, ..., z

Ext = IMG or TAB

Each CRISM data product of these types has a product ID that is unique within its data set. The product ID scheme for CRISM EDR, DDR, and TRDR products is as follows (see file naming convention for allowable values for each field):

CCCN>NNNNNNN\_XX\_AAAAAS\_TTTV

Where:

CCC	=	Class Type
NNNNNNNN	=	Observation ID as a hexadecimal number
XX	=	Counter within this observation
AAAAAA	=	Activity Type
S	=	Sensor ID
TTT	=	Product Type (EDR, DDR, LDR, "TRR" for TRDR)
V	=	Product version number

#### **2.3.4.2 EDR Validation Reports**

The file naming convention for EDR validation report is as follows.

(ClassType)(ObsID)\_(SensorID)\_VALIDATION.TXT

where:

ClassType =

FRT (Full Resolution Targeted Observation; discontinued 2012)

HRL (Half Resolution Long Targeted Observation; discontinued 2012)  
HRS (Half Resolution Short Targeted Observation; discontinued 2012)  
FRS (Full Resolution Short Targeted Observation; initiated 2012)  
ATO (Along-Track Oversampled Targeted Observation; initiated 2011)  
ATU (Along-Track Oversampled Targeted Observation; initiated 2012)  
EPF (Atmospheric Survey EPF; discontinued 2012)  
LMB (Limb Scan Observation; initiated 2009, discontinued 2017)  
TOD (Tracking Optical Depth Observation; initiated 2007, discontinued 2017)  
MSP (Multispectral Survey; discontinued 2018)  
HSP (Hyperspectral Survey; initiated 2010, discontinued 2018)  
HSV (Hyperspectral Survey - VNIR only, pixels 10x-binned; initiated 2010)  
MSV (Hyperspectral Survey - VNIR only, pixels 5x-binned; initiated 2012)  
MSW (Multispectral Window; discontinued 2008)  
FFC (Flat Field Calibration)  
CAL (Radiometric Calibration)  
ICL (Calibration source intercalibration)  
FUN (Functional test)  
UNK (no valid EDRs within observation that indicate class type)

ObsID = nnnnnnnn, Observation ID, unique for the whole CRISM mission, expressed as a hexadecimal number

SensorID = S or L

Each validation report has a product ID that is unique within its data set. The product ID scheme for CRISM EDR validation reports is as follows (see file naming convention for allowable values for each field):

CCCNNNNNNN\_S\_VALIDATION

Where:

CCC	=	Class Type
NNNNNNNN	=	Observation ID as a hexadecimal number
S	=	Sensor ID

#### **2.3.4.3 EDR Browse Products**

The file naming convention for the HTML browse products for EDRs is as follows.

(ClassType)(ObsID)\_BROWSE\_EDR(version).(Ext) where:

ClassType =

FRT (Full Resolution Targeted Observation; discontinued 2012)  
HRL (Half Resolution Long Targeted Observation; discontinued 2012)  
HRS (Half Resolution Short Targeted Observation; discontinued 2012)  
FRS (Full Resolution Short Targeted Observation; initiated 2012)  
ATO (Along-Track Oversampled Targeted Observation; initiated 2011)  
ATU (Along-Track Oversampled Targeted Observation; initiated 2012)  
EPF (Atmospheric Survey EPF; discontinued 2012)  
LMB (Limb Scan Observation; initiated 2009, discontinued 2017)  
TOD (Tracking Optical Depth Observation; initiated 2007, discontinued 2017)  
MSP (Multispectral Survey; discontinued 2018)  
HSP (Hyperspectral Survey; initiated 2010, discontinued 2018)  
HSV (Hyperspectral Survey - VNIR only, pixels 10x-binned; initiated 2010)  
MSV (Hyperspectral Survey - VNIR only, pixels 5x-binned; initiated 2012)  
MSW (Multispectral Window; discontinued 2008)  
FFC (Flat Field Calibration)  
CAL (Radiometric Calibration)  
ICL (Calibration source intercalibration)  
FUN (Functional test)  
UNK (no valid EDRs within observation that indicate class type)

ObsID= nnnnnnnn, Observation ID, unique for the whole CRISM mission, expressed as a hexadecimal number

version = 0, 1,...,9, a, ..., z

Ext = HTML

Each EDR HTML browse product has a product ID that is unique within its data set. The product ID scheme for CRISM EDR HTML browse products is as follows:

CCNNNNNNNN\_BROWSE\_EDRV

Where:

CCC	=	Class Type
NNNNNNNN	=	Observation ID as a hexadecimal number
TTT	=	Product Type (EDR)
V	=	Product version number

The file naming convention for the PNG browse products for EDRs is as follows.

(ClassType)(ObsID)\_ (Counter) \_ (Activity)(SensorID)\_ RAW(version).(Ext)

where:

Counter = nn, a monotonically increasing ordinal counter of EDRs from one Observation ID

Activity = for an EDR, type of observation, e.g.

BInnn – Bias measurements / Macro#

DFnnn – Dark field measurements / Macro#

LPnnn – Lamp measurements / Macro #

SPnnn – Sphere measurements / Macro #

SCnnn – Scene measurements / Macro #

T1nnn – Focal plane electronics test pattern 1 / Macro #

T2nnn – Focal plane electronics test pattern 2 / Macro #

T3nnn – Focal plane electronics test pattern 3 / Macro #

T4nnn – Focal plane electronics test pattern 4 / Macro #

T5nnn – Focal plane electronics test pattern 5 / Macro #

T6nnn – Focal plane electronics test pattern 6 / Macro #

T7nnn – Focal plane electronics test pattern 7 / Macro #

UNnnn – Instrument configuration does not match macro library / Macro #

SensorID= S for VNIR, or L for IR

version= 0, 1,...,9, a, ..., z

Ext= PNG

Each EDR PNG browse product will have a product ID that is unique within its data set. The product ID scheme for CRISM EDR PNG browse products is as follows:

CCCN>NNNNNNN\_XX\_AAAAAS\_RAWV

Where:

CCC = Class Type

NNNNNNNN = Observation ID as a hexadecimal number

XX = Counter within this observation

AAAAA = Activity Type

S = Sensor ID

V = Product version number

#### 2.3.4.4 MRDRs

The file naming convention for MRDR products is as follows.

(Tile)\_(ProductType)(Subtype)\_ (CLat)(Hemisphere) (CLon)\_(Resolution)\_version.(Ext)  
where:

Tile = Tnnnn, tile number with tile 0000 at the south pole, increasing spiraling east northward

Product Type = "MRR" for MRDR

Subtype of product, e.g.

IF – I/F

AL – Lambert albedo

SU – Summary Products

DE – Derived Products for I/F

DL – Derived Products for Lambert albedo

WV – List of wavelengths and wavelength ranges of radiance and I/F images

CLat = nn, Planetocentric latitude of tile center

Hemisphere = #, N or S for north or south latitude

CLon = nnn, East longitude of tile center

Resolution = nnnn, in map-projected pixels per degree, e.g. 0256 pixels per degree modified in the final delivery to 0330 pixels per degree

version = 0, 1,..., 9, a,..., z

Ext = IMG or TAB

The product ID scheme for the CRISM MRDRs is as follows:

TNNNN\_TTTSS\_XXDYYY\_RRRR\_V

Where:

TNNNN = Tile number

TTT = Product Type ("MRR" for MRDR)

SS = Product subtype, i.e., IF, AL, SU, DE, DL, or WV

XX = Planetocentric latitude of tile center

D = N or S for north or south latitude

YYY = East longitude of tile center

RRRR = Map resolution in pixels per degree, e.g. 0256 or 327

V = Product version number

#### **2.3.4.5 MRDR Browse Products**

The browse product nomenclature follows that of MRDRs except that browse products type (following the browse product types for TRDRs) is substituted for the type of image product:

(Tile)\_(ProductType)(BrowseProductType)\_(CLat)(Hemisphere)(CLon)(Resolution)\_version.(Ext)

where:

Tile = Tnnnn, tile number with tile 0000 at the south pole, increasing spiraling northward

Product Type = MRR

BrowseProductType = TRU, VNA, FEM, FM2, FAL, IRA, MAF, HYD, PHY, PFM, PAL, HYS, ICE, IC2, CAR, CR2, CHL, or TAN. The full list of products is described in section 3.11.3.

CLat = nn, Planetocentric latitude of tile center

Hemisphere = #, N or S for north or south latitude

CLon = nnn, East longitude of tile center

Resolution = nnnn, in map-projected pixels per degree, e.g. 0256 pixels per degree modified in the final delivery to 0327 pixels per degree

version = 0, 1,..., 9, a,..., z

Ext =

IMG – 3 band byte scaled image cube

HDR – Associated ENVI header

PNG – 3 band byte scaled binary image cube with alpha transparency channel

LBL – Associated PDS label

The product ID scheme for the CRISM MRDRs is as follows:

TNNNN\_TTTBBB\_XXDYYY\_RRRR\_V

Where:

TNNNN	=	Tile number
TTT	=	Product Type ("MRR" for MRDR)
BBB	=	Browse Product Type, TRU, VNA, FEM, FM2, FAL, IRA, MAF, HYD, PHY, PFM, PAL, HYS, ICE, IC2, CAR, CR2, CHL, or TAN
XX	=	Planetocentric latitude of tile center
D	=	N or S for north or south latitude
YYY	=	East longitude of tile center
RRRR	=	Map resolution in pixels per degree, e.g. 0256 or 0327
V	=	Product version number

#### **2.3.4.6 TERs and MTRDRs**

The file naming convention for TERs and MTRDRs closely parallels that for TRDRs, with the caveat that only those class types of hyperspectral targeted observations that are accompanied by 1- or 2-side EPF scans are processed to TERs or MTRDRs:

(ClassType)(ObsID)\_(Counter)\_(Activity)(SensorID)\_(Filetype)(version).(Ext)

where:

ClassType =

FRT (Full Resolution Targeted Observation)

HRL (Half Resolution Long Targeted Observation)

HRS (Half Resolution Short Targeted Observation)

ObsID = nnnnnnnn, Observation ID, unique for the whole CRISM mission, expressed as a hexadecimal number

Counter = nn, the ordinal counter carried through from the source EDR, expressed as a hexadecimal number

Activity = for a TER/MTRDR, type of product, e.g.

IFnnn – Corrected I/F / Macro #

SUnnn – Spectral summary parameters / Macro #

SRnnn – Refined spectral summary parameters / Macro #

INnnn – Data processing information maps / Macro #

DEnnn – Derived data product / Macro # (MTRDR only)

WVnnn – Wavelength information for the I/F image / Macro #

SensorID = J (for joined S and L)

A prefix of “BR” in the Activity portion of the filename identifies the file as a TER/MTRDR Browse Product, in which case it follows the naming convention specified in section 2.3.4.7.

Filetype =

TER (Targeted Empirical Record)

MTR (Map-projected Targeted Record – short for MTRDR)

version = 0, 1,...,9, a, ..., z

Ext =

IMG – Image cube

HDR – Associated ENVI header

LBL – PDS label

The product ID scheme for the CRISM TERs and MTRDRs is as follows:

CCCN>NNNNNNN\_XX\_AAAA AJ\_TTTV

Where:

CCC	=	Class Type
NNNNNNNN	=	Observation ID as a hexadecimal number
XX	=	Counter within this observation
AAAAAA	=	Activity Type
J	=	Sensor ID
TTT	=	Product Type (TER, MTR)
V	=	Radiometric calibration version number

#### **2.3.4.7 TRDR, TER, and MTRDR Browse Products**

Three data files and a single PDS detached label file comprise a given TRDR, TER, or MTRDR browse product file set. The file naming convention is the same across all four files and is as follows.

(ClassType)(ObsID)\_ (Counter) \_BR(BrowseProductType)(SensorID)\_ (Filetype)(version).(Ext)

where:

ClassType =

- FRT (Full Resolution Targeted Observation)
- HRL (Half Resolution Long Targeted Observation)
- HRS (Half Resolution Short Targeted Observation)

ObsID = nnnnnnnn, Observation ID, unique for the whole CRISM mission, expressed as a hexadecimal number

Counter = nn, the ordinal counter carried through from the source EDR, expressed as a hexadecimal number

BrowseProductType = TRU, VNA, FEM, FM2, FAL, IRA, MAF, HYD, PHY, PFM, PAL, HYS, ICE, IC2, CAR, CR2, CHL, or TAN. The full list of products is described in section 3.11.3.

SensorID = S, L, J (for joined S and L)

Filetype =

- TRR (Targeted Reduced Data Record)
- TER (Targeted Empirical Record)
- MTR (Map-projected Targeted Record – short for MTRDR)

version = 0, 1,...,9, a, ..., z

Ext =

IMG – 3 band byte scaled image cube

HDR – Associated ENVI header

PNG – 3 band byte scaled binary image cube with alpha transparency channel

LBL – Associated PDS label

Each TRDR/TER/MTRDR browse product has a product ID that is unique within its data set. The product ID scheme for CRISM TRDR/TER/MTRDR browse products is as follows:

CCCN>NNNNNNN\_XX\_BRAAAJ\_TTTV

Where:

CCC = Class Type

NNNNNNNN = Observation ID as a hexadecimal number

XX = Counter within this observation

AAA = Three character browse product type

J = Sensor ID

TTT = Product Type (TRR, TER, MTR)

V = Radiometric calibration version number

#### 2.3.4.8 CDRs

There are three formats for CDRs:

- tabulated ground or flight ancillary data used during processing from an EDR to radiance (level-6 CDRs)
- tables of scene and accompanying calibration EDRs, to process EDRA to CDR4s or TRDRs (level-6 CDRs, with distinct nomenclature to distinguish them from data-containing files)
- derived, image-format ground or flight data used during processing from an EDR to radiance or I/F (level-4 CDRs)

The file naming convention for data-containing level-6 CDRs is as follows.

(ProductType)(Level)\_(Partition)\_(Time)\_(Product)\_(SensorID)\_version.(Ext)

where:

ProductType = CDR

Level = 6

Partition = n, partition of the spacecraft clock.

Time = nnnnnnnnnn, spacecraft start time of applicability of data product; units are spacecraft clock counts, in units of whole seconds.

Product = nn, acronym describing data product from Table 3-5

SensorID = S or L (or J=joint)

Version = 0, 1,..., 9, a,..., z

Ext = TAB

The product ID scheme for data-containing CRISM level 6 CDRs is as follows:

CCCC\_P\_TTTTTTTT\_AA\_S\_V

Where:

CCCC = Product Type (CDR6)

P = Partition number of sclk counts

TTTTTTTTT = Start time of applicability, in units of sclk counts

AA = Acronym for contents of product

S = Sensor ID

V = Version

The file naming convention for EDR processing tables is as follows.

(Product)\_(Sensor)\_(YYYY)\_(DOY)\_version

where:

Product Type = BTF for before-the-fact predicted, or ATF for after-the-fact actual

Sensor = VN or IR

YYYY = year

DOY = day of year

Version = nn

The product ID scheme for the EDR processing tables is as follows:

CCCC\_P\_TTTTTTTT\_AA\_S\_V

Where:

CCC = Product (BTF or ATF)

S = Sensor ID

P = Partition number of sclk counts

YYYY = Year covered by table

DOY = Day of year covered by table

V = Version

The file naming convention for level-4 CDRs is as follows.

(ProductType)(Level)(Partition)(Time)\_  
(Product)(FrameRate)(Binning)(ExposureParameter)(WavelengthFilter)(Side)(SensorID)\_  
version.(Ext)

Product Type = CDR

Level = 4

Partition = n, partition of sclk counts

Time = nnnnnnnnnn, spacecraft start time of applicability of ground data product, or spacecraft mean time of acquisition of source EDR of flight data product; units are spacecraft clock counts, in units of whole seconds.

Product = nn, acronym describing data product from Table 3-19

FrameRate = n, rate in Hz at which data are taken (0=1 Hz, 1=3.75 Hz, 3=15 Hz, 4=30 Hz, 5 = N/A)

Binning = n, number of spatial pixels binned (0 = unbinned, 1 = 2x binned, 2 = 5x binned, 3 = 10x binned, 4 = N/A)

Exposure parameter = nnn, an integer 1-480 indicating commanded exposure time in units of (inverse frame rate)/480; 000 if inapplicable

Wavelength filter = n, and integer 0-3 indicating which onboard menu of rows of the detector are represented

Side = #, 1 or 2 for focal plane or sphere bulbs; or 0 if N/A

Sensor ID = S or L (or J=joint)

version = 0, 1,..., 9, a,..., z

Ext = IMG

The product ID scheme for CRISM level 4 CDRs is as follows:

CCCCPTTTTTTTT\_AARBEEWCS\_V

Where:		
CCCC	=	Product Type (CDR4)

P	=	Partition number of sclk counts
TTTTTTTTTT	=	Start time of applicability, in units of sclk counts
AA	=	Acronym for contents of product
R	=	Frame rate
B	=	Binning
EEE	=	Exposure parameter
W	=	Wavelength filter
C	=	Side
S	=	Sensor ID
V	=	Version

#### 2.3.4.9 ADRs

ADRs (if archived, which is not planned as of 2021) are hyperdimensional binary tables of derived values, where the axes of the matrix represent values of a layer of a DDR (e.g., incidence angle, thermal inertia, etc.), and the element in the matrix is a coefficient used either directly or as an input to correct I/F for predictived atmospheric, photometric, or thermal effects.

The file naming convention for ADRs is as follows.

(ProductType)\_ (ADR\_Type)\_ (Wavelength)\_ (Partition)\_ (Time)\_ version.(Ext)

where:

Product Type = ADR

ADR\_Type = CL, AC, or TE as described in section 3.8

Wavelength = nnnn, in nanometers; 0000 if not applicable

Partition = n, spacecraft clock partition.

Time = nnnnnnnnnn, spacecraft start time of applicability of data product; units are spacecraft clock counts, in units of whole seconds.

version = 0, 1,..., 9, a,..., z

Ext = DAT

The product ID scheme for CRISM ADRs is as follows:

CCC\_AA\_NNNN\_P\_TTTTTTTT\_V

Where:		
CCC	=	Product Type (ADR)
AA	=	Acronym for contents of product
NNNN	=	Wavelength in nearest whole nanometers
P	=	Partition number of sclk counts
TTTTTTTTTT	=	Start time of applicability, in units of sclk counts
V	=	Version

#### **2.3.4.10 SPICE Files**

The file naming convention CRISM-generated SPICE kernels is as follows.

MRO\_CRISM\_(KernelType)\_(YYYY\_DOY)\_(Filetype)\_(version).(Ext)

where:

Kernel Type =

FK (frames kernel)

IK (instrument kernel)

CK (gimbal C-kernel)

MK (metakernel)

YYYY\_DOY is the year and day of year of the start of a 2-week period covered in a single gimbal C kernel or metakernel; or else these fields are filled with zeroes

filetype =

P for predicted

R for reconstructed

N for not applicable

version = 0, 1,...,9, a, ..., z

Ext =

TI (text-format, instrument kernel)

TF (text-format, frames kernel)

BC (binary-format, gimbal C kernel)

BO (binary-format, gimbal offset C kernel)

TM (text-format, metakernel)

#### **2.3.4.11 Extra Products**

Files that document the history of instrument software settings have a format and nomenclature like that of level 6 CDRs, as described in section 2.3.4.8.

The file naming convention for the macro dictionary is as follows.

MacroDict(YYYYMMDD).PY

where:

YYYYMMDD = year, month, and day of the last onground revision of the macro dictionary

The file naming convention for the description of the image data generated by each macro is as follows.

MacroDict(YYYYMMDD)\_BURSTS.CSV

The file naming convention for the summary of each macro's function is as follows.

MacroDict(YYYYMMDD)\_SUM.CSV

The nomenclature of tables that connect specific observations with regions of interest on Mars, science objectives, and specific observation conditions is described in Table 2-13. For the SITE\_ID, ANCILLARY, REQ\_ID, and CORRESP tables may be one table for the mission, and the string YYYY\_MM\_DD is the date of the last update. For the OBS\_ID table, there are multiple tables, as indicated by YYYY\_MM\_00 for the year and month included in the table.

The file naming convention for the TER and MTR Extras products is presented in Appendix P2.

**Table 2-13. Nomenclature of Observation Tracking Tables**

File Name	File Contents
SITE_ID_YYYY_MM_DD.TAB	OPTIONAL: Description of the locations and physical features of sites of interest on Mars, compiled by the CRISM science team. Date is last update.
SITE_ID_YYYY_MM_DD.HDR	OPTIONAL: Header record to site ID table.
SITE_ID_YYYY_MM_DD.LBL	OPTIONAL: Label to site ID table.
ANCILLARY_YYYY_MM_DD.TAB	OPTIONAL: Tabulated statistics on physical properties of sites of interest on Mars, compiled by the CRISM science team . Date is last update.
ANCILLARY_YYYYMMDD.HDR	OPTIONAL: Header record to ancillary information table.
ANCILLARY_YYYYMMDD.LBL	OPTIONAL: Label to ancillary information table.
REQ_ID_MC##- ####_YYYY_MM_DD.TAB	OPTIONAL: A table of request IDs, with one or more entries, specifying the desired observing conditions such as Ls. One table per site ID (MC##-####).
REQ_ID_MC##- ####_YYYY_MM_DD.HDR	OPTIONAL: Generic header record to request ID tables.
REQ_ID_MC##- ####_YYYY_MM_DD.LBL	OPTIONAL: Label to request ID tables.
OBS_ID_YYYY_MM_DD.TAB	Table summarizing the date and characteristics of each observation actually taken.
OBS_ID_YYYY_MM_DD.HDR	Header record to observation ID table.
OBS_ID_YYYY_MM_DD.LBL	Label to observation ID table.
CORRESP_YYYY_MM_DD.TAB	OPTIONAL: Correspondence table in which one line gives a site ID, request ID, and target ID where there is geographic overlap.
CORRESP_YYYY_MM_DD.HDR	OPTIONAL: Header record to correspondence table.
CORRESP_YYYY_MM_DD.LBL	OPTIONAL: Label to correspondence table.

## 2.4 Standards Used in Generating Data Products

### 2.4.1 PDS Standards

The CRISM data product complies with the PDS standards for file formats and labels, specifically the PDS image and table data objects [Applicable Documents 6 and 7].

### 2.4.2 Time Standards

Two time standards are used in CRISM data products:

- spacecraft time in seconds (PDS label keywords SPACECRAFT\_CLOCK\_START\_COUNT and SPACECRAFT\_CLOCK\_STOP\_COUNT)

- UTC (PDS label keywords START\_TIME, STOP\_TIME, and PRODUCT\_CREATION\_TIME)

One additional time-related field is used in CRISM data products:

- target ID, which is a unique identifier associated with each MRO observation (PDS label keyword OBSERVATION\_ID)

### **2.4.3 Coordinate Systems**

The cartographic coordinate system used for the CRISM data products conforms to the IAU planetocentric system with East longitudes being positive. The IAU2000 reference system [7] for Mars cartographic coordinates and rotational elements was used for computing latitude and longitude coordinates.

## **2.5 Data Validation**

Data validation is an iterative process throughout the history of processing the data set. Key steps in the process are given below.

### **2.5.1 EDR level**

For each observation, every EDR is compared against frame-by-frame predictions of commanded instrument state. The results of the comparison are written as a data validation report that accompanies the EDRs for that observation.

In the case of a hardware or configuration discrepancy (shutter position, lamp status or level, pixel binning, frame rate, channel selection, power status of detectors), processing of the image data to RDR level does not occur in order to avoid introducing invalid results. Missing frames or portions of frames are replaced with a value of 65535 (this cannot be a valid data value) and only that portion of the EDR is not further processed.

If an expected calibration data set (background, focal plane lamp, or sphere) is not successfully acquired and downloaded, the next closest in time calibration can be used. In this case there is a discrepancy between the predicted EDR processing table and the actual one, and this is recorded in the data quality index upon processing of the scene EDR to the TRDR level.

### **2.5.2 EDR to RDR level**

A data quality keyword is used to encode Figures-of-Merit into one parameter that is included in each line of the list file with the EDR and TRDR. This begins with the EDR and is modified in the TRDR. At the EDR level, missing data, saturation, and basic hardware status are assessed.

At the TRDR level there is the additional option (not currently implemented) to add further information: whether a target's latitude and longitude are within the boundaries of an observation, for the central swath of a targeted observation; whether underexposure occurred; usage of temporally non-adjacent calibration files (due to loss of data from a background, bias, or sphere macro); or high spectrometer housing or detector temperature is flagged. Once the summary product backplanes are derived, an excessive violet I/F can be flagged as a possible indication of water ice clouds.

The 16-byte data quality field is interpreted as follows:

Byte 0: populated in EDR; 1 = focal planes not properly powered; 0 = focal planes properly powered;

Byte 1: populated in EDR; updated in RDR; 1 = saturated data (8-bit 255; 12-bit 4095; or within 10% of 14-bit saturation) present outside of bad pixel mask; 0 = saturated data not present;

Byte 2: populated in EDR; 1 = missing data (some pixels populated with 65535); 0 = no missing data;

Byte 3: populated in EDR; 1 = shutter out of commanded position; 0 = shutter in position;

Byte 4: populated in EDR; 1 = focal plane lamp setting out of commanded range; 0 = focal plane lamp setting in commanded range;

Byte 5: populated in EDR; 1 = sphere goal out of commanded range; 0 = sphere goal in commanded range;

Byte 6: populated in EDR; 1 = more lines or bands than expected; 0 = not more than expected;

Byte 7: populated in RDR; 1 = VNIR detector out of calibrated temperature range; 0 = VNIR detector within calibrated temperature range

(Byte 8: populated in RDR; 1 = IR detector out of calibrated temperature range; 0 = IR detector within calibrated temperature range)

(Byte 9: populated in RDR; 1 = sphere temperature out of calibrated range; 0 = temperature sphere within calibrated range)

(Byte 10: populated in RDR; 1= spectrometer housing temperature  $>-75^{\circ}\text{C}$ ; 0 = spectrometer housing temperature  $\leq-75^{\circ}\text{C}$ )

(Byte 11: populated in RDR; 1 = target not covered; 0 = target covered) (Note: not populated)

(Byte 12: populated in RDR; 1 = non-adjacent calibration files used; 0 = temporally adjacent calibration files used) (Note: not populated)

(Byte 13: populated in RDR; 1= violet I/F from summary product backplane suggests clouds or ice, value  $>0.1$ ; 0 = low violet I/F) (Note: not populated)

Byte 14 through Byte 15 spare

Missing frames or portions of frames or saturated data are indicated in an RDR with a value of 65535 (this cannot be a valid data value).

Note that for quality control purposes, IR data acquired at a detector temperature  $>127.5\text{K}$  ( $127.7\text{K}$  effective Feb. 2011) are delivered as EDRs but not as products processed further such as TRDRs.

### **2.5.3 RDR level**

Once data are calibrated to units of radiance, some of the pixels that are present in an EDR cannot have meaningful values. These include the regions at the edge of each detector which contain background measurements that are used during application of the calibration algorithm (see Appendix L). Those pixels are set to a value of exactly 65535, which cannot have a meaningful significant in the units used for radiance or I/F.

### 3. DETAILED DATA PRODUCT SPECIFICATIONS

#### 3.1 EDR

##### 3.1.1 Data Product Structure and Organization

At the SOC, EDRs are constructed from each observation with a distinct observation ID. An EDR consists of a part or all of the output from one of the constituent command macros that make up one observation tagged by a unique observation ID. The data in one EDR represent a consistent instrument configuration (shutter position, frame rate, pixel binning, compression, exposure time, on/off status and setting of different lamps). This is shown schematically in Figure 3-1. There is a single multiple-band image (suffix \*.IMG) stored in one file, plus a detached list file in which each record has information specific to one frame of the multiple-band image (suffix \*.TAB). One label points to both files.

The multiple-band image has dimensions of sample, line, and wavelength. The size of the multiple-band image varies according to the observation mode but is deterministic given the macro ID. A typical multiple-band image might have XX pixels in the sample (cross-track) dimension, YY pixels in the line (along-track) dimension, and ZZ pixels in the wavelength dimension, where

- XX=640/binning, where 640 is the number of columns read off the detector, and binning is 1, 2, 5, or 10,
- YY=the number of frames of data with a consistent instrument configuration , and
- ZZ=the number of detector rows (wavelengths) that are retained by the instrument.

Pixels are 16-bit unsigned integer values, most significant bit first.

Appended to the multiple-band image is a binary table of the detector rows that were used, as selected by the wavelength filter. This is a one-column table, with each row containing one detector row number expressed as a 16-bit unsigned integer values, most significant bit first.

Data are not precisely registered in the spectral direction. For one column, the projection onto Mars' surface may vary by as much as  $\pm 0.4$  detector elements in the XX dimension depending on position in the FOV (distortions are worst at the edges of the VNIR and IR FOVs). For a single wavelength, its location in the ZZ direction may vary by as much as  $\pm 1$  detector element depending on wavelength (distortions are worst at the short- and long-wavelength ends of the IR detector).

The detached comma-separated ASCII file is YY lines in length, containing raw instrument housekeeping plus other frame dependent information. Locations of the temperature sensors and heaters whose states are reported in the housekeeping are shown in Appendix M.

Most of the contents of an EDR represent unmodified but rearranged values from the data stream. The data stream downlinked by the spacecraft unpacks into a succession of image-like frames with binary headers containing housekeeping (Table 3-2). For each focal plane, there are 220 housekeeping items that contain full status of the instrument hardware, including data configuration, lamp and shutter status, gimbal position, a time stamp, and the target ID and macro within which the frame of data was taken.

To convert to an EDR format, the headers are stripped off and placed into the list file in text form, and the frames are merged into a multiple-band image. The list file is based on the 220 housekeeping items. 5 of the items are composite in that each bit of a 32-bit word encodes

particular information on gimbal status or control. These separate items are not broken out, except for the gimbal status at the beginning, middle, and end of each exposure, from which gimbal position is broken out (3 additional items). The housekeeping is pre-pended with spaces for 10 additional frame-specific items useful in data validation, processing, and sorting, for a total of 233 items per frame. Not all of the 10 additional items may be populated:

- A data quality parameter produced during data validation, as discussed in section 2.5
- $L_s$ , degrees
- Solar distance, km
- Time of day at center of FOV, hhmm.ss with 1 Mars solar day = 2400.00
- Preliminary latitude at center of FOV, degrees
- Preliminary longitude at center of FOV, degrees
- Preliminary  $i$  (incidence angle) at center of FOV, degrees
- Preliminary  $e$  (emission angle) at center of FOV, degrees
- Preliminary  $g$  (phase angle) at center of FOV, degrees
- Predicted dust opacity, unitless

The pointing and geometric information is derived from spacecraft positions and quaternions plus the gimbal position. Predicted dust opacity is interpolated from an ADR .

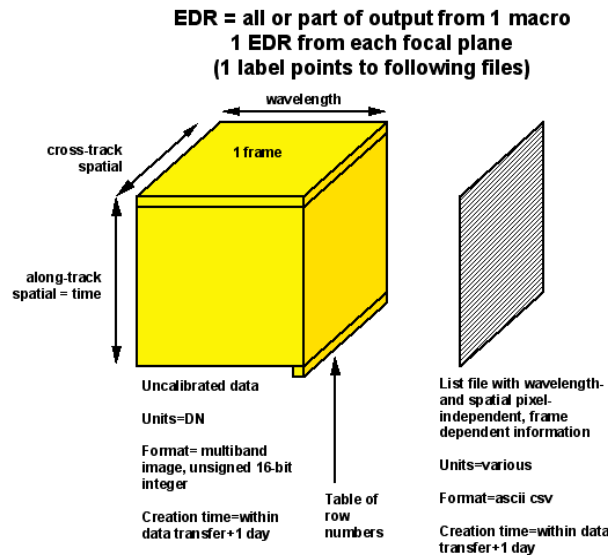


**Figure 3-1. Contents of a CRISM Experiment Data Record (EDR).**

**Table 3-2. Items in housekeeping list file**

Column	Mnemonic	Description	Source of information	Length (bytes)	Format (and range if applicable)	Notes
1	DATA_QUALITY_CODE	Data quality	Added parameter	16	Integer	1,2
2	SOLAR_LONGITUDE	Ls	Added parameter	7	Float	1,2
3	SOLAR_DISTANCE	Solar distance	Added parameter	12	Float	1,2
4	LOCAL_TIME	Local time (hh:mm:ss)	Added parameter	7	Character	1,2
5	CENTER_LATITUDE	Estimated latitude	Added parameter	7	Float	1,2
6	CENTER_LONGITUDE	Estimated longitude	Added parameter	7	Float	1,2
7	CENTER_INCIDENCE_ANGLE	Estimated incidence angle	Added parameter	7	Float	1,2
8	CENTER_EMISSION_ANGLE	Estimated emission angle	Added parameter	7	Float	1,2
9	CENTER_PHASE_ANGLE	Estimated phase angle	Added parameter	7	Float	1,2
10	PREDICTED_DUST_OPACITY	Predicted dust opacity	Added parameter	5	Float	1,2
11	SYNCHRONIZATION_PATTERN	Synchronization pattern	Spectrometer Image Header	10	Integer; valid value 4277809352	1,3
12	DATATYPE	Type of data (0 for image data; 1 for encoder diagnostics)	Spectrometer Image Header	5	Integer	1,3
13	NUMLINES	Amount of image data sent (lines, 0 - 480)	Spectrometer Image Header	3	Integer	1,3
14	EXPOSURE_MET	Spacecraft time of exposure, in spacecraft clock units	Spectrometer Image Header	10	Integer	1,3
15	EXPOSURE_SS	Time of exposure fractional second (1/2 <sup>16</sup> seconds)	Spectrometer Image Header	5	Integer	1,3
16	SCAN_MOTOR_STATUS1	Scan motor status word 1	Spectrometer Image Header	16	Character; see Table 3-3 for significance of each character	1,3
17	SCAN_MOTOR_STATUS2	Scan motor status word 2	Spectrometer Image Header	16	Character; see Table 3-3 for significance of each character	1,3
18	SCAN_MOTOR_STATUS3	Scan motor status word 3	Spectrometer Image Header	16	Character; see Table 3-3 for significance of each character	1,3
19	SCAN_MOTOR_ENCPOS1	Angular position of gimbal, beginning of frame	Derived from scan motor status word 1	8	Integer	1,3
20	SCAN_MOTOR_ENCPOS2	Angular position of gimbal, middle of frame	Derived from scan motor status word 2	8	Integer	1,3
21	SCAN_MOTOR_ENCPOS3	Angular position of gimbal, end of frame	Derived from scan motor status word 3	8	Integer	1,3
22	SPECT_ID	Spectrometer identifier	Spectrometer Image Header	1	Integer; 0 = IR, 1 = VNIR	1,3
23	TEMP_MON	Temperature monitoring enabled or disabled	Spectrometer Image Header	1	Integer; 0 = Off, 1 = On	1,3
24	EXPOSURE	Exposure time parameter; number of 1/480ths of inverse frame rate; specified separately for each detector	Spectrometer Image Header	3	0 - 480	1,3

Column	Mnemonic	Description	Source of information	Length (bytes)	Format (and range if applicable)	Notes
25	RATE	Rate of frame acquisition; 0 = 1 Hz; 1 = 3.75 Hz; 2 = 5 Hz; 3 = 15 Hz; 4 = 30 Hz	Spectrometer Image Header	1	Integer; 0-4	1,3
26	SOURCE	Data source, either actual detector or a test pattern	Spectrometer Image Header	1	Integer; 0 = Detector, 1 - 7 = Test pattern	1,3
27	FILTER	Wavelength filter; which onboard table is used to define which detector rows are recorded	Spectrometer Image Header	1	Integer; 0 – 3	1,3
28	BINNING	Pixel binning mode; 0 = 1:1, 1 = 2:1, 2 = 5:1, 3 = 10:1	Spectrometer Image Header	1	Integer; 0 – 3	1,3
29	LOSSY	Enable/disable lossy compression	Spectrometer Image Header	1	Integer; 0 = Disable, 1 = Enable	1,3
30	FAST	Enable/disable Fast compression	Spectrometer Image Header	1	Integer; 0 = Disable, 1 = Enable	1,3
31	DPU_BOARD_TEMP	DPU_PWR_0 (DPU power board temperature)	Analog Status	5	Integer	1,4
32	DPU_P5_VOLTAGE	DPU_PWR_1 (DPU +5 voltage)	Analog Status	5	Integer	1,4
33	DPU_P5_CURRENT	DPU_PWR_3 (DPU +5 current)	Analog Status	5	Integer	1,4
34	SCAN_MOT_CURR	DPU_PWR_4 (Scan motor current)	Analog Status	5	Integer	1,4
35	IR_BOARD_TEMP	IR_PWR_0 (IR power board temperature)	Analog Status	5	Integer	1,4
36	IR_FPU_P12_VOLTAGE	IR_PWR_1 (IR focal plane unit [FPU] +12 voltage)	Analog Status	5	Integer	1,4
37	IR_FPU_P7_VOLTAGE	IR_PWR_2 (IR FPU +7 voltage)	Analog Status	5	Integer	1,4
38	IR_FPU_CURRENT	IR_PWR_3 (IR FPU current)	Analog Status	5	Integer	1,4
39	HEATER_34_CURRENT	IR_PWR_4 (Heater 3 & 4 current)	Analog Status	5	Integer	1,4
40	VNIR_BOARD_TEMP	VNIR_PWR_0 (VNIR power board temperature)	Analog Status	5	Integer	1,4
41	VNIR_FPU_P12_VOLTAGE	VNIR_PWR_1 (VNIR FPU +12 voltage)	Analog Status	5	Integer	1,4
42	VNIR_FPU_P7_VOLTAGE	VNIR_PWR_2 (VNIR FPU +7 voltage)	Analog Status	5	Integer	1,4
43	VNIR_FPU_CURRENT	VNIR_PWR_3 (VNIR FPU current)	Analog Status	5	Integer	1,4
44	HEATER_12_CURRENT	VNIR_PWR_4 (Header 1 & 2 current)	Analog Status	5	Integer	1,4
45	COOL_BOARD_TEMP	COOL_PWR_0 (Cooler power board temperature)	Analog Status	5	Integer	1,4
46	COOL_P15_VOLTAGE	COOL_PWR_1 (Cooler +15 voltage)	Analog Status	5	Integer	1,4
47	COOL_CURRENT	COOL_PWR_3 (Cooler current)	Analog Status	5	Integer	1,4
48	HOP_HEATER_12_CURR	COOL_PWR_4 (High-output paraffin actuator [HOP] heater 1 & 2 current)	Analog Status	5	Integer	1,4

Column	Mnemonic	Description	Source of information	Length (bytes)	Format (and range if applicable)	Notes
49	SHUT_MOTOR_CURR_IR	IR_FP_0 (Shutter motor current (IR))	Analog Status	5	Integer	1,4
50	IR_DETECTOR_TEMP1	IR_FP_1 (IR detector temperature 1)	Analog Status	5	Integer	1,4
51	IR_DETECTOR_TEMP2	IR_FP_2 (IR detector temperature 2)	Analog Status	5	Integer	1,4
52	COOLER_TEMP1	IR_FP_3 (Cooler temperature 1)	Analog Status	5	Integer	1,4
53	COOLER_TEMP2	IR_FP_4 (Cooler temperature 2)	Analog Status	5	Integer	1,4
54	COOLER_TEMP3	IR_FP_5 (Cooler temperature 3)	Analog Status	5	Integer	1,4
55	SHUT_MOTOR_TEMP_IR	IR_FP_6 (Shutter motor temperature (IR))	Analog Status	5	Integer	1,4
56	SPHERE_TEMP_IR	IR_FP_7 (Integrating sphere temperature (IR))	Analog Status	5	Integer	1,4
57	SPIDER_TEMP_IR	IR_FP_8 (Telescope spider temperature (IR))	Analog Status	5	Integer	1,4
58	SPECT_CAVITY_TEMP_IR	IR_FP_9 (Spectral cavity temperature (IR))	Analog Status	5	Integer	1,4
59	OSU_CAVITY_TEMP_IR	IR_FP_10 (OSU cavity temperature (IR))	Analog Status	5	Integer	1,4
60	IR_FPU_BOARD_TEMP	IR_FP_11 (IR FPU board temperature)	Analog Status	5	Integer	1,4
61	IR_SPHERE_CURR	IR_FP_12 (IR sphere lamp current)	Analog Status	5	Integer	1,4
62	HOP_TEMP_IR	IR_FP_13 (HOP temperature (IR))	Analog Status	5	Integer	1,4
63	SHUT_MOTOR_CURR_VNIR	VNIR_FP_0 (Shutter motor current (VNIR))	Analog Status	5	Integer	1,4
64	VNIR_DETECTOR_TEMP1	VNIR_FP_1 (VNIR detector temperature 1)	Analog Status	5	Integer	1,4
65	VNIR_DETECTOR_TEMP2	VNIR_FP_2 (VNIR detector temperature 2)	Analog Status	5	Integer	1,4
66	TELESCOPE_TEMP	VNIR_FP_3 (Telescope temperature (VNIR))	Analog Status	5	Integer	1,4
67	OPTICAL_BENCH_TEMP	VNIR_FP_4 (Optical bench temperature (VNIR))	Analog Status	5	Integer	1,4
68	SPIDER_TEMP_VNIR	VNIR_FP_5 (Telescope spider temp. (VNIR))	Analog Status	5	Integer	1,4
69	SPECT_CAVITY_TEMP_VNIR	VNIR_FP_6 (Spectral cavity temperature (VNIR))	Analog Status	5	Integer	1,4
70	OSU_CAVITY_TEMP_VNIR	VNIR_FP_7 (OSU cavity temperature (VNIR))	Analog Status	5	Integer	1,4
71	VNIR_FPU_BOARD_TEMP	VNIR_FP_8 (VNIR FPU board temperature)	Analog Status	5	Integer	1,4
72	BAFFLETEMP	VNIR_FP_9 (Baffle temperature (VNIR))	Analog Status	5	Integer	1,4
73	SCAN_PWR	Scan motor power	Digital Status	1	Integer; 0 = Off, 3 = On	1,5
74	IR_PRI_PWR	IR FPU primary power	Digital Status	1	Integer; 0 = Off, 1 = On	1,5
75	HTR3_PWR	Heater 3 (on cooler radiator) power	Digital Status	1	Integer; 0 = Off, 1 = On	1,5

Column	Mnemonic	Description	Source of information	Length (bytes)	Format (and range if applicable)	Notes
76	HTR4_PWR	Heater 4 (on spectrometer housing) power	Digital Status	1	Integer; 0 = Off, 1 = On	1,5
77	VNIR_PRI_PWR	VNIR FPU primary power	Digital Status	1	Integer; 0 = Off, 1 = On	1,5
78	HTR1_PWR	Heater 1 (on gimbal electronics housing) power	Digital Status	1	Integer; 0 = Off, 1 = On	1,5
79	HTR2_PWR	Heater 2 (on gimbal electronics housing) power	Digital Status	1	Integer; 0 = Off, 1 = On	1,5
80	COOL_PRI_PWR	Cooler primary power	Digital Status	1	Integer; 0 = Off, 1 = On	1,5
81	HOP_HTR1_PWR	HOP heater 1 power	Digital Status	1	Integer; 0 = Off, 1 = On	1,5
82	HOP_HTR2_PWR	HOP heater 2 power	Digital Status	1	Integer; 0 = Off, 1 = On	1,5
83	COVER_TELLTALE_PWR	Imager cover telltale power	Digital Status	1	Integer; 0 = Off, 1 = On	1,5
84	COVER_TELLTALE	Cover Telltale	Digital Status	1	Integer; 0 = Not closed, 1 = Closed	1,5
85	IR_COOL1_LEVEL	IR Cooler 1 level	Digital Status	4	Integer; 0 - 4095	1,5
86	IR_COOL2_LEVEL	IR Cooler 2 level	Digital Status	4	Integer; 0 - 4095	1,5
87	IR_COOL3_LEVEL	IR Cooler 3 level	Digital Status	4	Integer; 0 - 4095	1,5
88	IR_FLOOD1_LEVEL	IR flood lamp 1 level	Digital Status	4	Integer; 0 - 4095	1,5
89	IR_FLOOD2_LEVEL	IR flood lamp 2 level	Digital Status	4	Integer; 0 - 4095	1,5
90	IR_SPHERE_GOAL	Sphere lamp 1 closed-loop goal (IR)	Digital Status	4	Integer; 0 - 4095	1,5
91	IR_SPHERE_LEVEL	Sphere lamp 1 level (IR); relevant to open-loop operation only	Digital Status	4	Integer; 0 - 4095	1,5
92	IR_SOURCE	IR data source, either actual detector or a test pattern	Digital Status	1	Integer; 0 = Detector, 1 - 7 = Test pattern	1,5
93	IR_SHUT_LED	Shutter fiducial light-emitting diode (LED) power (IR)	Digital Status	1	Integer; 0 = Off, 1 = On	1,5
94	IR_SPHERE_PWR	Sphere lamp 1 power (IR)	Digital Status	1	Integer; 0 = Off, 1 = On	1,5
95	IR_FLOOD1_PWR	IR flood lamp 1 power	Digital Status	1	Integer; 0 = Off, 1 = On	1,5
96	IR_FLOOD2_PWR	IR flood lamp 2 power	Digital Status	1	Integer; 0 = Off, 1 = On	1,5
97	IR_COOL1_PWR	IR cooler 1 power	Digital Status	1	Integer; 0 = Off, 1 = On	1,5
98	IR_COOL2_PWR	IR cooler 2 power	Digital Status	1	Integer; 0 = Off, 1 = On	1,5
99	IR_COOL3_PWR	IR cooler 3 power	Digital Status	1	Integer; 0 = Off, 1 = On	1,5
100	IR_LVDS_1	IR low-voltage differential signal (LVDS) driver #1 enable	Digital Status	1	Integer; 0 = Disable, 1 = Enable	1,5
101	IR_LVDS_2	IR LVDS driver #2 enable	Digital Status	1	Integer; 0 = Disable, 1 = Enable	1,5
102	IR_DAC_POWER	IR digital-to-analog converter (DAC) power (for coolers and lamps)	Digital Status	1	Integer; 0 = Off, 1 = On	1,5
103	IR_DAC_PD	IR DAC power down	Digital Status	1	Integer; 0 = Run, 1 = Power down	1,5

Column	Mnemonic	Description	Source of information	Length (bytes)	Format (and range if applicable)	Notes
104	IR_ANA_5V_PWR	IR analog 5V power	Digital Status	1	Integer; 0 = Off, 1 = On	1,5
105	IR_ADC_Q1_PWR	IR detector quadrant #1 analog-to-digital converter (ADC, or A/D) power	Digital Status	1	Integer; 0 = Off, 1 = On	1,5
106	IR_ADC_Q2_PWR	IR detector quadrant #2 A/D power	Digital Status	1	Integer; 0 = Off, 1 = On	1,5
107	IR_ADC_Q3_PWR	IR detector quadrant #3 A/D power	Digital Status	1	Integer; 0 = Off, 1 = On	1,5
108	IR_ADC_Q4_PWR	IR detector quadrant #4 A/D power	Digital Status	1	Integer; 0 = Off, 1 = On	1,5
109	IR_BIAS_PWR	IR detector bias power	Digital Status	1	Integer; 0 = Off, 1 = On	1,5
110	IR_AMP_HI_PWR	IR detector amp high power	Digital Status	1	Integer; 0 = Off, 1 = On	1,5
111	IR_CLOCK_DRIVE	IR detector clock driver	Digital Status	1	Integer; 0 = Off, 1 = On	1,5
112	IR_COOLER_TEMP3_CONV	IR cooler temperature 3 conversion enable; disabling turns off power to temperature sensor in case of introduced noise in detector	Digital Status	1	Integer; 0 = Disable, 1 = Enable	1,5
113	IR_COOLER_TEMP2_CONV	IR cooler temperature 2 conversion enable; disabling turns off power to temperature sensor in case of introduced noise in detector	Digital Status	1	Integer; 0 = Disable, 1 = Enable	1,5
114	IR_COOLER_TEMP1_CONV	IR cooler temperature 1 conversion enable; disabling turns off power to temperature sensor in case of introduced noise in detector	Digital Status	1	Integer; 0 = Disable, 1 = Enable	1,5
115	IR_TEMP2_CONV	IR detector temperature 2 conversion enable; disabling turns off power to temperature sensor in case of introduced noise in detector	Digital Status	1	Integer; 0 = Disable, 1 = Enable	1,5
116	IR_TEMP1_CONV	IR detector temperature 1 conversion enable; disabling turns off power to temperature sensor in case of introduced noise in detector	Digital Status	1	Integer; 0 = Disable, 1 = Enable	1,5
117	IR_SHUTTER_MOTOR_CURRENT_CONV	Shutter motor current conversion enable (IR); disabling turns off power to current sensor in case of introduced noise in detector	Digital Status	1	Integer; 0 = Disable, 1 = Enable	1,5

Column	Mnemonic	Description	Source of information	Length (bytes)	Format (and range if applicable)	Notes
118	IR_MUX_TEMP_CONV	IR multiplexed (MUX) temperature conversion enable; disabling turns off power to temperature sensor in case of introduced noise in detector	Digital Status	1	Integer; 0 = Disable, 1 = Enable	1,5
119	IR_SHUT_ENB	Shutter motor phase enabled (IR)	Digital Status	1	Integer; 0 - 3	1,5
120	IR_SHUT_PHASE	Shutter motor phase (IR)	Digital Status	1	Integer; 0 - 3	1,5
121	IR_DAC_STATE	IR DAC power state	Digital Status	1	Integer; 0 = Off, 1 = On	1,5
122	IR_SHUT_FID	Shutter fiducial LED (IR)	Digital Status	1	Integer; 0 = Off, 1 = On (fiduciated)	1,5
123	IR_ADC_Q1_STATE	IR detector quadrant #1 A/D latch-up	Digital Status	1	Integer; 0 = Ok, 1 = Latched	1,5
124	IR_ADC_Q2_STATE	IR detector quadrant #2 A/D latch-up	Digital Status	1	Integer; 0 = Ok, 1 = Latched	1,5
125	IR_ADC_Q3_STATE	IR detector quadrant #3 A/D latch-up	Digital Status	1	Integer; 0 = Ok, 1 = Latched	1,5
126	IR_ADC_Q4_STATE	IR detector quadrant #4 A/D latch-up	Digital Status	1	Integer; 0 = Ok, 1 = Latched	1,5
127	VNIR_FLOOD1_LEVEL	VNIR flood lamp 1 level	Digital Status	4	Integer; 0 - 4095	1,5
128	VNIR_FLOOD2_LEVEL	VNIR flood lamp 2 level	Digital Status	4	Integer; 0 - 4095	1,5
129	VNIR_SPHERE_GOAL	Sphere lamp 1 closed-loop goal (VNIR)	Digital Status	4	Integer; 0 - 4095	1,5
130	VNIR_SPHERE_LEVEL	Sphere lamp 1 level (VNIR); relevant to open-loop operation only	Digital Status	4	Integer; 0 - 4095	1,5
131	VNIR_HEATER	VNIR heater	Digital Status	1	0 = Off 1 = On	1,5
132	VNIR_SOURCE	VNIR data source, either actual detector or a test pattern	Digital Status	1	0 = Detector 1 - 7 = Test pattern	1,5
133	VNIR_SHUT_LED	Shutter fiducial LED power (VNIR)	Digital Status	1	Integer; 0 = Off, 1 = On	1,5
134	VNIR_SPHERE_PWR	Sphere lamp 2 power (VNIR)	Digital Status	1	Integer; 0 = Off, 1 = On	1,5
135	VNIR_FLOOD1_PWR	VNIR flood lamp 1 power	Digital Status	1	Integer; 0 = Off, 1 = On	1,5
136	VNIR_FLOOD2_PWR	VNIR flood lamp 2 power	Digital Status	1	Integer; 0 = Off, 1 = On	1,5
137	VNIR_LVDS_1	VNIR LVDS driver #1 enable	Digital Status	1	Integer; 0 = Disable, 1 = Enable	1,5
138	VNIR_LVDS_2	VNIR LVDS driver #2 enable	Digital Status	1	Integer; 0 = Disable, 1 = Enable	1,5
139	VNIR_DAC_POWER	VNIR DAC power (for lamps)	Digital Status	1	Integer; 0 = Off, 1 = On	1,5
140	VNIR_DAC_PD	VNIR DAC power down	Digital Status	1	0 = Run 1 = Power down	1,5
141	VNIR_ANA_5V_PWR	VNIR analog 5V power	Digital Status	1	Integer; 0 = Off, 1 = On	1,5
142	VNIR_ADC_Q1_PWR	VNIR detector quadrant #1 A/D power	Digital Status	1	Integer; 0 = Off, 1 = On	1,5
143	VNIR_ADC_Q2_PWR	VNIR detector quadrant #2 A/D power	Digital Status	1	Integer; 0 = Off, 1 = On	1,5
144	VNIR_ADC_Q3_PWR	VNIR detector quadrant #3 A/D power	Digital Status	1	Integer; 0 = Off, 1 = On	1,5

Column	Mnemonic	Description	Source of information	Length (bytes)	Format (and range if applicable)	Notes
145	VNIR_ADC_Q4_PWR	VNIR detector quadrant #4 A/D power	Digital Status	1	Integer; 0 = Off, 1 = On	1,5
146	VNIR_CHARGE_PUMP	VNIR detector charge pump power	Digital Status	1	Integer; 0 = off; 1 = 500 kHz; 2 = 250 kHz; 3 = 125 kHz (default)	1,5
147	VNIR_BIAS_PWR	VNIR detector bias power	Digital Status	1	Integer; 0 = Off, 1 = On	1,5
148	VNIR_AMP_HI_PWR	VNIR detector amp high power	Digital Status	1	Integer; 0 = Off, 1 = On	1,5
149	VNIR_CLOCK_DRIVE	VNIR detector clock driver	Digital Status	1	Integer; 0 = Off, 1 = On	1,5
150	VNIR_TEMP2_CONV	VNIR detector temperature 2 conversion enable; disabling turns off power to temperature sensor in case of introduced noise in detector	Digital Status	1	Integer; 0 = Disable, 1 = Enable	1,5
151	VNIR_TEMP1_CONV	VNIR detector temperature 1 conversion enable; disabling turns off power to temperature sensor in case of introduced noise in detector	Digital Status	1	Integer; 0 = Disable, 1 = Enable	1,5
152	VNIR_SHUTTER_MOTOR_CURRENT_CONV	Shutter motor current conversion enable (VNIR); disabling turns off power to current sensor in case of introduced noise in detector	Digital Status	1	Integer; 0 = Disable, 1 = Enable	1,5
153	VNIR_MUX_TEMP_CONV	VNIR multiplexed temperature conversion enable; disabling turns off power to temperature sensor in case of introduced noise in detector	Digital Status	1	Integer; 0 = Disable, 1 = Enable	1,5
154	VNIR_SHUT_ENB	Shutter motor phase enabled (VNIR)	Digital Status	1	Integer; 0 - 3	1,5
155	VNIR_SHUT_PHASE	Shutter motor phase (VNIR)	Digital Status	1	Integer; 0 - 3	1,5
156	VNIR_DAC_STATE	VNIR DAC power state	Digital Status	1	Integer; 0 = Off, 1 = On	1,5
157	VNIR_SHUTTER_FID	Shutter fiducial LED (VNIR)	Digital Status	1	Integer; 0 = Off, 1 = On (fiduciated)	1,5
158	VNIR_ADC_Q1_STATE	VNIR detector quadrant #1 A/D latch-up	Digital Status	1	Integer; 0 = Ok, 1 = Latched	1,5
159	VNIR_ADC_Q2_STATE	VNIR detector quadrant #2 A/D latch-up	Digital Status	1	Integer; 0 = Ok, 1 = Latched	1,5
160	VNIR_ADC_Q3_STATE	VNIR detector quadrant #3 A/D latch-up	Digital Status	1	Integer; 0 = Ok, 1 = Latched	1,5
161	VNIR_ADC_Q4_STATE	VNIR detector quadrant #4 A/D latch-up	Digital Status	1	Integer; 0 = Ok, 1 = Latched	1,5

Column	Mnemonic	Description	Source of information	Length (bytes)	Format (and range if applicable)	Notes
162	STATUS_INT	Status interval (seconds); interval at which analog digital and software status are reported in status packets to low-speed telemetry	Software Status	5	Integer; 1 – 65535 (0 = Off)	1,6
163	MACRO_BLOCKS	Number of macro blocks free	Software Status	5	Integer	1,6
164	TLM_VOLUME	Telemetry volume produced (KB) on the low speed engineering channel since the last CRM_STAT_CLR command	Software Status	5	Integer	1,6
165	WATCH_ADDR	Memory watch address	Software Status	5	Integer	1,6
166	WATCH_MEM_ID	Memory watch id (page no.)	Software Status	3	Integer	1,6
167	WATCH_DATA	Watched memory	Software Status	5	Integer	1,6
168	SW_VERSION	Software version number	Software Status	3	Integer	1,6
169	ALARM_ID	Latest alarm Id	Software Status	3	Integer; see Table 3-5	1,6
170	ALARM_TYPE	Latest alarm type	Software Status	1	Integer; 0 = Persistent, 1 = Transient	1,6
171	ALARM_COUNT	Count of alarms since the last CRM_STAT_CLR command	Software Status	3	Integer	1,6
172	CMD_EXEC	Commands executed since the last CRM_STAT_CLR command	Software Status	3	Integer	1,6
173	CMD_REJECT	Commands rejected since the last CRM_STAT_CLR command	Software Status	3	Integer	1,6
174	MAC_CMD_EXEC	Macro commands executed since the last CRM_STAT_CLR command	Software Status	3	Integer	1,6
175	MAC_CMD_REJECT	Macro commands rejected since the last CRM_STAT_CLR command	Software Status	3	Integer	1,6
176	MAC_ID	ID of most recent macro executed	Software Status	3	Integer	1,6
177	MACRO_LEARN	Macro learn mode; in learn mode commands are appended to a macro being loaded to memory; when not in learn mode commands are executed	Software Status	1	Integer; 0 = Not learning, 1 = Learning	1,6
178	MONITOR_RESPONSE	Monitor response enabling; if enabled a persistent out-of-limits condition will cause an onboard safing macro to be executed; 0 = disabled; 1 = enabled	Software Status	1	Integer; 0 = Disable, 1 = Enable	1,6

Column	Mnemonic	Description	Source of information	Length (bytes)	Format (and range if applicable)	Notes
179	MEM_WRITE	Memory write enable; required to upload data structures with commandable monitor limits or pixel processing value	Software Status	1	Integer; 0 = Disable, 1 = Enable	1,6
180	IR_SPECTRA	Last value for number of IR spectra to collect	Software Status	5	Integer; 0 – 65534 Remaining; 65535: Forever	1,6
181	VNIR_SPECTRA	Last value for number of VNIR spectra to collect	Software Status	5	Integer; 0 – 65534 Remaining; 65535: Forever	1,6
182	COOL_1_SETPOINT	Cooler 1 temperature goal; value corresponds to temperature goal for COOLER_TEMP1	Software Status	5	Integer	1,6
183	COOL_2_SETPOINT	Cooler 2 temperature goal; value corresponds to temperature goal for COOLER_TEMP2	Software Status	5	Integer	1,6
184	COOL_3_SETPOINT	Cooler 3 temperature goal; value corresponds to temperature goal for COOLER_TEMP3	Software Status	5	Integer	1,6
185	VNIR_HEATER_GOAL	VNIR heater temperature goal; value corresponds to temperature goal for VNIR_DETECTOR_TEMP1	Software Status	5	Integer	1,6
186	HEATER_1_GOAL	Heater 1 (on gimbal electronics housing) goal; value corresponds to temperature goal for OSU_CAVITY_TEMP_VNIR	Software Status	5	Integer	1,6
187	HEATER_2_GOAL	Heater 2 (on gimbal electronics housing) goal; value corresponds to temperature goal for OSU_CAVITY_TEMP_VNIR	Software Status	5	Integer	1,6
188	HEATER_3_GOAL	Heater 3 (on cooler radiator) goal; value corresponds to temperature goal for OSU_CAVITY_TEMP_IR	Software Status	5	Integer	1,6
189	HEATER_4_GOAL	Heater 4 (on spectrometer housing) goal; value corresponds to temperature goal for SPECT_CAVITY_TEMP_IR	Software Status	5	Integer	1,6
190	HEATER_1_HYSTERESIS	Heater 1 (on gimbal electronics housing) hysteresis	Software Status	3	Integer	1,6
191	HEATER_2_HYSTERESIS	Heater 2 (on gimbal electronics housing) hysteresis	Software Status	3	Integer	1,6
192	HEATER_3_HYSTERESIS	Heater 3 (on cooler radiator) hysteresis	Software Status	3	Integer	1,6

Column	Mnemonic	Description	Source of information	Length (bytes)	Format (and range if applicable)	Notes
193	HEATER_4_HYSTERESIS	Heater 4 (on spectrometer housing) hysteresis	Software Status	3	Integer	1,6
194	VNIR_HEATER_HYSTERESIS	VNIR heater hysteresis	Software Status	3	Integer	1,6
195	TARGET_ID	Target Id	Software Status	10	Integer	1,6
196	TARGET_TIME	Time of target closest approach (whole second component); same scale as EXPOSURE_MET	Software Status	10	Integer	1,6
197	TARGET_SUBSECONDS	Time of target fractional second ( $1/2^{16}$ seconds)	Software Status	5	Integer	1,6
198	PROFILE_ID	Profile Id	Software Status	5	Integer; 0 - 1819	1,6
199	SCAN_STATUS_WORD	Scan motor status word	Software Status	16	Character; see Table 3-3	1,6
200	SCAN_CONTROL_WORD	Scan motor control word	Software Status	16	Character; see Table 3-4	1,6
201	SLEW_ANGLE	Gimbal angle ( $\mu$ radians)	Software Status	11	Integer	1,6
202	OFFSET_ANGLE	Target for offset angle from gimbal profile defined in PROFILE_ID ( $\mu$ radians)	Software Status	11	Integer	1,6
203	OFFSET_RATE	Target for offset rate from gimbal profile defined in PROFILE_ID ( $\mu$ radians/s)	Software Status	11	Integer	1,6
204	GOAL_ANGLE	Gimbal goal angle from gimbal profile defined in PROFILE_ID ( $\mu$ radians)	Software Status	11	Integer	1,6
205	VNIR_HTR_MODE	VNIR heater control mode	Software Status	1	Integer; 0 = Off, 1 = On, 2 = Software control	1,6
206	OBSERVE	Observation state	Software Status	1	Integer; 0 = Idle, 1 = Observing	1,6
207	OFFSET_ADJUST	Scan offset adjustment	Software Status	1	Integer; 0 = Disable, 1 = Enable	1,6
208	HTR_1_MODE	Heater 1 (on gimbal electronics housing) control mode	Software Status	1	Integer; 0 = Off; 1 = On; 2 = Software control	1,6
209	HTR_2_MODE	Heater 2 (on gimbal electronics housing) control mode	Software Status	1	Integer; 0 = Off; 1 = On; 2 = Software control	1,6
210	HTR_3_MODE	Heater 3 (on cooler radiator) control mode	Software Status	1	Integer; 0 = Off; 1 = On; 2 = Software control	1,6
211	HTR_4_MODE	Heater 4 (on spectrometer housing) control mode	Software Status	1	Integer; 0 = Off; 1 = On; 2 = Software control	1,6
212	COVER_MODE	Cover deployment mode	Software Status	1	Integer; 0 = Disable deployment; 1 = Enable deployment	1,6

Column	Mnemonic	Description	Source of information	Length (bytes)	Format (and range if applicable)	Notes
213	SCAN_MODE	Scan platform control mode	Software Status	1	Integer; 0 = off; 1 = holding; the gimbal is held at the current position; 2 = slewing; the gimbal is moved to a commanded angle; 3 = following a profile; the gimbal follows a computed and uploaded profile; 4 = home; the gimbal searches for its index fiducial	1,6
214	OBS_MAC_ID	Id of most recent observation macro executed	Software Status	3	Integer	1,6
215	SHUTTER_POS	Shutter position from 0 to 32	Software Status	2	Integer; 0 - 32; nominal open is 3; viewing sphere is 17; closed is 32	1,6
216	SHUTTER_DRIVE	Shutter drive selection; VNIR channel for nominal use; IR is backup; both together is contingency for stuck shutter;	Software Status	1	Integer; 0 = IR side; 1 = VNIR side; 2 = both sides	1,6
217	SCAN_LOG_ENB	Scan platform logging enabling; with this enabled requests for spectra return high-rate scan diagnostic data	Software Status	1	Integer; 0 = Disable, 1 = Enable	1,6
218	IR_TEMP_MONITOR	IR temperature monitor enable/disable	Software Status	1	Integer; 0 = Off, 1 = On	1,6
219	IR_EXPOSE	IR exposure time parameter; number of 1/480ths of inverse frame rate	Software Status	3	Integer; 0 - 480	1,6
220	IR_RATE	IR frame acquisition rate	Software Status	1	Integer; 0 = 1 Hz; 1 = 3.75 Hz; 2 = 5 Hz; 3 = 15 Hz; 4 = 30 Hz	1,6
221	VNIR_TEMP_MONITOR	VNIR temperature monitor enable/disable	Software Status	1	Integer; 0 = Off, 1 = On	1,6
222	VNIR_EXPOSE	VNIR exposure time parameter; number of 1/480ths of inverse frame rate	Software Status	3	Integer; 0 - 480	1,6
223	VNIR_RATE	VNIR frame acquisition rate	Software Status	1	Integer; 0 = 1 Hz; 1 = 3.75 Hz; 2 = 5 Hz; 3 = 15 Hz; 4 = 30 Hz	1,6
224	IR_FILTER	IR wavelength filter table; which onboard table is used to define which detector rows are recorded	Software Status	1	Integer; 0 - 3	1,6
225	IR_BINNING	IR pixel binning mode	Software Status	1	Integer; 0 = 1:1, 1 = 2:1, 2 = 5:1, 3 = 10:1	1,6

Column	Mnemonic	Description	Source of information	Length (bytes)	Format (and range if applicable)	Notes
226	IR_LOSSY	IR lossy compression enabled or disabled; 12 to 8 bit look-up table commanded line by line in uploaded data structure	Software Status	1	Integer; 0 = Disable, 1 = Enable	1,6
227	IR_FAST	Enable/disable IR Fast compression	Software Status	1	Integer; 0 = Disable, 1 = Enable	1,6
228	VNIR_FILTER	VNIR wavelength filter table; which onboard table is used to define which detector rows are recorded	Software Status	1	Integer; 0 - 3	1,6
229	VNIR_BINNING	VNIR pixel binning mode	Software Status	1	Integer; 0 = 1:1, 1 = 2:1, 2 = 5:1, 3 = 10:1	1,6
230	VNIR_LOSSY	VNIR lossy compression enabled or disabled; 12 to 8 bit look-up table commanded line by line in uploaded data structure	Software Status	1	Integer; 0 = Disable, 1 = Enable	1,6
231	VNIR_FAST	Enable/disable Fast compression	Software Status	1	Integer; 0 = Disable, 1 = Enable	1,6
232	IR_PIXEL_PROC_CHECKSUM	IR pixel processing table CRC-CCITT checksum; the data structure containing gains offsets and which LUT to use is 480 rows and 3 columns; this is the least significant end of the sum and serves as a fingerprint	Software Status	5	Integer	1,6
233	VNIR_PIXEL_PROC_CHECKSUM	VNIR pixel processing table CRC-CCITT checksum; the data structure containing gains offsets and which LUT to use is 480 rows and 3 columns; this is the least significant end of the sum and serves as a fingerprint	Software Status	5	Integer	1,6

Notes:

- (1) Source of information describes whether information is a value-added field or part of original instrument housekeeping, and if so, the type of housekeeping represented.
- (2) The added parameters represent values calculated in post-processing that are useful to describe frame-dependent data quality, or approximate geometric, lighting, and atmospheric conditions at the time of the observation that are relevant to post-processing corrections.
- (3) The spectrometer image header describes the instrument configuration relevant to an individual frame of data such as exposure time, frame rate, data editing and compression, etc.
- (4) Analog status represents reading of voltage, current and temperature of different components of the CRISM instrument. Monitors are run by different electronics boards in the instrument. The nomenclature is as follows. DPU\_PWR\_0 represents the 0th status item monitored by the DPU power board, DPU\_PWR\_1 the 1st, etc. IR\_PWR is the IR power board in the DPU. VNIR\_PWR is the VNIR power board in the DPU. COOL\_PWR is the cooler power board in the DPU. IR\_FP is the IR focal plane electronics board in the base of the OSU. VNIR\_FP is the VNIR focal plane electronics board in the base

of the OSU.

(5) Digital status represents on/off settings of the instrument, levels of coolers or calibration lamps, or the source of data reported from each focal plane. The source may be measured data from the detector, or one of several test patterns stored in the focal plane electronics (for diagnostic purposes).

(6) Software status represents the status of RAM memory, the frequency of housekeeping reporting, the history of commanding, the history of reporting of alarms, commanded setting of coolers and heaters, and the commanded configuration of the instrument (as opposed to the actual configuration reported in the spectrometer image header).

**Table 3-3. Bit mapping of scan motor status word**

Name	Length (bits)	Value	Description
Direction	1	0 = Down 1 = Up	Platform direction
Index Latch	1	0 = No index 1 = Index seen	Latched (i.e. sticky) index pulse
Limit 2	1	0 = No limit 1 = Limit seen	Latched (i.e. sticky) limit switch #2
Limit 1	1	0 = No limit 1 = Limit seen	Latched (i.e. sticky) limit switch #1
Inphase	1	0 – 1	Raw inphase signal
Quadrature	1	0 – 1	Raw quadrature signal
Index	1	0 = No index 1 = Index	Raw index signal
Hall Sensor	3	0 – 7	Hall sensors
Encoder	22	Signed integer	Encoded scan platform position

**Table 3-4. Bit mapping of scan motor control word**

Name	Length (bits)	Value	Description
Enable Counter	1	0 = Disable 1 = Enable	Enable/disable encoder position counter
Reset Counter	1	0 = No operation 1 = Reset	Reset (i.e. zero) encoder position counter
Reset Index	1	0 = No operation 1 = Reset	Reset index latch
Motor Drive	1	0 = Disable 1 = Enable	Enable/disable motor drive
Test Clock	1	0 = Disable 1 = Enable	Enable/disable sending external clock (for ground testing)
Index Arm	1	0 = No operation 1 = Index	Arm index latch
Hall Latch	1	0 = No operation 1 = Latch	Latch Hall inputs
Hall Control	1	0 = Automatic 1 = Computer	Enable/disable computer control of Hall outputs
Fine Mode	1	0 = Coarse 1 = Fine	Coarse or fine control of motor drive DAC
Reset Limits	1	0 = No operation 1 = Reset	Reset limit latches
Hall Outputs	3	0 – 7	Hall outputs
Drive	12	Signed integer	Motor drive DAC

**Table 3-5. Alarms coded in housekeeping**

ID	Description	Information
0	<i>Unused</i>	
1	Bad packet	0
2	Out of macro contexts	Macro Id
3 ... 15	<i>Reserved</i>	
16	Invalid target id	
17	Scan platform loss of control	
18 ... 127	<i>Reserved</i>	
128 ... 169	Monitored value is too low; see Table 3-6	Value and limit
170 ... 191	<i>Reserved</i>	
192 ... 233	Monitored value is too high; see Table 3-6	Value and limit
234 ... 255	<i>Reserved</i>	

**Table 3-6. Alarms for monitored housekeeping and responses to out-of-limits conditions**

Source	Alarm Ids Low / High		Autonomy Macro Executed	
			Value too Low	Value too High
DPU power board temperature	128	192		
DPU +5 voltage	129	193		
DPU +5 current	130	194		
Scan motor current 1 & 2	131	195		10
IR power board temperature	132	196		5
IR FPU +12 voltage	133	197		
IR FPU +7 voltage	134	198		
IR FPU current	135	199		5
Heater 3 & 4 current	136	200		12
VNIR power board temperature	137	201		4
VNIR FPU +12 voltage	138	202		
VNIR FPU +7 voltage	139	203		
VNIR FPU current	140	204		4
Heater 1 & 2 current	141	205		11
Cooler power board temperature	142	206		8
Cooler +15 voltage	143	207		
Cooler current	144	208		8
HOP heater 1 & 2 current	145	209		13
Shutter motor current (IR)	146	210		7
IR detector temperature 1	147	211	8	
IR detector temperature 2	148	212	8	
Cooler temperature 1	149	213		8
Cooler temperature 2	150	214		8
Cooler temperature 3	151	215		8
Shutter motor temperature (IR)	152	216		
Integrating sphere temperature (IR)	153	217		
Telescope spider temperature (IR)	154	218		
Spectral cavity temperature (IR)	155	219		
OSU cavity temperature (IR)	156	220		
Sphere lamp current (IR)	157	221		14
IR FPU board temperature	158	222		5
HOP temperature (IR)	159	223		13
Shutter motor current (VNIR)	160	224		6
VNIR detector temperature 1	161	225		15
VNIR detector temperature 2	162	226		15
Telescope temperature	163	227		
Optical bench temperature	164	228		
Telescope spider temp. (VNIR)	165	229		
Spectral cavity temperature (VNIR)	166	230		
OSU cavity temperature (VNIR)	167	231		
VNIR FPU board temperature	168	232		4
Baffle temperature	169	233		

### **3.1.2 Label Description**

Each CRISM EDR is described by a PDS label stored in a separate text file with an extension ".LBL". A PDS label is object-oriented and describes objects in the data file. The PDS label contains keywords for product identification, along with descriptive information needed to interpret or process the data objects in the file.

PDS labels are written in Object Description Language (ODL) [5]. PDS label statements have the form of "keyword = value". Each label statement is terminated with a carriage return character (ASCII 13) and a line feed character (ASCII 10) sequence to allow the label to be read by many operating systems. Pointer statements with the following format are used to indicate the location of data objects:

^object = location

where the carat character (^, also called a pointer) is followed by the name of the specific data object. The location is the name of the file that contains the data object.

The CRISM EDR label is a combined-detached label (see reference 5) that describes both the image and table files that make up a CRISM EDR. An example EDR label is in Appendix A.

EDR label keywords with CRISM-specific values are listed in Table 3-7.

**Table 3-7. CRISM-specific values for EDR label keywords**

Keyword	Valid Values
PRODUCT_TYPE	EDR
OBSERVATION_TYPE	FRT (Full Resolution Targeted Observation) HRL (Half Resolution Long Targeted Observation) HRS (Half Resolution Short Targeted Observation) FRS (Full Resolution Short Targeted Observation) ATO (Along-Track Oversampled Targeted Observation) ATU (Along-Track Undersampled Targeted Observation) EPF (Atmospheric Survey EPF) TOD (Tracking Optical Depth Observation) LMB (Limb Scan Observation) MSP (Multispectral Survey) HSP (Hyperspectral Survey) HSV (Hyperspectral Survey, VNIR only) MSW (Multispectral Window) FFC (Flat-field calibration) CAL (Radiometric Calibration) ICL (Calibration source intercalibration) FUN (Functional test) UNK (no valid EDRs within observation that indicate class type)
OBSERVATION_ID	8-byte hexadecimal integer
MRO:OBSERVATION_NUMBER	Counter from product ID, hexadecimal

Keyword	Valid Values
MRO:ACTIVITY_ID	Type of measurement and macro ID ### used to execute it, i.e.: BI### – Bias measurement DF### – Dark field measurement LP### – Lamp measurement SP### – Sphere measurement SC### – Scene measurement T1### – Focal plane electronics test pattern 1 T2### – Focal plane electronics test pattern 1 T3### – Focal plane electronics test pattern 1 T4### – Focal plane electronics test pattern 1 T5### – Focal plane electronics test pattern 1 T6### – Focal plane electronics test pattern 1 T7### – Focal plane electronics test pattern 1 UN### – Instrument configuration does not match macro library
MRO:FRAME_RATE	"1", "3.75", "5", "15", or "30"
MRO:SENSOR_ID	"S" for VNIR, "L" for IR, or "J" for joint
SHUTTER_MODE_ID	"OPEN", "SPHERE", OR "CLOSED"
LIGHT_SOURCE_NAME	"NONE", "VNIR LAMP 1", "VNIR LAMP 2", "IR LAMP 1", "IR LAMP 1", "SPHERE LAMP 1", "SPHERE LAMP 2"
MRO:CALIBRATION_LAMP_STATUS	"OFF", "OPEN LOOP" or "CLOSED LOOP" (for integrating sphere only)
MRO:CALIBRATION_LAMP_LEVEL	Value between 0 and 4095
PIXEL_AVERAGING_WIDTH	1, 2, 5, or 10
COMPRESSION_TYPE	NONE, or 8_BIT
MRO:INSTRUMENT_POINTING_MODE	"DYNAMIC POINTING" if SCAN_MODE (housekeeping file column 213) equals 3; else "FIXED POINTING"
SCAN_MODE_ID	(If DYNAMIC POINTING): "SHORT" (for full-resolution or half-resolution short central swath or limb scan), "LONG" (for half-resolution long central swath), or "EPF" (for EPF even if part of a different class of observation), through 2012. The value has been designated "N/A" since truncated central scans without EPF images were adopted for targeted observations at that time.
SAMPLING_MODE_ID	"HYPERSPECTRAL" if wavelength filter used returns contiguous rows or "MULTISPECTRAL" if not
MRO:EXPOSURE_PARAMETER	The value supplied to the CRISM instrument to command the exposure time. At a given frame rate identified in MRO:FRAME_RATE, there are 480 possible exposure times ranging from 1 to 480.
MRO:WAVELENGTH_FILTER	Which of four onboard menus of rows was selected for downlink. The four choices are 0, 1, 2, or 3.

Keyword	Valid Values
MRO:WAVELENGTH_FILE_NAME	For an EDR, the wavelength file is a 5-column, 480-row text file. The five elements in each row are the row number and a 0 or 1 for each of MRO:WAVELENGTH_FILTER 0, 1, 2 and 3, indicating whether data from that row of the detector is included in the EDR when that option is selected in MRO:WAVELENGTH_FILTER. For a TRDR, the wavelength file is an image whose value at the location of a detector element is the center wavelength of that element, in nanometers.
MRO:PIXEL_PROC_FILE_NAME	For an EDR, the name of the ASCII file giving gain and offset to convert from 14 to 12 bits, and LUT used if lossy 12 to 8 bit compression is enabled (3 columns specified on a line-by-line basis)
MRO:LOOKUP_TABLE_FILE_NAME	(Not used in processing) For an EDR, the name of the ASCII file giving the 8-bit outputs from 12-bit inputs for each of the 8 onboard LUTs (8 columns specified for each 12-bit value 0-4095)

## 3.2 DDR

### 3.2.1 Data Product Structure and Organization

The DDR (Figure 3-8) consists of supporting data needed for the post-processing of a TRDR pointed at Mars' surface. There is a one-for-one spatial correspondence of each spatial pixel in a TRDR to each pixel in the DDR. The DDR for an observation is stored separately from the EDR and TRDR to minimize and streamline data product processing and updating. The EDR does not require highly accurate pointing information to construct, which the DDR does. Thus the EDR can be assembled promptly by having it decoupled from the DDR. A change in instrument calibration - not knowledge of its pointing - would require an update of the contents of the radiance portion of a TRDR but not the contents of the DDR. Thus having the DDR decoupled from the TRDR minimizes the amount of reprocessing necessary when knowledge of instrument radiometric characteristics changes.

The DDR contains one multiple-band image. The size of the multiple-band image varies according to the observation mode but is deterministic given the macro ID. A typical multiple-band image might have XX pixels in the sample (cross-track) dimension, YY pixels in the line (along-track) dimension, and ZZ pixels in the wavelength dimension, where:

- XX=640/binning, where 640 is the number of columns read off the detector, and binning is 1, 2, 5, or 10
- YY=the number of frames of data taken by the macro, and
- ZZ=the number layers in the DDR.

Due to optical distortions present in the EDRs and non-resampled TRDRs, not all wavelengths represent exactly the same spatial location. Therefore the spatial location for a DDR represent those of the VNIR band closest to 610 nm and the IR band closest to 2300 nm. There are separate DDAs for VNIR and IR data.

There are 14 layers in the DDR, all represented as 32-bit real numbers. The files are created at approximately 14 days after transfer of target ID files, when sufficiently accurate pointing information is available.

- Solar incidence angle relative to areoid, at same planetary radius as surface projection of pixel, units degrees
- Emission angle relative to areoid, at same planetary radius as surface projection of pixel, units degrees
- Solar phase angle, units degrees
- Areocentric latitude, units degrees N
- Areocentric longitude, units degrees E
- Solar incidence angle relative to planetary surface as estimated using MOLA shape model, units degrees
- Emission angle relative to planetary surface as estimated using MOLA shape model, units degrees
- Slope magnitude, using MOLA shape model and reference ellipsoid, units degrees
- Slope azimuth, using MOLA shape model and reference ellipsoid, units degrees clockwise from N
- Elevation relative to MOLA datum, units meters
- TES thermal inertia, units  $J\ m^{-2}\ K^{-1}\ s^{-0.5}$
- TES bolometric albedo
- Local solar time, hours
- Spare

Once image data are assembled into EDRs and calibrated into TRDRs, DDRs are created for the data. A version 0 DDR represents values based on predicted pointing, and is generated to provide quick-look information. Version 1 (and any) subsequent versions of a DDR are based on actual, reconstructed pointing.

**DDR = accompanies 1 shutter-open macro**

**1 DDR from each focal plane**

(label points to following files)

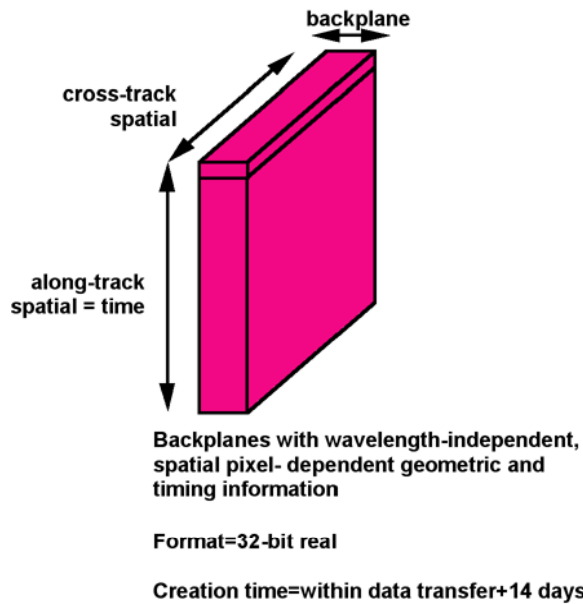


**Figure 3-8.  
Contents of a  
CRISM  
Derived Data  
Record (DDR).**

### **3.2.2 Label Description**

See section 2.3.4 for general information on CRISM product labels. A DDR label is detached and points to the single multiband image in the DDR. An example DDR label is in Appendix B.

DDR label keywords with CRISM-specific values are listed in Table 3-9.

**Table 3-9. CRISM-specific values for DDR label keywords**

Keyword	Valid Values
PRODUCT_TYPE	DDR
OBSERVATION_TYPE	FRT (Full Resolution Targeted Observation) HRL (Half Resolution Long Targeted Observation) HRS (Half Resolution Short Targeted Observation) FRS (Full Resolution Short Targeted Observation) ATO (Along-Track Oversampled Targeted Observation) ATU (Along-Track Undersampled Targeted Observation) EPF (Atmospheric Survey EPF) TOD (Tracking Optical Depth Observation) MSP (Multispectral Survey) HSP (Hyperspectral Survey) HSV (Hyperspectral Survey, VNIR only) MSW (Multispectral Window) FFC (Flat-field calibration)
OBSERVATION_ID	8-byte hexadecimal integer
MRO:OBSERVATION_NUMBER	Counter from product ID, hexadecimal
MRO:ACTIVITY_ID	Only valid value is: DE### – Derived Data
MRO:FRAME_RATE	""1", "3.75", "5", "15", or "30"
MRO:SENSOR_ID	"S" for VNIR, "L" for IR
SHUTTER_MODE_ID	"OPEN"
PIXEL_AVERAGING_WIDTH	1, 2, 5, or 10
MRO:INSTRUMENT_POINTING_MODE	"DYNAMIC POINTING" if SCAN_MODE (housekeeping file column 213) equals 3 ; else "FIXED POINTING"
SCAN_MODE_ID	(If DYNAMIC POINTING): "SHORT" (for full-resolution or half-resolution short central swath), "LONG" (for half-resolution long central swath), or "EPF" (for EPF even if part of a different class of observation), through 2012. The value has been designated "N/A" since truncated central scans without EPF images were adopted for targeted observations at that time.
BAND_NAME	Brief descriptive name of each layer of data in DDR

### 3.3 LDR

#### 3.3.1 Data Product Structure and Organization

The LDR consists of supporting data needed for the post-processing of a TRDR pointed at Mars' limb. The rationale for LDR structure and its geometric relation to a TRDR for a limb scan are similar to that of the DDR. The LDR contains one multiple-band image. The size of the multiple-band image is deterministic given the macro ID and typically the same for all images. A typical multiple-band image might have XX pixels in the sample (cross-track) dimension, YY pixels in the line (along-track) dimension, and ZZ pixels in the wavelength dimension, where:

- XX=640/binning, where 640 is the number of columns read off the detector, and binning is typically 10, for a dimension of 64,

- YY=the number of frames of data taken by the macro, typically 540, and
- ZZ=the number layers in the LDR.

Due to optical distortions present in the EDRs and non-resampled TRDRs, not all wavelengths represent exactly the same spatial location. The spatial location for a LDR represent those of the VNIR band closest to 610 nm and the IR band closest to 2300 nm. There are separate LDRs for VNIR and IR data.

There are 15 layers in the LDR, all represented as 32-bit real numbers. The files are created at approximately 14 days after transfer of target ID files, when sufficiently accurate pointing information is available.

- Solar incidence angle at the areoid, units degrees,
- Emission angle at the areoid, units degrees,
- Phase angle, units degrees,
- Planetocentric latitude at the tangent point of the line of sight, units degrees N,
- Longitude at the tangent point of the line of sight, units degrees E,
- Solar incidence angle at a surface intercept relative to a MOLA shape model, units degrees,
- Emission angle at a surface intercept relative to a MOLA shape model, units degrees,
- Elevation at the tangent point of the line of sight, units meters relative to areoid,
- Elevation at the tangent point of the line of sight, units meters relative to the MOLA shape model,
- Local Solar Time, units hours,
- Ephemeris Time of observation, seconds past noon January 1, 2000"
- Sub-solar planetocentric latitude, units degrees N,
- Sub-solar longitude, units degrees E,
- Sub-spacecraft planetocentric latitude, units degrees N,
- Sub-spacecraft longitude, units degrees E.

Once limb image data are assembled into EDRs, calibrated into TRDRs, and reconstructed pointing is available, LDRs are created for the data. There is no significance to a version 0 or 1.

### **3.3.2 Label Description**

See section 2.3.4 for general information on CRISM product labels. An LDR label is detached and points to the single multiband image in the LDR. An example LDR label is in Appendix H.

DDR label keywords with CRISM-specific values are listed in Table 3-10.

**Table 3-10. CRISM-specific values for LDR label keywords**

Keyword	Valid Values
PRODUCT_TYPE	LDR
OBSERVATION_TYPE	LMB (Limb Scan Observation)
OBSERVATION_ID	8-byte hexadecimal integer
MRO:OBSERVATION_NUMBER	Counter from product ID, hexadecimal
MRO:ACTIVITY_ID	Only valid value is: DE### – Derived data
MRO:FRAME_RATE	"3.75"
MRO:SENSOR_ID	"S" for VNIR, "L" for IR
PIXEL_AVERAGING_WIDTH	10
MRO:INSTRUMENT_POINTING_MODE	"DYNAMIC POINTING"
BAND_NAME	Brief descriptive name of each layer of data in LDR

### 3.4 Targeted RDR

#### 3.4.1 Data Product Structure and Organization

The TRDR consists of the output of one of the constituent macros associated with a target ID that contains scene data (Mars or other), as shown in Figure 3-11. Not all EDRs are processed to TRDR level; macros containing bias, background, sphere, or calibration lamp data are processed instead to CDRs. Only scene EDRs are processed to the TRDR level.

The TRDR contains one or more multiple-band images (suffix \*.IMG). One matches the dimensions of the multiple-band image of raw DN in an EDR, except that the data are in units of radiance. The size of the multiple-band image varies according to the observation mode but is deterministic given the ID of the command macro used to acquire the data. Appended to the multiple-band image is a binary table of the detector rows that were used, as selected by the wavelength filter. This is a one-column table, with each row containing one detector row number expressed as a 16-bit unsigned integer values, most significant bit first.

Other multiple-band images may contain I/F, Lambert albedo, or derived summary products (Table 3-12). The Lambert albedo image, if present, parallels the structure of the I/F image. The summary product image, if present, has the same spatial dimensions, but a different dimension in the spectral direction and it lacks the table of row numbers.

The size of the multiple-band image varies according to the observation mode but is deterministic given the macro ID. A typical multiple-band image might have XX pixels in the sample (cross-track) dimension, YY pixels in the line (along-track) dimension, and ZZ pixels in the wavelength dimension, where:

- XX=640/binning, where binning is 1, 2, 5, or 10
- YY=the number of frames of data taken by the macro, and
- ZZ=the number of detector rows (wavelengths) that are retained by the instrument.

The procedure for deriving this multiple-band image from an EDR is discussed in detail in Appendix L.

Improvements in calibration accuracy (and noise remediation) were added as versions of TRDRs incremented from v0 to v1 to v3 (v2 was developed but not released). Beginning with version 3 TRDRs, filtering is applied to the I/F version of the IR multiband image (not the VNIR multiband image) to reduce effects of propagated noise from ground or inflight calibrations, or from noise in scene measurements (especially those taken later in the mission at higher detector temperatures). The radiance multiband image in version 3 of the TRDRs remains unfiltered for reference. An overview of the filtering procedure is provided in Appendix N. Parameters of the filtering procedure are encoded in labels, beginning in version 3.

The data in a TRDR do not have optical distortions removed. In one column, the projection onto Mars' surface may vary by as much as  $\pm 0.4$  not-binned detector elements in the XX dimension depending on position in the FOV (distortions are worst at the edges of the VNIR and IR FOVs). For a single wavelength, its location in the ZZ direction may vary by as much as  $\pm 1$  not-binned detector elements depending on wavelength and position in the XX direction (distortions are worst at the short- and long-wavelength ends of the IR detector).

Components of the TRDR may be generated at different times. The list file can be created nearly as soon as data are received at the SOC; once the approximate spacecraft pointing information, gimbal position, and tables to convert telemetry from digital to physical units are available. The radiance or I/F multiple-band image requires bracketing sphere observations to process and so it might be delayed one day. Construction of the summary product or Lambert albedo multiband images, if present, requires coregistered MOLA derived data products and thus accurate, reconstructed spacecraft pointing for the data sets. That information will not be available for up to two weeks.

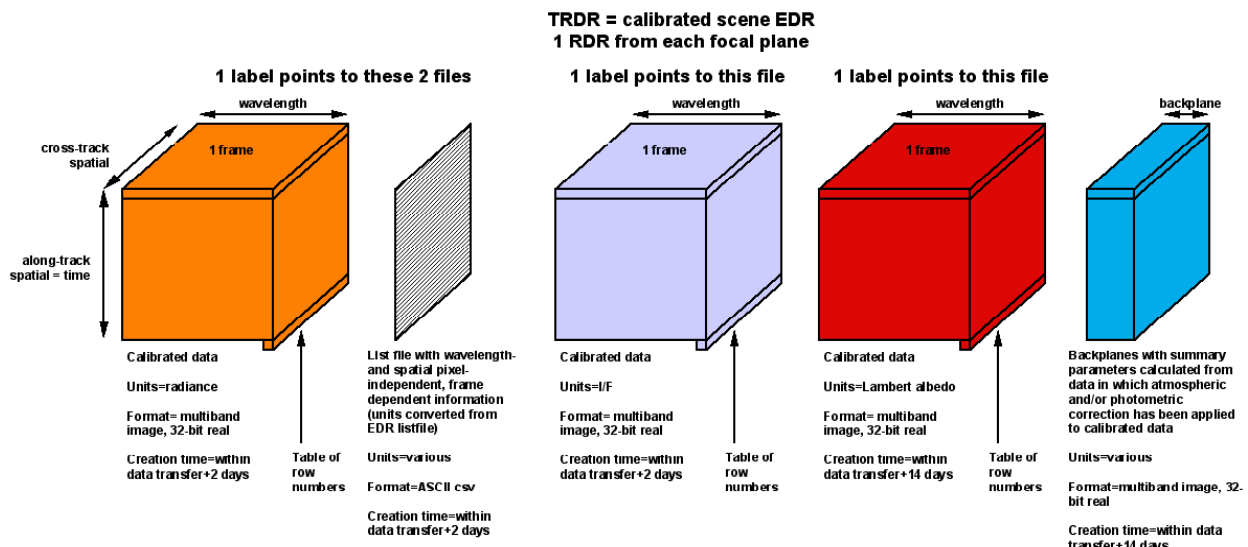


**Figure 3-11. Contents of a CRISM Reduced Data Record for a single observation (TRDR).**

Summary products (or “summary parameters”) are spectral indices that include reflectance at key wavelengths, spectral reflectance ratios, and measures of the wavelength position or depth of various absorptions, and that provide an overview of spectral signatures of phases on the Martian

surface or in the atmosphere. Although they do not by themselves provide definitive detections of phases, they are useful “pointers” and indicators of spatial variations in key spectral signatures. Forty-five summary products were in use at the beginning of CRISM’s orbital measurements of Mars, that were defined base on results from Mars Express OMEGA [Applicable Document 10]. Over the early 2010’s the definitions of products evolved to reduce false positive detections and to serve as indicators of phases previously undetected on Mars that were discovered in early analyses of CRISM measurements [Applicable Document 11]. Table 3-12 describes the various summary products in use during various phases of the MRO mission, their status following the last major revision to summary product definitions in 2014, and the rationales and caveats for the usage of each product. Those with a defined band number of the left-most column are parts of data deliveries after 2014.

Post-2014 (i.e., including TERs, MTRDRs, and v4 MRDRs) summary product definitions are able to work either on the selected wavelengths in multispectral mapping observations or on the continuous wavelength sampling in hyperspectral targeted observations. If the input is hyperspectral data (e.g., calculated from TERs or MTRDRs), the summary products are evaluated at the prescribed wavelengths, to optimize performance and to avoid along-slit wavelength drift. This evaluation is performed using a polynomial fit over the spectral kernel widths stated in Table 3-12. If the input is multispectral data (MRDRs) the evaluation is at the discrete channel nearest in wavelength. “Surface parameters” are evaluated on photometrically corrected I/F following whatever procedure is used to normalize out atmospheric gas absorptions; “atmospheric parameters” are evaluated on photometrically corrected I/F retaining gas features.

The summary parameters are the result of band math calculations – arithmetic functions of multiple spectral bands (Table 3-12) – and are floating point data type. In the majority of parameters (e.g. BD, INDEX type parameters) a featureless spectrum over the applicable wavelength range will result in a parameter value of zero, and the presence of the spectral feature being parameterized will result in a positive parameter value. A negative parameter value indicates that the underlying spectrum has structure that is inverted relative to what is expected for a feature detection – for example a ‘bump’ relative to the continuum where a detection would be a ‘dip’ (absorption feature). Due to residual noise, background spectral variability, and the overprinting of spectral features from differing surface and atmospheric constituents, it is common for the data distribution for a given zero-referenced parameter to be centered at or near zero but include both positive and negative values.

**Table 3-12. Formulation of parameters for summary products**

Summary product unmodified over mission
Minimally revised summary product
Fundamentally revised summary product
New summary product
Depreciated summary product (available in CRISM CAT)

#	NAME	STATUS	PARAMETER	FORMULATION	KERNEL WIDTH	RATIONALE	CAVEATS
<b>Surface Parameters (calculated using TRDR, MRDR, TER, MTRDR Lambert albedo)</b>							
1	R770	✓	0.77-µm reflectance	R770	R770: 5	Higher value more dusty or icy	Sensitive to slope effects, clouds
2	RBR	✓	Red/blue ratio	R770/R440	R440: 5 R770: 5	Higher value has more npFeOx	Sensitive to dust in atmosphere
	BD530	x	0.53-µm band depth	$1 - \left( \frac{R530}{a * R709 + b * R440} \right)$	R440: 5 R530: 5 R709: 5	-	-
3	BD530_2	✓	0.53-µm band depth	$1 - \left( \frac{R530}{a * R614 + b * R440} \right)$	R440: 5 R530: 5 R614: 5	Higher value has more crystalline hematite	-
	SH600	x	0.6-µm shoulder height	$1 - \left( \frac{a * R530 + b * R709}{R600} \right)$	-	-	-
4	SH600_2	✓	0.6-µm shoulder height	$1 - \left( \frac{a * R533 + b * R716}{R600} \right)$	R533: 5 R600: 5 R716: 3	Select ferric minerals, or compacted texture	Sensitive to high opacity in atmosphere
5	SH770	✓	0.77-µm shoulder height	$1 - \left( \frac{a * R716 + b * R860}{R775} \right)$	R716: 3 R775: 5 R860: 5	Select ferric minerals, less sensitive to LCP than SH600_2	Sensitive to high opacity in atmosphere
	BD640	x	0.64-µm band depth	$1 - \left( \frac{R648}{a * R600 + b * R709} \right)$	R600: 5 R648: 5 R709: 5	Select ferric minerals (esp. maghemite)	Obscured by VNIR detector artifact
6	BD640_2	✓	0.64-µm band depth	$1 - \left( \frac{R624}{a * R600 + b * R760} \right)$	R600: 5 R624: 3 R760: 5	Select ferric minerals (esp. maghemite)	Obscured by VNIR detector artifact
	BD860	x	0.86-µm band depth	$1 - \left( \frac{R860}{a * R800 + b * R984} \right)$	-	-	-
7	BD860_2	✓	0.86-µm band depth	$1 - \left( \frac{R860}{a * R755 + b * R977} \right)$	R755: 5 R860: 5 R977: 5	Select ferric minerals (esp. hematite)	-
	BD920	x	0.92 µm band depth	$1 - \left( \frac{R920}{a * R800 + b * R984} \right)$	-	-	-
8	BD920_2	✓	0.92 µm band depth	$1 - \left( \frac{R920}{a * R807 + b * R984} \right)$	R807: 5 R920: 5 R984: 5	Low-Ca pyroxene, crystalline ferric minerals	-
9	RPEAK1 *	✓	Reflectance peak 1	wavelength where 1st derivative=0 of 5th order polynomial fit to R442, R533, R600, R710, R740, R775, R800, R833, R860, R892, R925		Longer wavelength peak in dust	-
10	BDI1000VIS	✓	1-µm integrated band depth; VNIR wavelengths	divide R833, R860, R892, R925, R951, R984, R1023 by RPEAK1 then integrate over (1 - normalized radiances) to get integrated band depth		Crystalline ferrous silicates	-

#	NAME	STATUS	PARAMETER	FORMULATION	KERNEL WIDTH	RATIONALE	CAVEATS
11	BDI1000IR	✓	1-μm integrated band depth; IR wavelengths	divide R1030, R1050, R1080, R1150 by linear fit from peak R (of the 15) between 1.3-1.87μm to R2530 extrapolated backwards, then integrate over (1 – normalized radiances) to get integrated band depth		Ferrous silicate once corrected for aerosol induced slope	–
12	IRA	✓	IR albedo	R1330	R1330: 11	IR albedo	–
	OLINDEX2 (beginning with TRR3)	x	Olivine index 2	(RB1080 * 0.1) + (RB1210 * 0.1) + (RB1330 * 0.4) + (RB1470 * 0.4) Where RB#### = (RC#### - R####)/RC####. RC#### denotes the value of a point at a wavelength of #### nm along a modeled line that follows the average slope of the spectrum. Slope for RC#### anchored at R1750 and R2400.	R1080: 7 R1210: 7 R1330: 7 R1470: 7	Olivines strongly > 0	Also sensitive to HCP, Fe-phyllosilicates
13	OLINDEX3 (beginning with TER, MTRDR)	✓	Olivine index 3	RB1080 * 0.03 + RB1152 * 0.03 + RB1210 * 0.03 + RB1250 * 0.03 + RB1263 * 0.07 + RB1276 * 0.07 + RB1330 * 0.12 + RB1368 * 0.12 + RB1395 * 0.14 + RB1427 * 0.18 + RB1470 * 0.18 Slope for RC#### anchored at R1750 and R2400.	R1080: 7 R1152: 7 R1210: 7 R1250: 7 R1263: 7 R1276: 7 R1330: 7 R1368: 7 R1395: 7 R1427: 7 R1470: 7 R1750: 7 R2400: 7	Olivines strongly > 0	Also sensitive to HCP, Fe-phyllosilicates
	LCPINDEX	x	LCP index	$\frac{(R1330 - R1050)}{(R1330 + R1050)} * \frac{(R1330 - R1815)}{(R1330 + R1815)}$	–	Pyroxene is strongly +; Favors LCP	–
14	LCPINDEX2 (beginning with TER, MTRDR)	✓	Detect broad absorption centered at 1.81 μm (LCP index 2)	RB1690 * 0.20 + RB1750 * 0.20 + RB1810 * 0.30 + RB1870 * 0.30 Slope for RC#### anchored at R1560 and R2450.	R1560: 7 R1690: 7 R1750: 7 R1810: 7 R1870: 7 R2450: 7	Pyroxene is strongly +; Favors LCP	–
	HCPINDEX	x	HCP index	$\frac{(R1470 - R1050)}{(R1470 + R1050)} * \frac{(R1470 - R2067)}{(R1470 + R2067)}$	–	Pyroxene is strongly +; Favors HCP	LCP
15	HCPINDEX2 (beginning with MTRDR)	✓	Detect broad absorption centered at 2.12 μm (HCP index 2)	RB2120 * 0.10 + RB2140 * 0.10 + RB2230 * 0.15 + RB2250 * 0.30 + RB2430 * 0.20 + RB2460 * 0.15 Slope for RC#### anchored at R1810 and R2530.	R1810: 7 R2120: 5 R2140: 7 R2230: 7 R2250: 7 R2430: 7 R2460: 7 R2530: 7	Pyroxene is strongly +; Favors HCP	–
16	BD1300	✓	1.3-μm absorption associated with Fe <sup>2+</sup> substitution in plagioclase	$1 - \left( \frac{R1320}{a * R1080 + b * R1750} \right)$	R1080: 5 R1320: 15 R1750: 5	Plagioclase with Fe <sup>2+</sup> substitution	Fe-rich olivine can be > 0
17	VAR	✓	1.0-2.3-μm spectral variance	Fit a line from 1-2.3 microns and find variance of observed values from fit values by summing in quadrature over the # intervening wavelengths	–	OI & Px will have high values; (to be used w/ OL, PX indices)	–
18	ISLOPE1	✓	Spectral slope 1	$\frac{(R1815 - R2530)}{(W2530 - W1815)}$	R1815: 5 R2530: 5	ferric coating on dark rock	Sensitive to atmospheric hazes

#	NAME	STATUS	PARAMETER	FORMULATION	KERNEL WIDTH	RATIONALE	CAVEATS
19	BD1400	✓	1.4-µm H <sub>2</sub> O & -OH band depth	$1 - \left( \frac{R1395}{a * R1330 + b * R1467} \right)$	R1330: 5 R1395: 3 R1467: 5	Hydrated & hydroxylated minerals	–
20	BD1435	✓	1.435-µm CO <sub>2</sub> ice band depth	$1 - \left( \frac{R1435}{a * R1370 + b * R1470} \right)$	R1370: 3 R1432: 1 R1470: 3	CO <sub>2</sub> ice, some hydrated minerals	–
	BD1500	x	1.5-µm H <sub>2</sub> O ice band depth	$1 - \left( \frac{R1505 + R1558}{R1808 + R1367} \right)$	–	H <sub>2</sub> O ice	–
21	BD1500_2	✓	1.5-µm H <sub>2</sub> O ice band depth	$1 - \left( \frac{R1525}{a * R1367 + b * R1808} \right)$	R1367: 5 R1525: 11 R1808: 5	H <sub>2</sub> O ice	–
	ICER1	✓	CO <sub>2</sub> and H <sub>2</sub> O ice band depth ratio	$R1510/R1430$	R1510: 5 R1430: 5	CO <sub>2</sub> -H <sub>2</sub> O ice mixtures; > 1 for more CO <sub>2</sub> , < 1 for more water	–
22	ICER1_2	✓	CO <sub>2</sub> and H <sub>2</sub> O ice band depth ratio	$1 - \left( \frac{\left( \frac{R1510}{RC1510} \right)}{\left( \frac{R1435}{RC1435} \right)}$ Slope for RC##### anchored at R1850 and R2060.	R1850: 5 R1510: 5 R1435: 5 R2060: 5	CO <sub>2</sub> -H <sub>2</sub> O ice mixtures; > 1 for more CO <sub>2</sub> , < 1 for more water	–
	BD1750	x	1.7-µm H <sub>2</sub> O band depth	$1 - \left( \frac{R1750}{a * R1550 + b * R1815} \right)$	–	Gypsum Alunite	–
23	BD1750_2	✓	1.7-µm H <sub>2</sub> O band depth	$1 - \left( \frac{R1750}{a * R1690 + b * R1815} \right)$	R1690: 5 R1750: 3 R1815: 5	Gypsum Alunite	Don't use on pre-MRDR, TER, MTRDR products
	BD1900	x	1.9-µm H <sub>2</sub> O band depth	$1 - \left( \frac{\left( \frac{R1930 + R1985}{2} \right)}{a * 1875 + b * 2067} \right)$	–	H <sub>2</sub> O in minerals	Weakly sensitive to lo-Ca pyroxene, glass, H <sub>2</sub> O ice
24	BD1900_2	✓	1.9-µm H <sub>2</sub> O band depth	$0.5 * \left( 1 - \left( \frac{R1930}{a * R1850 + b * R2067} \right) \right) + 0.5 * \left( 1 - \left( \frac{R1985}{a * R1850 + b * R2067} \right) \right)$	R1850: 5 R1930: 5 R1985: 5 R2067: 5	H <sub>2</sub> O in minerals	Weakly sensitive to lo-Ca pyroxene, glass, H <sub>2</sub> O ice
	BD1900r	✓	1.95-µm H <sub>2</sub> O band depth	$1 - \left( \frac{R1908 + R1914 + R1921 + R1928 + R1934 + R1941}{R1862 + R1869 + R1875 + R2112 + R2120 + R2126} \right)$	R1862: 1 R1869: 1 R1875: 1 R1908: 1 R1914: 1 R1921: 1 R1928: 1 R1934: 1 R1941: 1 R2112: 1 R2120: 1 R2126: 1	H <sub>2</sub> O in minerals	Weakly sensitive to lo-Ca pyroxene, glass, H <sub>2</sub> O ice
25	BD1900r2	✓	1.95-µm H <sub>2</sub> O band depth	$1 - \left( \frac{\frac{R1908}{RC1908} + \frac{R1914}{RC1914} + \frac{R1921}{RC1921} + \frac{R1928}{RC1928} + \frac{R1934}{RC1934} + \frac{R1941}{RC1941}}{\frac{R1862}{RC1862} + \frac{R1869}{RC1869} + \frac{R1875}{RC1875} + \frac{R2112}{RC2112} + \frac{R2120}{RC2120} + \frac{R2126}{RC2126}} \right)$ Slope for RC##### anchored at R1850 and R2060.	R1850: 1 R1862: 1 R1869: 1 R1875: 1 R1908: 1 R1914: 1 R1921: 1 R1928: 1 R1934: 1 R1941: 1 R2112: 1 R2120: 1 R2126: 1	H <sub>2</sub> O in minerals	Weakly sensitive to lo-Ca pyroxene, glass, H <sub>2</sub> O ice
26	BDI2000	✓	2-µm integrated band depth	divide R1660, R1811, R2009, R2141, R2206, R2253, R2292, R2318, R2352, R2391, R2431, R2457 by linear fit from peak R (of 15) between 1.3-1.87 µm to R2530, then integrate over (1 – normalized radiances) to get integrated band depth	–	Pyroxene, glass	Weakly sensitive to H <sub>2</sub> O ice

#	NAME	STATUS	PARAMETER	FORMULATION	KERNEL WIDTH	RATIONALE	CAVEATS
	BD2100	x	2.1-μm shifted H <sub>2</sub> O band depth (multispectral)	$1 - \left( \frac{(R2120 + R2130)}{2} \right)$	-	H <sub>2</sub> O in monohydrated sulfate	Alunite, Serpentine
27	BD2100_2	✓	2.1-μm shifted H <sub>2</sub> O band depth (hyperspectral)	$1 - \left( \frac{R2132}{a * R1930 + b * R2250} \right)$	R1930: 5 R2132: 5 R2250: 5	H <sub>2</sub> O in monohydrated sulfates	Alunite, Serpentine
28	BD2165	✓	2.165-μm Al-OH band depth	$1 - \left( \frac{R2165}{a * R2120 + b * R2230} \right)$	R2120: 5 R2165: 3 R2230: 3	Pyrophyllite Kaolinite-group	Beidellite Allophane Imogolite
29	BD2190	✓	2.190-μm Al-OH band depth	$1 - \left( \frac{R2185}{a * R2120 + b * R2250} \right)$	R2120: 5 R2185: 3 R2250: 3	Beidellite Allophane Imogolite	Kaolinite-group
30	D2200	✓	2.2-μm dropoff	$1 - \left( \frac{R2210 + R2230}{\frac{RC2210 + RC2230}{2 * \frac{R2165}{RC2165}}} \right)$ Slope for RC##### anchored at R1815 and R2430.	R1815: 7 R2165: 5 R2210: 7 R2230: 7 R2430: 7	Al-OH minerals	Chlorite, Prehnite/Pumpellyite
	DOUB2200_H	x	2.16-μm Si-OH band depth and 2.21-μm H-bound Si-OH band depth (doublet)	$1 - \left( \frac{R2205 + R2258}{R2172 + R2311} \right)$	R2172: 5 R2205: 3 R2258: 3 R2311: 5	Opal and other Si-OH phases	-
31	MIN2200	✓	2.16-μm Si-OH band depth and 2.21-μm H-bound Si-OH band depth (doublet)	$\text{minimum} \left[ \left( 1 - \left( \frac{R2165}{a * R2120 + b * R2350} \right) \right), \left( 1 - \left( \frac{R2210}{a * R2120 + b * R2350} \right) \right) \right]$	R2120: 5 R2165: 3 R2120: 3 R2350: 5	Kaolinite group	-
	BD2210	x	2.21-μm Al-OH band depth	$1 - \left( \frac{R2210}{a * R2120 + b * R2250} \right)$	R2120: 5 R2210: 3 R2250: 5	Al-OH minerals	Gypsum, Alunite
32	BD2210_2	✓	2.21-μm Al-OH band depth	$1 - \left( \frac{R2210}{a * R2165 + b * R2290} \right)$	R2165: 5 R2210: 5 R2290: 5	Al-OH minerals	Gypsum, Alunite
33	BD2230	✓	2.23-μm band depth	$1 - \left( \frac{R2235}{a * R2210 + b * R2252} \right)$	R2210: 3 R2230: 3 R2252: 3	Hydroxylated ferric sulfate	Al-OH minerals
34	BD2250	✓	2.25-μm broad Al-OH and Si-OH band depth	$1 - \left( \frac{R2245}{a * R2120 + b * R2340} \right)$	R2120: 5 R2245: 7 R2340: 3	Opal and other Si-OH minerals	-
35	MIN2250 (beginning with TER, MTRDR)	✓	2.21-μm Si-OH band depth and 2.26-μm H-bound Si-OH band depth	$\text{minimum} \left[ \left( 1 - \left( \frac{R2210}{a * R2165 + b * R2350} \right) \right), \left( 1 - \left( \frac{R2265}{a * R2165 + b * R2350} \right) \right) \right]$	R2165: 5 R2210: 3 R2265: 3 R2350: 5	Opal	-
36	BD2265 (beginning with TER, MTRDR)	✓	2.265-μm band depth	$1 - \left( \frac{R2265}{a * R2210 + b * R2295} \right)$	R2210: 5 R2265: 3 R2295: 5	Jarosite Gibbsite Acid-treated nontronite	-
37	BD2290	✓	2.3-μm Mg,Fe-OH band depth / 2.292-μm CO <sub>2</sub> ice band depth	$1 - \left( \frac{R2290}{a * R2250 + b * R2350} \right)$	R2250: 5 R2290: 5 R2350: 5	Mg,Fe-OH minerals	Mg-Carbonate; Also CO <sub>2</sub> ice
38	D2300	✓	2.3-μm dropoff	$1 - \left( \frac{R2290 + R2320 + R2330}{\frac{RC2290 + RC2320 + RC2330}{\frac{R2120 + R2170 + R2210}{RC2120 + RC2170 + RC2210}}} \right)$ Slope for RC##### anchored at R1815 and R2530.	R1815: 5 R2120: 5 R2170: 5 R2210: 5 R2290: 3 R2320: 3 R2330: 3 R2530: 5	Mg,Fe-OH minerals	Mg-Carbonate; Also CO <sub>2</sub> ice

#	NAME	STATUS	PARAMETER	FORMULATION	KERNEL WIDTH	RATIONALE	CAVEATS
39	BD2355	✓	2.35-μm band depth	$1 - \left( \frac{R2355}{a * R2300 + b * R2450} \right)$	R2300: 5 R2355: 5 R2450: 5	Chlorite Prehnite Pumpellyite	Requires normalization of atmo. CO absorption
	SINDEX	x	Detects convexity at 2.29 μm due to absorptions at 1.9/2.1 μm & 2.4 μm	$1 - \left( \frac{R2100 + R2400}{2 * R2290} \right)$	—	Mono and polyhydrated sulfates) will be > 0	—
40	SINDEX2	✓	Inverse lever rule to detect convexity at 2.29 μm due to absorptions at 1.9/2.1 μm & 2.4 μm	$1 - \left( \frac{a * R2120 + b * R2400}{R2290} \right)$	R2120: 5 R2290: 7 R2400: 3	Mono and polyhydrated sulfates) will be > 0	—
	ICER2	x	2.7-μm CO2 ice band	$R2530/R2600$	—	CO2 vs water ice /soil; CO2 will be >>1, water and soil will be ~1	—
41	ICER2	✓	2.7-μm CO2 ice band	$RB2600$ Where $RB#### = (RC#### - R####)/RC####$ . $RC####$ denotes the value of a point at a wavelength of #### nm along a modeled line that follows the average slope of the spectrum. Slope for $RC####$ anchored at R2456 and R2530.	R2456: 5 R2530: 5 R2600: 5	CO2 vs water ice /soil; CO2 will be >>0, water and soil will be ~0	—
	BDCARB	x	Carbonate overtone band depth, or metal-OH band	$1 - \sqrt{\left( \frac{R2330}{a * R2230 + b * R2390} \right) * \left( \frac{R2530}{c * R2390 + d * R2600} \right)}$	—	Carbonates; both overtones need to be present to increase parameter value	Many hydroxylated silicate phases
42	MIN2295_2480 (beginning with TER, MTRDR)	✓	Mg Carbonate overtone band depth and metal-OH band	$minimum \left[ \left( 1 - \left( \frac{R2295}{a * R2165 + b * R2364} \right) \right), \left( 1 - \left( \frac{R2480}{a * R2364 + b * R2570} \right) \right) \right]$	R2165: 5 R2295: 5 R2364: 5 R2480: 5 R2570: 5	Mg -carbonates or hydroxylated silicate; both overtones need to be present to increase parameter value	—
43	MIN2345_2537 (beginning with MTRDR)	✓	Ca/Fe Carbonate overtone band depth and metal-OH band	$minimum \left[ \left( 1 - \left( \frac{R2345}{a * R2250 + b * R2430} \right) \right), \left( 1 - \left( \frac{R2537}{a * R2430 + b * R2602} \right) \right) \right]$	R2250: 5 R2345: 5 R2430: 5 R2537: 5 R2602: 5	Ca/Fe - carbonates or hydroxylated silicate; both overtones need to be present to increase parameter value	Prehnite, Serpentine
	BD2500H	x	Mg Carbonate overtone band depth	$1 - \left( \frac{R2500 + R2510}{R2540 + R2380} \right)$	R2380: 5 R2500: 5 R2510: 5 R2540: 5	Mg-carbonates	Some zeolites
44	BD2500_2	✓	Mg Carbonate overtone band depth	$1 - \left( \frac{R2480}{a * R2364 + b * R2570} \right)$	R2364: 5 R2480: 5 R2570: 5	Mg-carbonates	Some zeolites
45	BD3000	✓	3-μm H2O band depth	$1 - \left( \frac{R3000}{R2530 * \left( \frac{R2530}{R2210} \right)} \right)$	R2210: 5 R2530: 5 R3000: 5	bound H2O (accounts for spectral slope)	—
46	BD3100	✓	3.1-μm H2O ice band depth	$1 - \left( \frac{R3120}{a * R3000 + b * R3250} \right)$	R3000: 5 R3120: 5 R3250: 5	H2O ice	—
47	BD3200	✓	3.2-μm CO2 ice band depth	$1 - \left( \frac{R3320}{a * R3250 + b * R3390} \right)$	R3250: 5 R3320: 5 R3390: 5	CO2 ice	—
48	BD3400	✓	3.4-μm carbonate band depth	$1 - \left( \frac{a * R3390 + b * R3500}{c * R3250 + d * R3630} \right)$	—	carbonates	—

#	NAME	STATUS	PARAMETER	FORMULATION	KERNEL WIDTH	RATIONALE	CAVEATS
49	BD3400_2	✓	3.4-µm carbonate band depth	$1 - \left( \frac{R3420}{a * R3250 + b * R3630} \right)$	R3250: 10 R3420: 15 R3630: 10	carbonates	–
50	CINDEX	✓	3.9-µm carbonate index	$\left( \frac{R3750 + \frac{(R3750 - R3630)}{(3750 - 3630) * (3950 - 3750)}}{R3950} \right) - 1$	–	carbonates will be > 'bkgrnd' values > 0	–
51	CINDEX2	✓	Inverse lever rule to detect convexity at 3.6 µm due to absorptions at 3.4 µm & 3.9 µm	$1 - \left( \frac{a * R3450 + b * R3875}{R3610} \right)$	R3450: 9 R3610: 11 R3875: 7	carbonates will be > 'bkgrnd' values > 0	–

**Atmospheric Parameters (calculated using TRDR, MRDR, TER, MTRDR photometrically corrected I/F)**

52	R440	✓	0.44-µm reflectance	$R440$	R440: 5	Clouds/Hazes	–
53	IRR1	✓	IR ratio 1	$R800/R1020$	R800: 5 R1020: 5	Aphelion ice clouds (>1) vs. seasonal or dust (< 1)	–
54	BD2600	✓	2.6-µm H2O band depth	$1 - \left( \frac{R2600}{a * R2530 + b * R2630} \right)$	R2530: 5 R2600: 5 R2630: 5	H2O vapor (accounts for spectral slope)	–
55	IRR2	✓	IR ratio 2	$R2530/R2210$	R2210: 5 R2350: 5	aphelion ice clouds vs. seasonal or dust	–
56	IRR3	✓	IR ratio 3	$R3500/R3390$	R3390: 7 R3500: 7	aphelion ice clouds (higher values) vs. seasonal or dust	–

### **3.4.2 Label Description**

See section 2.3.4 for general information on CRISM product labels. A TRDR contains two labels, both detached. One points to both the multiband radiance image and the housekeeping listfile. A second label points to the multiband summary product image, if it is present. An example TRDR label is in Appendix C.

TRDR label keywords with CRISM-specific values are listed in Table 3-13.

**Table 3-13. CRISM-specific values for TRDR label keywords**

Keyword	Valid Values
PRODUCT_TYPE	TARGETED_RDR
OBSERVATION_TYPE	FRT (Full Resolution Targeted Observation) HRL (Half Resolution Long Targeted Observation) HRS (Half Resolution Short Targeted Observation) FRS (Full Resolution Short Targeted Observation) ATO (Along-Track Oversampled Targeted Observation) ATU (Along-Track Undersampled Targeted Observation) EPF (Atmospheric Survey EPF) TOD (Tracking Optical Depth Observation) LMB (Limb Scan Observation) MSP (Multispectral Survey) HSP (Hyperspectral Survey) HSV (Hyperspectral Survey - VNIR only, pixels 10x-binned) MSV (Hyperspectral Survey - VNIR only, pixels 5x-binned) MSW (Multispectral Window) FFC (Flat-field calibration)
OBSERVATION_ID	8-byte hexadecimal integer
MRO:OBSERVATION_NUMBER	Counter from product ID, hexadecimal
MRO:ACTIVITY_ID	RA### – Radiance IF### – I/F AL### – Lambert albedo SU### – Summary products
MRO:FRAME_RATE	""1", "3.75", "5", "15", or "30"
MRO:SENSOR_ID	"S" for VNIR, or "L" for IR
SHUTTER_MODE_ID	The only valid value is "OPEN"
LIGHT_SOURCE_NAME	The only valid value is "NONE"
MRO:CALIBRATION_LAMP_STATUS	The only valid value is "OFF"
MRO:CALIBRATION_LAMP_LEVEL	The only valid value is 0
PIXEL_AVERAGING_WIDTH	1, 2, 5, or 10

Keyword	Valid Values
MRO:INSTRUMENT_POINTING_MODE	"DYNAMIC POINTING" if SCAN_MODE (housekeeping file column 213) equals 3; else "FIXED POINTING"
SCAN_MODE_ID	(If DYNAMIC POINTING): "SHORT" (for full-resolution or half-resolution short central swath, or limb scan observation), "LONG" (for half-resolution long central swath), or "EPF" (for EPF even if part of a different class of observation), through 2012. The value has been designated "N/A" since truncated central scans without EPF images were adopted for targeted observations at that time.
SAMPLING_MODE_ID	"HYPERSPECTRAL" if wavelength filter used returns contiguous rows or "MULTISPECTRAL" if not
MRO:EXPOSURE_PARAMETER	The value supplied to the CRISM instrument to command the exposure time. At a given frame rate identified in MRO:FRAME_RATE, there are 480 possible exposure times ranging from 1 to 480.
MRO:WAVELENGTH_FILTER	Which of four onboard menus of rows was selected for downlink. The four choices are 0, 1, 2, or 3.
MRO:WAVELENGTH_FILE_NAME	For an EDR, the wavelength file is a 5-column, 480-row text file. The five elements in each row are the row number and a 0 or 1 for each of MRO:WAVELENGTH_FILTER 0, 1, 2 and 3, indicating whether data from that row of the detector is included in the EDR when that option is selected in MRO:WAVELENGTH_FILTER. For a TRDR, the wavelength file is an image whose value at the location of a detector element is the center wavelength of that element, in nanometers.
MRO:PIXEL_PROC_FILE_NAME	For a TRDR, the name of the ASCII file giving gain and offset to convert from 14 to 12 bits, and LUT used if lossy 12 to 8 bit compression is enabled (3 columns specified on a line-by-line basis)
MRO:INV_LOOKUP_TABLE_FILE_NAME	For a TRDR, the name of the ASCII file giving the inverse translation from 8 to 12 bits if 12 to 8 bit compression was enabled (not used in flight)
MRO:INVALID_PIXEL_LOCATION	(In v2 and earlier) X,Y,Z locations within a TRDR at which data values are invalid because they represent cosmic ray hits (not currently used)
MRO:REPLACED_PIXEL_LOCATION	(In v2 and earlier) X,Y,Z locations within a TRDR at which data values were replaced by interpolating from surrounding pixels

Keyword	Valid Values
MRO:ATMO_CORRECTION_FLAG	Whether or not a correction has been performed for photometric and atmospheric effects; "OFF" or "ON"
MRO:THERMAL_CORRECTION_MODE	Whether and what type of thermal correction has been performed to calibrated data. Valid values are "OFF", "CLIMATOLOGY;ADR_CL", "EMPIRICAL_MODEL_FROM_SPECTRUM;ALG_M", "PHYSICAL_MODEL;ADR_TE", or "N/A".
MRO:PHOTOCLIN_CORRECTION_FLAG	Valid only in the case where the value of keyword MRO:THERMAL_CORRECTION_MODE is PHYSICAL_MODEL;ADR_TE. If MRO:PHOTOCLIN_CORRECTION_FLAG is OFF, then slopes used to calculate temperature come from the companion DDR. If it is ON, then the slopes are calculated using photocalinometry of CRISM data (not used in flight)
MRO:SPATIAL_SUBSAMPLING_FLAG	If = 1, keystone corrected to 610 or 2300 nm by cubic resampling
MRO:SPATIAL_SUBSAMPLING_FILE	If MRO:SPATIAL_SUBSAMPLING_FLAG=1, name of instrument kernel or "CM" CDR used
MRO:SPATIAL_RESCALING_FLAG	If =1, VNIR rescaled to IR- 2300 nm - by cubic resampling
MRO:SPATIAL_RESCALING_FILE	If MRO:SPATIAL_RESCALING_FLAG=1, name of instrument kernel or "CM" CDR and frames kernel used
MRO:SPECTRAL_RESAMPLING_FLAG	If =1, nearest-neighbor spectral resampling has been performed
MRO:SPECTRAL_RESAMPLING_FILE	If MRO:SPECTRAL_RESAMPLING_FLAG=1, names of "PS" CDR used
MRO:HDF_SOFTWARE_NAME	Name of the CRISM hyperspectral data filter software used to process radiance TRDR data to I/F
MRO:HDF_SOFTWARE_VERSION_ID	Version of the software used by the CRISM hyperspectral data filter application
MRO:IF_MIN_VALUE	Control parameter for iterative kernel filter (IKF) used to convert IR radiance to I/F; minimum valid value of I/F. Values outside valid range are ignored during preprocessing
MRO:IF_MAX_VALUE	Maximum valid value of I/F for IR IKF
MRO:TRACE_MIN_VALUE	Control parameter for Ratio Shift Correction (RSC) used to convert VNIR and IR radiance to I/F; minimum valid value of a computed ratio. Values outside of the range are ignored during this processing step
MRO:TRACE_MAX_VALUE	Maximum valid value of I/F for RSC

Keyword	Valid Values
MRO:REFZ_MEDIAN_BOX_WIDTH	IKF control parameter; kernel size of a median filter used in the spectral direction in the computation of the reference cube during the preprocessing steps
MRO:REFZ_SMOOTH_BOX_WIDTH	IKF control parameter; kernel size of a boxcar smoothing filter used in the spectral direction in the computation of the reference cube during the preprocessing steps
MRO:FRAM_STAT_MEDIAN_BOX_WIDTH	IKF control parameter; kernel size of a median filter used on the frame median profile in the computation of bad frames during preprocessing steps
MRO:FRAM_STAT_MIN_DEVIATION	IKF control parameter; minimum deviation from the mean of an element of the normalized frame median profile necessary to be classified as a bad frame during preprocessing steps
MRO:FRAM_STAT_MEDIAN_CONF_LVL	IKF control parameter; the confidence level for the Grubb's Test used for outlier detection of elements of the normalized median frame profile in the detection of bad frames during preprocessing steps; typical values near 0.95
MRO:FRAM_STAT_IQR_CONF_LVL	IKF control parameter; the confidence level for the Grubb's Test used for outlier detection of elements of the normalized median profile of the frame interquartile range in the detection of bad frames during preprocessing steps; typical values near 0.95
MRO:RSC_REF_XY_MEDIAN_WIDTH	RSC control parameter; kernel size of a median filter used in the XY direction while computing the reference cube during the preprocessing steps
MRO:RSC_REF_XY_SMOOTH_WIDTH	RSC control parameter; kernel size of a boxcar smoothing filter used in the XY direction while computing the reference cube during the preprocessing steps
MRO:RSC_REF_YZ_MEDIAN_WIDTH	RSC control parameter; kernel size of a median filter used in the YZ direction while computing the reference cube during the preprocessing steps
MRO:RSC_REF_YZ_SMOOTH_WIDTH	RSC control parameter; kernel size of a boxcar smoothing filter used in the YZ direction while computing the reference cube during the preprocessing steps
MRO:RSC_RATIO_XY_MEDIAN_WIDTH	RSC control parameter; kernel size of a median filter used in the XY direction while computing the ratio cube during preprocessing steps
MRO:RSC_RATIO_XY_SMOOTH_WIDTH	RSC control parameter; kernel size of a smoothing boxcar filter used in the XY direction while computing the ratio cube during preprocessing steps

Keyword	Valid Values
MRO:RSC_RES_XY_PLY_ORDER	RSC control parameter; the order of the polynomial used to model low frequency content in the XY direction used as part of the RSC while computing the resolve cube during post processing steps
MRO:RSC_RES_XY_PLY_EXTND_WIDTH	RSC control parameter; number of pixels used to extend the trend of the column profiles when computing the polynomial used to model low frequency content in the XY direction used as part of the RSC while computing the resolve cube during the post processing steps
MRO:LOG_XFORM_NEG_CLIP_VALUE	IKF control parameter; value used for a negative I/F in the log base10 transform; represents minimum possible output pixel value for IKF procedure
MRO:IKF_NUM_REGIONS	IKF control parameter; number of spectral regions for application of IKF procedure
MRO:IKF_START_CHANNEL	IKF control parameter; number of first channel in a given spectral region for application of IKF procedure
MRO:IKF_STOP_CHANNEL	IKF control parameter; number of last channel in a given spectral region for application of IKF procedure
MRO:IKF_CONFIDENCE_LEVEL	IKF control parameter; confidence level for Grubb's Test used for outlier detection of elements of model residuals in IKF procedure; typical values near 0.95
MRO:IKF_WEIGHTING_STDDEV	IKF control parameter; weighting parameter for final model evaluation in IKF procedure
MRO:IKF_KERNEL_SIZE_X	IKF control parameter; size of the kernel in the X direction used in the IKF procedure
MRO:IKF_KERNEL_SIZE_Y	IKF control parameter; size of the kernel in the Y direction used in the IKF procedure
MRO:IKF_KERNEL_SIZE_Z	IKF control parameter; size of the kernel in the Z direction used in the IKF procedure
MRO:IKF_MODEL_ORDER_X	IKF control parameter; dimensionality of the model in the X direction used in the IKF procedure
MRO:IKF_MODEL_ORDER_Y	IKF control parameter; dimensionality of the model in the Y direction used in the IKF procedure
MRO:IKF_MODEL_ORDER_Z	IKF control parameter; dimensionality of the model in the Z direction used in the IKF procedure
BAND_NAME	Brief descriptive name of each layer of data in the summary product multi-band image. Values transitioned in 2014 following redefinition of summary product definitions. See Table 3-12.

## 3.5 Map-Projected Multispectral RDR

### 3.5.1 Data Product Structure and Organization

An MRDR (Figure 3-14) consists of mosaicked, map-projected VNIR+IR multispectral survey TRDRs, plus VNIR+IR hyperspectral survey TRDRs downsampled spectrally to earlier multispectral wavelengths. All data are represented as 32-bit real numbers. The files are updated infrequently, when a large amount of new coverage or new processing procedures are available. The multispectral map RDR contains up to five multiple-band images at 256 pixels/degree (v1, v3) or 327 pixels/degree (v4), and one list file containing wavelengths of the multispectral data.

The first multiple-band image, if present, is map-projected I/F without any further corrections applied, taken directly from the TRDR associated with a strip of multispectral data. Although in the TRDRs there are separate multiple-band images for the VNIR and IR detectors, in this case the data are merged. The size of the multiple-band image varies between map tiles. A typical multiple-band image might have 1280 pixels in the latitude direction, a variable number of pixels in the longitude direction, and approximately 72 pixels in the wavelength dimension, representing each of the selected channels in multispectral mode. This serves as a backup to the Lambert albedo image if it is not present, or for when Lambert albedo processing was in early development.

The second multiple-band image, if present, is geometrically identical to the map-projected I/F multiple-band image, except that the data have been processed using the ADR binary tables and other subsequent steps as described in Appendix P3 to Lambert albedo (the estimated surface contribution to reflected I/F, divided by  $\cos i$ ).

The third and fourth multiple-band images, if present, contain map-projected data from the DDRs associated with strips of multispectral data, used to derive I/F from radiance. One file corresponds to the I/F image, and one file corresponds to the Lambert albedo image (the component image strips may be fewer in the Lambert albedo file). In each of these, 11 additional layers are specific to individual multispectral strips used to assemble the tile, and are not contained in source DDRs.

- Solar longitude, units degrees
- Solar distance at time of measurement, units AU
- VNIR OBSERVATION\_ID of constituent measurement
- IR OBSERVATION\_ID of constituent measurement
- The VNIR OBSERVATION\_NUMBER carried through from the source scene EDRs;
- The IR OBSERVATION\_NUMBER carried through from the source scene EDRs;
- The VNIR LINE\_SAMPLE carried through from the temporary TRDR used to populate the MRDR; this identifies the VNIR wavelength calibration at the spatial pixel of the MRDR
- The IR LINE\_SAMPLE carried through from the temporary TRDR used to populate the MRDR; this identifies the IR wavelength calibration at the spatial pixel of the MRDR

- The LINE\_SAMPLE from the source VNIR TRDR; this together with column number, observation ID, and ordinal counter provides traceability back to a spatial pixel in a source EDR
- The LINE from the source IR TRDR
- The LINE from the source VNIR TRDR

The fifth multiple-band image contains map-projected summary products from multispectral data. The listfile, in ASCII format, contains wavelengths of each layer in the Lambert albedo and I/F images

Three versions of MRDRs have been released, with version numbers loosely keyed to calibration version numbers of input TRDRs. Which multiband images are present differ with version depending on the development status of the processing pipeline. Versions 1 and 3 have included content from TRDRs of mapping data having the corresponding version numbers. Summary product values at a given column within a strip are normalized to their along-track values as a first order correction for optical artifacts. There are no corrections for stochastic noise or inter-strip residuals due to calibration artifacts or differences in atmospheric opacity. V1 contains all five multiband images; V3 contains updated uncorrected I/F and the corresponding derived data.

Version 4 uses v3 radiometric calibration, but adopts a different approach to populating map tiles with strips of mapping data. For individual input mapping strips, the remediation of systematic optical and calibration artifacts is included at the input strip level (adapted from v3 TERs and MTRDRs). Prior to tile assembly, corrected I/F values for Lambert albedo and summary product files are subjected to a normalization procedure to minimize differences between overlapping strips of mapping data, using as reference data acquired under clear atmospheric conditions early in the mission when the IR detector was operated at its coldest with the least noise. Appendix P3 provides further detail. As this is the ultimate version of MRDRs, only Lambert albedo, corresponding derived data, and summary product multiband images are present.

### **3.5.2 Map projection standards**

Areocentric latitude and longitude, incidence, emission, and phase angles are derived from spacecraft attitude, gimbal position, pixel location, and MOLA shape model of Mars. The adopted projection convention is planetocentric, positive east, using the 2000 IAU prime meridian and pole of rotation. The projection varies in 5° latitude bands, using EQUIRECTANGULAR equatorward of 87.5° latitude and POLAR STEREOGRAPHIC poleward of that latitude. For the latitude bands projected equirectangularly, the center latitude of projection is the center of each tile to minimize "distortion." For the latitude band projected polar stereographically, in the north 0° longitude is down, and in the south 0° longitude is up.

For multispectral RDRs, the planet is divided into 1964 non-overlapping tiles as shown in Figure 2-10. Their longitude width increases poleward to keep tiles approximately the same in area. Through v3 they were structured with 256 pixels/degree (ppd). Beginning in v4, the map tiles are structured at 327 ppd to better match the native resolution of the data.

The multiband images are accompanied in the BROWSE directory by browse products, which are composed of thematically related byte-scaled spectral summary products and are described in detail in Section 3.11.3.

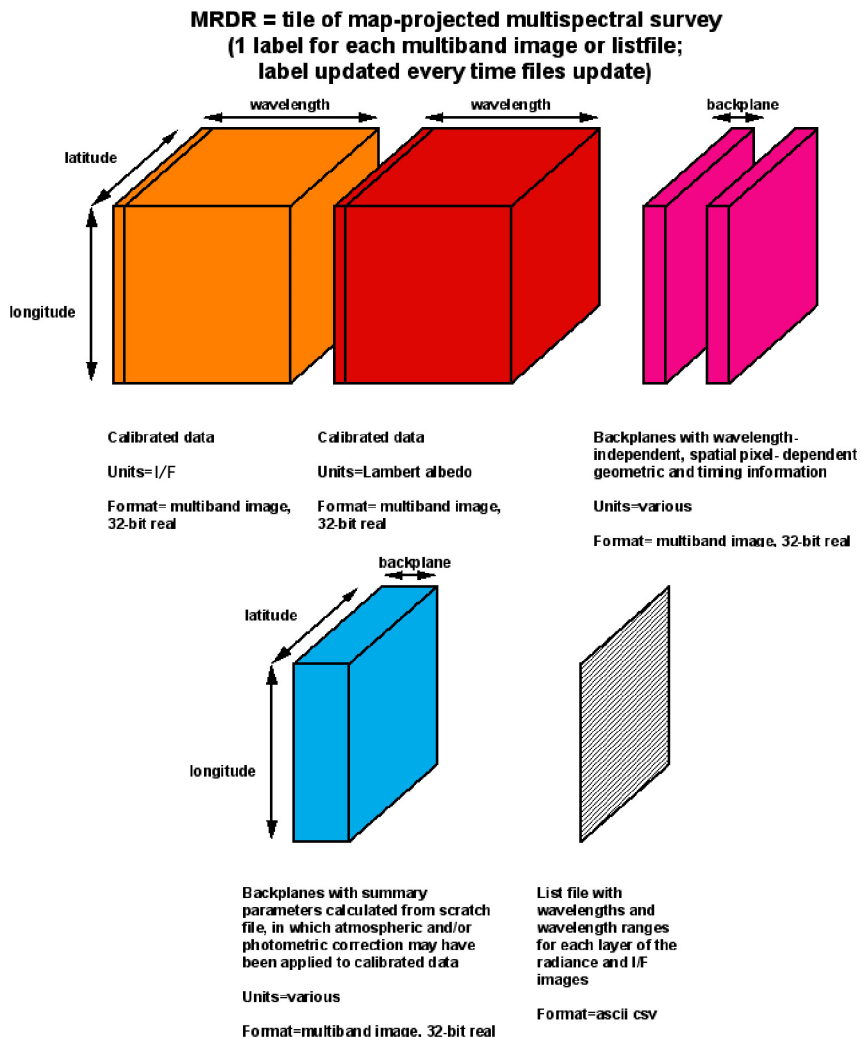


**Figure 3-14. Contents of a CRISM Reduced Data Record for a multispectral map tile (MRDR).**

### 3.5.3 Label Description

See section 2.3.4 for general information on CRISM product labels. Each component file of the MRDR has a single label pointing to it. An example MRDR label is in Appendix D.

MRDR label keywords with CRISM-specific values are listed in Table 3-15.

**Table 3-15. CRISM-specific values for MRDR label keywords**

Keyword	Valid Values
PRODUCT_TYPE	MAP_PROJECTED_MULTISPECTRAL_RDR
BAND_NAME	Brief descriptive name of each layer of data in the summary product multi-band image or the geometric/timing multi-band image. See Table 3-12.
MRO:ATMO_CORRECTION_FLAG	Whether or not a correction has been performed for photometric and atmospheric effects; "OFF" or "ON"
MRO:PHOTOCLIN_CORRECTION_FLAG	Validity only in the case where the value of keyword MRO:THERMAL_CORRECTION_MODE is PHYSICAL_MODEL;ADR_TE. If MRO:PHOTOCLIN_CORRECTION_FLAG is OFF, then slopes used to calculate temperature come from the companion DDR. If it is ON, then the slopes are calculated using photoclinometry of CRISM data
MRO:THERMAL_CORRECTION_MODE	Whether and what type of thermal correction has been performed to calibrated data. Valid values are "OFF", "CLIMATOLOGY;ADR_CL", "EMPIRICAL_MODEL_FROM_SPECTRUM;ALG_M", "PHYSICAL_MODEL;ADR_TE", or "N/A"

## 3.6 Targeted Empirical Record (TER) and Map-projected Targeted Reduced Data Record (MTRDR)

### 3.6.1 Data Product Structure and Organization

A Targeted Empirical Record (TER) spectral product is a spatially reconciled (coregistered VNIR and IR; S- and L- detector), full spectral range (VNIR and IR; S- and L- detector) I/F targeted observation central scan image cube in the IR (L-detector) sensor space that has been corrected for geometric, photometric, atmospheric, and instrumental effects. The corresponding Map-projected Targeted Reduced Data Record (MTRDR) (Figure 3-16) spectral product consists of the TER corrected I/F spectral information after map projection and the removal of spectral channels with suspect radiometry (“bad bands”). The MTRDR spectral product is similar in concept to a local, high-resolution map tile comparable to an MRDR, but at ~12 or ~6 times higher spatial resolution with hyperspectral sampling. The TER/MTRDR product set includes a hyperspectral image cube in units of corrected I/F (IF), spectral summary parameters (SU) derived from the corrected spectral reflectance data, residual noise-remediated refined spectral summary parameters (SR), browse products (BR) derived from the refined spectral summary parameters, data processing information maps (IN), a map projected version of the associated IR (L-detector) DDR (DE) (MTR product only), and a text table that lists wavelength information (WV) for the spectral image cube. All of the image cubes are 32-bit real, with the exception of the browse products which have been byte-scaled (8-bit). A detailed description of the TER/MTRDR data processing is provided in Appendix P1.

The primary TER/MTRDR data products are hyperspectral images cubes (IF) with units of corrected I/F in the IR (L-detector) sensor space (TER) and map-projected according to MRO

project standards (MTR). A typical MTR hyperspectral image cube (with an equirectangular map projection) has XX pixels in the longitude dimension, YY pixels in the latitude dimension, and ZZ pixels in the wavelength dimension, where XX and YY depend on the source data characteristics and target location, and ZZ is the number of channels retained in the product across the full spectral range. Spatial dimensions are consistent across all genetically related (common source Target ID) TER and MTR product sets.

The spectral summary products (SU; defined in Table 3-12) are multi-band image cubes composed of the results of a suite of spectral band math calculations designed to parameterize the known surface mineralogical diversity. The CRISM spectral summary parameter library has been significantly revised and expanded in association with the TER/MTRDR development and is documented in Applicable Document [11]. The refined summary parameter products (SR) have been post-processed to remove the most egregious effects of spectral noise.

The browse products are composed of thematically related byte-scaled spectral summary products and are described in detail in Section 3.11.3.

The data processing information (IN) products are multi-band image cubes that provide visibility into TER/MTRDR data processing pipeline residuals in a spatial frame consistent with the TER/MTRDR data product suite.

The table file, in ASCII format, contains wavelength information for each spectral band in the corrected I/F image cube.

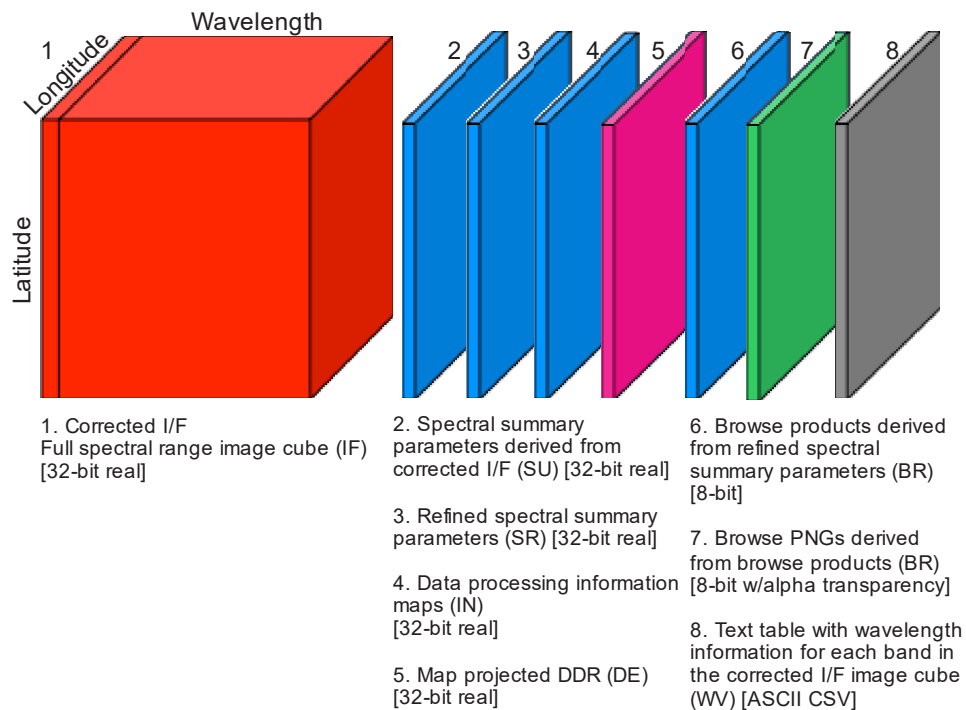


**Figure 3-16. Contents of a CRISM Map-projected Targeted Reduced Data Record (MTRDR) Data Product Set**

### **3.6.2 Label Description**

See section 2.3.4 for general information on CRISM product labels. Example TER and MTRDR labels are provided in Appendix E.

TER/MTRDR label keywords with CRISM-specific values are listed in Table 3-17.

**Table 3-17. CRISM-specific values for TER/MTRDR label keywords**

Keyword	Valid Values
PRODUCT_TYPE	MPTARGETED_RDR, MPTARGETED_BROWSE, MAP_PROJECTED_DDR, TER, TARGETED_BROWSE
OBSERVATION_TYPE	FRT (Full Resolution Targeted Observation) HRL (Half Resolution Long Targeted Observation) HRS (Half Resolution Short Targeted Observation)
OBSERVATION_ID	8-byte hexadecimal integer
MRO:OBSERVATION_NUMBER	Counter from product ID
MRO:ACTIVITY_ID	IF### – Scene measurement
MRO:SENSOR_ID	"J" for joined
MRO:WAVELENGTH_FILE_NAME	The name of the companion file with wavelength information for each spectral band.
MRO:PHOTOMETRIC_CORR_FLAG	Indicates the application of a Lambertian photometric correction. Valid values are: "ON", "OFF"
MRO:ATMOSPHERIC_CORR_FLAG	Indicates the application of a correction for atmospheric gas absorptions. Valid values are: "ON", "OFF"
MRO:RATIO_SHIFT_CORR_FLAG	Indicates the application of the Ratio Shift Correction (RSC), a robust column-oriented 'destriping' procedure. Valid values are: "ON", "OFF"
MRO:EMPIRICAL_GEOM_NORM_FLAG	Indicates the application of the Empirical Geometric Normalization (EGN) procedure which normalizes the contribution of atmospheric I/F to that at the minimum emergence angle in the image. Valid values are: "ON", "OFF".
MRO:EMPIRICAL_SMILE_CORR_FLAG	Indicates the application of the Empirical Smile Correction (ESC) procedure. Valid values are: "ON", "OFF".
MRO:SENSOR_SPACE_TRANSFORM_FLAG	Indicates the application of a spatial transform that maps CRISM VNIR data from a given targeted observation into the corresponding IR data sensor space. Valid values are: "ON", "OFF"

## 3.7 Level-6 CDR

### 3.7.1 Data Product Structure and Organization

A level-6 CDR (Figure 3-18) consists of tabulated derived data. Typically it is used for calibration of EDRs to CDRs, radiance or I/F. Derivation of the level-6 CDRs from flight data is described in Appendix M. The different types of calibration-related level-6 CDRs are given in Table 3-19.

The CDR6 format is also used to store operationally significant engineering information that the user may find helpful, but that are beyond the scope of the required elements of the archive. This includes a time ordered history of observations and the characteristics of the sites observed, as well as the configuration-managed history of the hardware and software state of the CRISM instrument. These "operational CDRs" are described in Table 3-20.

File format is comparable to that of EDR and RDR list files. The tables are ASCII comma-separated value (CSV) format.

### 3.7.2 Label Description

See section 2.3.4 for general information on CRISM product labels. An example level-6 CDR label is in Appendix F.

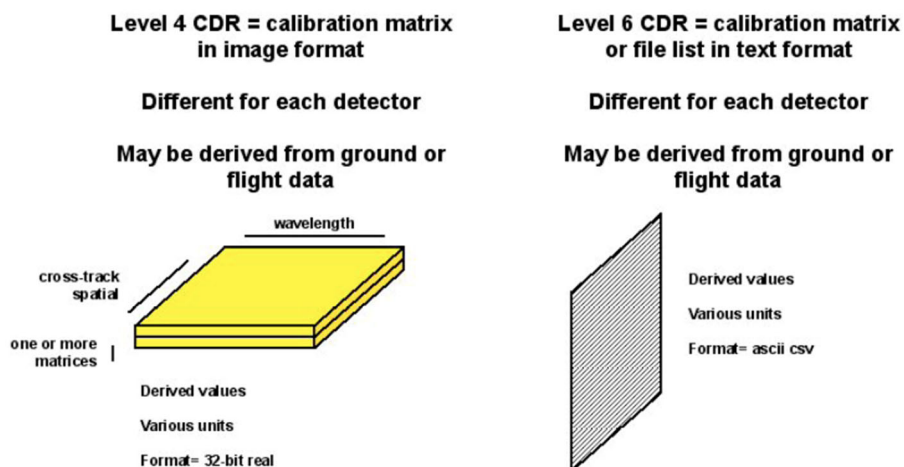


**Figure 3-18. Contents of a CRISM Calibration Data Record (CDR).  
Level 4 is image data; level 6 is text.**

**Table 3-19. Descriptions of calibration-related level-6 CDRs**

PRODUCTS	FORM FOR EACH FOCAL PLANE	PRODUCT ACRONYM
<b>INFREQUENTLY UPDATED PRODUCTS</b>		
Coefficients for correcting raw housekeeping for effects of lamps, coolers, frame rate	ASCII table , 11 columns (only one file applicable to both VNIR and IR)	HD
Coefficients for calibrating housekeeping from digital to physical units	ASCII table , 5 columns (only one file applicable to both VNIR and IR)	HK
Coefficients to convert housekeeping voltages for perturbations due to current	ASCII table , 7 columns (only one file applicable to both VNIR and IR)	HV
Gain and offset to use for each row for 12 to 14 bit conversion; 12 to 8 bit lookup tables for each row (if used)	ASCII table, 4 columns, 1 per detector	PP
Wavelength tables	ASCII table, 5 columns, 1 per detector	WV
Bandwidth for each row (band) in central columns of each detector at which spectral smile and keystone are minimum.	ASCII table, 2 cols VNIR and 11 cols IR, 1 per detector	BW
Center wavelength for each row (band) in central columns of each detector at which spectral smile and keystone are minimum.	ASCII table, 2 columns, 1 per detector	SW
12 to 8 bit lookup tables	ASCII table, 1 col. of 12-bit input, 8 cols. of 8-bit output	LK
8 to 12 bit lookup tables (inverse of 12 to 8)	ASCII table, 8 cols. of 8-bit input, 1 col. of 12-bit output	LI
Linearity correction	ASCII table, 7 columns, 1 per detector	LC
Bias step function as a function of frame rate and quadrant	ASCII table, 3 columns, 1 per detector	BS
Additive correction of bias to nominal detector operating temperature	ASCII table, 3 columns, 1 per detector	DB
Additive correction of bias to nominal focal plane electronics operating temperature	ASCII table, 3 columns, 1 per detector	EB
Interquadrant ghost removal scaling factors	ASCII table, 6 columns, 1 per detector	GH
Average Mars spectrum for limiting cases in different operating modes	ASCII table, 6 columns, 1 per detector	AS
Saturation limit for each detector quadrant and frame rate	ASCII table, 3 columns, 1 per detector	SL
Valid limits for each detector quadrant and frame rate for 14-bit DN level and noise	ASCII table, 5 columns, 1 per detector	VL
Atmospheric transmission for each wavelength bin averaged over IR columns 270-369 or VNIR columns 260-359, the part of each detector at which spectral smile and keystone are minimum	ASCII table, 2 columns, 1 per detector	CT

PRODUCTS	FORM FOR EACH FOCAL PLANE	PRODUCT ACRONYM
<b>FREQUENTLY UPDATED PRODUCTS</b>		
Standard telemetry file: CRISM low-rate telemetry in raw counts, from the beginning of a UTC calendar day to its end. This is used in preference to the telemetry attached to each image for correction of thermal effects.	ASCII table, 224 columns	ST
Predicted EDR processing table: Predicted table of EDRs containing scene data and the corresponding EDRs containing time-dependent calibration measurements. It is constructed from uplinked commands	ASCII table, 21 columns	BTF
EDR processing table: Table of EDRs containing scene data and the corresponding EDRs containing time-dependent calibration measurements. Used to process scene EDRs to TRDRs, and calibration EDRs to CDRs. If there is a discrepancy between the actual and predicted EDRs used for calibration, the TRDRs resulting from scene EDRs are quality-flagged.	ASCII table, 6 columns	ATF

**Table 3-20. Descriptions of operational level-6 CDRs**

PRODUCTS	FORM FOR EACH FOCAL PLANE	PRODUCT ACRONYM
Digital values of alarm limits and instrument parameters. Used for validation of uplinked sequences.	ASCII table with columns of start time of applicability, raw digital value, and comments (only one file applicable to both VNIR and IR)	DR
Calibrated physical values of alarm limits. Used for validation of uplinked sequences.	ASCII table with columns of start time of applicability, value as Celsius, volts, or amps, and comments (only one file applicable to both VNIR and IR)	DC
Digital values of heater and cooler settings. Used for validation of uplinked sequences.	ASCII table with columns of start time of applicability, raw digital value, and comments (only one file applicable to both VNIR and IR)	SR
Calibrated physical values of heater and cooler settings. Used for validation of uplinked sequences.	ASCII table with columns of start time of applicability, value as Celsius, and comments (only one file applicable to both VNIR and IR)	SC
Expected compression ratio of data in different instrument configurations. Used for management of solid state recorder usage.	ASCII table with columns activity, wavelength filter, binning, lossy compression setup, lossless compression setup, and expected compression ratio of data with that configuration.	CP
Mission event log. Includes times of updates to instrument software or settings, command loads, flight tests, or other notable events.	ASCII table with columns of start time and comments (only one file applicable to both VNIR and IR)	EL

## **3.8 Level-4 CDR**

### ***3.8.1 Data Product Structure and Organization***

A level-4 CDR (Figure 3-18) consists of a derived image product needed for calibration to radiance or I/F. Derivation of the level-4 CDRs from flight data is described in Appendix L. The different types of level-4 CDRs are given in Table 3-21. The data may be bitmap or 32-bit real numbers, depending on the product.

A level-4 CDR contains one or more images. The size varies according to pixel binning. The dimensions are XX' pixels in the sample (cross-track) dimension, YY pixels in the wavelength dimension, where:

- XX'=(640)/binning, where 640 is the number of columns read off the detector, and binning is 1, 2, 5, or 10
- YY= the number of rows (wavelength) that are retained by the instrument.

### ***3.8.2 Label Description***

See section 2.3.4 for general information on CRISM product labels. An example level-4 CDR label is in Appendix G.

**Table 3-21. Descriptions of level-4 CDRs**

PRODUCTS	FORM FOR EACH FOCAL PLANE	VERSIONS FOR DIFFERENT PIXEL BINNING / CHANNEL SELECTION?	VERSIONS FOR DIFFERENT FRAME RATE?	ACRONYM
<b>GROUND CALIBRATION PRODUCTS</b>				
Masks of detector dark columns, scattered light columns, scene columns	2D matrix per detector, 8 bit	Y	N	DM
Nonuniformity file: time-tagged, row-normalized measurement of detector nonuniformity	Two 2D matrices, 32 bit	Y	Y	NU
Matrices to remove estimated leaked higher order light	Four 2D matrices per detector, 16 bit integer, row numbers Four 2D matrices per detector, 32 bit, weighting coefficients	Y	N	LL
Sphere spectral radiance at set point (pixel by pixel coefficients to a 2nd order polynomial function of optical bench temperature)	Three 2D matrices per detector, 32 bit, for each sphere bulb	Y	N	SS
Shutter position reproducibility correction to sphere radiance (pixel by pixel coefficients to a linear function of the ratio of corrected sphere image to sphere spectral radiance model)	2 2D matrices per detector, 32 bit, for each sphere bulb	Y	N	SH
Temperature dependence of detector responsivity (pixel by pixel coefficients to a 2nd order polynomial function of detector temperature)	Three 2D matrices per detector, 32 bit	Y	N	TD
Along-slit angle measured from slit center	2D matrix per detector, 32 bit	Y	N	CM
Number of lines by which to shift each column (sample) of an image to minimize the effects of spectral smile	2D matrix per detector, 32 bit	Y	N	PS
Wavelength image (each pixel) determined onground	2D matrix per detector, 32 bit	Y	N	WA
Nearest-neighbor resampled wavelength image (each pixel) determined onground	2D matrix per detector, 32 bit	Y	N	RW
Spectral bandpass, or full width half maximum (each pixel) determined onground	One (VNIR) or ten(IR) 2D matrices per detector, 32 bit	Y	N	SB

PRODUCTS	FORM FOR EACH FOCAL PLANE	VERSIONS FOR DIFFERENT PIXEL BINNING / CHANNEL SELECTION?	VERSIONS FOR DIFFERENT FRAME RATE?	ACRONYM
Solar flux at 1 AU (for each pixel to take into account spectral smile effects)	2D matrix per detector, 32 bit	Y	N	SF
Nearest-neighbor resampled solar flux at 1 AU (for each pixel to take into account spectral smile effects)	2D matrix per detector, 32 bit	Y	N	RF
Atmospheric transmission as measured from a nadir-pointed hyperspectral scan across Olympus Mons	2D matrix per detector, 32 bit	Y	N	AT
Atmospheric transmission as measured from a nadir-pointed hyperspectral scan across Olympus Mons, nearest-neighbor resampled in the wavelength direction	2D matrix per detector, 32 bit	Y	N	RT
<b>FREQUENTLY UPDATED PRODUCTS</b>				
Bad pixel mask: time-tagged bitmap of bad pixels	2D matrix, 8 bits, per detector	Y	Y	BP
Bias file: time-tagged, fitted VNIR and IR images extrapolated to zero exposure time	2D matrix, 32 bit, per detector	Y	Y	BI
Background file: time-tagged, bias- and ghost-subtracted, linearized, averaged VNIR and IR background frames	2D matrix, 32 bit, per detector	Y	Y	BK
Noise file: time-tagged, image of pixel-by-pixel uncertainties in background images	2D matrix, 32 bit, per detector	Y	Y	UB
Processed sphere image in units of DN/ms	2D matrix, 32 bit, per detector (1 for each sphere bulb)	Y	N	SP

CDR label keywords with CRISM-specific values are listed in Table 3-22.

**Table 3-22. CRISM-specific values for CDR label keywords**

Keyword	Valid Values
PRODUCT_TYPE	CDR
OBSERVATION_TYPE	If produced from flight data: FRT (Full Resolution Targeted Observation) HRL (Half Resolution Long Targeted Observation) HRS (Half Resolution Short Targeted Observation) FRS (Full Resolution Short Targeted Observation) ATO (Along-Track Oversampled Targeted Observation) ATU (Along-Track Undersampled Targeted Observation) EPF (Atmospheric Survey EPF) TOD (Tracking Optical Depth Observation) MSP (Multispectral Survey, losslessly compressed) MSW (Multispectral Window) HSP (Hyperspectral Survey, losslessly compressed) HSV (Hyperspectral Survey - VNIR only, pixels 10x-binned) MSV (Hyperspectral Survey - VNIR only, pixels 5x-binned) CAL (Radiometric Calibration) FFC (Flat-field calibration) ICL (Calibration source intercalibration)
OBSERVATION_ID	10-digit hexadecimal integer (if produced from flight data)
MRO:OBSERVATION_NUMBER	Counter from product ID (if produced from flight data)
MRO:ACTIVITY_ID	Valid values (if produced from flight data) are: BI### – Bias measurement DF### – Dark field measurement LP### – Lamp measurement SP### – Sphere measurement SC### – Scene measurement (for flat-field calibration)
SOURCE_PRODUCT_ID	The product ID of the EDR from which a CDR was constructed (if produced from flight data)
MRO:EXPOSURE_PARAMETER	The value supplied to the CRISM instrument to command the exposure time. At a given frame rate identified in MRO:FRAME_RATE, there are 480 possible exposure times ranging from 1 to 480.
MRO:WAVELENGTH_FILTER	Which of four onboard menus of rows was selected for downlink. The four choices are 0, 1, 2, or 3.
MRO:SENSOR_ID	"S" for VNIR, or "L" for IR
SHUTTER_MODE_ID	"OPEN", "SPHERE", OR "CLOSED" (if produced from flight data)
LIGHT_SOURCE_NAME	"NONE", "VNIR LAMP 1", "VNIR LAMP 2", "IR LAMP 1", "IR LAMP 2", "SPHERE LAMP 1", "SPHERE LAMP 2"

Keyword	Valid Values
MRO:CALIBRATION_LAMP_STATUS	"OFF", "OPEN LOOP" or "CLOSED LOOP" (for integrating sphere only)
MRO:CALIBRATION_LAMP_LEVEL	Value between 0 and 4095
PIXEL_AVERAGING_WIDTH	1, 2, 5, or 10
MRO:DETECTOR_TEMPERATURE	Physical units; used to correct bias or responsivity for detector temperature. On each detector there are two temperature sensors. The primary source of IR detector temperature is IR temperature sensor 1 (column 50 in the EDR list file). The backup source of IR detector temperature is IR temperature sensor 2 (column 51 in the EDR list file). The primary source of VNIR detector temperature is VNIR temperature sensor 2 (column 65 in the EDR list file). The backup source of VNIR detector temperature is VNIR temperature sensor 1 (column 64 in the EDR list file)."
MRO:FPE_TEMPERATURE	Physical units; used to correct bias for electronics temperature. The temperature of the IR focal plane electronics (if MRO:SENSOR_ID = "L"), or the VNIR focal plane electronics (if MRO:SENSOR_ID = "S").
MRO:OPTICAL_BENCH_TEMPERATURE	Physical units; backup to correct sphere radiance for sphere temperature
MRO:SPHERE_TEMPERATURE	Physical units; used to correct sphere radiance for sphere temperature
MRO:SPECTROMETER_HOUSING_TEMP	Physical units; used in backup correction of background for spectrometer housing temperature. The primary source of this temperature is a measurement digitized by the VNIR focal plane electronics, column 58 in the EDR list file. The backup source of this temperature is a measurement digitized by the IR focal plane electronics, column 69 in the EDR list file
BAND_NAME	Brief descriptive name of each layer of data in the CDR

### 3.9 ADR

An Ancillary Data Record or ADR, if archived, contains a hyperdimensional binary table of derived values, where the axes of the matrix represent values of a layer of a DDR (e.g., incidence angle, thermal inertia, etc.), the output of another ADR, or a value extracted from a TRDR.

The overall objective of ADRs is to correct I/F in a TRDR for a strip of multispectral survey data for atmospheric, photometric, or (possibly) thermal effects to isolate the surface-reflected component of I/F as Lambert albedo. There are three types of ADRs:

1. The "CL" ADR is a table of surface temperatures and atmospheric dust and ice opacities, given for a latitude and longitude from the DDR and Ls and local solar time from the TRDR label.

2. The "AC" ADR is a table of correction from I/F to Lambert albedo, for an incidence, emission, and phase angle and surface elevation from the DDR, dust and ice optical depths and surface temperature from the CL ADR, and observed I/F from a TRDR. There is a separate AC ADR for each wavelength that is corrected; nominal wavelengths are those used in multispectral mapping, in wavelength filter 1.
3. The "TE" ADR is a table of calculated surface temperature for latitude, thermal inertia, elevation, and slope magnitude and azimuth from the DDR, dust and ice opacity from the CL ADR, Ls and local solar time from the TRDR label, and bolometric albedo estimated from Lambert albedo at wavelengths <2300 nm. This supplants surface temperature that is returned from the CL ADR.

ADR contents are described in Tables 3-23 through 3-25. Whether archived or not, they are used in the process of converting I/F to Lambert albedo during production of MRDRs. In that processing the thermal correction to the longest IR wavelengths is not implemented.

**Table 3-23. LUT for atmospheric opacity (ADR type = CL)**

VARIABLE	RANGE	UNIT
Latitude	-90-90°	degrees
Longitude	-90-90°	degrees
Ls	0-360°	degrees
Local time	15	(assumed local time)r
Surface temperature	180-310	°K
Dust opacity	0-1.0	dimensionless opacity
Ice opacity	0-1.0	dimensionless opacity

**Table 3-24. LUT for predicted atmospheric / photometric / thermal correction (ADR type = AC)**

VARIABLE	RANGE	WAVELENGTH
Wavelength	410-3920 nm	(separate table for each wavelength)
Incidence angle at areoid	25-75°	degrees
Emission angle at areoid	0-45°	degrees
Phase angle at areoid	45-135°	degrees
Elevation	-8000-26000	meters
Dust optical depth	0-1	dimensionless opacity
Ice optical depth	0-0.6	dimensionless opacity
Surface temperature	140-300 K	°K
Observed I/F	0.03-0.50	dimensionless

**Table 3-25. LUT for local surface temperature (ADR type = TE)**

VARIABLE	RANGE	UNITS
Latitude	-90-90°	degrees
Slope magnitude	0-10	degrees
Slope azimuth	0-270	degrees clockwise from north
Elevation	-8000-26000	meters
Thermal inertia	5-5000	J m^-2 K^-1 s^-0.5
Dust+ice opacity	0-1.0	dimensionless opacity
Ls	0-360°	degrees
Local time	13-17	(assumed local time)r
Bolometric albedo	0.15-0.35	dimensionless

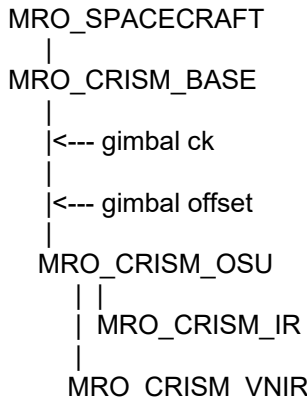
### 3.10 CRISM-Generated SPICE Files

Four types of SPICE kernels are needed to calculate CRISM's pointing:

1) Frames kernel (FK). This file defines the relationships of the of CRISM's field of view to the spacecraft, with the gimbal at "nadir". These transformations in frames of reference include:

- gimbal base (MRO\_CRISM\_BASE) -> spacecraft (MRO\_SPACECRAFT)
- optical axis at gimbal "nadir" (MRO\_CRISM\_OSU) -> gimbal base (MRO\_CRISM\_BASE)
- (the gimbal C kernel defines the relationship of optic axis at a gimbal position to the gimbal nadir)
- (the gimbal offset defines the software offset between commanded nadir and physical nadir)
- IR zero position for IK (MRO\_CRISM\_IR) -> optical axis (MRO\_CRISM\_OSU); nominal there two are coaligned and offsets of the IR FOV from the optical axis are entirely accounted for in the IK
- VNIR zero position for IK (MRO\_CRISM\_VNIR) -> optical axis (MRO\_CRISM\_OSU); nominal there two are coaligned and offsets of the VNIR FOV from the optical axis are entirely accounted for in the IK

Graphically, this is:



The CRISM frames kernel is delivered to NAIF and is incorporated into the MRO frames kernel.

2) Instrument kernel (IK). This file describes the relationship of position of each detector element (at a row or wavelength and spatial or column position) to a zero position within the field of view. Nominally, that is in the VNIR row closest to 610 nm or the IR row closest to 2300 nm, at the column position closest to the optical axis. Due to keystone distortion, there is a different relationship for every row number of either detector.

The CRISM instrument kernel is delivered to NAIF.

3) Gimbal C kernel. This file gives a time history of the angle of the gimbal within the gimbal plane, relative to its commanded nadir. It is constructed from gimbal attitude measurements in

image headers, i.e., from the TAB file part of an EDR. One file covers a 2-week time span of CRISM data.

CRISM gimbal C kernels are delivered to NAIF.

4) Metakernel. This file gives, for any time span covered by a gimbal C kernel, the MRO and CRISM SPICE kernels used to create DDRs for observations occurring during that time period. Note that kernels are loaded in the order listed., so the highest priority kernel is listed last.

## **3.11 Browse Products**

Browse products are synoptic versions of data products to help identify products of interest. There are browse products for EDRs, TRDRs, TERs, MTRDRs, and MRDRs.

### **3.11.1 *EDR Browse Products***

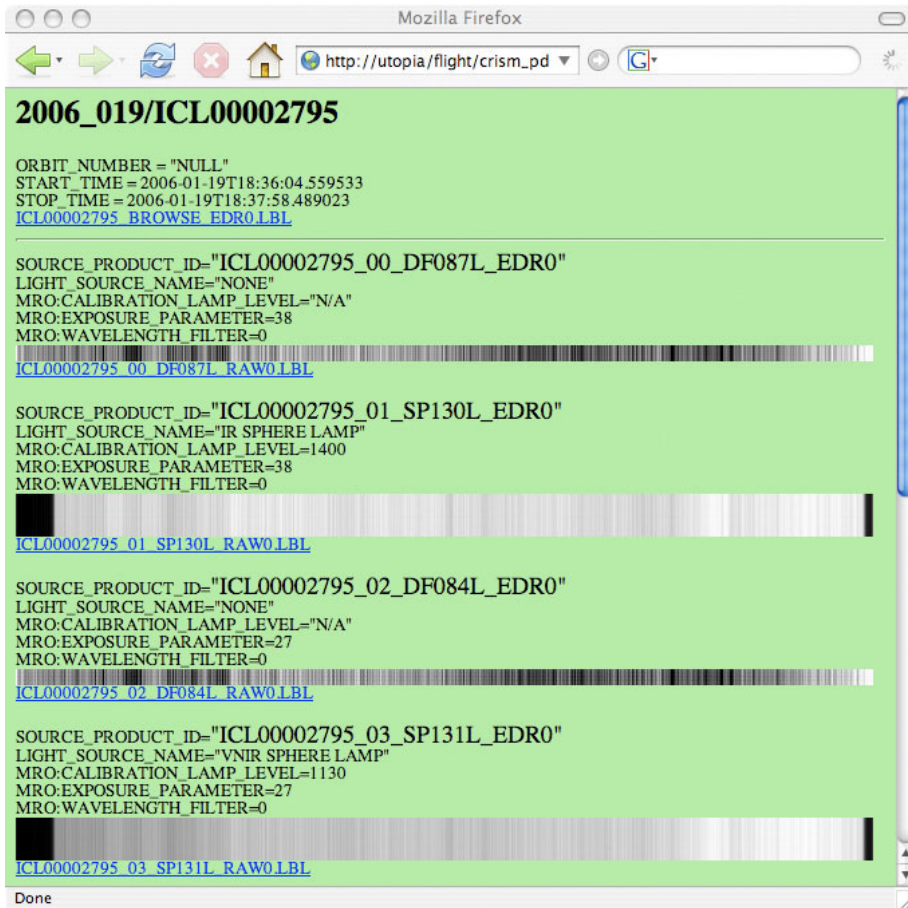
There are two types of products. One is an HTML file that gives the key parameters of the component EDRs for each observation, and links to PNG files for each EDR in the observation. A detached label to the HTML file describes the observation at a high level.

The browse product for each EDR is a scaled (0-255), median DN value from selected wavelengths for each spatial element in an EDR multiband image, stored in PNG format. The dimensions of the PNG file, XX pixels in the sample (cross-track) dimension and YY pixels in the line (along-track) dimension, match the spatial dimensions of the source EDR. A detached label to the PNG file describes the source EDR and the scaling between its raw data values and the PNG file.

Figure 3-26 shows an example EDR HTML browse product, linking to the PNG files for the component EDRs and to all of the associated labels.

An example set of EDR browse product labels is in Appendix I.

**Figure 3-26. Example EDR browse product**



### 3.11.2 TRDR Browse Products

Each hyperspectral targeted (gimbaled) observation TRDR IF data product has one browse product in a directory structure that parallels that of the TRDR directory. This is by year and DOY, e.g. /2006/2006\_350/, with subdirectories for each observation named according to the combination of class type and observation ID unique to a single observation, e.g. "FRT00001270". Each VNIR (S-detector) TRDR has a TRU browse product visualization and each IR (L-detector) TRDR has a FAL browse product visualization (see definitions in sections 3.11.3). As with TER MTRDR browse products (section 3.11.3), three data files and one detached PDS label file describing the three files constitutes a single TRDR browse product set. The three data files are:

1. A .IMG file which stores the browse image as a 3-band 8-bit raw binary PDS image object.
2. A .HDR file which stores ENVI Header information associated with the IMG file. This file is provided as a convenience to users of the ENVI software and allows the TRDR browse products to be loaded directly into ENVI.
3. A .PNG file which stores the 3-band 8-bit browse image in Portable Network Graphics (PNG) format with an alpha transparency channel that corresponds to the non-scene edge pixels.

The spatial dimensions of each PNG and IMG file match the spatial dimensions of the source TRDR.

### **3.11.3 MRDR, TER, and MTRDR Browse Products**

A MRDR, TER, or MTRDR browse product set consists of three data files and a detached PDS label file. The label file contains the metadata and pointers to the three data files. The three data files are

- 1) an IMG file containing the browse product image as a three-band PDS IMAGE object;
- 2) a PNG file containing the browse product image in the Portable Network Graphics file format (three bands and an alpha transparency channel); and
- 3) a HDR file associated with the IMG file which stores file format (and map projection information for MTRs) in the ENVI header format. This allows users of the ENVI image processing software to readily read in the image data. The SOURCE\_PRODUCT\_ID keyword in the PDS label links the browse products to the source TER/MTRDR.

There are up to four PNG browse product images sourced to the VNIR detector and up to thirteen PNG browse product images sourced to the IR detector. One browse product is constructed from data from both detectors. The spatial dimensions of each PNG file match the source MRDR, TER, or MTRDR. The detached PDS label describes the scaling between the source 32-bit spectral summary parameter data and the byte scaled data in the IMG and PNG files.

All TER/MTRDR browse products (BR) are constructed from refined spectral summary parameters (SR) calculated for targeted observations using the revised CRISM spectral summary parameter library [Applicable Document 11] as described in Appendix P1. All MRDR browse products are constructed from comparably refined summary product versions of strips of mapping data from which strip-to-strip residuals are removed using the optimization process described in Appendix P3. In the byte-scaled browse products, spectral parameters that sample selected channels (e.g. R770) or capture spectral slope (e.g. ISLOPE1) or a band ratio (e.g. IRR2) are stretched according to the scene statistics. All other parameters are stretched according to meaningful values of the underlying band math calculation and the parameter distribution both within the product and across the product set.

Note that browse products for MRDRs are not one-for-one comparable with TER and MTRDR browse products, for reasons having to do with the component red, green, or blue bands which typically are summary products. For TERs and MTRDRs, summary product band math is evaluated at precise wavelengths of the formulae evaluated using polynomial fits to multiple channels over the kernel widths summarized in Table 3-12. In contrast for MRDRs summary product band math is evaluated at the channels present that are nearest to the wavelengths in the formulae, yielding a non-identical solution.

#### **1. VNIR Browse Products**

1.1 TRU (“True Color”) is an enhanced natural color representation of the scene composed of spectral channels across the visible spectrum.

red = (R600) 600-nm I/F

green = (R530) 530-nm I/F

blue = (R440) 440-nm I/F

1.2 VNA (“VNIR Albedo”) shows I/F at 770 nm (near the typical VNIR peak of the reflectance spectrum) as a proxy for VNIR albedo and may be used to correlate spectral variations with morphology. For consistency with the browse product suite, the single source parameter band is replicated into all three RGB channels.

red = (R770) 770-nm I/F

green = (R770) 770-nm I/F

blue = (R770) 770-nm I/F

1.3 FEM (“Fe Mineralogy”) shows information related to iron-bearing minerals and represents the spectral curvature at the visible and near-infrared wavelengths related to iron.

red = (BD530\_2) 530-nm band depth, highlighting nanophase or crystalline ferric oxides

green = (BD600\_2) 600-nm shoulder highlighting textural and/or coating effects

blue = (BDI1000VIS) 1000-nm VNIR band depth highlighting dust-free or more mafic surfaces

1.4 FM2 (“Fe Mineralogy, Version 2”) shows complementary information related to Fe minerals and is particularly sensitive to olivine and pyroxene, as well as nanophase ferric oxide and crystalline ferric or ferrous minerals.

red = (BD530) 530-nm band depth indicating the presence of nanophase ferric oxides

green = (BD920) 920-nm band depth highlighting coarser-grained ferric minerals or low-Ca pyroxene

blue = (BDI1000VIS) 1000-nm VNIR band depth highlighting dust-free or more mafic surfaces

## 2. IR Browse Products

2.1 FAL (“False Color”) is an enhanced infrared false color representation of the scene with the constituent wavelengths chosen to highlight differences between key mineral groups. Red to orange coloration is typically characteristic of olivine-rich for Fe-phyllosilicate-rich material, blue/green colors is often indicative of clay mineralogy, green colors may indicate carbonate, and gray/brown colors often indicate basaltic material.

red = (R2529) 2529-nm I/F

green = (R1506) 1506-nm I/F

blue = (R1080) 1080-nm I/F

2.2 IRA (“IR Albedo”) shows I/F at 1330 nm as a proxy for IR albedo and may be used to correlate spectral variations with morphology. For consistency with the browse product suite, the single source parameter band is replicated into all three RGB channels.

red = (R1330) 1330-nm I/F

green = (R1330) 1330-nm I/F

blue = (R1330) 1330-nm I/F

2.3 MAF (“Mafic Mineralogy”) shows information related to mafic mineralogy. Olivine and Fe-phyllosilicate share a 1000-1700 nm bowl-shaped absorption and will appear red in the MAF browse product. Low- and high-Ca pyroxene display an additional ~2000-nm absorption and appear green/cyan and blue/magenta.

red = (OLINDEX3) Spectral index keyed to fayalitic olivine (also highlights iron-bearing phyllosilicates)

green = (LCPINDEX2) Spectral index keyed to low-Ca pyroxene

blue = (HCPINDEX2) Spectral index keyed to high-Ca pyroxene

2.4 HYD (“Hydrated Mineralogy”) shows information related to bound water in minerals. Polyhydrated sulfates have strong 1900 nm and 2400 nm absorption bands, and thus appear magenta in the HYD browse product. Monohydrated sulfates have a strong 2100 nm absorption and a weak 2400 nm absorption band, and thus appear yellow/green in the HYD browse product. Blue colors are indicative of other hydrated minerals (such as clays, glass, carbonate, or zeolite).

red = (SINDEX2) Spectral index keyed to bound water bands indicative of hydrated sulfates

green = (BD2100\_2) 2100-nm band depth attributable to a shifted H<sub>2</sub>O band exhibited by monohydrated sulfates

blue = (BD1900\_2) 1900-nm band depth attributable to bound molecular H<sub>2</sub>O

2.5 PHY (“Phyllosilicates”) shows information related to hydroxylated minerals including phyllosilicate. Fe/Mg-OH bearing minerals (e.g., Fe/Mg-phyllosilicate) will appear red, or magenta (when hydrated). Al/Si-OH bearing minerals (e.g., Al-phyllosilicates or hydrated silica) will appear green, or cyan (when hydrated). Blue colors are indicative of other hydrated minerals (such as sulfates, glass, carbonate, or water ice).

red = (D2300) 2300-nm spectral drop-off associated with Fe/Mg phyllosilicate or Mg-carbonate

green = (D2200) 2200-nm spectral drop-off associated with Al-phyllosilicate or hydrated silica

blue = (BD1900R2) 1900-nm band depth attributable to bound molecular H<sub>2</sub>O

2.6 PFM (“Phyllosilicate with Fe and Mg”) shows information related to the cation composition of hydroxylated minerals including Fe/Mg-phyllosilicate. Red/yellow colors indicate the presence of prehnite, chlorite, epidote, or Ca/Fe carbonate, while cyan colors indicate the presence of Fe/Mg-smectites or Mg-carbonate.

red = (BD2355) 2355-nm band depth indicating the presence of prehnite, chlorite, epidote, or Ca/Fe carbonate

green = (D2300) 2300-nm spectral drop-off associated with Fe/Mg phyllosilicate or Mg-carbonate

blue = (BD2290) 2290-nm band depth consistent with an Mg- or Fe- OH cation-hydroxyl absorption

2.7 PAL (“Phyllosilicate with Al”) shows information related to the cation composition of hydroxylated minerals including Al-phyllosilicate and hydrated silica. Red/yellow colors indicate the presence of Al-smectites or hydrated silica, cyan colors may indicate the alunite, and light/white colors indicate the presence of kaolinite group minerals.

red = (BD2210\_2) 2210-nm band depth consistent with an Al-OH cation-hydroxyl absorption

green = (BD2190) 2190-nm band depth

blue = (BD2165) 2165-nm band depth consistent with Al-OH structure in Kaolininte-group minerals.

2.8 HYS (“Hydrated Silica”) shows information related to Si/Al-hydroxylated minerals that can be used to differentiate between hydrated silica and Al-phyllosilicates. Light red/yellow colors indicate the presence of hydrated silica, whereas cyan colors indicate Al-OH minerals. Additionally, jarosite will appear yellow. Blue colors are indicative of other hydrated minerals (such as sulfates, clays, glass, carbonate, or water ice).

red = (MIN2250) Minimum band depth of paired 2210-nm and 2260-nm Si-OH features

green = BD2250 2250-nm band depth consistent with Al-OH and Si-OH cation-hydroxyl

blue = (BD1900R2) 1900-nm band depth attributable to bound molecular H<sub>2</sub>O

2.9 ICE (“Ices”) shows information related to water or carbon dioxide frost or ice. CO<sub>2</sub> frost or ice displays a sharp 1435-nm absorption and thus appears blue in the ICE browse product. Water ice or frost has a strong 1500 nm absorption and thus appears green in the ICE browse product. Red colors are indicative of hydrated minerals (such as sulfates, clays, glass, carbonate, or water ice).

red = (BD1900\_2) 1900-nm band depth attributable to bound molecular H<sub>2</sub>O

green = (BD1500\_2) 1500-nm band depth diagnostic of H<sub>2</sub>O ice

blue = (BD1435) 1435-nm band depth diagnostic of CO<sub>2</sub> ice

2.10 IC2 (“Ices, Version 2”) shows complementary information related to water or carbon dioxide frost or ice. CO<sub>2</sub> frost or ice displays a sharp 1435-nm absorption and thus appears blue in the IC2 browse product. Water ice or frost has a strong 1500 nm absorption and thus appears green in the IC2 browse product. The 3920-nm spectral channel is a discriminator for icy vs. ice-free material with ices having a lower solar reflected and thermal emission radiance at this wavelength.

red = (R3920) 3920-nm I/F highlighting comparatively warm ice-free surfaces

green = (BD1500\_2) 1500-nm band depth diagnostic of H<sub>2</sub>O ice

blue = (BD1435) 1435-nm band depth diagnostic of CO<sub>2</sub> ice

2.11 CHL (“Chloride”) shows information related to inferred chloride deposits in THEMIS DCS glowing terrain and spatially associated hydrated mineral deposits. The chloride material has a relatively positive near-infrared spectral slope and is comparatively desiccated, so appears blue in the CHL browse product. Yellow/green colors are indicative of hydrated minerals, especially phyllosilicates.

red = (ISLOPE1) spectral slope over the 1815-nm to 2530-nm interval

green = (BD3000) 3000-nm band depth attributable to bound H<sub>2</sub>O

blue = (IRR2) 2530-nm to 2210-nm spectral ratio

2.12 CAR (“Carbonates”) shows information related to Mg carbonate minerals. Blueish- or yellowish-white colors indicate Mg-carbonate, while red/magenta colors indicate Fe/Mg-phyllosilicate. Blue colors are indicative of other hydrated minerals (such as sulfates, clays, glass, or carbonate).

red = (D2300) 2300-nm spectral drop-off associated with Fe/Mg phyllosilicate or Mg-carbonate

green = (BD2500H) 2500-nm band depth corresponding to an Mg-carbonate overtone

blue = (BD1900\_2) 1900-nm band depth attributable to bound molecular H<sub>2</sub>O

2.13 CR2 (“Carbonates, Version 2”) shows information distinguishing carbonate minerals. Red/magenta colors indicate Mg-carbonates, while green/cyan colors indicate Fe/Ca-carbonates.

red = (MIN2295\_2480) Minimum band depth of paired 2295-nm and 2480-nm Mg-carbonate overtone features

green = (MIN2345\_2537) Minimum band depth of paired 2345-nm and 2537-nm Ca/Fe-carbonate overtone features

blue = (CINDEX2) Spectral index keyed to ~3400-nm and ~3900-nm carbonate spectral features.

### 3. Joined (VNIR and IR) Browse Products

3.1 TAN (“Tandem”) shows an enhanced visible to infrared false color representation of the scene, incorporating spectral data from both (VNIR and IR) detectors. This is the designated browse product visualization for the TER/MTR IF data products.

red = (R2529) 2529-nm I/F

green = (R1330) 1330-nm I/F

blue = (R770) 770-nm I/F

Example TER and MTRDR browse product labels are provided in Appendix J. An example set of MRDR browse product labels is in Appendix K.

## 3.12 Extra Products

### 3.12.1 *EDR Extras Products*

See section 3.10.1 in Applicable Document [5] for descriptions of the potential products in this directory.

In the Observation Tracking Table (OTT) directory, only OBS\_ID table is regularly generated. It provides a synopsis of the disposition and quality of CRISM observations that have actually been commanded to the instrument. Its contents are described in Table 3-27. There is one row per commanded EDR.

**Table 3-27. Contents of OBS\_ID Table.**

Information	Description
REQUEST_ID	May be null if it is not site-related, such as calibration or functional test (class = FUN or CAL).
PARTICIPATING_INSTRUMENTS	Any combination of the characters CHX to indicate instruments planning to participate.
COORDINATED_TARGET	1 if true
MEP_TARGET	1 if true
RIDEALONG	1 if true
OBSERVATION_ID	8-byte hexadecimal integer, if in integrated target list.
OBSERVATION_TYPE	FRT, HRL, HRS, FRS, ATO, ATU, EPF, TOD, MSW, MSP, HSP, HSV, MSV, CAL, FFC, ICL, or FUN

Information	Description
ACTIVITY_ID	AC### where AC is a 2-letter designation of the type of measurement made, and ### as a 3-numeral designation of the instrument command macro that was executed to acquire the data. Macro numbers are in the range 0-255. BI is measurement of detector bias, DF is a measurement of background including dark current and thermal background, LP is measurement of a focal plane lamp, SP is measurement of the internal integrating sphere, and SC is measurement of an external scene. TP indicates that the EDR contains any test pattern produced by instrument electronics. T1 through T7 specify the test pattern, test pattern 1 through test pattern 7. UN indicates data in which housekeeping does not match the commanded instrument configuration.
PLAN_OBSERVATION_NUMBER	Monotonically increasing ordinal counter of the EDRs generated from one spectrometer for a single OBSERVATION_ID.
PLAN_SENSOR_ID	Spectrometer identifier. 0 = IR; 1 = VNIR.
PLAN_LINES	Number of frames
PLAN_BANDS	Number of wavelengths
PLAN_BINNING	Spatial pixel binning mode; specified separately for each detector; 0 = 1:1; 1 = 2:1; 2 = 5:1; 3 = 10:1
PLAN_RATE	Rate of frame acquisition; 0 = 1 Hz; 1 = 3.75 Hz; 2 = 5 Hz; 3 = 15 Hz; 4 = 30 Hz; specified separately for each detector
PLAN_EXPOSURE_PARAMETER	At a given frame rate there are 480 possible exposure times ranging from 1 to 480. An exposure parameter of 480 yields an exposure time equal to the inverse of the frame rate. An exposure time parameter of 1 yields an exposure time 1/480 as large.
PLAN_SHUTTER_POS	Shutter position from 0 to 32; nominal open is 3; viewing sphere is 17; closed is 32.
PLAN_FILTER	Wavelength filter table; which of uploadable tables 0-3; specified separately for each detector
PLAN_FAST	Lossless Fast compression enabled or disabled; specified separately for each detector; 0 = disabled; 1 = enabled
PLAN_LOSSY	Lossy compression enabled or disabled; 12 to 8 bit look-up table commanded line by line in uploaded data structure; specified separately for each detector; 0 = disabled; 1 = enabled
PLAN_IR_FLOOD1_PWR	IR flood lamp 1 power (IR); 0 = off; 1 = on.
PLAN_IR_FLOOD1_LEVEL	IR flood lamp 1 level 0-4095.
PLAN_IR_FLOOD2_PWR	IR flood lamp 2 power (IR); 0 = off; 1 = on.
PLAN_IR_FLOOD2_LEVEL	IR flood lamp 2 level 0-4095.
PLAN_IR_SPHERE_PWR	IR sphere lamp power; 0 = off; 1 = on.
PLAN_IR_SPHERE_GOAL	Closed-loop goal, 0-4095.
PLAN_VNIR_FLOOD1_PWR	VNIR flood lamp 1 power (VNIR); 0 = off; 1 = on.
PLAN_VNIR_FLOOD1_LEVEL	VNIR flood lamp 1 level 0-4095.
PLAN_VNIR_FLOOD2_PWR	VNIR flood lamp 2 power (VNIR); 0 = off; 1 = on.
PLAN_VNIR_FLOOD2_LEVEL	VNIR flood lamp 2 level 0-4095.
PLAN_VNIR_SPHERE_PWR	VNIR sphere lamp power; 0 = off; 1 = on.
PLAN_VNIR_SPHERE_GOAL	Closed-loop goal, 0-4095.
PLAN_COMPRESSION_RATIO	Compression ratio used to model data volume.
PLAN_CLOSEST_APPROACH_TIME	yyyy-mm-ddThh:mm:ss.sss, ISO UTC time format
PLAN_START_TIME	yyyy-mm-ddThh:mm:ss.sss, ISO UTC time format
PLAN_STOP_TIME	yyyy-mm-ddThh:mm:ss.sss, ISO UTC time format

Information	Description
PLAN_LOWER_RIGHT_LATITUDE	Planned latitude of the surface point at the edge of the FOV on the antisunward (right-hand) side of the groundtrack at the observation start.
PLAN_LOWER_RIGHT_LONGITUDE	Planned longitude of the surface point at the edge of the FOV on the antisunward (right-hand) side of the groundtrack at the observation start.
PLAN_LOWER_LEFT_LATITUDE	Planned latitude of the surface point at the edge of the FOV on the sunward (left-hand) side of the groundtrack at the observation start.
PLAN_LOWER_LEFT_LONGITUDE	Planned longitude of the surface point at the edge of the FOV on the sunward (left-hand) side of the groundtrack at the observation start.
PLAN_UPPER_RIGHT_LATITUDE	Planned latitude of the surface point at the edge of the FOV on the antisunward (right-hand) side of the groundtrack at the observation end.
PLAN_UPPER_RIGHT_LONGITUDE	Planned longitude of the surface point at the edge of the FOV on the antisunward (right-hand) side of the groundtrack at the observation end.
PLAN_UPPER_LEFT_LATITUDE	Planned latitude of the surface point at the edge of the FOV on the sunward (left-hand) side of the groundtrack at the observation end.
PLAN_UPPER_LEFT_LONGITUDE	Planned longitude of the surface point at the edge of the FOV on the sunward (left-hand) side of the groundtrack at the observation end.
RECEIPT	Received on ground; 0 = no, 1 = partially received with no gap filled, 2 = partially received with gap filled, 3 = received.
PRODUCT_ID	CCCN>NNNNNNN_XX_AAAAAS_EDRV where CCC = OBSERVATION_TYPE, NNNNNNNN = OBSERVATION_ID as a hexadecimal number, XX = OBSERVATION_NUMBER, AAAA = ACTIVITY_ID, S = SENSOR_ID S or L, V = Product version number
ENCODING_COMPRESSION_RATIO	Actual compression ratio of data.
CLOSEST_APPROACH_TIME	yyyy-mm-ddThh:mm:ss.sss, ISO UTC time format
START_TIME	yyyy-mm-ddThh:mm:ss.sss, ISO UTC time format
STOP_TIME	yyyy-mm-ddThh:mm:ss.sss, ISO UTC time format
LOWER_RIGHT_LATITUDE	Actual latitude of the surface point at the edge of the FOV on the antisunward (right-hand) side of the groundtrack at the observation start.
LOWER_RIGHT_LONGITUDE	Actual longitude of the surface point at the edge of the FOV on the antisunward (right-hand) side of the groundtrack at the observation start.
LOWER_LEFT_LATITUDE	Actual latitude of the surface point at the edge of the FOV on the sunward (left-hand) side of the groundtrack at the observation start.
LOWER_LEFT_LONGITUDE	Actual longitude of the surface point at the edge of the FOV on the sunward (left-hand) side of the groundtrack at the observation start.
UPPER_RIGHT_LATITUDE	Actual latitude of the surface point at the edge of the FOV on the antisunward (right-hand) side of the groundtrack at the observation end.
UPPER_RIGHT_LONGITUDE	Actual longitude of the surface point at the edge of the FOV on the antisunward (right-hand) side of the groundtrack at the observation end.

Information	Description
UPPER_LEFT_LATITUDE	Actual latitude of the surface point at the edge of the FOV on the sunward (left-hand) side of the groundtrack at the observation end.
UPPER_LEFT_LONGITUDE	Actual longitude of the surface point at the edge of the FOV on the sunward (left-hand) side of the groundtrack at the observation end.
DATA_QUALITY_INDEX	See description in section 2.5.2
FILE_SPECIFICATION_NAME	Pathname of image EDR in data directory, e.g., EDR/2006_350/FRT00001270/FRT00001270_01_SC001S_EDR0.IMG
LINES	Number of frames
COMMENT	Text string describing nature of observation

### **3.12.2 TRDR Extras Products**

The TRDR EXTRAS visualizations are Portable Network Graphics (PNG) format files that depict the geometry and structure of CRISM hyperspectral targeted observations. The TRDR detector specific visualizations have file names with the form [Class Type][Target ID]\_[Sensor]\_[Name].PNG where [Class Type] is a three letter observation type code (e.g. FRT, HRL, HRS), [Target ID] is an eight character hexadecimal observation identifier, [Sensor] is a single character indicating the VNIR (S-detector) or IR (L-detector) wavelength range, and [Name] indicates the plot contents.

See section 3.10.2 in Applicable Document [5] for descriptions of the products in this directory.

### **3.12.3 TER/MTRDR Extras Products**

See section 3.10.3 in Applicable Document [5] for descriptions of the products in this directory. Examples of TER and MTR Extras products are detailed in this document in Appendix P2.

## **4. APPLICABLE SOFTWARE**

### **4.1 Utility Programs**

To facilitate timely and consistent analysis of CRISM data, the CRISM Analysis Tool (CAT) has been developed and provided to the community shortly after MRO's orbital mission began. CAT is based on the commercially available ENVI software package which requires IDL to run. A companion software package with lesser functionality, JCAT, does not require ENVI or IDL, and was developed and made available in 2019.

The CRISM Team has also developed a spectral library of well-characterized Mars analog materials, measured under dry N<sub>2</sub>-purged conditions over CRISM's wavelength range and convolved with the CRISM's slit function. This special measurement environment is necessary because many lithologies of interest adsorb water strongly and under ambient conditions are spectrally dissimilar to their state on Mars. In 2014, a companion set of Mars type spectra of various phases. The spectral libraries are found at Applicable Documents [11] and [12].

CAT, JCAT, and the spectral libraries are available at the PDS Geosciences Node web site <https://pds-geosciences.wustl.edu/missions/mro/crism.htm>, along with tutorial information to operate the CAT.

Key data-reduction and management capabilities of the CRISM analysis tool (CAT) include:

- The CAT has the ability to read EDRs, TRDRs, DDRs, MRDRs, CDRs, TERs and MTRDRs.
- The CAT has the ability to map-project data following the conventions given in section 3.4.2.
- The CAT has the ability to access the SOC and to download and apply current CDRs for correction of atmospheric and photometric effects.
- The CAT has the ability to create site-specific browse products.
- The CAT also has the ability to apply all of the extensive analysis capabilities already built into ENVI, including classification (e.g. spectral angle mapping), mixture modeling, principal components analysis, and techniques that use the spectral library as input.

## **4.2 Applicable PDS Software Tools**

PDS-labeled images and tables can be viewed with the program NASAView, developed by the PDS and available for a variety of computer platforms from the PDS web site <http://pds.nasa.gov/tools>.

## APPENDIX A. EDR LABEL

```
PDS_VERSION_ID      = PDS3
LABEL_REVISION_NOTE = "2003-11-19, S. Slavney (GEO);
                      2005-02-01, C. Hash (ACT);
                      2006-01-04, C. Hash (ACT);"

/* EDR Identification */

DATA_SET_ID        = "MRO-M-CRISM-2-EDR-V1.0"
PRODUCT_ID         = "FRT00004ECA_07_SC166L_EDR0"
/* cccnnnnnnn_xx_oaaas_EDRv */
/* ccc = Class Type           */
/* nnnnnnnn = Observation ID (hex)   */
/* xx = counter within observation (hex) */
/* oaaaa = obs type, macro number    */
/* s = sensor ID (S or L)          */
/* v = version number             */

INSTRUMENT_HOST_NAME = "MARS RECONNAISSANCE ORBITER"
SPACECRAFT_ID       = MRO
INSTRUMENT_NAME     = "COMPACT RECONNAISSANCE IMAGING
                      SPECTROMETER FOR MARS"
INSTRUMENT_ID        = CRISM
TARGET_NAME          = MARS
PRODUCT_TYPE         = EDR
PRODUCT_CREATION_TIME = 2007-04-06T16:41:28
START_TIME           = 2007-03-23T03:02:31.910417
STOP_TIME            = 2007-03-23T03:04:39.644669
SPACECRAFT_CLOCK_START_COUNT = "2/0859086170.55396"
SPACECRAFT_CLOCK_STOP_COUNT = "2/0859086298.37980"
ORBIT_NUMBER         = "NULL"
OBSERVATION_TYPE    = "FRT"
OBSERVATION_ID      = "16#00004ECA#"
MRO:OBSERVATION_NUMBER = 16#07#
MRO:ACTIVITY_ID     = "SC166"
MRO:SENSOR_ID       = "L"
PRODUCT_VERSION_ID  = "0"
PRODUCER_INSTITUTION_NAME = "JOHNS HOPKINS UNIVERSITY
                           APPLIED PHYSICS LABORATORY"
SOFTWARE_NAME        = "pipe_edrslice"
SOFTWARE_VERSION_ID = "4.3"

/* EDR Instrument and Observation Parameters */
/* for first frame */
TARGET_CENTER_DISTANCE = NULL <KM>
SOLAR_DISTANCE         = NULL <KM>
SHUTTER_MODE_ID        = OPEN
LIGHT_SOURCE_NAME       = "NONE"
MRO:CALIBRATION_LAMP_STATUS = "OFF"
MRO:CALIBRATION_LAMP_LEVEL = "N/A"
PIXEL_AVERAGING_WIDTH = 1
MRO:INSTRUMENT_POINTING_MODE = "DYNAMIC POINTING"
SCAN_MODE_ID           = SHORT
MRO:FRAME_RATE          = 3.75 <HZ>
MRO:EXPOSURE_PARAMETER = 301
SAMPLING_MODE_ID        = "HYPERSPEC"
COMPRESSION_TYPE        = "NONE"
MRO:WAVELENGTH_FILTER = 0
MRO:WAVELENGTH_FILE_NAME = "CDR6_1_0000000000_WV_L_1.TAB"
MRO:PIXEL_PROC_FILE_NAME = "CDR6_1_0000000000_PP_L_1.TAB"
```

```

MRO:LOOKUP_TABLE_FILE_NAME = "CDR6_1_0000000000_LK_J_0.TAB"

/* This EDR label describes two data files. The first file contains */
/* the first two objects and the second file contains the third: */
/* 1. A multiple-band image file containing uncalibrated EDR data, */
/* 2. A binary table of selected image row numbers from detector, */
/* 3. A table of ancillary and housekeeping data. */
/* Description of EDR IMAGE file */

OBJECT = FILE
^IMAGE      = "FRT00004ECA_07_SC166L_EDR0.IMG"
^ROWNUM_TABLE = ("FRT00004ECA_07_SC166L_EDR0.IMG", 210241)
RECORD_TYPE = FIXED_LENGTH
RECORD_BYTES = 1280
FILE_RECORDS = 210241

OBJECT = IMAGE
LINES      = 480
LINE_SAMPLES = 640
SAMPLE_TYPE = MSB_UNSIGNED_INTEGER
SAMPLE_BITS = 16
BANDS      = 438
BAND_STORAGE_TYPE = LINE_INTERLEAVED
MISSING_CONSTANT = 65535
CHECKSUM    = "NULL"
END_OBJECT = IMAGE

OBJECT = ROWNUM_TABLE
NAME        = "SELECTED ROWS FROM DETECTOR"
INTERCHANGE_FORMAT = "BINARY"
ROWS        = 438
COLUMNS     = 1
ROW_BYTES   = 2
DESCRIPTION = "The detector is subsampled in the spectral direction
by selecting specific rows to be downlinked. This
table provides a list of the rows selected for all
frames in this multidimensional image cube."

OBJECT = COLUMN
NAME        = DETECTOR_ROW_NUMBER
DATA_TYPE   = MSB_UNSIGNED_INTEGER
BIT_MASK    = 2#0000000111111111#
START_BYTE  = 1
BYTES       = 2
MISSING_CONSTANT = 65535
DESCRIPTION  = "Detector row number from which the data was taken."
END_OBJECT = COLUMN

END_OBJECT = ROWNUM_TABLE

END_OBJECT = FILE

/* Description of EDR HOUSEKEEPING TABLE file */

OBJECT = FILE
^EDR_HK_TABLE = "FRT00004ECA_07_SC166L_HKP0.TAB"
RECORD_TYPE = FIXED_LENGTH
RECORD_BYTES = 1038
FILE_RECORDS = 480

OBJECT = EDR_HK_TABLE
NAME        = "EDR HOUSEKEEPING TABLE"

```

```
INTERCHANGE_FORMAT = "ASCII"
ROWS          = 480
COLUMNS        = 233
ROW_BYTES      = 1038

/* Columns in the table are described in this external file: */
^STRUCTURE      = "EDRHK.FMT"

END_OBJECT = EDR_HK_TABLE

END_OBJECT = FILE
END
```

## APPENDIX B. DDR LABEL

```
PDS_VERSION_ID      = PDS3
LABEL_REVISION_NOTE = "2004-11-22, S. Slavney (GEO);
                      2006-04-05, S. Murchie (JHU/APL);"

/* DDR Identification */

DATA_SET_ID          = "MRO-M-CRISM-6-DDR-V1.0"
PRODUCT_ID           = "FRT00004ECA_07_DE166L_DDR1"
/* cccnnnnnnn_xx_ooaaas_DDRv */
/* ccc = Class Type */
/* nnnnnnnn = Observation ID (hex) */
/* xx = counter this observation (hex) */
/* ooaaa = obs type, macro number */
/* s = sensor ID (S or L) */
/* v = version number */

INSTRUMENT_HOST_NAME = "MARS RECONNAISSANCE ORBITER"
SPACECRAFT_ID        = MRO
INSTRUMENT_NAME       = "COMPACT RECONNAISSANCE IMAGING
                           SPECTROMETER FOR MARS"
INSTRUMENT_ID         = CRISM
TARGET_NAME           = MARS
PRODUCT_TYPE          = DDR
PRODUCT_CREATION_TIME = 2007-04-07T07:48:44
START_TIME            = 2007-03-23T03:02:31.499
STOP_TIME             = 2007-03-23T03:04:39.233
SPACECRAFT_CLOCK_START_COUNT = "2/859086170:55396"
SPACECRAFT_CLOCK_STOP_COUNT = "2/859086298:37980"

ORBIT_NUMBER          = 0
OBSERVATION_TYPE     = "FRT"
OBSERVATION_ID        = "16#00004ECA#"
MRO:OBSERVATION_NUMBER = 16#07#
MRO:ACTIVITY_ID      = "DE166"
MRO:SENSOR_ID         = "L"
PRODUCT_VERSION_ID    = "1"
SOURCE_PRODUCT_ID     = {
  "MRO_SCLKSCET.00021.65536.tsc",
  "mro_v08.tf",
  "MRO_CRISM_FK_0000_000_N_1.TF",
  "MRO_CRISM_IK_0000_000_N_1.TI",
  "naif0008.tls",
  "pck00008.tpc",
  "mro_sc_psp_070313_070319.bc",
  "mro_sc_psp_070320_070326.bc",
  "mro_sc_2007-03-27.bc",
  "mro_sc_2007-03-28.bc",
  "spck_2007_081_r_1.bc",
  "spck_2007_082_r_1.bc",
  "spck_2007_083_r_1.bc",
  "spck_2007_084_r_1.bc",
  "spck_2007_085_r_1.bc",
  "spck_2007_086_r_1.bc",
  "de410.bsp",
  "mro_cruise.bsp",
  "mro_ab.bsp",
  "mro_psp.bsp",
  "mro_psp_rec.bsp"
}
```

```

PRODUCER_INSTITUTION_NAME = "APPLIED PHYSICS LABORATORY"
SOFTWARE_NAME           = "crism_ddr"
SOFTWARE_VERSION_ID     = "1.9"

/* DDR Instrument and Observation Parameters */

TARGET_CENTER_DISTANCE   = 3675.164588 <KM>
                           /* distance to Mars center at first frame */
SOLAR_DISTANCE           = 212137794.935710 <KM>
SOLAR_LONGITUDE          = 205.303815 <DEGREES>
MRO:FRAME_RATE           = 3.75 <HZ>
PIXEL_AVERAGING_WIDTH    = 1
MRO:INSTRUMENT_POINTING_MODE = "DYNAMIC POINTING"
SCAN_MODE_ID              = "LONG"

/* This DDR label describes one data file: */  

/* 1. A multiple-band backplane image file with wavelength-independent, */  

/* spatial pixel-dependent geometric and timing information. */  

/* See the CRISM Data Products SIS for more detailed description. */

OBJECT                  = FILE
^IMAGE                 = "FRT00004ECA_07_DE166L_DDR1.IMG"
RECORD_TYPE             = FIXED_LENGTH
RECORD_BYTES            = 2560
FILE_RECORDS           = 6720

OBJECT                  = IMAGE
LINES                  = 480
LINE_SAMPLES           = 640
SAMPLE_TYPE            = PC_REAL
SAMPLE_BITS             = 32
BANDS                  = 14
BAND_STORAGE_TYPE      = BAND_SEQUENTIAL
BAND_NAME              = ("INA at areoid, deg",
                           "EMA at areoid, deg",
                           "Phase angle, deg",
                           "Latitude, areocentric, deg N",
                           "Longitude, areocentric, deg E",
                           "INA at surface from MOLA, deg",
                           "EMA at surface from MOLA, deg",
                           "Slope magnitude from MOLA, deg",
                           "MOLA slope azimuth, deg clkwise from N",
                           "Elevation, meters relative to MOLA",
                           "Thermal inertia, J m^-2 K^-1 s^-0.5",
                           "Bolometric albedo",
                           "Local solar time, hours",
                           "Spare")

END_OBJECT              = IMAGE

END_OBJECT              = FILE

END

```

## APPENDIX C1. TRDR LABEL (RADIANCE IMAGE + LISTFILE)

```
PDS_VERSION_ID      = PDS3
LABEL_REVISION_NOTE = "2004-11-22, S. Slavney (GEO);
                      2005-12-20, H. Taylor (JHU/APL);
                      2006-04-05, S. Murchie (JHU/APL);
                      2006-09-18, P. Cavender (JHU/APL);
                      2007-04-30, P. Cavender (JHU/APL);
                      Version 1, Improved SS CDRs and
                      added post-processing bad pixel
                      correction
                      2007-09-13, D. Humm (JHU/APL);
                      Version 2, Improved calibration
                      motivated by Deimos observation
                      2010-06-01, D. Humm (JHU/APL);
                      Version 3, shutter mirror correction
                      and other calibration tweaks
                      2010-10-12, C. Hash (ACT);
                      Version 3, Added data filter control
                      parameters"
DATA_SET_ID         = "MRO-M-CRISM-3-RDR-TARGETED-V1.0"
PRODUCT_ID          = "FRT00004ECA_07_RA166L_TRR3"

/* cccnnnnnnn_xx_oaaaaas_TRRv      */
/* ccc = Class Type                */
/* nnnnnnnn = Observation ID, hexadecimal */
/* oaaaa = Image type, Macro number   */
/* s = Sensor ID (S or L)          */
/* v = Version number              */

INSTRUMENT_HOST_NAME = "MARS RECONNAISSANCE ORBITER"
SPACECRAFT_ID        = MRO
INSTRUMENT_NAME       = "COMPACT RECONNAISSANCE IMAGING
                           SPECTROMETER FOR MARS"
INSTRUMENT_ID         = CRISM
TARGET_NAME           = MARS
PRODUCT_TYPE          = TARGETED_RDR
PRODUCT_CREATION_TIME = 2010-11-09T00:34:29
START_TIME             = 2007-03-23T03:02:31.499
STOP_TIME              = 2007-03-23T03:04:39.233
SPACECRAFT_CLOCK_START_COUNT = "2/0859086170.55396"
SPACECRAFT_CLOCK_STOP_COUNT  = "2/0859086298.37980"
ORBIT_NUMBER          = "NULL"
OBSERVATION_TYPE      = "FRT"
OBSERVATION_ID         = "16#00004ECA#"
MRO:OBSERVATION_NUMBER = 16#07#
MRO:ACTIVITY_ID        = "RA166"
MRO:SENSOR_ID          = "L"
MRO:DETECTOR_TEMPERATURE = -165.838
MRO:OPTICAL_BENCH_TEMPERATURE = -48.411
MRO:SPECTROMETER_HOUSING_TEMP = -72.699
MRO:SPHERE_TEMPERATURE = -48.064
MRO:FPE_TEMPERATURE    = 0.812
PRODUCT_VERSION_ID     = "3"
SOURCE_PRODUCT_ID = {
  "CDR410000000000_DM0000000L_3",
  "CDR410000000000_LL0000000L_4",
  "CDR410000000000_SH0000001L_4",
  "CDR410000000000_SS0000001L_6",
  "CDR410000000000_TD0000000S_2",
  "CDR410803692813_SF0000000L_4",
```

```

"CDR420847411200_NU1000001L_5",
"CDR420859086160_BK1030100L_3",
"CDR420859086162_BP1000000L_3",
"CDR420859086162_UB1030100L_3",
"CDR420859086234_BP1000000L_3",
"CDR420859086302_BK1030100L_3",
"CDR420859086303_BP1000000L_3",
"CDR420859086303_UB1030100L_3",
"CDR420859087293_BK0003800L_3",
"CDR420859087299_UB0003800L_3",
"CDR420859087333_SP0003801L_3",
"CDR420859087333_SP0042501S_3",
"CDR420859087355_BK0003800L_3",
"CDR420859087361_UB0003800L_3",
"CDR420859127820_BI1000000L_3",
"CDR420861470430_BI0000000L_3",
"CDR6_1_0000000000_AS_L_0",

"CDR6_1_0000000000_BS_L_0",
"CDR6_1_0000000000_DB_L_0",
"CDR6_1_0000000000_EB_L_0",
"CDR6_1_0000000000_GH_L_2",
"CDR6_1_0000000000_HD_J_1",
"CDR6_1_0000000000_HK_J_1",
"CDR6_1_0000000000_HV_J_1",
"CDR6_1_0000000000_LC_L_1",
"CDR6_1_0000000000_LI_J_0",
"CDR6_1_0000000000_VL_L_0",
"CDR6_2_0835294537_PP_L_0",
"CDR6_2_0859075219_ST_J_0",
"FRT00004ECA_07_SC166L_EDR0"
}

MRO:INVALID_PIXEL_LOCATION = {
}

PRODUCER_INSTITUTION_NAME = "JOHNS HOPKINS UNIVERSITY
APPLIED PHYSICS LABORATORY"
SOFTWARE_NAME = "crism_imagecal"
SOFTWARE_VERSION_ID = "2.5.3"

/* Targeted RDR Instrument and Observation Parameters */

TARGET_CENTER_DISTANCE = "NULL" <KM>
SOLAR_DISTANCE = 212139419.063420 <KM>
SOLAR_LONGITUDE = 205.304261
SHUTTER_MODE_ID = "OPEN"
LIGHT_SOURCE_NAME = "NONE"
MRO:CALIBRATION_LAMP_STATUS = "OFF"
MRO:CALIBRATION_LAMP_LEVEL = "N/A"
PIXEL_AVERAGING_WIDTH = 1
MRO:INSTRUMENT_POINTING_MODE = "DYNAMIC POINTING"
SCAN_MODE_ID = "SHORT"
MRO:FRAME_RATE = 3.75 <HZ>
MRO:EXPOSURE_PARAMETER = 301
SAMPLING_MODE_ID = "HYPERSPEC"
COMPRESSION_TYPE = "NONE"
MRO:WAVELENGTH_FILTER = "0"
MRO:WAVELENGTH_FILE_NAME = "CDR410803692813_WA0000000L_3.IMG"
MRO:PIXEL_PROC_FILE_NAME = "CDR6_2_0835294537_PP_L_0.TAB"
MRO:INV_LOOKUP_TABLE_FILE_NAME = "CDR6_1_0000000000_LI_J_0.TAB"
MRO:ATMO_CORRECTION_FLAG = "OFF"
MRO:THERMAL_CORRECTION_MODE = "OFF"
MRO:PHOTOCLIN_CORRECTION_FLAG = "OFF"

```

```

MRO:SPATIAL_RESAMPLING_FLAG = "OFF"
MRO:SPATIAL_RESAMPLING_FILE = "N/A"

MRO:SPATIAL_RESCALING_FLAG = "OFF"
MRO:SPATIAL_RESCALING_FILE = "N/A"
MRO:SPECTRAL_RESAMPLING_FLAG = "OFF"
MRO:SPECTRAL_RESAMPLING_FILE = "N/A"

/* Hyperspectral Data Filter Control Parameters */

MRO:HDF_SOFTWARE_NAME      = "N/A"

MRO:HDF_SOFTWARE_VERSION_ID = "N/A"
MRO:IF_MIN_VALUE           = "N/A"
MRO:IF_MAX_VALUE           = "N/A"
MRO:TRACE_MIN_VALUE        = "N/A"
MRO:TRACE_MAX_VALUE        = "N/A"
MRO:REFZ_MEDIAN_BOX_WIDTH  = "N/A"
MRO:REFZ_SMOOTH_BOX_WIDTH  = "N/A"
MRO:FRAM_STAT_MEDIAN_BOX_WIDTH = "N/A"
MRO:FRAM_STAT_MIN_DEVIATION = "N/A"
MRO:FRAM_STAT_MEDIAN_CONF_LVL = "N/A"
MRO:FRAM_STAT_IQR_CONF_LVL = "N/A"
MRO:RSC_REF_XY_MEDIAN_WIDTH = "N/A"
MRO:RSC_REF_XY_SMOOTH_WIDTH = "N/A"
MRO:RSC_REF_YZ_MEDIAN_WIDTH = "N/A"
MRO:RSC_REF_YZ_SMOOTH_WIDTH = "N/A"
MRO:RSC_RATIO_XY_MEDIAN_WIDTH = "N/A"
MRO:RSC_RATIO_XY_SMOOTH_WIDTH = "N/A"
MRO:RSC_RES_XY_PLY_ORDER   = "N/A"
MRO:RSC_RES_XY_PLY_EXTND_WIDTH = "N/A"
MRO:LOG_XFORM_NEG_CLIP_VALUE = "N/A"
MRO:IKF_NUM_REGIONS        = "N/A"
MRO:IKF_START_CHANNEL      = ("N/A", "N/A")
MRO:IKF_STOP_CHANNEL       = ("N/A", "N/A")
MRO:IKF_CONFIDENCE_LEVEL   = ("N/A", "N/A")
MRO:IKF_WEIGHTING_STDDEV   = ("N/A", "N/A")
MRO:IKF_KERNEL_SIZE_X      = ("N/A", "N/A")
MRO:IKF_KERNEL_SIZE_Y      = ("N/A", "N/A")
MRO:IKF_KERNEL_SIZE_Z      = ("N/A", "N/A")
MRO:IKF_MODEL_ORDER_X      = ("N/A", "N/A")
MRO:IKF_MODEL_ORDER_Y      = ("N/A", "N/A")
MRO:IKF_MODEL_ORDER_Z      = ("N/A", "N/A")

/* This Targeted RDR label describes two data files. The first file */
/* contains the first two objects and the second file contains the */
/* third: */
/* 1. A multiple-band image file containing calibrated RDR data, */
/*    in units of radiance, */
/* 2. A binary table of selected image row numbers from detector, */
/* 3. A table of ancillary and housekeeping data converted to */
/*    engineering units. */

OBJECT      = FILE
^IMAGE      = "FRT00004ECA_07_RA166L_TRR3.IMG"
^ROWNUM_TABLE = ("FRT00004ECA_07_RA166L_TRR3.IMG", 210241 )
RECORD_TYPE = FIXED_LENGTH
RECORD_BYTES = 2560
FILE_RECORDS = 210241

OBJECT      = IMAGE
LINES       = 480

```

```

LINE_SAMPLES      = 640
SAMPLE_TYPE      = PC_REAL
SAMPLE_BITS       = 32
UNIT              = "W / (m**2 micrometer sr)"
BANDS             = 438
BAND_STORAGE_TYPE = LINE_INTERLEAVED
END_OBJECT = IMAGE

OBJECT          = ROWNUM_TABLE
NAME            = "SELECTED ROWS FROM DETECTOR"
INTERCHANGE_FORMAT = "BINARY"
ROWS             = 438
COLUMNS          = 1
ROW_BYTES        = 2
DESCRIPTION      = "The detector is subsampled in the spectral direction
                    by selecting specific rows to be downlinked. This
                    table provides a list of the rows selected for all
                    frames in this multidimensional image cube."
OBJECT = COLUMN
NAME            = DETECTOR_ROW_NUMBER
DATA_TYPE        = MSB_UNSIGNED_INTEGER
COLUMN_NUMBER    = 1
BIT_MASK         = 2#000000011111111#
START_BYTE       = 1
BYTES            = 2
DESCRIPTION      = "Detector row number from which the data was taken."
END_OBJECT = COLUMN
END_OBJECT      = ROWNUM_TABLE

END_OBJECT = FILE

OBJECT = FILE
^TRDR_HK_TABLE   = "FRT0004ECA_07_RA166L_HKP3.TAB"
RECORD_TYPE       = FIXED_LENGTH
RECORD_BYTES      = 1221
FILE_RECORDS     = 480
OBJECT           = TRDR_HK_TABLE
NAME             = "TARGETED RDR HOUSEKEEPING TABLE"
INTERCHANGE_FORMAT = ASCII
ROWS              = 480
COLUMNS          = 233
ROW_BYTES         = 1221
^STRUCTURE        = "TRDRHK.FMT"
END_OBJECT        = TRDR_HK_TABLE
END_OBJECT = FILE
END

```

## APPENDIX C2. TRDR LABEL (I/F IMAGE)

```
PDS_VERSION_ID      = PDS3
LABEL_REVISION_NOTE = "2004-11-22, S. Slavney (GEO);
                      2005-12-20, H. Taylor (JHU/APL);
                      2006-04-05, S. Murchie (JHU/APL);
                      2006-09-18, P. Cavender (JHU/APL);
                      2007-04-30, P. Cavender (JHU/APL);
                      Version 1, Improved SS CDRs and
                      added post-processing bad pixel
                      correction
                      2007-09-13, D. Humm (JHU/APL);
                      Version 2, Improved calibration
                      motivated by Deimos observation
                      2010-06-01, D. Humm (JHU/APL);
                      Version 3, shutter mirror correction
                      and other calibration tweaks
                      2010-10-12, C. Hash (ACT);
                      Version 3, Added data filter control
                      parameters"
DATA_SET_ID         = "MRO-M-CRISM-3-RDR-TARGETED-V1.0"
PRODUCT_ID          = "FRT00004ECA_07_IF166L_TRR3"

/* cccnnnnnnn_xx_oaaaaas_TRRv      */
/* ccc = Class Type                */
/* nnnnnnnn = Observation ID, hexadecimal */
/* oaaaa = Image type, Macro number   */
/* s = Sensor ID (S or L)          */
/* v = Version number              */

INSTRUMENT_HOST_NAME = "MARS RECONNAISSANCE ORBITER"
SPACECRAFT_ID        = MRO
INSTRUMENT_NAME       = "COMPACT RECONNAISSANCE IMAGING
                           SPECTROMETER FOR MARS"
INSTRUMENT_ID         = CRISM
TARGET_NAME           = MARS
PRODUCT_TYPE          = TARGETED_RDR
PRODUCT_CREATION_TIME = 2010-11-11T04:21:39
START_TIME             = 2007-03-23T03:02:31.499
STOP_TIME              = 2007-03-23T03:04:39.233
SPACECRAFT_CLOCK_START_COUNT = "2/0859086170.55396"
SPACECRAFT_CLOCK_STOP_COUNT  = "2/0859086298.37980"
ORBIT_NUMBER          = "NULL"
OBSERVATION_TYPE      = "FRT"
OBSERVATION_ID         = "16#00004ECA#"
MRO:OBSERVATION_NUMBER = 16#07#
MRO:ACTIVITY_ID        = "IF166"
MRO:SENSOR_ID          = "L"
MRO:DETECTOR_TEMPERATURE = -165.838
MRO:OPTICAL_BENCH_TEMPERATURE = -48.411
MRO:SPECTROMETER_HOUSING_TEMP = -72.699
MRO:SPHERE_TEMPERATURE = -48.064
MRO:FPE_TEMPERATURE    = 0.812
PRODUCT_VERSION_ID     = "3"
SOURCE_PRODUCT_ID = {
  "CDR410000000000_DM0000000L_3",
  "CDR410000000000_LL0000000L_4",
  "CDR410000000000_SH0000001L_4",
  "CDR410000000000_SS0000001L_6",
  "CDR410000000000_TD0000000S_2",
  "CDR410803692813_SF0000000L_4",
```

```

"CDR420847411200_NU1000001L_5",
"CDR420859086160_BK1030100L_3",
"CDR420859086162_BP1000000L_3",
"CDR420859086162_UB1030100L_3",
"CDR420859086234_BP1000000L_3",
"CDR420859086302_BK1030100L_3",
"CDR420859086303_BP1000000L_3",
"CDR420859086303_UB1030100L_3",
"CDR420859087293_BK0003800L_3",
"CDR420859087299_UB0003800L_3",
"CDR420859087333_SP0003801L_3",
"CDR420859087333_SP0042501S_3",
"CDR420859087355_BK0003800L_3",
"CDR420859087361_UB0003800L_3",
"CDR420859127820_BI1000000L_3",
"CDR420861470430_BI0000000L_3",
"CDR6_1_0000000000_AS_L_0",

"CDR6_1_0000000000_BS_L_0",
"CDR6_1_0000000000_DB_L_0",
"CDR6_1_0000000000_EB_L_0",
"CDR6_1_0000000000_GH_L_2",
"CDR6_1_0000000000_HD_J_1",
"CDR6_1_0000000000_HK_J_1",
"CDR6_1_0000000000_HV_J_1",
"CDR6_1_0000000000_LC_L_1",
"CDR6_1_0000000000_LI_J_0",
"CDR6_1_0000000000_VL_L_0",
"CDR6_2_0835294537_PP_L_0",
"CDR6_2_0859075219_ST_J_0",
"FRT00004ECA_07_SC166L_EDR0"
}

MRO:INVALID_PIXEL_LOCATION = {
}

PRODUCER_INSTITUTION_NAME = "JOHNS HOPKINS UNIVERSITY
APPLIED PHYSICS LABORATORY"
SOFTWARE_NAME = "crism_imagecal"
SOFTWARE_VERSION_ID = "2.5.3"

/* Targeted RDR Instrument and Observation Parameters */

TARGET_CENTER_DISTANCE = "NULL" <KM>
SOLAR_DISTANCE = 212139419.063420 <KM>
SOLAR_LONGITUDE = 205.304261
SHUTTER_MODE_ID = "OPEN"
LIGHT_SOURCE_NAME = "NONE"
MRO:CALIBRATION_LAMP_STATUS = "OFF"
MRO:CALIBRATION_LAMP_LEVEL = "N/A"
PIXEL_AVERAGING_WIDTH = 1
MRO:INSTRUMENT_POINTING_MODE = "DYNAMIC POINTING"
SCAN_MODE_ID = "SHORT"
MRO:FRAME_RATE = 3.75 <HZ>
MRO:EXPOSURE_PARAMETER = 301
SAMPLING_MODE_ID = "HYPERSPEC"
COMPRESSION_TYPE = "NONE"
MRO:WAVELENGTH_FILTER = "0"
MRO:WAVELENGTH_FILE_NAME = "CDR410803692813_WA0000000L_3.IMG"
MRO:PIXEL_PROC_FILE_NAME = "CDR6_2_0835294537_PP_L_0.TAB"
MRO:INV_LOOKUP_TABLE_FILE_NAME = "CDR6_1_0000000000_LI_J_0.TAB"
MRO:ATMO_CORRECTION_FLAG = "OFF"
MRO:THERMAL_CORRECTION_MODE = "OFF"

```

```

MRO:PHOTOCLIN_CORRECTION_FLAG = "OFF"
MRO:SPATIAL_RESAMPLING_FLAG = "OFF"
MRO:SPATIAL_RESAMPLING_FILE = "N/A"

MRO:SPATIAL_RESCALING_FLAG = "OFF"
MRO:SPATIAL_RESCALING_FILE = "N/A"
MRO:SPECTRAL_RESAMPLING_FLAG = "OFF"
MRO:SPECTRAL_RESAMPLING_FILE = "N/A"

/* Hyperspectral Data Filter Control Parameters */

MRO:HDF_SOFTWARE_NAME = "crismhdf"
MRO:HDF_SOFTWARE_VERSION_ID = "1.0.4"
MRO:IF_MIN_VALUE = 0.000000
MRO:IF_MAX_VALUE = 1.000000
MRO:TRACE_MIN_VALUE = 0.01
MRO:TRACE_MAX_VALUE = 100.00
MRO:REFZ_MEDIAN_BOX_WIDTH = 35
MRO:REFZ_SMOOTH_BOX_WIDTH = 9
MRO:FRAM_STAT_MEDIAN_BOX_WIDTH = 5
MRO:FRAM_STAT_MIN_DEVIATION = 0.00500000
MRO:FRAM_STAT_MEDIAN_CONF_LVL = 0.99999900
MRO:FRAM_STAT_IQR_CONF_LVL = 0.99999900
MRO:RSC_REF_XY_MEDIAN_WIDTH = 15
MRO:RSC_REF_XY_SMOOTH_WIDTH = 5
MRO:RSC_REF_YZ_MEDIAN_WIDTH = 15
MRO:RSC_REF_YZ_SMOOTH_WIDTH = 5
MRO:RSC_RATIO_XY_MEDIAN_WIDTH = 25
MRO:RSC_RATIO_XY_SMOOTH_WIDTH = 13
MRO:RSC_RES_XY_PLY_ORDER = 5
MRO:RSC_RES_XY_PLY_EXTND_WIDTH = 38
MRO:LOG_XFORM_NEG_CLIP_VALUE = 0.00000100
MRO:IKF_NUM_REGIONS = 2
MRO:IKF_START_CHANNEL = ( 0, 179 )
MRO:IKF_STOP_CHANNEL = ( 178, 437 )
MRO:IKF_CONFIDENCE_LEVEL = ( 0.900, 0.900 )
MRO:IKF_WEIGHTING_STDDEV = ( 1.500, 1.250 )
MRO:IKF_KERNEL_SIZE_X = ( 5, 5 )
MRO:IKF_KERNEL_SIZE_Y = ( 3, 3 )
MRO:IKF_KERNEL_SIZE_Z = ( 5, 5 )
MRO:IKF_MODEL_ORDER_X = ( 1, 1 )
MRO:IKF_MODEL_ORDER_Y = ( 1, 1 )
MRO:IKF_MODEL_ORDER_Z = ( 1, 4 )

/* This Targeted RDR label describes two data files. The first file */
/* contains the first two objects and the second file contains the */
/* third: */
/* 1. A multiple-band image file containing calibrated RDR data, */
/*    in units of radiance, */
/* 2. A binary table of selected image row numbers from detector, */
/* 3. A table of ancillary and housekeeping data converted to */
/*    engineering units. */

OBJECT = FILE
^IMAGE = "FRT00004ECA_07_IF166L_TRR3.IMG"
^ROWNUM_TABLE = ("FRT00004ECA_07_IF166L_TRR3.IMG", 210241 )
RECORD_TYPE = FIXED_LENGTH
RECORD_BYTES = 2560
FILE_RECORDS = 210241

OBJECT = IMAGE
LINES = 480

```

```

LINE_SAMPLES    = 640
SAMPLE_TYPE     = PC_REAL
SAMPLE_BITS      = 32
UNIT            = "I_OVER_F"
BANDS           = 438
BAND_STORAGE_TYPE = LINE_INTERLEAVED
END_OBJECT = IMAGE

OBJECT          = ROWNUM_TABLE
NAME            = "SELECTED ROWS FROM DETECTOR"
INTERCHANGE_FORMAT = "BINARY"
ROWS             = 438
COLUMNS          = 1
ROW_BYTES        = 2
DESCRIPTION      = "The detector is subsampled in the spectral direction
                    by selecting specific rows to be downlinked. This
                    table provides a list of the rows selected for all
                    frames in this multidimensional image cube."
OBJECT = COLUMN
NAME            = DETECTOR_ROW_NUMBER
DATA_TYPE        = MSB_UNSIGNED_INTEGER
COLUMN_NUMBER   = 1
BIT_MASK         = 2#000000011111111#
START_BYTE       = 1
BYTES            = 2
DESCRIPTION      = "Detector row number from which the data was taken."
END_OBJECT = COLUMN
END_OBJECT      = ROWNUM_TABLE

END_OBJECT = FILE

OBJECT = FILE
^TRDR_HK_TABLE  = "FRT0004ECA_07_RA166L_HKP3.TAB"
RECORD_TYPE      = FIXED_LENGTH
RECORD_BYTES     = 1221
FILE_RECORDS    = 480
OBJECT          = TRDR_HK_TABLE
NAME            = "TARGETED RDR HOUSEKEEPING TABLE"
INTERCHANGE_FORMAT = ASCII
ROWS             = 480
COLUMNS          = 233
ROW_BYTES        = 1221
^STRUCTURE       = "TRDRHK.FMT"
END_OBJECT      = TRDR_HK_TABLE
END_OBJECT = FILE
END

```

## APPENDIX D1. MRDR LABEL (I/F OR AL IMAGE)

```
PDS_VERSION_ID      = PDS3
RECORD_TYPE        = FIXED_LENGTH
RECORD_BYTES       = 4544
FILE_RECORDS      = 92160
LABEL_REVISION_NOTE = "2003-11-19, S. Slavney (GEO);
                      2005-09-25, S. Murchie (JHU/APL);
                      2007-03-09, E. Malaret (ACT Corp.);
                      2007-09-14, C. Hash (ACT Corp)"

^IMAGE              = "T1396_MRRIF_30N088_0256_1.IMG"

/* Map-projected Multispectral RDR Identification */

DATA_SET_ID         = "MRO-M-CRISM-5-RDR-MULTISPECTRAL-V1.0"
PRODUCT_ID          = "T1396_MRRIF_30N088_0256_1"
/*( TNNNN_MRRss_yydxxx_rrrr_v )*/
/*( NNNN = tile number           )*/
/*( ss = subtype of image product )*/
/*( yy = latitude of upper left corner )*/
/*( d = N or S for north or south latitude )*/
/*( xxx = east longitude of upper left corner )*/
/*( rrrr = resolution in pixels/degree )*/
/*( v = version number           )*/

INSTRUMENT_HOST_NAME = "MARS RECONNAISSANCE ORBITER"
SPACECRAFT_ID       = MRO
INSTRUMENT_NAME      = "COMPACT RECONNAISSANCE IMAGING
                        SPECTROMETER FOR MARS"
INSTRUMENT_ID        = CRISM
TARGET_NAME          = MARS
PRODUCT_TYPE         = MAP_PROJECTED_MULTISPECTRAL_RDR
PRODUCT_CREATION_TIME = 2008-12-09T07:58:41.208
START_TIME           = "N/A"
STOP_TIME            = "N/A"
SPACECRAFT_CLOCK_START_COUNT = "N/A"
SPACECRAFT_CLOCK_STOP_COUNT  = "N/A"
PRODUCT_VERSION_ID   = "1"
PRODUCER_INSTITUTION_NAME = "APPLIED PHYSICS LABORATORY"
SOFTWARE_NAME         = "PIPE_create_crism_mrdr_product"
SOFTWARE_VERSION_ID   = "12.05.08"
MRO:WAVELENGTH_FILE_NAME = "T1396_MRRWV_30N088_0256_1.TAB"

/* This Map Projected Multispectral RDR label describes one data file: */
/* 1. A multiple-band image file of calibrated RDR data in radiance, */
/* This RDR represents one latitude-longitude bin in a global map. */
/* See the Map Projection Object below for bin coordinates and resolution.*/
/* See the CRISM Data Products SIS for more detailed description. */

/* Description of MAP PROJECTED MULTISPECTRAL RDR RADIANCE IMAGE file */

OBJECT              = IMAGE
LINES               = 1280
LINE_SAMPLES        = 1136
SAMPLE_TYPE         = PC_REAL
SAMPLE_BITS         = 32
UNIT                = "I over F"
BANDS               = 72
BAND_STORAGE_TYPE   = BAND_SEQUENTIAL
END_OBJECT          = IMAGE
```

```

/* Map projection information about this RDR is in the IMAGE_MAP_PROJECTION */
/* object below. */

OBJECT      = IMAGE_MAP_PROJECTION
^DATA_SET_MAP_PROJECTION  = "MRR_MAP.CAT"
MAP_PROJECTION_TYPE    = "EQUIRECTANGULAR"
A_AXIS_RADIUS        = 3396 <KM>
B_AXIS_RADIUS        = 3396 <KM>
C_AXIS_RADIUS        = 3396 <KM>
FIRST_STANDARD_PARALLEL = "N/A"
SECOND_STANDARD_PARALLEL = "N/A"
POSITIVE_LONGITUDE_DIRECTION = "EAST"
CENTER_LATITUDE       = 27.50000 <DEGREE>
CENTER_LONGITUDE      = 87.50000 <DEGREE>
REFERENCE_LATITUDE    = "N/A"
REFERENCE_LONGITUDE   = "N/A"
LINE_FIRST_PIXEL      = 1 /* North edge */
LINE_LAST_PIXEL       = 1280 /* South edge */
SAMPLE_FIRST_PIXEL    = 1 /* West edge */
SAMPLE_LAST_PIXEL     = 1136 /* East edge */
MAP_PROJECTION_ROTATION = 0.0
MAP_RESOLUTION         = 256 <PIXEL/DEGREE>
MAP_SCALE              = 0.231528833585 <KM/PIXEL>
MAXIMUM_LATITUDE       = 32.50000 <DEGREE>
MINIMUM_LATITUDE       = 27.50000 <DEGREE>
WESTERNMOST_LONGITUDE = 85.00000 <DEGREE>
EASTERNMOST_LONGITUDE = 90.00000 <DEGREE>
LINE_PROJECTION_OFFSET = 8320.000
SAMPLE_PROJECTION_OFFSET = 640.000
COORDINATE_SYSTEM_TYPE = "BODY-FIXED ROTATING"
COORDINATE_SYSTEM_NAME = "PLANETOCENTRIC"
END_OBJECT            = IMAGE_MAP_PROJECTION

```

END

## APPENDIX D2. MRDR LABEL (DERIVED DATA IMAGE)

```

PDS_VERSION_ID      = PDS3
RECORD_TYPE        = FIXED_LENGTH
RECORD_BYTES       = 4544
FILE_RECORDS      = 30720
LABEL_REVISION_NOTE = "2003-11-19, S. Slavney (GEO);
                      2005-09-25, S. Murchie (JHU/APL);
                      2007-03-09, E. Malaret (ACT Corp.);
                      2007-09-14, C. Hash (ACT Corp)"

^IMAGE              = "T1396_MRRDE_30N088_0256_1.IMG"

/* Map-projected Multispectral RDR Identification */

DATA_SET_ID         = "MRO-M-CRISM-5-RDR-MULTISPECTRAL-V1.0"
PRODUCT_ID          = "T1396_MRRDE_30N088_0256_1"
/*( TNNNN_MRRss_yydxxx_rrrr_v           )*/
/*( NNNN = tile number                  )*/
/*( ss = subtype of image product      )*/
/*( yy = latitude of upper left corner )*/
/*( d = N or S for north or south latitude )*/
/*( xxx = east longitude of upper left corner )*/
/*( rrrr = resolution in pixels/degree   )*/
/*( v = version number                 )*/

INSTRUMENT_HOST_NAME = "MARS RECONNAISSANCE ORBITER"
SPACECRAFT_ID       = MRO
INSTRUMENT_NAME     = "COMPACT RECONNAISSANCE IMAGING
                      SPECTROMETER FOR MARS"
INSTRUMENT_ID        = CRISM
TARGET_NAME          = MARS
PRODUCT_TYPE         = MAP_PROJECTED_MULTISPECTRAL_RDR
PRODUCT_CREATION_TIME = 2008-12-09T07:58:41.208
START_TIME           = "N/A"
STOP_TIME            = "N/A"
SPACECRAFT_CLOCK_START_COUNT = "N/A"
SPACECRAFT_CLOCK_STOP_COUNT  = "N/A"
PRODUCT_VERSION_ID   = "1"
PRODUCER_INSTITUTION_NAME = "APPLIED PHYSICS LABORATORY"
SOFTWARE_NAME         = "PIPE_create_crism_mrdr_product"
SOFTWARE_VERSION_ID   = "12.05.08"
MRO:WAVELENGTH_FILE_NAME = "T1396_MRRWV_30N088_0256_1.TAB"

/* This Map Projected Multispectral RDR label describes one data file: */
/* 1. A multiple-band image file of calibrated RDR data in radiance, */
/* This RDR represents one latitude-longitude bin in a global map. */
/* See the Map Projection Object below for bin coordinates and resolution.*/
/* See the CRISM Data Products SIS for more detailed description. */

/* Description of MAP PROJECTED MULTISPECTRAL RDR RADIANCE IMAGE file */

OBJECT              = IMAGE
LINES               = 1280
LINE_SAMPLES        = 1136
SAMPLE_TYPE         = PC_REAL
SAMPLE_BITS         = 32

BANDS               = 24
BAND_STORAGE_TYPE   = BAND_SEQUENTIAL
BAND_NAME            = ("Solar longitude, deg",

```

```

    "Solar distance, AU",
    "Observation ID, VNIR",
    "Observation ID, IR",
    "Ordinal counter, VNIR",
    "Ordinal counter, IR",
    "Column number, VNIR",
    "Column number, IR",
    "Line, or frame number, VNIR",
    "Line, or frame number, IR",
    "INA at areoid, deg",
    "EMA at areoid, deg",
    "Phase angle, deg",
    "Latitude, areocentric, deg N",
    "Longitude, areocentric, deg E",
    "INA at surface from MOLA, deg",
    "EMA at surface from MOLA, deg",
    "Slope magnitude from MOLA, deg",
    "MOLA slope azimuth, deg clkwise from N",
    "Elevation, meters relative to MOLA",
    "Thermal inertia, J m^-2 K^-1 s^-0.5",
    "Bolometric albedo",
    "Local solar time, hours",
    "Spare")
END_OBJECT          = IMAGE

/* Map projection information about this RDR is in the IMAGE_MAP_PROJECTION */
/* object below. */

OBJECT              = IMAGE_MAP_PROJECTION
"DATA_SET_MAP_PROJECTION" = "MRR_MAP.CAT"
MAP_PROJECTION_TYPE = "EQUIRECTANGULAR"
A_AXIS_RADIUS       = 3396 <KM>
B_AXIS_RADIUS       = 3396 <KM>
C_AXIS_RADIUS       = 3396 <KM>
FIRST_STANDARD_PARALLEL = "N/A"
SECOND_STANDARD_PARALLEL = "N/A"
POSITIVE_LONGITUDE_DIRECTION = "EAST"
CENTER_LATITUDE     = 27.50000 <DEGREE>
CENTER_LONGITUDE    = 87.50000 <DEGREE>
REFERENCE_LATITUDE  = "N/A"
REFERENCE_LONGITUDE = "N/A"
LINE_FIRST_PIXEL    = 1 /* North edge */
LINE_LAST_PIXEL     = 1280 /* South edge */
SAMPLE_FIRST_PIXEL  = 1 /* West edge */
SAMPLE_LAST_PIXEL   = 1136 /* East edge */
MAP_PROJECTION_ROTATION = 0.0
MAP_RESOLUTION      = 256 <PIXEL/DEGREE>
MAP_SCALE           = 0.231528833585 <KM/PIXEL>
MAXIMUM_LATITUDE    = 32.50000 <DEGREE>
MINIMUM_LATITUDE    = 27.50000 <DEGREE>
WESTERNMOST_LONGITUDE = 85.00000 <DEGREE>
EASTERNMOST_LONGITUDE = 90.00000 <DEGREE>
LINE_PROJECTION_OFFSET = 8320.000
SAMPLE_PROJECTION_OFFSET = 640.000
COORDINATE_SYSTEM_TYPE = "BODY-FIXED ROTATING"
COORDINATE_SYSTEM_NAME = "PLANETOCENTRIC"
END_OBJECT          = IMAGE_MAP_PROJECTION

```

END

## APPENDIX D3. MRDR LABEL (SUMMARY PRODUCT IMAGE)

```
PDS_VERSION_ID      = PDS3
RECORD_TYPE        = FIXED_LENGTH
RECORD_BYTES       = 4544
FILE_RECORDS      = 57600
LABEL_REVISION_NOTE = "2003-11-19, S. Slavney (GEO);
                      2005-09-25, S. Murchie (JHU/APL);
                      2007-03-09, E. Malaret (ACT Corp.);
                      2007-09-14, C. Hash (ACT Corp)"

^IMAGE              = "T1396_MRRSU_30N088_0256_1.IMG"

/* Map-projected Multispectral RDR Identification */

DATA_SET_ID         = "MRO-M-CRISM-5-RDR-MULTISPECTRAL-V1.0"
PRODUCT_ID          = "T1396_MRRSU_30N088_0256_1"
/*( TNNNN_MRRss_yydxxx_rrrr_v           )*/
/*( NNNN = tile number                  )*/
/*( ss = subtype of image product      )*/
/*( yy = latitude of upper left corner )*/
/*( d = N or S for north or south latitude )*/
/*( xxx = east longitude of upper left corner )*/
/*( rrrr = resolution in pixels/degree   )*/
/*( v = version number                 )*/

INSTRUMENT_HOST_NAME = "MARS RECONNAISSANCE ORBITER"
SPACECRAFT_ID       = MRO
INSTRUMENT_NAME     = "COMPACT RECONNAISSANCE IMAGING
                      SPECTROMETER FOR MARS"
INSTRUMENT_ID        = CRISM
TARGET_NAME          = MARS
PRODUCT_TYPE         = MAP_PROJECTED_MULTISPECTRAL_RDR
PRODUCT_CREATION_TIME = 2008-08-03T11:32:50.342
START_TIME           = "N/A"
STOP_TIME            = "N/A"
SPACECRAFT_CLOCK_START_COUNT = "N/A"
SPACECRAFT_CLOCK_STOP_COUNT  = "N/A"
PRODUCT_VERSION_ID   = "1"
PRODUCER_INSTITUTION_NAME = "APPLIED PHYSICS LABORATORY"
SOFTWARE_NAME         = "PIPE_create_crism_mrdr_product"
SOFTWARE_VERSION_ID   = "04.21.08"
MRO:WAVELENGTH_FILE_NAME = "N/A"

/* This Map Projected Multispectral RDR label describes one data file: */
/* 1. A multiple-band image file of calibrated RDR data in radiance, */
/* This RDR represents one latitude-longitude bin in a global map. */
/* See the Map Projection Object below for bin coordinates and resolution.*/
/* See the CRISM Data Products SIS for more detailed description. */

/* Description of MAP PROJECTED MULTISPECTRAL RDR RADIANCE IMAGE file */

OBJECT              = IMAGE
LINES               = 1280
LINE_SAMPLES        = 1136
SAMPLE_TYPE         = PC_REAL
SAMPLE_BITS         = 32

BANDS               = 45
BAND_STORAGE_TYPE   = BAND_SEQUENTIAL
```

```

BAND_NAME      = ("R770",
                  "RBR",
                  "BD530",
                  "SH600",
                  "BD640",
                  "BD860",
                  "BD920",
                  "RPEAK1",
                  "BDI1000VIS",
                  "BDI1000IR",
                  "IRAC",
                  "OLINDEX",
                  "LCPINDEX",
                  "HCPXINDEX",
                  "VAR",
                  "ISLOPE1",
                  "BD1435",
                  "BD1500",
                  "ICER1",
                  "BD1750",
                  "BD1900",
                  "BDI2000",
                  "BD2100",
                  "BD2210",
                  "BD2290",
                  "D2300",
                  "SINDEX",
                  "ICER2",
                  "BDCARB",
                  "BD3000",
                  "BD3100",
                  "BD3200",
                  "BD3400",
                  "CINDEX",
                  "R440",
                  "IRR1",
                  "BD1270O2",
                  "BD1400H2O",
                  "BD2000CO2",
                  "BD2350",
                  "BD2600",
                  "IRR2",
                  "R2700",
                  "BD2700",
                  "IRR3")
END_OBJECT     = IMAGE

/* Map projection information about this RDR is in the IMAGE_MAP_PROJECTION */
/* object below. */
```

```

OBJECT          = IMAGE_MAP_PROJECTION
^DATA_SET_MAP_PROJECTION = "MRR_MAP.CAT"
MAP_PROJECTION_TYPE = "EQUIRECTANGULAR"
A_AXIS_RADIUS    = 3396 <KM>
B_AXIS_RADIUS    = 3396 <KM>
C_AXIS_RADIUS    = 3396 <KM>
FIRST_STANDARD_PARALLEL = "N/A"
SECOND_STANDARD_PARALLEL = "N/A"
POSITIVE_LONGITUDE_DIRECTION = "EAST"
CENTER_LATITUDE   = 27.50000 <DEGREE>
CENTER_LONGITUDE  = 87.50000 <DEGREE>
REFERENCE_LATITUDE = "N/A"
```

```
REFERENCE_LONGITUDE      = "N/A"
LINE_FIRST_PIXEL        = 1    /* North edge */
LINE_LAST_PIXEL         = 1280 /* South edge */
SAMPLE_FIRST_PIXEL      = 1    /* West edge */
SAMPLE_LAST_PIXEL       = 1136 /* East edge */
MAP_PROJECTION_ROTATION = 0.0
MAP_RESOLUTION          = 256 <PIXEL/DEGREE>
MAP_SCALE               = 0.231528833585 <KM/PIXEL>
MAXIMUM_LATITUDE        = 32.50000 <DEGREE>
MINIMUM_LATITUDE        = 27.50000 <DEGREE>
WESTERNMOST_LONGITUDE   = 85.00000 <DEGREE>
EASTERNMOST_LONGITUDE   = 90.00000 <DEGREE>
LINE_PROJECTION_OFFSET  = 8320.000
SAMPLE_PROJECTION_OFFSET = 640.000
COORDINATE_SYSTEM_TYPE  = "BODY-FIXED ROTATING"
COORDINATE_SYSTEM_NAME   = "PLANETOCENTRIC"
END_OBJECT              = IMAGE_MAP_PROJECTION
```

END

## APPENDIX D4. MRDR LABEL (WAVELENGTH FILE)

```

PDS_VERSION_ID      = PDS3
RECORD_TYPE        = FIXED_LENGTH
RECORD_BYTES       = 16
FILE_RECORDS      = 72
LABEL_REVISION_NOTE = "2003-11-19, S. Slavney (GEO);
                      2006-09-25, S. Murchie (JHU/APL)
                      2006-09-27, S. Murchie (JHU/APL)
                      2007-09-14, C. Hash (ACT Corp)"

^TABLE              = "T1396_MRRWV_30N088_0256_1.TAB"

/* Map-projected Multispectral RDR Identification */
DATA_SET_ID         = "MRO-M-CRISM-5-RDR-MULTISPECTRAL-V1.0"
PRODUCT_ID          = "T1396_MRRWV_30N088_0256_1"
/*( Tnnnn_MRRss_xx yyyy rrrr_v )*/
/*( nnnn = tile number           )*/
/*( ss = subtype of image product )*/
/*( xx = latitude of tile center )*/
/*( d = N or S for north or south latitude )*/
/*( yyyy = east longitude of tile center )*/
/*( rrrr = resolution in pixels/degree )*/
/*( v = version number          )*/

INSTRUMENT_HOST_NAME = "MARS RECONNAISSANCE ORBITER"
SPACECRAFT_ID       = MRO
INSTRUMENT_NAME      = "COMPACT RECONNAISSANCE IMAGING
                      SPECTROMETER FOR MARS"
INSTRUMENT_ID        = CRISM
TARGET_NAME          = MARS
PRODUCT_TYPE         = MAP_PROJECTED_MULTISPECTRAL_RDR
PRODUCT_CREATION_TIME = 2008-12-09T08:00:39.178
START_TIME           = "N/A"
STOP_TIME            = "N/A"
SPACECRAFT_CLOCK_START_COUNT = "N/A"
SPACECRAFT_CLOCK_STOP_COUNT  = "N/A"
PRODUCT_VERSION_ID   = "1"
PRODUCER_INSTITUTION_NAME = "APPLIED PHYSICS LABORATORY"
SOFTWARE_NAME         = "PIPE_create_crism_tile_wv"
SOFTWARE_VERSION_ID   = "12.05.08"

/* This Map Projected Multispectral RDR label describes four data files: */
/* 6. A listfile including detector row numbers and wavelengths in the */
/* I.F and Lambert albedo images.          */
/* This RDR represents one latitude-longitude bin in a global map.      */
/* See the Map Projection Object below for bin coordinates and resolution.*/
/* See the CRISM Data Products SIS for more detailed description.      */
/* Description of MAP PROJECTED MULTISPECTRAL RDR LISTFILE */

OBJECT              = TABLE
NAME                = "CRISM MRDR WAVELENGTH TABLE"
INTERCHANGE_FORMAT   = "ASCII"
ROWS                = 72
COLUMNS              = 3
ROW_BYTES            = 14
DESCRIPTION          = "CRISM MRDR wavelength table "
OBJECT              = COLUMN
COLUMN_NUMBER        = 1
NAME                = SPECT_ID
DATA_TYPE            = ASCII_INTEGER
START_BYTE           = 214

```

```
BYTES      = 1
DESCRIPTION = "Spectrometer identifier; 0 = IR; 1 = VNIR"
END_OBJECT = COLUMN
OBJECT     = COLUMN
COLUMN_NUMBER = 2
NAME       = ROWNUM
DATA_TYPE   = ASCII_INTEGER
START_BYTE  = 3
BYTES      = 3
DESCRIPTION = "detector row number (0-479)"
END_OBJECT = COLUMN
OBJECT     = COLUMN
COLUMN_NUMBER = 3
NAME       = SAMPL_WAV
DATA_TYPE   = ASCII_REAL
START_BYTE  = 7
BYTES      = 8
DESCRIPTION = "Standard sampling center wavelength in nm"
UNIT       = "NM"
END_OBJECT = COLUMN
END_OBJECT = TABLE
END
```

## **APPENDIX E1. TER LABEL (CORRECTED I/F FILE)**

```

SOFTWARE_NAME           = "mtrdr_pipeline"
SOFTWARE_VERSION_ID     = "1.0"

SOURCE_PRODUCT_ID      = (
    "FRT00002F7F_07_DE168L_DDR1",
    "FRT00002F7F_07_DE168S_DDR1",
    "FRT00002F7F_07_IF168L_TRR3",
    "FRT00002F7F_07_IF168S_TRR3",
    "CDR410803692813_WA0000000L_3",
    "CDR410803692813_WA0000000S_2",
    "CDR6_1_0000000000_SW_L_3",
    "CDR6_1_0000000000_SW_S_2"
)
/* Targeted RDR Observation and Processing Parameters */

SOLAR_DISTANCE          = 236036552.409150 <KILOMETER>
SOLAR_LONGITUDE          = 133.840086
MRO:WAVELENGTH_FILE_NAME = "FRT00002F7F_07_WV168J_TER3.TAB"
MRO:PHOTOMETRIC_CORR_FLAG = "ON"
MRO:ATMOSPHERIC_CORR_FLAG = "ON"
MRO:RATIO_SHIFT_CORR_FLAG = "ON"
MRO:EMPIRICAL_GEOM_NORM_FLAG = "ON"
MRO:EMPIRICAL_SMILE_CORR_FLAG = "ON"
MRO:SENSOR_SPACE_TRANSFORM_FLAG = "ON"

/* ENVI header description */
/* The ENVI header is a separate ASCII file that includes basic image */
/* data file characteristics and allows the image data to be loaded */
/* directly into the ENVI image processing software available bands */
/* list. */

OBJECT                  = ENVI_HEADER
HEADER_TYPE              = "ENVI"
INTERCHANGE_FORMAT        = "ASCII"
BYTES                   = 17855
DESCRIPTION              = "This text file can be used by ENVI image
processing software to read in the image."
END_OBJECT               = ENVI_HEADER

/* This Targeted Empirical Record label describes a multiple-band */
/* image file containing calibrated and corrected spectral data */
/* in units of corrected I over F. */

OBJECT                  = IMAGE
LINES                   = 540
LINE_SAMPLES             = 640
SAMPLE_TYPE              = PC_REAL
SAMPLE_BITS               = 32
UNIT                    = "CORRECTED_I_OVER_F"
BANDS                   = 545
BAND_STORAGE_TYPE        = BAND_SEQUENTIAL
END_OBJECT = IMAGE

END

```

## APPENDIX E2. TER LABEL (DATA PROCESSING INFORMATION FILE)

```

PDS_VERSION_ID = PDS3

RECORD_TYPE = FIXED_LENGTH
RECORD_BYTES = 2560
FILE_RECORDS = 4860
LABEL_REVISION_NOTE =
    "2012-03-06, H. Taylor, F. Seelos (JHU/APL)
    Initial TER/MTRDR labels for CRISM Data Users' Workshop;
    2014-01-09, G. Romeo, J. Aiello, F. Seelos (JHU/APL)
    Complete TER/MTRDR label set for preliminary PDS review;
    2014-04-08, G. Romeo, J. Aiello, R. Espiritu, F. Seelos (JHU/APL)
    TER/MTRDR label set revisions completed for PDS peer review;
    2014-08-14, G. Romeo, J. Aiello, F. Seelos (JHU/APL)
    PDS peer review TER/MTRDR label set liens retired;"

^ENVI_HEADER = "FRT00002F7F_07_IN168J_TER3.HDR"
^IMAGE = "FRT00002F7F_07_IN168J_TER3.IMG"

/* DDR Identification */
DATA_SET_ID = "MRO-M-CRISM-4-RDR-TARGETED-V1.0"
PRODUCT_ID = "FRT00002F7F_07_IN168J_TER3"

/*
/*          cccnnnnnnn_xx_ooaaas_TERv      */
/*          ccc = Class Type             */
/*          nnnnnnnn = Observation ID (hex) */
/*          xx = counter this observation (hex) */
/*          ooaaa = obs type, macro number */
/*          s = sensor ID (J for Joined)   */
/*          v = version number           */
*/

INSTRUMENT_HOST_NAME = "MARS RECONNAISSANCE ORBITER"
SPACECRAFT_ID = MRO
INSTRUMENT_NAME = "COMPACT RECONNAISSANCE IMAGING
                  SPECTROMETER FOR MARS"
INSTRUMENT_ID = CRISM
TARGET_NAME = MARS
PRODUCT_TYPE = TARGETED_RDR
PRODUCT_CREATION_TIME = 2015-06-10T16:40:53
START_TIME = 2006-11-11T13:21:36.054
STOP_TIME = 2006-11-11T13:23:59.788
SPACECRAFT_CLOCK_START_COUNT = "2/0847718514.58200"
SPACECRAFT_CLOCK_STOP_COUNT = "2/0847718658.40771"

ORBIT_NUMBER = 1374
OBSERVATION_TYPE = "FRT"
OBSERVATION_ID = "16#00002F7F#"
MRO:OBSERVATION_NUMBER = 16#07#
MRO:ACTIVITY_ID = "IF168"
MRO:SENSOR_ID = "J"
PRODUCT_VERSION_ID = "3"
PRODUCER_INSTITUTION_NAME = "JOHNS HOPKINS UNIVERSITY
                             APPLIED PHYSICS LABORATORY"
SOFTWARE_NAME = "mtrdr_pipeline"

```

```

SOFTWARE_VERSION_ID          = "1.0"
SOURCE_PRODUCT_ID           =
  "FRT00002F7F_07_DE168L_DDR1",
  "FRT00002F7F_07_DE168S_DDR1",
  "FRT00002F7F_07_IF168J_TER3"
)

/* Targeted RDR Observation and Processing Parameters */

SOLAR_DISTANCE              = 236036552.409150 <KILOMETER>
SOLAR_LONGITUDE              = 133.840086
MRO:PHOTOMETRIC_CORR_FLAG   = "ON"
MRO:ATMOSPHERIC_CORR_FLAG   = "ON"
MRO:RATIO_SHIFT_CORR_FLAG   = "ON"
MRO:EMPIRICAL_GEOM_NORM_FLAG = "ON"
MRO:EMPIRICAL_SMILE_CORR_FLAG = "ON"
MRO:SENSOR_SPACE_TRANSFORM_FLAG = "ON"

/* ENVI header description */
/* The ENVI header is a separate ASCII file that includes basic image */
/* data file characteristics and allows the image data to be loaded */
/* directly into the ENVI image processing software available bands */
/* list. */

OBJECT                      = ENVI_HEADER
  HEADER_TYPE                = "ENVI"
  INTERCHANGE_FORMAT          = "ASCII"
  BYTES                      = 664
  DESCRIPTION                = "This text file can be used by ENVI image
processing software to read in the image."
END_OBJECT                  = ENVI_HEADER

/* This Targeted Empirical Record label describes a multiple-band */
/* image file containing TER/MTRDR data processing information. */

OBJECT                      = IMAGE
  LINES                      = 540
  LINE_SAMPLES               = 640
  SAMPLE_TYPE                = PC_REAL
  SAMPLE_BITS                = 32
  DESCRIPTION                = "TER_MTRDR_PROCESSING_INFORMATION"
  BANDS                      = 9
  BAND_STORAGE_TYPE          = BAND_SEQUENTIAL
  BAND_NAME                  =
    ( "VNIR/IR Spectral Continuity Residual",
      "VNIR/IR Spatial Gradient Residual",
      "ATM Correction Spectral Shift Artifact",
      "VNIR Sample",
      "VNIR Line",
      "IR Sample",
      "IR Line",
      "VNIR/IR Ground Sampling Offset",
      "VNIR/IR Mask" )
END_OBJECT                  = IMAGE

END

```

## APPENDIX E3. TER LABEL (REFINED SUMMARY PRODUCT FILE)

```

PDS_VERSION_ID = PDS3

RECORD_TYPE = FIXED_LENGTH
RECORD_BYTES = 2560
FILE_RECORDS = 32400
LABEL_REVISION_NOTE =
    "2012-03-06, H. Taylor, F. Seelos (JHU/APL)
    Initial TER/MTRDR labels for CRISM Data Users' Workshop;
    2014-01-09, G. Romeo, J. Aiello, F. Seelos (JHU/APL)
    Complete TER/MTRDR label set for preliminary PDS review;
    2014-04-08, G. Romeo, J. Aiello, R. Espiritu, F. Seelos (JHU/APL)
    TER/MTRDR label set revisions completed for PDS peer review;
    2014-08-14, G. Romeo, J. Aiello, F. Seelos (JHU/APL)
    PDS peer review TER/MTRDR label set liens retired;"

^ENVI_HEADER = "FRT00002F7F_07_SR168J_TER3.HDR"
^IMAGE = "FRT00002F7F_07_SR168J_TER3.IMG"

/* DDR Identification */
DATA_SET_ID = "MRO-M-CRISM-4-RDR-TARGETED-V1.0"
PRODUCT_ID = "FRT00002F7F_07_SR168J_TER3"

/*
/*          cccnnnnnnn_xx_ooaaas_TERv      */
/*          ccc = Class Type             */
/*          nnnnnnnn = Observation ID (hex) */
/*          xx = counter this observation (hex) */
/*          ooaaa = obs type, macro number */
/*          s = sensor ID (J for Joined)   */
/*          v = version number           */
*/

INSTRUMENT_HOST_NAME = "MARS RECONNAISSANCE ORBITER"
SPACECRAFT_ID = MRO
INSTRUMENT_NAME = "COMPACT RECONNAISSANCE IMAGING
                  SPECTROMETER FOR MARS"
INSTRUMENT_ID = CRISM
TARGET_NAME = MARS
PRODUCT_TYPE = TARGETED_RDR
PRODUCT_CREATION_TIME = 2015-06-11T04:42:23
START_TIME = 2006-11-11T13:21:36.054
STOP_TIME = 2006-11-11T13:23:59.788
SPACECRAFT_CLOCK_START_COUNT = "2/0847718514.58200"
SPACECRAFT_CLOCK_STOP_COUNT = "2/0847718658.40771"

ORBIT_NUMBER = 1374
OBSERVATION_TYPE = "FRT"
OBSERVATION_ID = "16#00002F7F#"
MRO:OBSERVATION_NUMBER = 16#07#
MRO:ACTIVITY_ID = "IF168"
MRO:SENSOR_ID = "J"
PRODUCT_VERSION_ID = "3"
PRODUCER_INSTITUTION_NAME = "JOHNS HOPKINS UNIVERSITY
                             APPLIED PHYSICS LABORATORY"
SOFTWARE_NAME = "mtrdr_pipeline"

```

```

SOFTWARE_VERSION_ID          = "1.0"
SOURCE_PRODUCT_ID           =
    "FRT00002F7F_07_SU168J_TER3"
)

/* Targeted RDR Observation and Processing Parameters */

SOLAR_DISTANCE              = 236036552.409150 <KILOMETER>
SOLAR_LONGITUDE              = 133.840086
MRO:PHOTOMETRIC_CORR_FLAG   = "ON"
MRO:ATMOSPHERIC_CORR_FLAG   = "ON"
MRO:RATIO_SHIFT_CORR_FLAG   = "ON"
MRO:EMPIRICAL_GEOM_NORM_FLAG = "ON"
MRO:EMPIRICAL_SMILE_CORR_FLAG = "ON"
MRO:SENSOR_SPACE_TRANSFORM_FLAG = "ON"

/* ENVI header description */
/* The ENVI header is a separate ASCII file that includes basic image      */
/* data file characteristics and allows the image data to be loaded       */
/* directly into the ENVI image processing software available bands      */
/* list.                                                               */
/*                                                                       */

OBJECT                      = ENVI_HEADER
HEADER_TYPE                 = "ENVI"
INTERCHANGE_FORMAT          = "ASCII"
BYTES                       = 987
DESCRIPTION                 = "This text file can be used by ENVI image
processing software to read in the image."
END_OBJECT                  = ENVI_HEADER

/* This Targeted Empirical Record label describes a multiple-band      */
/* image file containing refined spectral summary parameters           */
/* calculated from calibrated and corrected spectral data.            */
/*                                                                       */

OBJECT                      = IMAGE
LINES                       = 540
LINE_SAMPLES                = 640
SAMPLE_TYPE                 = PC_REAL
SAMPLE_BITS                 = 32
DESCRIPTION                 = "REFINED_SPECTRAL_SUMMARY_PARAMETERS"
BANDS                       = 60
BAND_STORAGE_TYPE          = BAND_SEQUENTIAL
BAND_NAME                   =
    ( "R770",
      "RBR",
      "BD530_2",
      "SH600_2",
      "SH770",
      "BD640_2",
      "BD860_2",
      "BD920_2",
      "RPEAK1",
      "BDI1000VIS",
      "R440",
      "IRR1",
      "BDI1000IR",
      "OLINDEX3",
      )

```

```

    "R1330" for v0-v3,
    "R1337" for v4,
    "BD1300",
    "LCPINDEX2",
    "HCPINDEX2",
    "VAR",
    "ISLOPE1",
    "BD1400",
    "BD1435",
    "BD1500_2",
    "ICER1_2",
    "BD1750_2",
    "BD1900_2",
    "BD1900R2",
    "BDI2000",
    "BD2100_2",
    "BD2165",
    "BD2190",
    "MIN2200",
    "BD2210_2",
    "D2200",
    "BD2230",
    "BD2250",
    "MIN2250",
    "BD2265",
    "BD2290",
    "D2300",
    "BD2355",
    "SINDEX2",
    "ICER2_2",
    "MIN2295_2480",
    "MIN2345_2537",
    "BD2500_2",
    "BD3000",
    "BD3100",
    "BD3200",
    "BD3400_2",
    "CINDEX2",
    "BD2600",
    "IRR2",
    "IRR3",
    "R530",
    "R600",
    "R1080",
    "R1506",
    "R2529",
    "R3920" )
END_OBJECT
= IMAGE
END

```

## APPENDIX E4. TER LABEL (SUMMARY PRODUCT FILE)

```

PDS_VERSION_ID = PDS3

RECORD_TYPE = FIXED_LENGTH
RECORD_BYTES = 2560
FILE_RECORDS = 32400
LABEL_REVISION_NOTE =
    "2012-03-06, H. Taylor, F. Seelos (JHU/APL)
    Initial TER/MTRDR labels for CRISM Data Users' Workshop;
    2014-01-09, G. Romeo, J. Aiello, F. Seelos (JHU/APL)
    Complete TER/MTRDR label set for preliminary PDS review;
    2014-04-08, G. Romeo, J. Aiello, R. Espiritu, F. Seelos (JHU/APL)
    TER/MTRDR label set revisions completed for PDS peer review;
    2014-08-14, G. Romeo, J. Aiello, F. Seelos (JHU/APL)
    PDS peer review TER/MTRDR label set liens retired;"

^ENVI_HEADER = "FRT00002F7F_07_SU168J_TER3.HDR"
^IMAGE = "FRT00002F7F_07_SU168J_TER3.IMG"

/* DDR Identification */
DATA_SET_ID = "MRO-M-CRISM-4-RDR-TARGETED-V1.0"
PRODUCT_ID = "FRT00002F7F_07_SU168J_TER3"

/*
/*          cccnnnnnnn_xx_ooaaas_TERv      */
/*          ccc = Class Type             */
/*          nnnnnnnn = Observation ID (hex) */
/*          xx = counter this observation (hex) */
/*          ooaaa = obs type, macro number */
/*          s = sensor ID (J for Joined)   */
/*          v = version number           */
*/

INSTRUMENT_HOST_NAME = "MARS RECONNAISSANCE ORBITER"
SPACECRAFT_ID = MRO
INSTRUMENT_NAME = "COMPACT RECONNAISSANCE IMAGING
                  SPECTROMETER FOR MARS"
INSTRUMENT_ID = CRISM
TARGET_NAME = MARS
PRODUCT_TYPE = TARGETED_RDR
PRODUCT_CREATION_TIME = 2015-06-11T02:24:10
START_TIME = 2006-11-11T13:21:36.054
STOP_TIME = 2006-11-11T13:23:59.788
SPACECRAFT_CLOCK_START_COUNT = "2/0847718514.58200"
SPACECRAFT_CLOCK_STOP_COUNT = "2/0847718658.40771"

ORBIT_NUMBER = 1374
OBSERVATION_TYPE = "FRT"
OBSERVATION_ID = "16#00002F7F#"
MRO:OBSERVATION_NUMBER = 16#07#
MRO:ACTIVITY_ID = "IF168"
MRO:SENSOR_ID = "J"
PRODUCT_VERSION_ID = "3"
PRODUCER_INSTITUTION_NAME = "JOHNS HOPKINS UNIVERSITY
                             APPLIED PHYSICS LABORATORY"
SOFTWARE_NAME = "mtrdr_pipeline"

```

```

SOFTWARE_VERSION_ID          = "1.0"
SOURCE_PRODUCT_ID           =
    "FRT00002F7F_07_IF168J_TER3"
)

/* Targeted RDR Observation and Processing Parameters */

SOLAR_DISTANCE              = 236036552.409150 <KILOMETER>
SOLAR_LONGITUDE              = 133.840086
MRO:PHOTOMETRIC_CORR_FLAG   = "ON"
MRO:ATMOSPHERIC_CORR_FLAG   = "ON"
MRO:RATIO_SHIFT_CORR_FLAG   = "ON"
MRO:EMPIRICAL_GEOM_NORM_FLAG = "ON"
MRO:EMPIRICAL_SMILE_CORR_FLAG = "ON"
MRO:SENSOR_SPACE_TRANSFORM_FLAG = "ON"

/* ENVI header description */
/* The ENVI header is a separate ASCII file that includes basic image      */
/* data file characteristics and allows the image data to be loaded       */
/* directly into the ENVI image processing software available bands      */
/* list.                                                               */
/*                                                                     */

OBJECT                      = ENVI_HEADER
    HEADER_TYPE            = "ENVI"
    INTERCHANGE_FORMAT     = "ASCII"
    BYTES                  = 987
    DESCRIPTION             = "This text file can be used by ENVI image
                                processing software to read in the image."
END_OBJECT                   = ENVI_HEADER

/* This Targeted Empirical Record label describes a multiple-band      */
/* image file containing spectral summary parameters calculated      */
/* from calibrated and corrected spectral data.                         */
/*                                                                     */

OBJECT                      = IMAGE
    LINES                  = 540
    LINE_SAMPLES            = 640
    SAMPLE_TYPE             = PC_REAL
    SAMPLE_BITS              = 32
    DESCRIPTION             = "SPECTRAL_SUMMARY_PARAMETERS"
    BANDS                  = 60
    BAND_STORAGE_TYPE       = BAND_SEQUENTIAL
    BAND_NAME               =
        ( "R770",
          "RBR",
          "BD530_2",
          "SH600_2",
          "SH770",
          "BD640_2",
          "BD860_2",
          "BD920_2",
          "RPEAK1",
          "BDI1000VIS",
          "R440",
          "IRR1",
          "BDI1000IR",
          "OLINDEX3",

```

```

    "R1330",
    "BD1300",
    "LCPINDEX2",
    "HCPIINDEX2",
    "VAR",
    "ISLOPE1",
    "BD1400",
    "BD1435",
    "BD1500_2",
    "ICER1_2",
    "BD1750_2",
    "BD1900_2",
    "BD1900R2",
    "BDI2000",
    "BD2100_2",
    "BD2165",
    "BD2190",
    "MIN2200",
    "BD2210_2",
    "D2200",
    "BD2230",
    "BD2250",
    "MIN2250",
    "BD2265",
    "BD2290",
    "D2300",
    "BD2355",
    "SINDEX2",
    "ICER2_2",
    "MIN2295_2480",
    "MIN2345_2537",
    "BD2500_2",
    "BD3000",
    "BD3100",
    "BD3200",
    "BD3400_2",
    "CINDEX2",
    "BD2600",
    "IRR2",
    "IRR3",
    "R530",
    "R600",
    "R1080",
    "R1506",
    "R2529",
    "R3920" )
END_OBJECT      = IMAGE
END

```

## APPENDIX E5. TER LABEL (WAVELENGTH FILE)

```

PDS_VERSION_ID = PDS3

RECORD_TYPE = FIXED_LENGTH
RECORD_BYTES = 30
FILE_RECORDS = 545
LABEL_REVISION_NOTE =
    "2012-03-06, H. Taylor, F. Seelos (JHU/APL)
    Initial TER/MTRDR labels for CRISM Data Users' Workshop;
    2014-01-09, G. Romeo, J. Aiello, F. Seelos (JHU/APL)
    Complete TER/MTRDR label set for preliminary PDS review;
    2014-04-08, G. Romeo, J. Aiello, R. Espiritu, F. Seelos (JHU/APL)
    TER/MTRDR label set revisions completed for PDS peer review;
    2014-08-14, G. Romeo, J. Aiello, F. Seelos (JHU/APL)
    PDS peer review TER/MTRDR label set liens retired;"

^WAVELENGTH_SOURCE_TABLE = "FRT00002F7F_07_WV168J_TER3.TAB"

/* Map-Projected Targeted RDR Identification */
DATA_SET_ID = "MRO-M-CRISM-4-RDR-TARGETED-V1.0"
PRODUCT_ID = "FRT00002F7F_07_WV168J_TER3"

/*
   cccnnnnnnn_xx_ooaaaas_TERv      */
/*   ccc = Class Type               */
/*   nnnnnnnn = Observation ID, hexadecimal */
/*   xx = counter this observation (hex) */
/*   ooooo = Image type, Macro number */
/*   s = Sensor ID (J for Joined)   */
/*   v = Version number            */

INSTRUMENT_HOST_NAME = "MARS RECONNAISSANCE ORBITER"
SPACECRAFT_ID = MRO
INSTRUMENT_NAME = "COMPACT RECONNAISSANCE IMAGING
                  SPECTROMETER FOR MARS"
INSTRUMENT_ID = CRISM
TARGET_NAME = MARS
PRODUCT_TYPE = TARGETED_RDR
PRODUCT_CREATION_TIME = 2015-06-10T16:38:51
START_TIME = 2006-11-11T13:21:36.054
STOP_TIME = 2006-11-11T13:23:59.788
SPACECRAFT_CLOCK_START_COUNT = "2/0847718514.58200"
SPACECRAFT_CLOCK_STOP_COUNT = "2/0847718658.40771"

PRODUCT_VERSION_ID = "3"
PRODUCER_INSTITUTION_NAME = "JOHNS HOPKINS UNIVERSITY
                            APPLIED PHYSICS LABORATORY"
SOFTWARE_NAME = "mtrdr_pipeline"
SOFTWARE_VERSION_ID = "1.0"

/* A listfile including spectrometer identifier, detector row numbers,*/
/* wavelengths, full width half max, and bad band identifier in the*/
/* Targeted Empirical Record and Map-Projected Targeted RDR images. */

OBJECT = WAVELENGTH_SOURCE_TABLE
NAME = "CRISM JOINED WAVELENGTH TABLE"

```

```

INTERCHANGE_FORMAT = "ASCII"
ROWS                = 545
COLUMNS              = 5
ROW_BYTES            = 30
DESCRIPTION          = "CRISM JOINED WAVELENGTH table"
OBJECT
  COLUMN_NUMBER      = 1
  NAME               = SPECT_ID
  DATA_TYPE           = ASCII_INTEGER
  START_BYTE          = 1
  BYTES               = 2
  DESCRIPTION         = "Spectrometer identifier; 0 = IR; 1 = VNIR"
END_OBJECT
OBJECT
  COLUMN_NUMBER      = 2
  NAME               = ROWNUM
  DATA_TYPE           = ASCII_INTEGER
  START_BYTE          = 4
  BYTES               = 4
  DESCRIPTION         = "detector row number (0-479)"
END_OBJECT
OBJECT
  COLUMN_NUMBER      = 3
  NAME               = SAMPL_WAV
  DATA_TYPE           = ASCII_REAL
  START_BYTE          = 9
  BYTES               = 8
  DESCRIPTION         = "Standard sampling center wavelength in nm"
  UNIT                = "NM"
END_OBJECT
OBJECT
  COLUMN_NUMBER      = 4
  NAME               = FWHM
  DATA_TYPE           = ASCII_REAL
  START_BYTE          = 18
  BYTES               = 8
  DESCRIPTION         = "Full Width Half Max in nm"
  UNIT                = "NM"
END_OBJECT
OBJECT
  COLUMN_NUMBER      = 5
  NAME               = BAD_BAND_ID
  DATA_TYPE           = ASCII_INTEGER
  START_BYTE          = 27
  BYTES               = 2
  DESCRIPTION         = "Bad Band Identifier; 0 = BAD; 1 = GOOD"
END_OBJECT
END_OBJECT
= WAVELENGTH_SOURCE_TABLE
END

```

## **APPENDIX E6. MTRDR LABEL (CORRECTED I/F FILE)**

```

PRODUCT_VERSION_ID      = "3"
PRODUCER_INSTITUTION_NAME = "JOHNS HOPKINS UNIVERSITY
                           APPLIED PHYSICS LABORATORY"
SOFTWARE_NAME           = "mtrdr_pipeline"
SOFTWARE_VERSION_ID     = "1.0"
SOURCE_PRODUCT_ID       =
  ("FRT00002F7F_07_IF168J_TER3",
   "FRT00002F7F_07_DE168L_DDR1"
)

/*
 * Targeted RDR Observation and Processing Parameters */

SOLAR_DISTANCE          = 236036552.409150 <KILOMETER>
SOLAR_LONGITUDE          = 133.840086
MRO:WAVELENGTH_FILE_NAME = "FRT00002F7F_07_WV168J_MTR3.TAB"
MRO:PHOTOMETRIC_CORR_FLAG = "ON"
MRO:ATMOSPHERIC_CORR_FLAG = "ON"
MRO:RATIO_SHIFT_CORR_FLAG = "ON"
MRO:EMPIRICAL_GEOM_NORM_FLAG = "ON"
MRO:EMPIRICAL_SMILE_CORR_FLAG = "ON"
MRO:SENSOR_SPACE_TRANSFORM_FLAG = "ON"

/* Map projection information about this RDR is in the */
/* IMAGE_MAP_PROJECTION object below. */

OBJECT                  = IMAGE_MAP_PROJECTION
  ^DATA_SET_MAP_PROJECTION = "MTR_MAP.CAT"
  MAP_PROJECTION_TYPE     = "POLAR STEREOGRAPHIC"
  A_AXIS_RADIUS           = 3396.190000000000 <KILOMETER>
  B_AXIS_RADIUS           = 3396.190000000000 <KILOMETER>
  C_AXIS_RADIUS           = 3376.200000000000 <KILOMETER>
  POSITIVE_LONGITUDE_DIRECTION = EAST
  CENTER_LATITUDE         = 90.0000000 <DEGREE>
  CENTER_LONGITUDE        = 0.0000000 <DEGREE>
  LINE_FIRST_PIXEL        = 1 <PIXEL>
  LINE_LAST_PIXEL         = 761 <PIXEL>
  SAMPLE_FIRST_PIXEL      = 1 <PIXEL>
  SAMPLE_LAST_PIXEL       = 880 <PIXEL>
  MAP_PROJECTION_ROTATION = 0.0000000 <DEGREE>
  MAP_RESOLUTION          = 3293.0387513
  MAP_SCALE                = 0.0180000
  MINIMUM_LATITUDE        = 84.8928520 <DEGREE>
  MAXIMUM_LATITUDE        = 85.2014640 <DEGREE>
  WESTERNMOST_LONGITUDE   = -22.8965470 <DEGREE>
  EASTERNMOST_LONGITUDE   = -19.0829150 <DEGREE>
  LINE_PROJECTION_OFFSET  = -14945.9116667 <PIXEL>
  SAMPLE_PROJECTION_OFFSET = 6313.7611111 <PIXEL>
  COORDINATE_SYSTEM_TYPE  = "BODY-FIXED ROTATING"
  COORDINATE_SYSTEM_NAME   = "PLANETOCENTRIC"
END_OBJECT               = IMAGE_MAP_PROJECTION

/*
 * ENVI header description */
/* The ENVI header is a separate ASCII file that includes basic image */
/* data file characteristics and allows the image data to be loaded */
/* directly into the ENVI image processing software available bands */
/* list. */

OBJECT                  = ENVI_HEADER
  HEADER_TYPE            = "ENVI"
  INTERCHANGE_FORMAT     = "ASCII"
  BYTES                  = 14781
  DESCRIPTION             = "This text file can be used by ENVI image
                                processing software to read in the image."

```

```
END_OBJECT          = ENVI_HEADER

/* This Map-Projected Targeted RDR label describes a multiple-band */
/* image file containing calibrated and corrected spectral data      */
/* in units of corrected I over F.                                     */

OBJECT              = IMAGE
LINES               = 761
LINE_SAMPLES        = 880
SAMPLE_TYPE         = PC_REAL
SAMPLE_BITS         = 32
UNIT                = "CORRECTED_I_OVER_F"
BANDS               = 489
BAND_STORAGE_TYPE  = BAND_SEQUENTIAL
END_OBJECT = IMAGE

END
```

## APPENDIX E7. MTRDR LABEL (DATA PROCESSING INFORMATION FILE)

```

PDS_VERSION_ID = PDS3

RECORD_TYPE = FIXED_LENGTH
RECORD_BYTES = 3520
FILE_RECORDS = 6849
LABEL_REVISION_NOTE =
    "2012-03-06, H. Taylor, F. Seelos (JHU/APL)
     Initial TER/MTRDR labels for CRISM Data Users' Workshop;
     2014-01-09, G. Romeo, J. Aiello, F. Seelos (JHU/APL)
     Complete TER/MTRDR label set for preliminary PDS review;
     2014-04-08, G. Romeo, J. Aiello, R. Espiritu, F. Seelos (JHU/APL)
     TER/MTRDR label set revisions completed for PDS peer review;
     2014-08-14, G. Romeo, J. Aiello, F. Seelos (JHU/APL)
     PDS peer review TER/MTRDR label set liens retired;"

^ENVI_HEADER = "FRT00002F7F_07_IN168J_MTR3.HDR"
^IMAGE = "FRT00002F7F_07_IN168J_MTR3.IMG"

/* DDR Identification */
DATA_SET_ID = "MRO-M-CRISM-5-RDR-MPTARGETED-V1.0"
PRODUCT_ID = "FRT00002F7F_07_IN168J_MTR3"

/*
/*          cccnnnnnnn_xx_oaaaaas_MTRv      */
/*          ccc = Class Type                */
/*          nnnnnnnn = Observation ID (hex) */
/*          xx = counter this observation (hex) */
/*          ooooo = obs type, macro number   */
/*          s = sensor ID (J for Joined)    */
/*          v = version number             */
*/

INSTRUMENT_HOST_NAME = "MARS RECONNAISSANCE ORBITER"
SPACECRAFT_ID = MRO
INSTRUMENT_NAME = "COMPACT RECONNAISSANCE IMAGING
                  SPECTROMETER FOR MARS"
INSTRUMENT_ID = CRISM
TARGET_NAME = MARS
PRODUCT_TYPE = MPTARGETED_RDR
PRODUCT_CREATION_TIME = 2015-06-11T20:21:43
START_TIME = 2006-11-11T13:21:36.054
STOP_TIME = 2006-11-11T13:23:59.788
SPACECRAFT_CLOCK_START_COUNT = "2/0847718514.58200"
SPACECRAFT_CLOCK_STOP_COUNT = "2/0847718658.40771"

ORBIT_NUMBER = 1374
OBSERVATION_TYPE = "FRT"
OBSERVATION_ID = "16#00002F7F#"
MRO:OBSERVATION_NUMBER = 16#07#
MRO:ACTIVITY_ID = "IF168"
MRO:SENSOR_ID = "J"
PRODUCT_VERSION_ID = "3"
PRODUCER_INSTITUTION_NAME = "JOHNS HOPKINS UNIVERSITY
                             APPLIED PHYSICS LABORATORY"

```

```

SOFTWARE_NAME = "mtrdr_pipeline"
SOFTWARE_VERSION_ID = "1.0"
SOURCE_PRODUCT_ID =
    "FRT00002F7F_07_DE168L_DDR1",
    "FRT00002F7F_07_DE168S_DDR1",
    "FRT00002F7F_07_IF168J_MTR3"
)

/* Targeted RDR Observation and Processing Parameters */

SOLAR_DISTANCE = 236036552.409150 <KILOMETER>
SOLAR_LONGITUDE = 133.840086
MRO:PHOTOMETRIC_CORR_FLAG = "ON"
MRO:ATMOSPHERIC_CORR_FLAG = "ON"
MRO:RATIO_SHIFT_CORR_FLAG = "ON"
MRO:EMPIRICAL_GEOM_NORM_FLAG = "ON"
MRO:EMPIRICAL_SMILE_CORR_FLAG = "ON"
MRO:SENSOR_SPACE_TRANSFORM_FLAG = "ON"

/* Map projection information about this RDR is in the */
/* IMAGE_MAP_PROJECTION object below. */

OBJECT = IMAGE_MAP_PROJECTION
  ^DATA_SET_MAP_PROJECTION = "MTR_MAP.CAT"
  MAP_PROJECTION_TYPE = "POLAR STEREOGRAPHIC"
  A_AXIS_RADIUS = 3396.190000000000 <KILOMETER>
  B_AXIS_RADIUS = 3396.190000000000 <KILOMETER>
  C_AXIS_RADIUS = 3376.200000000000 <KILOMETER>
  POSITIVE_LONGITUDE_DIRECTION = EAST
  CENTER_LATITUDE = 90.0000000 <DEGREE>
  CENTER_LONGITUDE = 0.0000000 <DEGREE>
  LINE_FIRST_PIXEL = 1 <PIXEL>
  LINE_LAST_PIXEL = 761 <PIXEL>
  SAMPLE_FIRST_PIXEL = 1 <PIXEL>
  SAMPLE_LAST_PIXEL = 880 <PIXEL>
  MAP_PROJECTION_ROTATION = 0.0000000 <DEGREE>
  MAP_RESOLUTION = 3293.0387513
  MAP_SCALE = 0.0180000
  MINIMUM_LATITUDE = 84.8928520 <DEGREE>
  MAXIMUM_LATITUDE = 85.2014640 <DEGREE>
  WESTERNMOST_LONGITUDE = -22.8965470 <DEGREE>
  EASTERNMOST_LONGITUDE = -19.0829150 <DEGREE>
  LINE_PROJECTION_OFFSET = -14945.9116667 <PIXEL>
  SAMPLE_PROJECTION_OFFSET = 6313.7611111 <PIXEL>
  COORDINATE_SYSTEM_TYPE = "BODY-FIXED ROTATING"
  COORDINATE_SYSTEM_NAME = "PLANETOCENTRIC"
END_OBJECT = IMAGE_MAP_PROJECTION

/* ENVI header description */
/* The ENVI header is a separate ASCII file that includes basic image */
/* data file characteristics and allows the image data to be loaded */
/* directly into the ENVI image processing software available bands */
/* list. */

OBJECT = ENVI_HEADER
  HEADER_TYPE = "ENVI"
  INTERCHANGE_FORMAT = "ASCII"

```

```

BYTES          = 1418
DESCRIPTION      = "This text file can be used by ENVI image
                   processing software to read in the image."
END_OBJECT      = ENVI_HEADER

/* This Map-Projected Targeted RDR label describes a multiple-band */
/* image file containing TER/MTRDR data processing information. */

OBJECT          = IMAGE
LINES            = 761
LINE_SAMPLES     = 880
SAMPLE_TYPE      = PC_REAL
SAMPLE_BITS       = 32
DESCRIPTION       = "TER_MTRDR_PROCESSING_INFORMATION"
BANDS            = 9
BAND_STORAGE_TYPE = BAND_SEQUENTIAL
BAND_NAME        = ( "VNIR/IR Spectral Continuity Residual",
                     "VNIR/IR Spatial Gradient Residual",
                     "ATM Correction Spectral Shift Artifact",
                     "VNIR Sample",
                     "VNIR Line",
                     "IR Sample",
                     "IR Line",
                     "VNIR/IR Ground Sampling Offset",
                     "VNIR/IR Mask" )
END_OBJECT      = IMAGE

END

```

## APPENDIX E8. MTRDR LABEL (DERIVED INFORMATION FILE)

```

PDS_VERSION_ID = PDS3

RECORD_TYPE = FIXED_LENGTH
RECORD_BYTES = 3520
FILE_RECORDS = 10654
LABEL_REVISION_NOTE =
    "2012-03-06, H. Taylor, F. Seelos (JHU/APL)
    Initial TER/MTRDR labels for CRISM Data Users' Workshop;
    2014-01-09, G. Romeo, J. Aiello, F. Seelos (JHU/APL)
    Complete TER/MTRDR label set for preliminary PDS review;
    2014-04-08, G. Romeo, J. Aiello, R. Espiritu, F. Seelos (JHU/APL)
    TER/MTRDR label set revisions completed for PDS peer review;
    2014-08-14, G. Romeo, J. Aiello, F. Seelos (JHU/APL)
    PDS peer review TER/MTRDR label set liens retired;"

^ENVI_HEADER = "FRT00002F7F_07_DE168L_MTR1.HDR"
^IMAGE = "FRT00002F7F_07_DE168L_MTR1.IMG"

/* DDR Identification */
DATA_SET_ID = "MRO-M-CRISM-5-RDR-MPTARGETED-V1.0"
PRODUCT_ID = "FRT00002F7F_07_DE168L_MTR1"

/*
/*          cccnnnnnnn_xx_ooaaas_MTRv      */
/*          ccc = Class Type             */
/*          nnnnnnnn = Observation ID (hex) */
/*          xx = counter this observation (hex) */
/*          ooaaa = obs type, macro number */
/*          s = sensor ID (J for Joined)   */
/*          v = version number           */
*/

INSTRUMENT_HOST_NAME = "MARS RECONNAISSANCE ORBITER"
SPACECRAFT_ID = MRO
INSTRUMENT_NAME = "COMPACT RECONNAISSANCE IMAGING
                  SPECTROMETER FOR MARS"
INSTRUMENT_ID = CRISM
TARGET_NAME = MARS
PRODUCT_TYPE = MAP_PROJECTED_DDR
PRODUCT_CREATION_TIME = 2015-06-11T20:21:39
START_TIME = 2006-11-11T13:21:36.055
STOP_TIME = 2006-11-11T13:23:59.789
SPACECRAFT_CLOCK_START_COUNT = "2/847718514:58200"
SPACECRAFT_CLOCK_STOP_COUNT = "2/847718658:40771"

ORBIT_NUMBER = 1374
OBSERVATION_TYPE = "FRT"
OBSERVATION_ID = "16#00002F7F#"
MRO:OBSERVATION_NUMBER = 16#07#
MRO:ACTIVITY_ID = "DE168"
MRO:SENSOR_ID = "L"
PRODUCT_VERSION_ID = "1"
PRODUCER_INSTITUTION_NAME = "JOHNS HOPKINS UNIVERSITY
                             APPLIED PHYSICS LABORATORY"
SOFTWARE_NAME = "mtrdr_pipeline"

```

```

SOFTWARE_VERSION_ID          = "1.0"
SOURCE_PRODUCT_ID           =
    "FRT00002F7F_07_DE168L_DDR1"
)

/* DDR Instrument and Observation Parameters */

TARGET_CENTER_DISTANCE      = 3691.650462 <KILOMETER>
                                /* distance to Mars center at first frame */
SOLAR_DISTANCE               = 236035146.305619 <KILOMETER>
SOLAR_LONGITUDE              = 133.839681

/* Map projection information about this RDR is in the */
/* IMAGE_MAP_PROJECTION object below.                      */

OBJECT                      = IMAGE_MAP_PROJECTION
^DATA_SET_MAP_PROJECTION    = "MTR_MAP.CAT"
MAP_PROJECTION_TYPE         = "POLAR STEREOGRAPHIC"
A_AXIS_RADIUS                = 3396.190000000000 <KILOMETER>
B_AXIS_RADIUS                = 3396.190000000000 <KILOMETER>
C_AXIS_RADIUS                = 3376.200000000000 <KILOMETER>
POSITIVE_LONGITUDE_DIRECTION = EAST
CENTER_LATITUDE              = 90.000000 <DEGREE>
CENTER_LONGITUDE              = 0.000000 <DEGREE>
LINE_FIRST_PIXEL              = 1 <PIXEL>
LINE_LAST_PIXEL               = 761 <PIXEL>
SAMPLE_FIRST_PIXEL            = 1 <PIXEL>
SAMPLE_LAST_PIXEL             = 880 <PIXEL>
MAP_PROJECTION_ROTATION      = 0.000000 <DEGREE>
MAP_RESOLUTION                = 3293.0387513
MAP_SCALE                     = 0.018000
MINIMUM_LATITUDE              = 84.8928520 <DEGREE>
MAXIMUM_LATITUDE              = 85.2014640 <DEGREE>
WESTERNMOST_LONGITUDE         = -22.8965470 <DEGREE>
EASTERNMOST_LONGITUDE         = -19.0829150 <DEGREE>
LINE_PROJECTION_OFFSET        = -14945.9116667 <PIXEL>
SAMPLE_PROJECTION_OFFSET      = 6313.7611111 <PIXEL>
COORDINATE_SYSTEM_TYPE        = "BODY-FIXED ROTATING"
COORDINATE_SYSTEM_NAME        = "PLANETOCENTRIC"
END_OBJECT                   = IMAGE_MAP_PROJECTION

/* ENVI header description */
/* The ENVI header is a separate ASCII file that includes basic image */
/* data file characteristics and allows the image data to be loaded   */
/* directly into the ENVI image processing software available bands   */
/* list.                                                               */

OBJECT                      = ENVI_HEADER
HEADER_TYPE                  = "ENVI"
INTERCHANGE_FORMAT            = "ASCII"
BYTES                        = 1601
DESCRIPTION                  = "This text file can be used by ENVI image
processing software to read in the image."
END_OBJECT                   = ENVI_HEADER

/* This map-projected DDR label describes one data file:                 */

```

```

/* 1. A multiple-band backplane image file with wavelength-independent, */
/* spatial pixel-dependent geometric and timing information.          */
/* See the CRISM Data Products SIS for more detailed description.      */

OBJECT                  = IMAGE
  LINES                 = 761
  LINE_SAMPLES          = 880
  SAMPLE_TYPE           = PC_REAL
  SAMPLE_BITS            = 32
  BANDS                = 14
  BAND_STORAGE_TYPE     = BAND_SEQUENTIAL
  BAND_NAME              = ("INA at areoid, deg",
                           "EMA at areoid, deg",
                           "Phase angle, deg",
                           "Latitude, areocentric, deg N",
                           "Longitude, areocentric, deg E",
                           "INA at surface from MOLA, deg",
                           "EMA at surface from MOLA, deg",
                           "Slope magnitude from MOLA, deg",
                           "MOLA slope azimuth, deg clkwise from N",
                           "Elevation, meters relative to MOLA",
                           "Thermal inertia, J m^-2 K^-1 s^-0.5",
                           "Bolometric albedo",
                           "Local solar time, hours",
                           "Spare")
END_OBJECT               = IMAGE

END

```

## APPENDIX E9. MTRDR LABEL (REFINED SUMMARY PRODUCT FILE)

```

PDS_VERSION_ID = PDS3

RECORD_TYPE = FIXED_LENGTH
RECORD_BYTES = 3520
FILE_RECORDS = 45660
LABEL_REVISION_NOTE =
    "2012-03-06, H. Taylor, F. Seelos (JHU/APL)
    Initial TER/MTRDR labels for CRISM Data Users' Workshop;
    2014-01-09, G. Romeo, J. Aiello, F. Seelos (JHU/APL)
    Complete TER/MTRDR label set for preliminary PDS review;
    2014-04-08, G. Romeo, J. Aiello, R. Espiritu, F. Seelos (JHU/APL)
    TER/MTRDR label set revisions completed for PDS peer review;
    2014-08-14, G. Romeo, J. Aiello, F. Seelos (JHU/APL)
    PDS peer review TER/MTRDR label set liens retired;"

^ENVI_HEADER = "FRT00002F7F_07_SR168J_MTR3.HDR"
^IMAGE = "FRT00002F7F_07_SR168J_MTR3.IMG"

/* DDR Identification */
DATA_SET_ID = "MRO-M-CRISM-5-RDR-MPTARGETED-V1.0"
PRODUCT_ID = "FRT00002F7F_07_SR168J_MTR3"

/*
   cccnnnnnnn_xx_ooaaas_MTRv      */
/*   ccc = Class Type             */
/*   nnnnnnnn = Observation ID (hex) */
/*   xx = counter this observation (hex) */
/*   ooaaa = obs type, macro number */
/*   s = sensor ID (J for Joined) */
/*   v = version number           */

INSTRUMENT_HOST_NAME = "MARS RECONNAISSANCE ORBITER"
SPACECRAFT_ID = MRO
INSTRUMENT_NAME = "COMPACT RECONNAISSANCE IMAGING
                  SPECTROMETER FOR MARS"
INSTRUMENT_ID = CRISM
TARGET_NAME = MARS
PRODUCT_TYPE = MPTARGETED_RDR
PRODUCT_CREATION_TIME = 2015-06-11T20:20:38
START_TIME = 2006-11-11T13:21:36.054
STOP_TIME = 2006-11-11T13:23:59.788
SPACECRAFT_CLOCK_START_COUNT = "2/0847718514.58200"
SPACECRAFT_CLOCK_STOP_COUNT = "2/0847718658.40771"

ORBIT_NUMBER = 1374
OBSERVATION_TYPE = "FRT"
OBSERVATION_ID = "16#00002F7F#"
MRO:OBSERVATION_NUMBER = 16#07#
MRO:ACTIVITY_ID = "IF168"
MRO:SENSOR_ID = "J"
PRODUCT_VERSION_ID = "3"
PRODUCER_INSTITUTION_NAME = "JOHNS HOPKINS UNIVERSITY
                             APPLIED PHYSICS LABORATORY"
SOFTWARE_NAME = "mtrdr_pipeline"

```

```

SOFTWARE_VERSION_ID          = "1.0"
SOURCE_PRODUCT_ID           =
    "FRT00002F7F_07_SU168J_MTR3"
)

/* Targeted RDR Observation and Processing Parameters */

SOLAR_DISTANCE              = 236036552.409150 <KILOMETER>
SOLAR_LONGITUDE              = 133.840086
MRO:PHOTOMETRIC_CORR_FLAG   = "ON"
MRO:ATMOSPHERIC_CORR_FLAG   = "ON"
MRO:RATIO_SHIFT_CORR_FLAG   = "ON"
MRO:EMPIRICAL_GEOM_NORM_FLAG = "ON"
MRO:EMPIRICAL_SMILE_CORR_FLAG = "ON"
MRO:SENSOR_SPACE_TRANSFORM_FLAG = "ON"

/* Map projection information about this RDR is in the */
/* IMAGE_MAP_PROJECTION object below. */

OBJECT                      = IMAGE_MAP_PROJECTION
  ^DATA_SET_MAP_PROJECTION   = "MTR_MAP.CAT"
  MAP_PROJECTION_TYPE        = "POLAR STEREOGRAPHIC"
  A_AXIS_RADIUS              = 3396.190000000000 <KILOMETER>
  B_AXIS_RADIUS              = 3396.190000000000 <KILOMETER>
  C_AXIS_RADIUS              = 3376.200000000000 <KILOMETER>
  POSITIVE_LONGITUDE_DIRECTION = EAST
  CENTER_LATITUDE            = 90.000000 <DEGREE>
  CENTER_LONGITUDE            = 0.000000 <DEGREE>
  LINE_FIRST_PIXEL            = 1 <PIXEL>
  LINE_LAST_PIXEL             = 761 <PIXEL>
  SAMPLE_FIRST_PIXEL          = 1 <PIXEL>
  SAMPLE_LAST_PIXEL           = 880 <PIXEL>
  MAP_PROJECTION_ROTATION    = 0.000000 <DEGREE>
  MAP_RESOLUTION              = 3293.0387513
  MAP_SCALE                   = 0.0180000
  MINIMUM_LATITUDE            = 84.8928520 <DEGREE>
  MAXIMUM_LATITUDE            = 85.2014640 <DEGREE>
  WESTERNMOST_LONGITUDE       = -22.8965470 <DEGREE>
  EASTERNMOST_LONGITUDE       = -19.0829150 <DEGREE>
  LINE_PROJECTION_OFFSET      = -14945.9116667 <PIXEL>
  SAMPLE_PROJECTION_OFFSET    = 6313.7611111 <PIXEL>
  COORDINATE_SYSTEM_TYPE      = "BODY-FIXED ROTATING"
  COORDINATE_SYSTEM_NAME      = "PLANETOCENTRIC"
END_OBJECT                   = IMAGE_MAP_PROJECTION

/* ENVI header description */
/* The ENVI header is a separate ASCII file that includes basic image */
/* data file characteristics and allows the image data to be loaded */
/* directly into the ENVI image processing software available bands */
/* list. */

OBJECT                      = ENVI_HEADER
  HEADER_TYPE                = "ENVI"
  INTERCHANGE_FORMAT          = "ASCII"
  BYTES                       = 1741
  DESCRIPTION                 = "This text file can be used by ENVI image
processing software to read in the image."

```

```

END_OBJECT          = ENVI_HEADER

/* This Map-Projected Targeted RDR label describes a multiple-band */
/* image file containing refined spectral summary parameters      */
/* calculated from calibrated and corrected spectral data.       */

OBJECT              = IMAGE
LINES               = 761
LINE_SAMPLES        = 880
SAMPLE_TYPE         = PC_REAL
SAMPLE_BITS         = 32
DESCRIPTION         = "REFINED_SPECTRAL_SUMMARY_PARAMETERS"
BANDS              = 60
BAND_STORAGE_TYPE  = BAND_SEQUENTIAL
BAND_NAME           = ( "R770",
                         "RBR",
                         "BD530_2",
                         "SH600_2",
                         "SH770",
                         "BD640_2",
                         "BD860_2",
                         "BD920_2",
                         "RPEAK1",
                         "BDI1000VIS",
                         "R440",
                         "IRR1",
                         "BDI1000IR",
                         "OLINDEX3",
                         "R1330",
                         "BD1300",
                         "LCPINDEX2",
                         "HCPINDEX2",
                         "VAR",
                         "ISLOPE1",
                         "BD1400",
                         "BD1435",
                         "BD1500_2",
                         "ICER1_2",
                         "BD1750_2",
                         "BD1900_2",
                         "BD1900R2",
                         "BDI2000",
                         "BD2100_2",
                         "BD2165",
                         "BD2190",
                         "MIN2200",
                         "BD2210_2",
                         "D2200",
                         "BD2230",
                         "BD2250",
                         "MIN2250",
                         "BD2265",
                         "BD2290",
                         "D2300",
                         "BD2355",
                         "SINDEX2",

```

```
"ICER2_2",
"MIN2295_2480",
"MIN2345_2537",
"BD2500_2",
"BD3000",
"BD3100",
"BD3200",
"BD3400_2",
"CINDEX2",
"BD2600",
"IRR2",
"IRR3",
"R530",
"R600",
"R1080",
"R1506",
"R2529",
"R3920" )
END_OBJECT
= IMAGE
```

END

## APPENDIX E10. MTRDR LABEL (SUMMARY PRODUCT FILE)

```

PDS_VERSION_ID = PDS3

RECORD_TYPE = FIXED_LENGTH
RECORD_BYTES = 3520
FILE_RECORDS = 45660
LABEL_REVISION_NOTE =
    "2012-03-06, H. Taylor, F. Seelos (JHU/APL)
    Initial TER/MTRDR labels for CRISM Data Users' Workshop;
    2014-01-09, G. Romeo, J. Aiello, F. Seelos (JHU/APL)
    Complete TER/MTRDR label set for preliminary PDS review;
    2014-04-08, G. Romeo, J. Aiello, R. Espiritu, F. Seelos (JHU/APL)
    TER/MTRDR label set revisions completed for PDS peer review;
    2014-08-14, G. Romeo, J. Aiello, F. Seelos (JHU/APL)
    PDS peer review TER/MTRDR label set liens retired;"

^ENVI_HEADER = "FRT00002F7F_07_SU168J_MTR3.HDR"
^IMAGE = "FRT00002F7F_07_SU168J_MTR3.IMG"

/* DDR Identification */
DATA_SET_ID = "MRO-M-CRISM-5-RDR-MPTARGETED-V1.0"
PRODUCT_ID = "FRT00002F7F_07_SU168J_MTR3"

/*
/*          cccnnnnnnn_xx_ooaaas_MTRv */
/*          ccc = Class Type           */
/*          nnnnnnnn = Observation ID (hex) */
/*          xx = counter this observation (hex) */
/*          ooaaa = obs type, macro number */
/*          s = sensor ID (J for Joined) */
/*          v = version number        */
*/

INSTRUMENT_HOST_NAME = "MARS RECONNAISSANCE ORBITER"
SPACECRAFT_ID = MRO
INSTRUMENT_NAME = "COMPACT RECONNAISSANCE IMAGING
                  SPECTROMETER FOR MARS"
INSTRUMENT_ID = CRISM
TARGET_NAME = MARS
PRODUCT_TYPE = MPTARGETED_RDR
PRODUCT_CREATION_TIME = 2015-06-11T20:20:11
START_TIME = 2006-11-11T13:21:36.054
STOP_TIME = 2006-11-11T13:23:59.788
SPACECRAFT_CLOCK_START_COUNT = "2/0847718514.58200"
SPACECRAFT_CLOCK_STOP_COUNT = "2/0847718658.40771"

ORBIT_NUMBER = 1374
OBSERVATION_TYPE = "FRT"
OBSERVATION_ID = "16#00002F7F#"
MRO:OBSERVATION_NUMBER = 16#07#
MRO:ACTIVITY_ID = "IF168"
MRO:SENSOR_ID = "J"
PRODUCT_VERSION_ID = "3"
PRODUCER_INSTITUTION_NAME = "JOHNS HOPKINS UNIVERSITY
                             APPLIED PHYSICS LABORATORY"
SOFTWARE_NAME = "mtrdr_pipeline"

```

```

SOFTWARE_VERSION_ID          = "1.0"
SOURCE_PRODUCT_ID           =
    "FRT00002F7F_07_IF168J_MTR3"
)

/* Targeted RDR Observation and Processing Parameters */

SOLAR_DISTANCE              = 236036552.409150 <KILOMETER>
SOLAR_LONGITUDE              = 133.840086
MRO:PHOTOMETRIC_CORR_FLAG   = "ON"
MRO:ATMOSPHERIC_CORR_FLAG   = "ON"
MRO:RATIO_SHIFT_CORR_FLAG   = "ON"
MRO:EMPIRICAL_GEOM_NORM_FLAG = "ON"
MRO:EMPIRICAL_SMILE_CORR_FLAG = "ON"
MRO:SENSOR_SPACE_TRANSFORM_FLAG = "ON"

/* Map projection information about this RDR is in the */
/* IMAGE_MAP_PROJECTION object below. */

OBJECT                      = IMAGE_MAP_PROJECTION
  ^DATA_SET_MAP_PROJECTION   = "MTR_MAP.CAT"
  MAP_PROJECTION_TYPE        = "POLAR STEREOGRAPHIC"
  A_AXIS_RADIUS              = 3396.190000000000 <KILOMETER>
  B_AXIS_RADIUS              = 3396.190000000000 <KILOMETER>
  C_AXIS_RADIUS              = 3376.200000000000 <KILOMETER>
  POSITIVE_LONGITUDE_DIRECTION = EAST
  CENTER_LATITUDE             = 90.000000 <DEGREE>
  CENTER_LONGITUDE            = 0.000000 <DEGREE>
  LINE_FIRST_PIXEL            = 1 <PIXEL>
  LINE_LAST_PIXEL              = 761 <PIXEL>
  SAMPLE_FIRST_PIXEL           = 1 <PIXEL>
  SAMPLE_LAST_PIXEL            = 880 <PIXEL>
  MAP_PROJECTION_ROTATION     = 0.000000 <DEGREE>
  MAP_RESOLUTION               = 3293.0387513
  MAP_SCALE                   = 0.0180000
  MINIMUM_LATITUDE             = 84.8928520 <DEGREE>
  MAXIMUM_LATITUDE             = 85.2014640 <DEGREE>
  WESTERNMOST_LONGITUDE        = -22.8965470 <DEGREE>
  EASTERNMOST_LONGITUDE        = -19.0829150 <DEGREE>
  LINE_PROJECTION_OFFSET       = -14945.9116667 <PIXEL>
  SAMPLE_PROJECTION_OFFSET     = 6313.7611111 <PIXEL>
  COORDINATE_SYSTEM_TYPE       = "BODY-FIXED ROTATING"
  COORDINATE_SYSTEM_NAME        = "PLANETOCENTRIC"
END_OBJECT                   = IMAGE_MAP_PROJECTION

/* ENVI header description */
/* The ENVI header is a separate ASCII file that includes basic image */
/* data file characteristics and allows the image data to be loaded */
/* directly into the ENVI image processing software available bands */
/* list. */

OBJECT                      = ENVI_HEADER
  HEADER_TYPE                = "ENVI"
  INTERCHANGE_FORMAT          = "ASCII"
  BYTES                       = 1741
  DESCRIPTION                 = "This text file can be used by ENVI image
processing software to read in the image."

```

```

END_OBJECT          = ENVI_HEADER

/* This Map-Projected Targeted RDR label describes a multiple-band */
/* image file containing spectral summary parameters calculated      */
/* from calibrated and corrected spectral data.                      */

OBJECT              = IMAGE
LINES               = 761
LINE_SAMPLES        = 880
SAMPLE_TYPE         = PC_REAL
SAMPLE_BITS         = 32
DESCRIPTION         = "SPECTRAL_SUMMARY_PARAMETERS"
BANDS              = 60
BAND_STORAGE_TYPE  = BAND_SEQUENTIAL
BAND_NAME           = ( "R770",
                         "RBR",
                         "BD530_2",
                         "SH600_2",
                         "SH770",
                         "BD640_2",
                         "BD860_2",
                         "BD920_2",
                         "RPEAK1",
                         "BDI1000VIS",
                         "R440",
                         "IRR1",
                         "BDI1000IR",
                         "OLINDEX3",
                         "R1330",
                         "BD1300",
                         "LCPINDEX2",
                         "HCPINDEX2",
                         "VAR",
                         "ISLOPE1",
                         "BD1400",
                         "BD1435",
                         "BD1500_2",
                         "ICER1_2",
                         "BD1750_2",
                         "BD1900_2",
                         "BD1900R2",
                         "BDI2000",
                         "BD2100_2",
                         "BD2165",
                         "BD2190",
                         "MIN2200",
                         "BD2210_2",
                         "D2200",
                         "BD2230",
                         "BD2250",
                         "MIN2250",
                         "BD2265",
                         "BD2290",
                         "D2300",
                         "BD2355",
                         "SINDEX2",

```

```
"ICER2_2",
"MIN2295_2480",
"MIN2345_2537",
"BD2500_2",
"BD3000",
"BD3100",
"BD3200",
"BD3400_2",
"CINDEX2",
"BD2600",
"IRR2",
"IRR3",
"R530",
"R600",
"R1080",
"R1506",
"R2529",
"R3920" )
END_OBJECT
= IMAGE
```

END

## APPENDIX E11. MTRDR LABEL (WAVELENGTH FILE)

```

PDS_VERSION_ID = PDS3

RECORD_TYPE = FIXED_LENGTH
RECORD_BYTES = 30
FILE_RECORDS = 489
LABEL_REVISION_NOTE =
    "2012-03-06, H. Taylor, F. Seelos (JHU/APL)
    Initial TER/MTRDR labels for CRISM Data Users' Workshop;
    2014-01-09, G. Romeo, J. Aiello, F. Seelos (JHU/APL)
    Complete TER/MTRDR label set for preliminary PDS review;
    2014-04-08, G. Romeo, J. Aiello, R. Espiritu, F. Seelos (JHU/APL)
    TER/MTRDR label set revisions completed for PDS peer review;
    2014-08-14, G. Romeo, J. Aiello, F. Seelos (JHU/APL)
    PDS peer review TER/MTRDR label set liens retired;"

^WAVELENGTH_SOURCE_TABLE = "FRT00002F7F_07_WV168J_MTR3.TAB"

/* Map-Projected Targeted RDR Identification */
DATA_SET_ID = "MRO-M-CRISM-5-RDR-MPTARGETED-V1.0"
PRODUCT_ID = "FRT00002F7F_07_WV168J_MTR3"

/*
   cccnnnnnnn_xx_ooaaaas_MTRv      */
/*   ccc = Class Type               */
/*   nnnnnnnn = Observation ID, hexadecimal */
/*   xx = counter this observation (hex) */
/*   ooooo = Image type, Macro number */
/*   s = Sensor ID (J for Joined)   */
/*   v = Version number            */

INSTRUMENT_HOST_NAME = "MARS RECONNAISSANCE ORBITER"
SPACECRAFT_ID = MRO
INSTRUMENT_NAME = "COMPACT RECONNAISSANCE IMAGING
                  SPECTROMETER FOR MARS"
INSTRUMENT_ID = CRISM
TARGET_NAME = MARS
PRODUCT_TYPE = MPTARGETED_RDR
PRODUCT_CREATION_TIME = 2015-06-11T20:19:43
START_TIME = 2006-11-11T13:21:36.054
STOP_TIME = 2006-11-11T13:23:59.788
SPACECRAFT_CLOCK_START_COUNT = "2/0847718514.58200"
SPACECRAFT_CLOCK_STOP_COUNT = "2/0847718658.40771"

PRODUCT_VERSION_ID = "3"
PRODUCER_INSTITUTION_NAME = "JOHNS HOPKINS UNIVERSITY
                            APPLIED PHYSICS LABORATORY"
SOFTWARE_NAME = "mtrdr_pipeline"
SOFTWARE_VERSION_ID = "1.0"

/* A listfile including spectrometer identifier, detector row numbers,*/
/* wavelengths, full width half max, and bad band identifier in the*/
/* Targeted Empirical Record and Map-Projected Targeted RDR images. */

OBJECT_NAME = WAVELENGTH_SOURCE_TABLE
             = "CRISM JOINED WAVELENGTH TABLE"

```

```

INTERCHANGE_FORMAT = "ASCII"
ROWS
    = 489
COLUMNS
    = 5
ROW_BYTES
    = 30
DESCRIPTION
    = "CRISM JOINED WAVELENGTH table"
OBJECT
    COLUMN_NUMBER
        = 1
    NAME
        = SPECT_ID
    DATA_TYPE
        = ASCII_INTEGER
    START_BYTE
        = 1
    BYTES
        = 2
    DESCRIPTION
        = "Spectrometer identifier; 0 = IR; 1 = VNIR"
END_OBJECT
OBJECT
    COLUMN_NUMBER
        = 2
    NAME
        = ROWNUM
    DATA_TYPE
        = ASCII_INTEGER
    START_BYTE
        = 4
    BYTES
        = 4
    DESCRIPTION
        = "detector row number (0-479)"
END_OBJECT
OBJECT
    COLUMN_NUMBER
        = 3
    NAME
        = SAMPL_WAV
    DATA_TYPE
        = ASCII_REAL
    START_BYTE
        = 9
    BYTES
        = 8
    DESCRIPTION
        = "Standard sampling center wavelength in nm"
    UNIT
        = "NM"
END_OBJECT
OBJECT
    COLUMN_NUMBER
        = 4
    NAME
        = FWHM
    DATA_TYPE
        = ASCII_REAL
    START_BYTE
        = 18
    BYTES
        = 8
    DESCRIPTION
        = "Full Width Half Max in nm"
    UNIT
        = "NM"
END_OBJECT
OBJECT
    COLUMN_NUMBER
        = 5
    NAME
        = BAD_BAND_ID
    DATA_TYPE
        = ASCII_INTEGER
    START_BYTE
        = 27
    BYTES
        = 2
    DESCRIPTION
        = "Bad Band Identifier; 0 = BAD; 1 = GOOD"
END_OBJECT
END_OBJECT
    = WAVELENGTH_SOURCE_TABLE
END

```

## APPENDIX F. LEVEL 6 CDR LABEL

```
PDS_VERSION_ID      = PDS3
LABEL_REVISION_NOTE = "2005-12-22, P. Cavender;
                      2006-09-18, MRO CRISM:HWT line length fix;
                      2009-04-03, Scott Murchie; modified
                      table 2 to contain hyperspectral survey,
                      and put old table 2 into table 3
                      2009-08-07, C. Hash; modified table 2
                      to be a superset of table 1."
/* Level 6 CDR (Calibration Data Record) Identification */
DATA_SET_ID         = "MRO-M-CRISM-4/6-CDR-V1.0"
PRODUCT_ID          = "CDR6_9_0947778566_WV_L_0"
PRODUCT_TYPE        = CDR
SPACECRAFT_ID       = MRO
INSTRUMENT_ID       = CRISM
START_TIME          = 2010-01-12T15:48:55
STOP_TIME           = NULL
SPACECRAFT_CLOCK_START_COUNT = "9/0947778566"
SPACECRAFT_CLOCK_STOP_COUNT  = NULL
PRODUCT_CREATION_TIME = 2010-02-19T18:58:00
MRO:SENSOR_ID       = "L"
PRODUCT_VERSION_ID   = "0"

/* Description of CDR6 TABLE file */

OBJECT              = FILE
^TABLE              = "CDR6_9_0947778566_WV_L_0.TAB"
RECORD_TYPE         = FIXED_LENGTH
RECORD_BYTES        = 13
FILE_RECORDS        = 480

OBJECT              = TABLE
NAME                = "WAVELENGTH TABLE"
INTERCHANGE_FORMAT  = "ASCII"
ROWS                = 4804
COLUMNS             = 5
ROW_BYTES           = 13
DESCRIPTION         = "Wavelength Table"

OBJECT              = COLUMN
COLUMN_NUMBER        = 1
NAME                = IR_ROW
DATA_TYPE            = ASCII_INTEGER
START_BYTE           = 1
BYTES               = 3
DESCRIPTION         = "IR detector row; low numbers are at the long
wavelength end"
END_OBJECT           = COLUMN

OBJECT              = COLUMN
COLUMN_NUMBER        = 2
NAME                = IR_FILTER_0
DATA_TYPE            = ASCII_INTEGER
START_BYTE           = 5
BYTES               = 1
DESCRIPTION         = "IR wavelength table 0; in housekeeping file
when SPECT_ID=0 this column is applicable
when FILTER=0; if value is 0 then data from
that row of the detector is not returned; if
```

value is 1 then data from that row of the  
 detector is returned"

```

END_OBJECT      = COLUMN

OBJECT          = COLUMN
COLUMN_NUMBER   = 3
NAME            = IR_FILTER_1
DATA_TYPE       = ASCII_INTEGER
START_BYTE     = 7
BYTES          = 1
DESCRIPTION     = "IR wavelength table 1; in housekeeping file
when SPECT_ID=0 this column is applicable
when FILTER=1; if value is 0 then data from
that row of the detector is not returned; if
value is 1 then data from that row of the
detector is returned"
END_OBJECT      = COLUMN

OBJECT          = COLUMN
COLUMN_NUMBER   = 4
NAME            = IR_FILTER_2
DATA_TYPE       = ASCII_INTEGER
START_BYTE     = 9
BYTES          = 1
DESCRIPTION     = "IR wavelength table 2; in housekeeping file
when SPECT_ID=0 this column is applicable
when FILTER=2; if value is 0 then data from
that row of the detector is not returned; if
value is 1 then data from that row of the
detector is returned"
END_OBJECT      = COLUMN

OBJECT          = COLUMN
COLUMN_NUMBER   = 5
NAME            = IR_FILTER_3
DATA_TYPE       = ASCII_INTEGER
START_BYTE     = 11
BYTES          = 1
DESCRIPTION     = "IR wavelength table 3; in housekeeping file
when SPECT_ID=0 this column is applicable
when FILTER=3; if value is 0 then data from
that row of the detector is not returned; if
value is 1 then data from that row of the
detector is returned"
END_OBJECT      = COLUMN

END_OBJECT      = TABLE

END_OBJECT      = FILE

END
  
```

## APPENDIX G. LEVEL 4 CDR LABEL

```
PDS_VERSION_ID      = PDS3
LABEL_REVISION_NOTE = "2006-04-11 D. Humm (APL), modified;
                      version 0 prelim Rob Green cal <2500 nm
                      and 5x5 >2500 nm; version 1 D. Humm,
                      replace all non-scene with 65535. ;
                      version 2 2006-09-21 D. Humm,
                      final ground Rob Green cal
                      <2500 nm and 5x5 >2500 nm;
                      version 3 2007-01-23 D. Humm,
                      adjust by 1.5-3 nm wavelength
                      shift as a function of column #
                      supplied by Rob Green 2007-01-03"
/*( NOTE: Comments in this label that are delimited with parentheses,      )*/
/*( for example:                                )*/
/*( comment )*/
/*( are notes to the data provider. These comments should be removed      )*/
/*( from the final label. Comments without parentheses, for example:      )*/
/*(   /* comment */                                )*/
/*( are intended to be part of the final label.                           )*/
/* Level 4 CDR (Calibration Data Record) Identification */

DATA_SET_ID          = "MRO-M-CRISM-4/6-CDR-V1.0"
PRODUCT_ID           = "CDR410803692813_WA0000000L_3"

/*( CDR4Pttttttt_pprbeewsn_v      )*/
/*( P = partition of sclk time      )*/
/*( tttttttt = s/c start or mean time      )*/
/*( pp = calib. type from SIS table 2-8      )*/
/*( r = frame rate identifier, 0-4      )*/
/*( b = binning identifier, 0-3      )*/
/*( eee = exposure time parameter, 0-480  )*/
/*( w = wavelength filter, 0-3      )*/
/*( s = side: 1 or 2, or 0 if N/A      )*/
/*( n = sensor ID: S, L, or J      )*/
/*( v = version      )*/

PRODUCT_TYPE          = CDR
SPACECRAFT_ID         = MRO
INSTRUMENT_ID          = CRISM
START_TIME             = 2005-06-19T23:59:59.999
STOP_TIME              = NULL
SPACECRAFT_CLOCK_START_COUNT = "1/0803692813"
SPACECRAFT_CLOCK_STOP_COUNT  = NULL
OBSERVATION_TIME        = NULL
PRODUCT_CREATION_TIME    = 2007-01-23T23:26:00

OBSERVATION_TYPE        = NULL
OBSERVATION_ID           = NULL
MRO:OBSERVATION_NUMBER     = NULL
MRO:ACTIVITY_ID          = NULL
SOURCE_PRODUCT_ID         = NULL
MRO:SENSOR_ID             = "L"
PRODUCT_VERSION_ID        = "3"

/* CDR Instrument and Observation Parameters */
```

```

SAMPLING_MODE_ID      = "HYPERSPEC"
MRO:WAVELENGTH_FILE_NAME    = "CDR410803692813_WA0000000L_3.IMG"
MRO:DETECTOR_TEMPERATURE    = NULL
MRO:OPTICAL_BENCH_TEMPERATURE = NULL
MRO:SPECTROMETER_HOUSING_TEMP = NULL
MRO:SPHERE_TEMPERATURE    = NULL
SHUTTER_MODE_ID      = "OPEN"
LIGHT_SOURCE_NAME     = "NONE"
MRO:CALIBRATION_LAMP_STATUS  = "OFF"
MRO:CALIBRATION_LAMP_LEVEL  = 0
MRO:FRAME_RATE        = NULL
PIXEL_AVERAGING_WIDTH   = 1 /*( pixel bin size, across track ) */
MRO:EXPOSURE_PARAMETER   = NULL
MRO:WAVELENGTH_FILTER    = "0"

/* This Level 4 CDR label describes one calibration data file. The file */
/* is a mutiple-band, single-frame image file derived from ground data. */
/* It consists of a binary image followed by a list of row numbers */
/* corresponding to the wavelength filter. */

/* The WA level 4 CDR gives the center wavelength in nm of each pixel, */
/* assuming a given spatial binning and wavelength filter. */

/* Description of CDR IMAGE file */

OBJECT          = FILE
^IMAGE          = "CDR410803692813_WA0000000L_3.IMG"

/* offset is in file records, which is just (imgbands*imgrlines) + 1 */
^ROWNUM_TABLE = ("CDR410803692813_WA0000000L_3.IMG",439 )

RECORD_TYPE = FIXED_LENGTH
RECORD_BYTES = 2560 /* one row now, not one frame to save space in table */
FILE_RECORDS = 439 /* compute by ROUND ((imgbands * imgrlines * */
/*                  line_samples * samplebits/8 + */
/*                  tablerows * tablerowbytes) / */
/*                  record_bytes + 0.5 ) */

OBJECT          = IMAGE
LINES           = 1
LINE_SAMPLES     = 640
SAMPLE_TYPE      = PC_REAL
SAMPLE_BITS       = 32
BANDS           = 438
BAND_NAME        = NULL
BAND_STORAGE_TYPE = LINE_INTERLEAVED
DESCRIPTION       = "Center wavelength in nm for each
                      detector pixel"
UNIT             = "NM"
END_OBJECT       = IMAGE

/* be sure to pad this object to a full record (2560/bin bytes here) */
OBJECT = ROWNUM_TABLE
NAME      = "SELECTED ROWS FROM DETECTOR"
INTERCHANGE_FORMAT = "BINARY"
ROWS      = 438
COLUMNS    = 1
ROW_BYTES   = 2
DESCRIPTION = "The detector is subsampled in the spectral direction
                by selecting specific rows to be downlinked. This
                table provides a list of the rows selected for all
                frames in this multidimensional image cube."

```

```
OBJECT = COLUMN
  NAME      = DETECTOR_ROW_NUMBER
  DATA_TYPE  = MSB_UNSIGNED_INTEGER
  BIT_MASK   = 2#00000011111111#
  START_BYTE = 1
  BYTES     = 2
  DESCRIPTION = "Detector row number from which the data was taken."
END_OBJECT = COLUMN

END_OBJECT = ROWNUM_TABLE

END_OBJECT      = FILE

END
```

## APPENDIX H. LDR LABEL

```
PDS_VERSION_ID      = PDS3
LABEL_REVISION_NOTE = "2009-04-07, S. Murchie (JHU/APL);"

/* LDR Identification */

DATA_SET_ID          = "MRO-M-CRISM-6-LDR-V1.0"
PRODUCT_ID           = "LMB00002B61_0B_DE227S_LDR0"
/* cccnnnnnnn_xx_oaaas_LDRv */
/* ccc = Class Type */
/* nnnnnnnn = Observation ID (hex) */
/* xx = counter this observation (hex) */
/* oaaaa = obs type, macro number */
/* s = sensor ID (S or L) */
/* v = version number */

INSTRUMENT_HOST_NAME = "MARS RECONNAISSANCE ORBITER"
SPACECRAFT_ID        = MRO
INSTRUMENT_NAME       = "COMPACT RECONNAISSANCE IMAGING
                           SPECTROMETER FOR MARS"
INSTRUMENT_ID         = CRISM
TARGET_NAME           = MARS
PRODUCT_TYPE          = LDR
PRODUCT_CREATION_TIME = 2009-09-03T19:50:25
START_TIME            = 2009-07-11T09:12:06.267
STOP_TIME             = 2009-07-11T09:14:30.001
SPACECRAFT_CLOCK_START_COUNT = "6/931770748:44476"
SPACECRAFT_CLOCK_STOP_COUNT = "6/931770892:27045"

ORBIT_NUMBER          = 0
OBSERVATION_TYPE     = "LMB"
OBSERVATION_ID        = "16#00002B61#"
MRO:OBSERVATION_NUMBER = 16#0B#
MRO:ACTIVITY_ID      = "DE227"
MRO:SENSOR_ID         = "S"
PRODUCT_VERSION_ID    = "0"
SOURCE_PRODUCT_ID      = {
    "mro.tsc",
    "mro_v14.tf",
    "MRO_CRISM_FK_0000_000_N_01.TF",
    "MRO_CRISM_IK_0000_000_N_10.TI",
    "naif0009.tls",
    "pck00008.tpc",
    "mro_sc_psp_090707_090713.bc",
    "spck_2009_191_r_1.bc",
    "spck_2009_192_r_1.bc",
    "de410.bsp",
    "mro_cruise.bsp",
    "mro_ab.bsp",
    "mro_psp.bsp",
    "mro_psp1.bsp",
    "mro_psp2.bsp",
    "mro_psp_rec.bsp"
}
PRODUCER_INSTITUTION_NAME = "APPLIED PHYSICS LABORATORY"
SOFTWARE_NAME           = "crism_ldr"
SOFTWARE_VERSION_ID      = "1.0"

/* LDR Instrument and Observation Parameters */
```

```

SOLAR_DISTANCE      = 213229293.617318 <KM>
SOLAR_LONGITUDE     = 301.331137 <DEGREES>
MRO:FRAME_RATE      = 3.75 <HZ>
PIXEL_AVERAGING_WIDTH = 10
MRO:INSTRUMENT_POINTING_MODE = "DYNAMIC POINTING"

/* This LDR label describes one data file:          */
/* 1. A multiple-band backplane image file with wavelength-independent, */
/* spatial pixel-dependent geometric and timing information.      */

/* See the CRISM Data Products SIS for more detailed description.      */

OBJECT              = FILE
^IMAGE              = "LMB00002B61_0B_DE227S_LDR0.IMG"
RECORD_TYPE         = FIXED_LENGTH
RECORD_BYTES        = 256
FILE_RECORDS       = 8100

OBJECT              = IMAGE
LINES               = 540
LINE_SAMPLES        = 64
SAMPLE_TYPE         = PC_REAL
SAMPLE_BITS         = 32
BANDS               = 15
BAND_STORAGE_TYPE   = BAND_SEQUENTIAL
BAND_NAME           = ("INA at areoid, deg",
                      "EMA at areoid, deg",
                      "Phase angle, deg",
                      "Latitude, areocentric, deg N",
                      "Longitude, areocentric, deg E",
                      "INA at surface from MOLA, deg",
                      "EMA at surface from MOLA, deg",
                      "Elevation, meters relative to areoid",
                      "Elevation, meters relative to MOLA",
                      "Local Solar Time, hours",
                      "Ephemeris Time of observation, seconds past noon January 1, 2000",
                      "Sub-Solar Latitude, areocentric, deg N",
                      "Sub-Solar Longitude, areocentric, deg E",
                      "Sub-Spacecraft Latitude, areocentric, deg N",
                      "Sub-Spacecraft Longitude, areocentric, deg E")

END_OBJECT          = IMAGE

END_OBJECT          = FILE

END

```

## APPENDIX I1. EDR BROWSE PRODUCT HTML FILE LABEL

```
PDS_VERSION_ID      = PDS3
LABEL_REVISION_NOTE = "2006-02-25, S.Murchie (APL)"

/* This browse product provides an overview of the MRO CRISM EDRs */
/* from a single observation */

^HTML_DOCUMENT      = "FRT00004ECA_BROWSE_EDR0.HTML"

DATA_SET_ID         = "MRO-M-CRISM-2-EDR-V1.0"
PRODUCT_ID          = "FRT00004ECA_BROWSE_EDR0"
/* EDR browse product */
/* cccnnnnnnn_BROWSE_EDRv           */
/* ccc = Class Type                 */
/* nnnnnnnn = Observation ID (hex) */
/* v = Version number               */

INSTRUMENT_HOST_NAME = "MARS RECONNAISSANCE ORBITER"
SPACECRAFT_ID        = MRO
INSTRUMENT_NAME       = "COMPACT RECONNAISSANCE IMAGING
                           SPECTROMETER FOR MARS"
INSTRUMENT_ID         = CRISM
TARGET_NAME           = MARS
PRODUCT_TYPE          = BROWSE
PRODUCT_CREATION_TIME = 2007-04-25T11:17:50.529
PRODUCER_INSTITUTION_NAME = "JOHNS HOPKINS UNIVERSITY
                           APPLIED PHYSICS LABORATORY"
SOFTWARE_NAME          = "pipe_crism_create_browse"
SOFTWARE_VERSION_ID    = "1.0"

/* The following information is relevant to an entire observation */

ORBIT_NUMBER         = NULL
OBSERVATION_TYPE     = "FRT"
OBSERVATION_ID        = "16#00004ECA#"
PRODUCT_VERSION_ID    = "0"
SOLAR_DISTANCE        = NULL <KM>

/* These times are from the beginning of the first EDR of the observation */
/* to the end of the last EDR of the observation */

START_TIME            = 2007-03-23T02:59:55.113681
STOP_TIME              = 2007-03-23T03:06:55.910109
SPACECRAFT_CLOCK_START_COUNT = "2/0859086014.03181"
SPACECRAFT_CLOCK_STOP_COUNT = "2/0859086434.55376"

OBJECT                = HTML_DOCUMENT
DOCUMENT_NAME          = "EDR BROWSE OVERVIEW"
RECORD_TYPE             = UNDEFINED
PUBLICATION_DATE       = 2007-04-25
DOCUMENT_TOPIC_TYPE    = "HTML NAVIGATION"
INTERCHANGE_FORMAT      = ASCII
DOCUMENT_FORMAT          = HTML
DESCRIPTION             = "This document provides an overview of the MRO
                           CRISM EDRs from a single observation."
END_OBJECT              = HTML_DOCUMENT

END
```

## APPENDIX I2. EDR BROWSE PRODUCT PNG FILE LABEL

```
PDS_VERSION_ID = PDS3
LABEL_REVISION_NOTE = "2003-11-19, S. Slavney (GEO);
    2005-02-01, C. Hash (ACT);
    2006-01-04, C. Hash (ACT);"

/* EDR Identification */

DATA_SET_ID      = "MRO-M-CRISM-2-EDR-V1.0"
PRODUCT_ID       = "FRT00004ECA_07_SC166L_RAW0"
/* cccnnnnnnn_xx_ooaaas_RAWv */
/* ccc = Class Type */
/* nnnnnnnn = Observation ID (hex) */
/* xx = counter within observation (hex) */
/* oaaaa = obs type, macro number */
/* s = sensor ID (S or L) */
/* v = version number */

INSTRUMENT_HOST_NAME = "MARS RECONNAISSANCE ORBITER"
SPACECRAFT_ID     = MRO
INSTRUMENT_NAME   = "COMPACT RECONNAISSANCE IMAGING
                      SPECTROMETER FOR MARS"
INSTRUMENT_ID     = CRISM
TARGET_NAME        = MARS
PRODUCT_TYPE       = BROWSE
PRODUCT_CREATION_TIME = 2007-04-06T13:22:26
START_TIME         = 2007-03-23T03:02:31.910417
STOP_TIME          = 2007-03-23T03:04:39.644669
SPACECRAFT_CLOCK_START_COUNT = "2/0859086170.55396"
SPACECRAFT_CLOCK_STOP_COUNT = "2/0859086298.37980"
ORBIT_NUMBER       = "NULL"
OBSERVATION_TYPE  = "FRT"
OBSERVATION_ID    = "16#00004ECA#"
MRO:OBSERVATION_NUMBER = 16#07#
MRO:ACTIVITY_ID   = "SC166"
MRO:SENSOR_ID     = "L"
PRODUCT_VERSION_ID = "0"
PRODUCER_INSTITUTION_NAME = "JOHNS HOPKINS UNIVERSITY
                           APPLIED PHYSICS LABORATORY"
SOFTWARE_NAME      = "pipe_edrslice"
SOFTWARE_VERSION_ID = "4.3"

/* EDR Instrument and Observation Parameters */
/* for first frame */
TARGET_CENTER_DISTANCE = NULL <KM>
SOLAR_DISTANCE         = NULL <KM>
SHUTTER_MODE_ID        = OPEN
LIGHT_SOURCE_NAME       = "NONE"
MRO:CALIBRATION_LAMP_STATUS = "OFF"
MRO:CALIBRATION_LAMP_LEVEL = "N/A"
PIXEL_AVERAGING_WIDTH = 1
MRO:INSTRUMENT_POINTING_MODE = "DYNAMIC POINTING"
SCAN_MODE_ID           = SHORT
MRO:FRAME_RATE          = 3.75 <HZ>
MRO:EXPOSURE_PARAMETER = 301
SAMPLING_MODE_ID        = "HYPERSPEC"
COMPRESSION_TYPE        = "NONE"
MRO:WAVELENGTH_FILTER = 0
MRO:WAVELENGTH_FILE_NAME = "CDR6_1_0000000000_WV_L_1.TAB"
MRO:PIXEL_PROC_FILE_NAME = "CDR6_1_0000000000_PP_L_1.TAB"
```

```
MRO:LOOKUP_TABLE_FILE_NAME = "CDR6_1_0000000000_LK_J_0.TAB"

/* These parameters describe the browse image as a PDS document. */

^DOCUMENT      = "FRT00004ECA_07_SC166L_RAW0.PNG"
OBJECT        = DOCUMENT
DOCUMENT_NAME   = "FRT00004ECA_07_SC166L_RAW0"
DOCUMENT_FORMAT  = PNG
DOCUMENT_TOPIC_TYPE = "BROWSE IMAGE"
INTERCHANGE_FORMAT = BINARY
PUBLICATION_DATE = 2007-04-06
SOURCE_PRODUCT_ID = "FRT00004ECA_07_SC166L_EDR0"
LINES          = 480
LINE_SAMPLES    = 640
SAMPLE_TYPE     = MSB_UNSIGNED_INTEGER
SAMPLE_BITS     = 8
DERIVED_MINIMUM = 0
DERIVED_MAXIMUM = 250
OFFSET          = -145.522
SCALING_FACTOR  = 0.299
MISSING_CONSTANT = 255
DESCRIPTION      = "This file is a scaled median image of raw DN level
in a CRISM EDR. The x-y coordinates of the image
are spatial and in sensor space (not map-
projected), where x = detector column and y = frame
number within an EDR. The encoded 8-bit value at
each x-y location is the scaled median of the
values at all wavelengths."
END_OBJECT      = DOCUMENT
END
```

## APPENDIX J1. TER ‘TAN’ BROWSE PRODUCT LABEL

```

PDS_VERSION_ID = PDS3

RECORD_TYPE = UNDEFINED
LABEL_REVISION_NOTE =
    "2012-03-06, H. Taylor, F. Seelos (JHU/APL)
    Initial TER/MTRDR labels for CRISM Data Users' Workshop;
    2014-01-09, G. Romeo, J. Aiello, F. Seelos (JHU/APL)
    Complete TER/MTRDR label set for preliminary PDS review;
    2014-04-08, G. Romeo, J. Aiello, R. Espiritu, F. Seelos (JHU/APL)
    TER/MTRDR label set revisions completed for PDS peer review;
    2014-08-14, G. Romeo, J. Aiello, F. Seelos (JHU/APL)
    PDS peer review TER/MTRDR label set liens retired;"

^PNG_DOCUMENT = "FRT00002F7F_07_BRTANJ_TER3.PNG"
^ENVI_HEADER = "FRT00002F7F_07_BRTANJ_TER3.HDR"
^IMAGE = "FRT00002F7F_07_BRTANJ_TER3.IMG"

/* Targeted RDR Browse Product Identification */

DATA_SET_ID = "MRO-M-CRISM-4-RDR-TARGETED-V1.0"
PRODUCT_ID =
    "FRT00002F7F_07_BRTANJ_TER3"
    /* cccnnnnnnn_xx_oaaaaas_TERv */          */
    /* ccc = Class Type */                     */
    /* nnnnnnnn = Observation ID, hexadecimal */
    /* oaaaa = Image type, browse type */      */
    /* xx = counter this observation (hex)   */
    /* s = Sensor ID (J for Joined) */        */
    /* v = Version number */                  */
INSTRUMENT_HOST_NAME = "MARS RECONNAISSANCE ORBITER"
SPACECRAFT_ID = MRO
INSTRUMENT_NAME = "COMPACT RECONNAISSANCE IMAGING
    SPECTROMETER FOR MARS"
INSTRUMENT_ID = CRISM
TARGET_NAME = MARS
PRODUCT_TYPE = TARGETED_BROWSE
PRODUCT_CREATION_TIME = 2015-06-11T04:43:17
START_TIME = 2006-11-11T13:21:36.054
STOP_TIME = 2006-11-11T13:23:59.788
SPACECRAFT_CLOCK_START_COUNT = "2/0847718514.58200"
SPACECRAFT_CLOCK_STOP_COUNT = "2/0847718658.40771"

ORBIT_NUMBER = 1374
OBSERVATION_TYPE = "FRT"
OBSERVATION_ID = "16#00002F7F#"
MRO:OBSERVATION_NUMBER = 16#07#
MRO:ACTIVITY_ID = "IF168"
MRO:SENSOR_ID = "J"

/* Detector and FPE temperature refer to IR component of observation */

MRO:DETECTOR_TEMPERATURE = -163.287
MRO:OPTICAL_BENCH_TEMPERATURE = -52.315
MRO:SPECTROMETER_HOUSING_TEMP = -75.764
MRO:SPHERE_TEMPERATURE = -52.275
MRO:FPE_TEMPERATURE = -0.375

PRODUCT_VERSION_ID = "3"

```

```

PRODUCER_INSTITUTION_NAME      = "JOHNS HOPKINS UNIVERSITY
                                  APPLIED PHYSICS LABORATORY"
SOFTWARE_NAME                  = "mtrdr_pipeline"
SOFTWARE_VERSION_ID            = "1.0"

/* Targeted RDR Observation and Processing Parameters */

SOLAR_DISTANCE                = 236036552.409150 <KILOMETER>
SOLAR_LONGITUDE                = 133.840086
MRO:PHOTOMETRIC_CORR_FLAG     = "ON"
MRO:ATMOSPHERIC_CORR_FLAG     = "ON"
MRO:RATIO_SHIFT_CORR_FLAG     = "ON"
MRO:EMPIRICAL_GEOM_NORM_FLAG  = "ON"
MRO:EMPIRICAL_SMILE_CORR_FLAG = "ON"
MRO:SENSOR_SPACE_TRANSFORM_FLAG= "ON"

/* These parameters describe the browse image as a PDS document. */

/* The browse IMG and PNG products are identical in the RED, GREEN, */
/* and BLUE channels. The PNG product includes an additional ALPHA */
/* transparency channel in which the non-scene pixels are marked */
/* as transparent. */

OBJECT                         = PNG_DOCUMENT
DOCUMENT_NAME                  = "FRT00002F7F_07_BRTANJ_TER3"
DOCUMENT_FORMAT                 = PNG
DOCUMENT_TOPIC_TYPE            = "BROWSE IMAGE"
INTERCHANGE_FORMAT              = BINARY
PUBLICATION_DATE               = 2013-12-15
DESCRIPTION                     = "An enhanced visible to infrared false color
                                 representation of the scene."
END_OBJECT                      = PNG_DOCUMENT

/* ENVI header description */
/* The ENVI header is a separate ASCII file that includes basic image */
/* data file characteristics and allows the image data to be loaded */
/* directly into the ENVI image processing software available bands */
/* list. */

OBJECT                         = ENVI_HEADER
HEADER_TYPE                     = "ENVI"
INTERCHANGE_FORMAT              = "ASCII"
BYTES                           = 479
DESCRIPTION                     = "This text file can be used by ENVI image
                                 processing software to read in the image."
END_OBJECT                      = ENVI_HEADER

/* This Targeted Empirical Record label describes a multiple-band */
/* image file containing a byte scaled browse product derived from */
/* selected refined spectral summary parameters. */

OBJECT                         = IMAGE
LINES                           = 540
LINE_SAMPLES                    = 640
SAMPLE_TYPE                     = LSB_UNSIGNED_INTEGER
SAMPLE_BITS                     = 8
DESCRIPTION                     = "TAN_BROWSE_PRODUCT"
BANDS                           = 3
BAND_STORAGE_TYPE               = BAND_SEQUENTIAL
BAND_SEQUENCE                   = "(RED, GREEN, BLUE)"
BAND_NAME                       = ( "R2529", "R1330", "R770")
/* The following information to scale from real numbers to an */

```

```
/* 8-bit integer for this type of browse image. */  
DERIVED_MINIMUM      = ( 0, 0, 0)  
DERIVED_MAXIMUM      = ( 254, 254, 254 )  
OFFSET               = ( 1.0480E-01, 1.4055E-01, 1.6392E-01)  
SCALING_FACTOR       = ( 1.7353E-03, 1.2948E-03, 1.1004E-03)  
END_OBJECT = IMAGE  
  
END
```

## APPENDIX J2. MTRDR 'TAN' BROWSE PRODUCT LABEL

```

PDS_VERSION_ID = PDS3

RECORD_TYPE = UNDEFINED
LABEL_REVISION_NOTE =
    "2012-03-06, H. Taylor, F. Seelos (JHU/APL)
    Initial TER/MTRDR labels for CRISM Data Users' Workshop;
    2014-01-09, G. Romeo, J. Aiello, F. Seelos (JHU/APL)
    Complete TER/MTRDR label set for preliminary PDS review;
    2014-04-08, G. Romeo, J. Aiello, R. Espiritu, F. Seelos (JHU/APL)
    TER/MTRDR label set revisions completed for PDS peer review;
    2014-08-14, G. Romeo, J. Aiello, F. Seelos (JHU/APL)
    PDS peer review TER/MTRDR label set liens retired;"

^PNG_DOCUMENT = "FRT00002F7F_07_BRTANJ_MTR3.PNG"
^ENVI_HEADER = "FRT00002F7F_07_BRTANJ_MTR3.HDR"
^IMAGE = "FRT00002F7F_07_BRTANJ_MTR3.IMG"

/* Map-Projected Targeted RDR Browse Product Identification */

DATA_SET_ID = "MRO-M-CRISM-5-RDR-MPTARGETED-V1.0"
PRODUCT_ID = "FRT00002F7F_07_BRTANJ_MTR3"
/* cccnnnnnnn_xx_oaaaaas_MTRv */ /*/
/* ccc = Class Type */ /*/
/* nnnnnnnnn = Observation ID, hexadecimal */ /*/
/* oaaaa = Image type, browse type */ /*/
/* xx = counter this observation (hex) */ /*/
/* s = Sensor ID (J for Joined) */ /*/
/* v = Version number */ /*/
INSTRUMENT_HOST_NAME = "MARS RECONNAISSANCE ORBITER"
SPACECRAFT_ID = MRO
INSTRUMENT_NAME = "COMPACT RECONNAISSANCE IMAGING
                  SPECTROMETER FOR MARS"
INSTRUMENT_ID = CRISM
TARGET_NAME = MARS
PRODUCT_TYPE = MPTARGETED_BROWSE
PRODUCT_CREATION_TIME = 2015-06-11T20:21:31
START_TIME = 2006-11-11T13:21:36.054
STOP_TIME = 2006-11-11T13:23:59.788
SPACECRAFT_CLOCK_START_COUNT = "2/0847718514.58200"
SPACECRAFT_CLOCK_STOP_COUNT = "2/0847718658.40771"

ORBIT_NUMBER = 1374
OBSERVATION_TYPE = "FRT"
OBSERVATION_ID = "16#00002F7F#"
MRO:OBSERVATION_NUMBER = 16#07#
MRO:ACTIVITY_ID = "IF168"
MRO:SENSOR_ID = "J"

/* Detector and FPE temperature refer to IR component of observation */

MRO:DETECTOR_TEMPERATURE = -163.287
MRO:OPTICAL_BENCH_TEMPERATURE = -52.315
MRO:SPECTROMETER_HOUSING_TEMP = -75.764
MRO:SPHERE_TEMPERATURE = -52.275
MRO:FPE_TEMPERATURE = -0.375

```

```

PRODUCT_VERSION_ID      = "3"
PRODUCER_INSTITUTION_NAME = "JOHNS HOPKINS UNIVERSITY
                           APPLIED PHYSICS LABORATORY"
SOFTWARE_NAME           = "mtrdr_pipeline"
SOFTWARE_VERSION_ID     = "1.0"

/* Targeted RDR Observation and Processing Parameters */

SOLAR_DISTANCE          = 236036552.409150 <KILOMETER>
SOLAR_LONGITUDE          = 133.840086
MRO:PHOTOMETRIC_CORR_FLAG = "ON"
MRO:ATMOSPHERIC_CORR_FLAG = "ON"
MRO:RATIO_SHIFT_CORR_FLAG = "ON"
MRO:EMPIRICAL_GEOM_NORM_FLAG = "ON"
MRO:EMPIRICAL_SMILE_CORR_FLAG = "ON"
MRO:SENSOR_SPACE_TRANSFORM_FLAG = "ON"

/* These parameters describe the browse image as a PDS document. */

/* The browse IMG and PNG products are identical in the RED, GREEN, */
/* and BLUE channels. The PNG product includes an additional ALPHA */
/* transparency channel in which the non-scene pixels are marked */
/* as transparent. */

OBJECT                  = PNG_DOCUMENT
DOCUMENT_NAME           = "FRT00002F7F_07_BRTANJ_MTR3"
DOCUMENT_FORMAT          = PNG
DOCUMENT_TOPIC_TYPE     = "BROWSE IMAGE"
INTERCHANGE_FORMAT      = BINARY
PUBLICATION_DATE        = 2013-12-15
DESCRIPTION              = "An enhanced visible to infrared false color
                           representation of the scene."
END_OBJECT               = PNG_DOCUMENT

/* ENVI header description */
/* The ENVI header is a separate ASCII file that includes basic image */
/* data file characteristics and allows the image data to be loaded */
/* directly into the ENVI image processing software available bands */
/* list. */

OBJECT                  = ENVI_HEADER
HEADER_TYPE              = "ENVI"
INTERCHANGE_FORMAT       = "ASCII"
BYTES                   = 1233
DESCRIPTION              = "This text file can be used by ENVI image
                           processing software to read in the image."
END_OBJECT               = ENVI_HEADER

/* This Map-Projected Targeted RDR label describes a multiple-band */
/* image file containing a byte scaled browse product derived from */
/* selected refined spectral summary parameters. */

OBJECT                  = IMAGE
LINES                   = 761
LINE_SAMPLES             = 880
SAMPLE_TYPE              = LSB_UNSIGNED_INTEGER
SAMPLE_BITS              = 8
DESCRIPTION              = "TAN_BROWSE_PRODUCT"
BANDS                  = 3
BAND_STORAGE_TYPE        = BAND_SEQUENTIAL
BAND_SEQUENCE            = "(RED, GREEN, BLUE)"
BAND_NAME                = ( "R2529", "R1330", "R770")

```

```

/* The following information to scale from real numbers to an */
/* 8-bit integer for this type of browse image. */
DERIVED_MINIMUM      = (    0,    0,    0)
DERIVED_MAXIMUM      = ( 254, 254, 254 )
OFFSET               = ( 1.0480E-01, 1.4055E-01, 1.6392E-01)
SCALING_FACTOR       = ( 1.7353E-03, 1.2948E-03, 1.1004E-03)
END_OBJECT = IMAGE

/* Map projection information about this RDR is in the */
/* IMAGE_MAP_PROJECTION object below. */

OBJECT                = IMAGE_MAP_PROJECTION
^DATA_SET_MAP_PROJECTION = "MTR_MAP.CAT"
MAP_PROJECTION_TYPE   = "POLAR STEREOGRAPHIC"
A_AXIS_RADIUS         = 3396.190000000000 <KILOMETER>
B_AXIS_RADIUS         = 3396.190000000000 <KILOMETER>
C_AXIS_RADIUS         = 3376.200000000000 <KILOMETER>
POSITIVE_LONGITUDE_DIRECTION = EAST
CENTER_LATITUDE       = 90.0000000 <DEGREE>
CENTER_LONGITUDE      = 0.0000000 <DEGREE>
LINE_FIRST_PIXEL      = 1 <PIXEL>
LINE_LAST_PIXEL        = 761 <PIXEL>
SAMPLE_FIRST_PIXEL    = 1 <PIXEL>
SAMPLE_LAST_PIXEL     = 880 <PIXEL>
MAP_PROJECTION_ROTATION = 0.0000000 <DEGREE>
MAP_RESOLUTION         = 3293.0387513
MAP_SCALE              = 0.0180000
MINIMUM_LATITUDE      = 84.8928520 <DEGREE>
MAXIMUM_LATITUDE      = 85.2014640 <DEGREE>
WESTERNMOST_LONGITUDE = -22.8965470 <DEGREE>
EASTERNMOST_LONGITUDE = -19.0829150 <DEGREE>
LINE_PROJECTION_OFFSET = -14945.9116667 <PIXEL>
SAMPLE_PROJECTION_OFFSET = 6313.7611111 <PIXEL>
COORDINATE_SYSTEM_TYPE = "BODY-FIXED ROTATING"
COORDINATE_SYSTEM_NAME = "PLANETOCENTRIC"
END_OBJECT             = IMAGE_MAP_PROJECTION

```

END

## APPENDIX K. MRDR BROWSE PRODUCT 'TRU' PNG FILE LABEL

```

PDS_VERSION_ID      = PDS3
RECORD_TYPE        = UNDEFINED
LABEL_REVISION_NOTE = "2003-11-19, S. Slavney (GEO);
                      2005-09-25, S. Murchie (JHU/APL);
                      2007-09-14, C. Hash (ACT Corp)"
/* Map-projected Multispectral RDR Identification */
DATA_SET_ID        = "MRO-M-CRISM-5-RDR-MULTISPECTRAL-V1.0"
PRODUCT_ID         = "T1396_MRRTRU_30N088_0256_2"
    /*( Tnnnn_MRRsss_xx yyyy_rrrr_v           )*/
    /*( nnnn = tile number                  )*/
    /*( sss = subtype of browse product    )*/
    /*( xx = latitude of tile center       )*/
    /*( d = N or S for north or south latitude )*/
    /*( yyyy = east longitude of tile center )*/
    /*( rrrr = resolution in pixels/degree   )*/
    /*( v = version number                 )*/
INSTRUMENT_HOST_NAME = "MARS RECONNAISSANCE ORBITER"
SPACECRAFT_ID      = MRO
INSTRUMENT_NAME     = "COMPACT RECONNAISSANCE IMAGING
                      SPECTROMETER FOR MARS"
INSTRUMENT_ID       = CRISM
TARGET_NAME         = MARS
PRODUCT_TYPE        = BROWSE
PRODUCT_CREATION_TIME = 2009-12-02T16:48:56
START_TIME          = "N/A"
STOP_TIME           = "N/A"
SPACECRAFT_CLOCK_START_COUNT = "N/A"
SPACECRAFT_CLOCK_STOP_COUNT = "N/A"
PRODUCT_VERSION_ID = "2"
PRODUCER_INSTITUTION_NAME = "APPLIED PHYSICS LABORATORY"
SOFTWARE_NAME       = "PIPE_create_crism_mrdr_browse"
SOFTWARE_VERSION_ID = "09.01.09"
MRO:WAVELENGTH_FILE_NAME = "N/A"
/* These parameters describe the browse image as a PDS document. */
^PNG_DOCUMENT        = "T1396_MRRTRU_30N088_0256_2.PNG"
OBJECT              = PNG_DOCUMENT
DOCUMENT_NAME        = "T1396_MRRTRU_30N088_0256_2"
DOCUMENT_FORMAT      = PNG
DOCUMENT_TOPIC_TYPE = "BROWSE IMAGE"
INTERCHANGE_FORMAT  = BINARY
PUBLICATION_DATE    = 2009-12-02
SOURCE_PRODUCT_ID   = "T1396_MRRAL_30N088_0256_2"
SAMPLE_TYPE          = LSB_UNSIGNED_INTEGER
SAMPLE_BITS          = 8
BANDS               = 3
BAND_SEQUENCE        = ("RED","GREEN","BLUE")
BAND_NAME            = ("598 nm","533 nm","442 nm")
/* The following information to scale from real numbers to an */
/* 8-bit integer is hard-coded for this type of browse image. */
DERIVED_MINIMUM     = (0,0,0)
DERIVED_MAXIMUM      = (250,250,250)
OFFSET               = (0.00000,0.00000,0.00000)
SCALING_FACTOR       = (0.00120,0.00120,0.00120)
MISSING_CONSTANT     = (255,255,255)
DESCRIPTION          = "This file is a true color VNIR image assembled
                      from calibrated radiance, solar distance, and
                      solar flux as sampled in the wavelength filter
                      and binning state being used: radiance_factor =
                      I*D^2/(pi*F) where I = spectral radiance,

```

D = solar distance in AU, and F = solar flux at 1 AU. Subsequently a correction was made for atmospheric and photometric effects either predictively from climatology or after the fact from CRISM measurements."

```

END_OBJECT      = PNG_DOCUMENT
/* Map projection information about this RDR is in the IMAGE_MAP_PROJECTION */
/* object below. */
OBJECT          = IMAGE_MAP_PROJECTION
  ^DATA_SET_MAP_PROJECTION    = "MRR_MAP.CAT"
  MAP_PROJECTION_TYPE        = "EQUIRECTANGULAR"
  A_AXIS_RADIUS              = 3396 <KM>
  B_AXIS_RADIUS              = 3396 <KM>
  C_AXIS_RADIUS              = 3396 <KM>
  FIRST_STANDARD_PARALLEL    = "N/A"
  SECOND_STANDARD_PARALLEL   = "N/A"
  POSITIVE_LONGITUDE_DIRECTION = "EAST"
  CENTER_LATITUDE             = 27.50000 <DEGREE>
  CENTER_LONGITUDE            = 87.50000 <DEGREE>
  REFERENCE_LATITUDE          = "N/A"
  REFERENCE_LONGITUDE         = "N/A"
  LINE_FIRST_PIXEL            = 1
  LINE_LAST_PIXEL             = 1280
  SAMPLE_FIRST_PIXEL          = 1
  SAMPLE_LAST_PIXEL           = 1136
  MAP_PROJECTION_ROTATION    = 0.0
  MAP_RESOLUTION               = 256 <PIXEL/DEG>
  MAP_SCALE                   = 0.231528833585 <KM/PIXEL>
  MAXIMUM_LATITUDE             = 32.50000 <DEGREE>
  MINIMUM_LATITUDE             = 27.50000 <DEGREE>
  WESTERNMOST_LONGITUDE        = 85.00000 <DEGREE>
  EASTERNMOST_LONGITUDE        = 90.00000 <DEGREE>
  LINE_PROJECTION_OFFSET       = 1280.000
  SAMPLE_PROJECTION_OFFSET     = 640.000
  COORDINATE_SYSTEM_TYPE      = "BODY-FIXED ROTATING"
  COORDINATE_SYSTEM_NAME       = "PLANETOCENTRIC"
END_OBJECT      = IMAGE_MAP_PROJECTION
END
```

## APPENDIX L. RADIOMETRIC CALIBRATION DETAILS

Dave Humm and Scott Murchie

Updated 2/1/2018

(Describes the TRDR calibration pipeline, v3)

### 1. CALIBRATION OVERVIEW

#### 1.1 Collection of calibration data in flight

Darks will be taken bracketing every targeted measurement as part of the macro for that targeted measurement. Darks will be taken every 5 minutes in mapping mode.

Onboard integrating sphere calibration data will be taken with the IR lamp at nominally fixed intervals in time. The plan is to take sphere calibrations once every 1.5 orbits, bracketing scene observations with a dayside and nightside sphere observation. The idea is that the IR detector will be relatively warm (by a degree or so, maybe much less) on the dayside and relatively cool on the nightside. To correct the radiometric calibration for detector temperature, we interpolate in indicated detector temperature between the dayside and nightside sphere calibrations. In some cases, we will skip an extra orbit or two between the dayside and nightside due to restrictions on scheduling. The primary sphere lamp is lamp 1, the IR-controlled “cross-slit” lamp, and these data are used for all calibrations (as of 12/16/2008). Integrating sphere data with lamp 2, the VNIR-controlled “along-slit” lamp, will be taken on the same schedule for redundancy. As of 12/28/2010, the dayside and nightside calibration observations are taken, and the software has the capacity to interpolate between them, but that capacity is not used. Only one sphere observation is used to calibrate a given scene. The temperature changes have not proven significant, and using just one sphere observation reduces the injection of noise.

Bias calibration data, darks with multiple integration times, will be taken at nominally fixed intervals for the IR detector only. Currently, the default is to take a bias set with every integrating sphere calibration measurement. There is a specific macro for the bias calibration.

Focal plane lamp data are taken occasionally. The focal plane lamp data are not used in the calibration algorithm, so this is just for verification and engineering checkout. There is a specific macro for the focal plane lamp calibration.

A nadir-pointed hyperspectral swath of a featureless region of Mars is taken at a nominally fixed interval. Currently, the plan is to take these data monthly. These data will be used to flat-field the VNIR detector at all wavelengths and the IR detector at wavelengths where there are no sharp atmospheric spectral features. As of 12/28/2010 (the “TRR3 calibration”), hundreds of flat field swathes had been taken, and a median of all of them was used for flat-fielding.

#### 1.2 Reduction of flight target image data using calibration data

1. Use pixel processing table and LUT tables to convert 8-bit data to 12-bit if data are 8-bit. Section 2.2.
2. Use pixel processing table to convert 12-bit data to 14-bit data. Section 2.2.

3. Subtract bias calculated from nearest available flight bias calibration data set. For IR only. Apply to scene images and darks. Sections 2.3 and 3.1.
4. Subtract darks from scene images. VNIR only. Use a weighted average of darks taken before and after the target image, with the weighting factors derived from the relative time at which each dark was taken with respect to the scene image. Sections 2.3 and 3.2.
5. Make detector quadrant ghost correction applying coefficients from ground calibration to each quadrant within each image. For IR, apply to darks as well. Section 2.4.
6. Subtract median of masked pixels in each image frame. For VNIR only. The IR correction is done later in the pipeline. Section 2.5.
7. Apply a priori bad pixel mask to all images, replacing bad pixels with a linear spatial nearest-neighbor interpolation. For VNIR there's a single dead pixel only in full-resolution images, defined by a CDR. For IR, we calculate the bad pixel mask for each image using the set of associated dark and bias images. Replace saturated pixels with 65535. Sections 2.6 and **Error! Reference source not found.**
8. Apply overall detector nonlinearity correction to scene images. For IR, apply to darks as well. Section **Error! Reference source not found...**
9. Divide by integration time to get counts/millisecond. Section **Error! Reference source not found..**
10. Subtract processed darks from processed scene images. Use a weighted average of darks taken before and after the scene image, with the weighting factors derived from the relative time at which each dark was taken with respect to the scene image. For IR only. Sections **Error! Reference source not found.** and 3.2.
11. Subtract median of masked pixels in each image frame. For IR only. The VNIR correction is done earlier in the pipeline. Section **Error! Reference source not found..**
12. Apply stray light subtraction using stray light pixels within each image. VNIR only. For IR, the sphere radiance is adjusted to account for stray light and there is no explicit correction. The formula for the VNIR correction is complex. Section **Error! Reference source not found..**
13. Apply subtraction of 2<sup>nd</sup> order leaked light in Zone 3 of IR detector using Zone 1 and 2 counts from same image and ground-derived coefficients. For IR only. Section **Error! Reference source not found.**
14. Apply shutter mirror nonrepeatability correction to ground integrating sphere radiance. This corrects the ground-measured radiance of the integrating sphere to the shutter mirror position in the flight calibration sphere data. Uses flight calibration sphere data to correct ground sphere radiance. No effect on flight scene or calibration images, but it does use data from the flight calibration image, so it must be performed in sequence after the previous calibration steps. Section 3.4.
15. Calculate spectroradiometric responsivity using nearest available flight integrating sphere data and ground sphere radiance. This spectrum is a function of wavelength pixel and spatial pixel. For VNIR detector rows 185-215 (short wavelengths), the responsivity is simply read from a CDR, not calculated from a sphere image, because the sphere is too dim. Sections 3.5 and **Error! Reference source not found.**
16. Apply binning to responsivity for the different modes. Section 2.14.
17. Divide corrected counts/second in the scene images by the binned responsivity to get radiance at the instrument aperture. Note that before the radiance is calculated, the scene

- data sets should be processed using steps 1-14 above. Section **Error! Reference source not found..**
18. Divide radiance image by image of external flat field. Section **Error! Reference source not found..**
  19. Apply ex post facto bad pixel removal algorithm to scene images. Section **Error! Reference source not found..**
  20. Replace non-scene pixels with the value 65535. Section **Error! Reference source not found..**

## 2. CALIBRATION DESCRIPTION

### 2.1 Overview of calibration equation

Radiometric calibration to units of radiance follows the equation

$$RD_{x,\lambda,r} = M_{x,\lambda,Hz} \left( ( K_{x,\lambda,Hz} ( D14_{\lambda} ( DN_{x,\lambda,TaV,TaW,TaI,TaJ,Ta2,Hz,t,r} ) - BiaT_{x,\lambda,TaV,TaW,TaI,TaJ,Hz,t} ) / t - Bkgd_{x,\lambda,TaI,Ta2,Hz} - Scat_{x,\lambda,TaV,TaI,Ta2,Hz,r} ) / ( RST_{x,\lambda,TaV,TaI,Ta2} * FF_{x,\lambda,Hz} ) \right)$$

Diffuse spectral reflectivity (I/F) is calculated by

$$IF_{x,\lambda} = \pi \cdot RD_{x,\lambda,r} / ( SF_{x,\lambda} / r^2 )$$

Subscripts include:

- $x$ , **spatial position** in a row on the focal plane, in detector elements
- $\lambda$ , **wavelength** in spectral direction on the focal plane, in detector elements or nm
- $Hz$ , **frame rate, wavelength table, and binning mode**
- $T_{aI}$ , **IR detector temperature** in K for scene measurement
- $T_{aV}$ , **VNIR detector temperature** in K for scene measurement
- $T_{a2}$ , **spectrometer housing temperature** in K
- $T_{c3}$ , **temperature of the integrating sphere** in K for flight calibration measurement
- $T_{aJ}$ , **IR focal plane board temperature** in K for scene measurement
- $T_{aW}$ , **VNIR focal plane board temperature** in K for scene measurement
- $t$ , **integration time** in seconds
- $s$ , **choice of sphere bulb**, side 1 or 2

Temperatures are given for scene measurements, bias measurements, calibration measurements, or first and second dark measurements according to the lowercase subscripts a, b, c, d, and e respectively. So, for example,  $T_{aI}$  would be the IR detector temperature for the scene image,  $T_{dI}$  would be the IR detector temperature for the “before” dark image,  $T_{eI}$  for the “after” dark image,  $T_{cI}$  would be the IR detector temperature for the associated flight calibration images, and  $T_{bI}$  would be the IR detector temperature for the associated bias measurement. The algorithm uses temperatures from the low-rate telemetry. The temperatures are taken once per second and a 10-point median smoothing is applied.

Subscripts indicate which terms in the equation are dependent on which parameters. This includes both explicit and implicit dependence, and excludes when an implicit dependence has been explicitly subtracted out. For example, the  $Bkgd_{x,\lambda,TaI,Ta2,HZ}$  term includes background from the IR glow of the inside walls of the spectrometer, so it depends on the spectrometer temperature  $T_{a2}$ .  $Bkgd_{x,\lambda,TaI,Ta2,HZ}$  is calculated from dark images with spectrometer temperatures  $T_{d2}$  and  $T_{e2}$ , but the calculation is designed to give the level of the background for the target measurement spectrometer temperature  $T_{a2}$ . The explicit dependence on  $T_{d2}$  and  $T_{e2}$  has been subtracted out, leaving an implicit dependence on  $T_{a2}$ , so  $T_{a2}$  is in the subscript.

Description of the terms of the equation:

$D14_\lambda()$  converts from raw DN to 14-bit DN.

$BiaT_{x,\lambda,TaV,TaW,TaI,TaJ,HZ,t}$  is the detector bias (DN at zero integration time).

$K_{x,\lambda,HZ}()$  flags saturated pixels and applies the detector ghost, VNIR dark column subtract, initial bad pixel, and detector nonlinearity corrections.

$Bkgd_{x,\lambda,TaI,Ta2,HZ}$  is the dark subtraction term calculated from shutter-closed measurements and IR dark column subtract.

$Scat_{x,\lambda,TaV,TaI,Ta2,HZ,r}$  is the stray light subtraction, including diffuse scatter for VNIR and 2nd order light for IR.

$RST_{x,\lambda,TaV,TaI,Ta2}$  is the responsivity calculated from flight onboard sphere calibration images.

$M_{x,\lambda,HZ}()$  applies the detector mask and the final scene bad pixel correction.

$FF_{x,\lambda,HZ}$  is the flat field.

$RD_{x,\lambda,r}$  is the observed spectral radiance in  $W/(m^2 \text{ micrometer sr})$  at the instrument aperture.

$SF_{x,\lambda}$  is solar spectral irradiance for a normally illuminated surface 1 AU from the Sun, convolved to the CRISM spectral profiles.

$r$  is the distance of Mars from the Sun in astronomical units.

$IF_{x,\lambda}$  is the I/F of the scene (unitless), a measure of diffuse reflectivity.

Definition of the terms of the equation:

The value 65535 is treated as a flag and any pixel with that value does not receive any further calibration. Pixels with the value 65535 may be replaced as part of the ex post facto bad pixel correction, however. See Section **Error! Reference source not found..**

$$D14_\lambda(DN_{x,\lambda,TaV,TaI,Ta2,HZ,t,r}) = Offset_\lambda + ILUT_\lambda(DN_{x,\lambda,TaV,TaI,Ta2,HZ,t,r}) / Gain_\lambda$$

This is conversion from raw DN (raw DN has fast lossless compression undone) to 14-bit DN. See section 2.2.

$$\begin{aligned} BiaT_{x,\lambda,TaI,TaJ,HZ,t} = & Bias_{x,\lambda,TbI,TbJ,HZ} - a0_I \cdot Hv(\text{row}_\lambda + 1 - (502/480) \cdot (480-\text{integ}(t))) \\ & + \beta_{I,HZ} \cdot (TaI - TbI) - \beta_{J,HZ} \cdot (TaJ - TbJ) \end{aligned}$$

for IR and

$$\begin{aligned} BiaT_{x,\lambda,TaV,TaW,HZ,t} = & (\alpha_{ea} \cdot Bias_{x,\lambda,TdV,TdW,HZ,t} + \alpha_{ad} \cdot Bias_{x,\lambda,TeV,TeW,HZ,t}) / (\alpha_{ad} + \alpha_{ea}) \\ & + \beta_{V,HZ} \cdot [\alpha_{ea} \cdot (TaV - TdV) + \alpha_{ad} \cdot (TeV - TaV)] / (\alpha_{ad} + \alpha_{ea}) \\ & + \beta_{W,HZ} \cdot [\alpha_{ea} \cdot (TaW - TdW) + \alpha_{ad} \cdot (TeV - TaW)] / (\alpha_{ad} + \alpha_{ea}) \end{aligned}$$

for VNIR is the temperature-corrected bias subtraction. The masked pixel subtraction renders the detector temperature correction redundant, but it is still performed. See section 2.3 and section 3.1.

$K_{x,\lambda,HZ}( ) = F_{HZ}( S( B_{x,\lambda,HZ}(H( )) ) )$  for IR and

$K_{x,\lambda,HZ}( ) = F_{HZ}( S( B_{x,\lambda,HZ}(H( ) - \text{median}_{x,\lambda}( DN14^{b_{x1...xn,\lambda,0...2s,TaV,TaW,HZ,t,r}} ) ) )$  for VNIR applies the detector ghost correction, applies the masked pixel (dark column) subtract for VNIR only, applies the a priori bad pixel correction, flags saturated pixels, and applies the detector nonlinearity correction. See sections 2.4 through **Error! Reference source not found..**

$H( DN14^{a_{x,\lambda,TaV,TaI,Ta2,HZ,t,r}} ) = DN14^{a_{x,\lambda,TaV,TaI,Ta2,HZ,t,r}} - \sum_{n=0}^{n=3} G( DN14^{a_{x0+n\delta,\lambda,TaV,TaI,Ta2,HZ,t,r}} )$  applies the detector quadrant ghost correction. See section 2.4.

$B_{x,\lambda,HZ}( )$  is the a priori bad pixel removal function. See section 2.6.

$S( DN14^{d_{x,\lambda,TaV,TaI,Ta2,HZ,t,r}} ) = 65565$  if  $DN14^{c_{x,\lambda,TaV,TaI,Ta2,HZ,t,r}} > DN14^{c_{maxI}}$  for IR or  $DN14^{c_{maxV}}$  for VNIR. See section **Error! Reference source not found..**

$Bkgd_{x,\lambda,TaI,Ta2,HZ} = Bkgd_{x,\lambda,TdI,TdI,Td2,Td2,HZ,ta1,td1,te1}$  is the dark-subtraction term. It is zero for VNIR. The parameters in the subscripts on the right-hand side are explicitly used to calculate a value of the background that should be implicitly dependent only on the parameters in the subscripts on the left-hand side. See section **Error! Reference source not found..** The dark-subtraction term in the calibration equation also includes an IR masked pixel (dark column) correction term described in section **Error! Reference source not found..** Note those masked pixels themselves have dark subtraction applied before they are used for the masked pixel correction.

$Scat_{x,\lambda,TaI,Ta2,HZ,r} = \sum_{n=1}^{n=6} K_{x,\lambda,n,HZ} \cdot RT14^{i_{x,\lambda,y_n,HZ,TaI,Ta2,HZ,r}}$

for IR comprises the stray light correction for second order. See section **Error! Reference source not found..**

$Scat_{x,\lambda,TaI,Ta2,HZ,r} = \{ <RT14^{hh_{x1...xn,\lambda,TaV,TaI,Ta2,HZ,r}} \cdot SW^{hh_{x,TaV,TaI,Ta2,HZ}}\} \text{ for } \lambda < 563 \text{ nm and } \{ <RT14^{hh_{x1...xn,\lambda,TaV,TaI,Ta2,HZ,r}} \cdot CS^{hh_{x,\lambda,TaV,TaI,Ta2,HZ}}\} \text{ for } \lambda > 563 \text{ nm}$

for VNIR comprises the stray light correction for scattered light. See section **Error! Reference source not found..**

$RST_{x,\lambda,TaI,Ta2} = ( RSP^j_{x,\lambda,TcI,Tc2} \cdot ( T_{aI} - T_{fl} ) + RSP^j_{x,\lambda,TfI,Tf2} \cdot ( T_{cI} - T_{aI} ) ) / ( T_{cI} - T_{fl} )$

for IR, where  $T_{cI}$  and  $T_{fl}$  are the IR detector temperatures for the dayside and nightside sphere calibrations respectively. As of 12/30/2008, this capability is in the code but is not being utilized. We just use the nearest IR flight integrating sphere data twice.

$RST_{x,\lambda,TaV,Ta2} = RSP^j_{x,\lambda,TcV,Tc2} \cdot ( \mu_{x,\lambda} + v_{x,\lambda} \cdot T_{av} + \pi_{x,\lambda} \cdot T_{av}^2 ) / ( \mu_{x,\lambda} + v_{x,\lambda} \cdot T_{cv} + \pi_{x,\lambda} \cdot T_{cv}^2 )$

for VNIR is the temperature-corrected CRISM responsivity calculated from the flight onboard sphere calibration measurements. As of 12/30/2008,  $\mu=1$ ,  $v=0$ , and  $\pi=0$ , so the correction is not applied. See section 3.4, section 3.5, and section **Error! Reference source not found..**

$FF_{x,\lambda,HZ} = FL_{x,\lambda,HZ} + EP_{x,\lambda,HZ} \cdot \log( RT^j_{x,\lambda,TaV,TaI,Ta2,HZ,r} / RSP^j_{x,\lambda,TaV,TaI,Ta2,HZ} )$

where  $FL_{x,\lambda,HZ}$  is the radiance image of an external flat field scene, run through the whole calibration pipeline and then normalized so the scene pixels in each row average to 1. See

section 3.3 and section **Error! Reference source not found.** As of 1/28/2009,  $EP_{x,\lambda}$  is zero, so it is a straight flat field with no allowance for pixel-dependent nonlinearity.

$M_{x,\lambda,Hz}()$  replaces non-scene pixels with the value 65535. For IR, it also applies the ex post facto bad pixel correction. See section **Error! Reference source not found.**

$RD_{x,\lambda,r}$  is the observed spectral radiance in  $W/(m^2 \text{ micrometer sr})$  at the instrument aperture for scene or EPF measurements. See section **Error! Reference source not found.**

$IF_{x,\lambda}$  is I/F, a measure of the observed diffuse reflectivity of the Martian surface as a function of wavelength. The normalization is such that the I/F of a normally illuminated perfect white Lambertian surface is 1. See section 2.18.

## 2.2 Uncompression and conversion to 14-bit DN

Before any calibration steps are taken, the lossless fast compression is undone, yielding **raw DN**.

The first term in the calibration equation,  $DN_{x,\lambda,Hz,t}$ , is **raw DN** for some column x and row  $\lambda$ , taken at some frame rate Hz with exposure time t. Raw DN levels are in EDRs named according to the convention `cccnxxxxxx_xx_aaaaas_EDRv.IMG` where ccc=class of observation (targeted, multispectral windows, etc.), nnnnnnnn=observation ID in hex, xx=counter of EDRs within that observation, aaaaa=activity type, s=sensor ID, and v=version number.

Some raw DN values may be 65535. These are unphysical values used as flags for data dropout pixels. For later steps in the calibration algorithm, the value 65535 will be used to flag saturated and non-scene pixels. Whenever the value of 65535 is encountered, the calibration algorithm assumes it is a flag, not a true DN, and simply passes the value through rather than applying the calibration calculation to that pixel. The ex post facto bad pixel correction (Section **Error! Reference source not found.**) is an exception and replaces 65535 with values calculated from neighboring pixels.

- Although raw DN has the lossless fast compression undone, it is still always written to an EDR compressed from a 14-bit state. This compression is performed in the DPU before lossless fast compression. Raw DN is restored to 14 bits using a pixel processing table which has one line per detector row, with 3 elements per line. This step occurs after the EDRs are generated, as part of the conversion of the EDRs to radiance units.

The conversion needs to know:

- Which one of 8 look-up tables was used to convert 12 to 8 bits on that line, if the data are 8 bits
- An inverted version of the lookup table used for each line, to convert back to 12 bits
- A gain, by which the 12-bit DN should be divided
- An offset, which should be added to the gain-corrected DN

For 8-bit raw DN (lossy compression on), there are two steps to the conversion, converting raw

DN to 12-bit DN12, and converting 12-bit DN12 to 14-bit DN14. For 12-bit raw DN (lossy compression off), the first step is skipped.

The formula for generating 12-bit DN12 is

$$DN12_{x,\lambda,TaV,TaW,TaI,TaJ,Ta2,Hz,t,r} = ILUT_{\lambda}(DN_{x,\lambda,TaV,TaW,TaI,TaJ,Ta2,Hz,t,r})$$

for 8-bit raw DN, and

$$DN12_{x,\lambda,TaV,TaW,TaI,TaJ,Ta2,Hz,t,r} = DN_{x,\lambda,TaV,TaW,TaI,TaJ,Ta2,Hz,t,r}$$

for 12-bit raw DN.  $ILUT_{\lambda}$  is the inverse of the original look-up table used by the flight DPU to perform the lossy compression. In addition to the above formulas, the values of 65535 in the data drop-out pixels are simply passed forward as always.

The formula for converting 12-bit DN12 to 14-bit DN14 is

$$DN14_{x,\lambda,TaV,TaW,TaI,TaJ,Ta2,Hz,t,r} = Offset_{\lambda} + DN12_{x,\lambda,TaV,TaW,TaI,TaJ,Ta2,Hz,t,r} / Gain_{\lambda}$$

The offset, gain, and lookup tables are all given row-by-row, and tables are valid over specified time ranges.

Which LUTs were used for each row is maintained as the last column in the level 6 pixel processing CDR, named  $CDR6\_#\_\#\#\#\#\#\#\#\_PP\_n\_v.TAB$ , where #=spacecraft time SCLK partition at the beginning time of validity of the CDR,  $\#\#\#\#\#\#\#$ =spacecraft time SCLK at the beginning time of validity of the CDR, n=sensor ID and v=version number. The LUTs themselves are maintained as  $CDR6\_1\_0000000000\_LK\_n\_v.TAB$ , and the conversion back to 14 bits uses the inverse lookup table, maintained as  $CDR6\_1\_0000000000\_LI\_n\_v.TAB$ . The gains are maintained as the second column of the level 6 pixel processing CDR, and the offsets are maintained as the third column of the level 6 pixel processing CDR.

## 2.3 Remove bias

Next the bias is removed from the data. The bias subtraction formula for the IR is

$$\begin{aligned} DN14^a_{x,\lambda,TaI,Ta2,Hz,t,r} &= DN14_{x,\lambda,TaJ,Ta2,Hz,t,r} + a0_I \cdot Hv(\text{row}_{\lambda}+1-(502/480)) \cdot (480-\text{integ}(t)) \\ &\quad - Bias_{x,\lambda,TbI,TbJ,Hz} - \beta_{I,Hz} \cdot (TaI - TbI) - \beta_{J,Hz} \cdot (TaJ - TbJ) \end{aligned}$$

The superscript “a” indicates the first step in the calibration algorithm has been applied, and we continue through the alphabet for subsequent steps of the calibration algorithm. As discussed earlier, any values of 65535 are treated as flags and simply passed through in this step with no further calibration performed on them.

Bias is different and more complicated for the IR detector as compared to the VNIR detector. Bias is the DN level extrapolated to zero exposure time, in image form, taken at a particular

frame rate. This represents an electronics bias added to the measured signal, to prevent near-zero DNs from going negative (and being clipped) due to superimposed noise. In detector-level testing it was found that bias has a nearly fixed pattern pixel to pixel, but that its magnitude varies weakly with temperature and strongly with frame rate.

In flight, bias for the IR detector is derived from a dedicated calibration, performed periodically, in which, at each frame rate, a burst of 10 images is taken with the shutter closed at each of several short exposure times. These data are taken at IR detector temperature  $T_{bI}$ . After making a correction for a step in the bias that is a function of integration time parameter, the DN values are fit linearly on a pixel-by-pixel basis and the exposure time=0 y-intercept image is used as the bias estimate. This process is described in section 3.1.

The IR bias images  $Bias_{x,\lambda,T_{bI},T_{bJ},Hz}$  are corrected for the step function  $-a_0 \cdot Hv(\text{row}_\lambda + 1 - (502/480) \cdot (480-\text{integ}(t)))$ . This term results from details of the readout of the image in the electronics. It is entirely predetermined, and contains the entire dependence of the bias on the integration time. The constant  $a_0$  is determined from ground calibration data,  $Hv()$  is the Heaviside function,  $\text{row}_\lambda$  is the detector row number (counting from zero), and  $\text{integ}(t)$  is the integration time parameter  $\text{integ}$  using the formula  $t = 1000 \cdot (502 - \text{floor}((502/480) \cdot (480-\text{integ}))) / (502 \cdot \text{rate})$ , where  $\text{floor}()$  is the function that creates an integer from a real number by rounding down. Since the bias images  $Bias_{x,\lambda,T_{bI},T_{bJ},Hz}$  do not include the step function, it is subtracted explicitly in the equation above.

The IR bias images  $Bias_{x,\lambda,T_{bI},T_{bJ},Hz}$  are stored as level 4 calibration data records (CDRs) named  $CDR4\#tttttttt\_BIRbeeewsl_v.IMG$ , where # = spacecraft SCLK partition for the mean time at which that bias data was taken, tttttttt = mean spacecraft time SCLK for that bias data, r = frame rate, b = binning, eee = exposure time parameter, w = wavelength filter, s = 0, L = detector (IR), and v = version number. The calibration software uses the partition # and the mean SCLK tttttttt to calculate encoded SCLK for the bias measurement. It uses the SCLK given in the .TAB list file that goes with each frame of the EDR along with a partition # from the .LBL file that goes with that EDR to calculate encoded SCLK for that EDR. It then uses the CDR4 file with the value of encoded SCLK that is closest to the value of encoded SCLK for the scene measurement. The keyword "MRO:EXPOSURE\_PARAMETER" in the .LBL file is the integration time parameter.

The bias calibration may be taken at an IR detector temperature  $T_{bI}$  different from that of the data being corrected,  $T_{aI}$ . The term  $\beta_{I,Hz} \cdot (T_{aI} - T_{bI})$  represents the scalar difference between two modeled values of averaged, temperature-dependent bias. This scalar value is intended to correct the bias image for small temperature differences between the time of its acquisition and the time of the data being corrected. The coefficients  $\beta_{I,Hz}$  are given in a level 6 CDR named  $CDR6\#_0000000000\_DB\_L_v.TAB$ . Separate coefficients are defined for the 4 detector quadrants, but as of this writing (11/4/2005) the values are the same for all the quadrants so there is no subscript to represent the quadrant dependence.

The bias calibration may be taken at an IR focal plane electronics board temperature  $T_{bJ}$  different from that of the data being corrected,  $T_{aJ}$ . The term  $\beta_{J,Hz} \cdot (T_{aJ} - T_{bJ})$  represents the scalar difference between two modeled values of averaged, temperature-dependent bias. This scalar value is

intended to correct the bias image for small temperature differences between the time of its acquisition and the time of the data being corrected. The coefficients  $\beta_{j,\text{Hz}}$  are given in a level 6 CDR named CDR6 #\_0000000000\_EB\_L\_v.TAB. Separate coefficients are defined for the 4 detector quadrants, but as of this writing (11/4/2005) the values are the same for all the quadrants so there is no subscript to represent the quadrant dependence.

For the VNIR images, the dark current and thermal photons are nil, so the bias is directly measured when the shutter is closed (the dark measurements taken before and after a scene or calibration image). For the IR, a separate bias subtraction is necessary because there is background due to dark current and thermal photons, and it is necessary to separate that background from the bias in order to make an accurate linearity correction.

The bias subtraction formula for VNIR is

$$\begin{aligned} \text{DN14}^a_{x,\lambda,\text{TaV},\text{Hz},t,r} = & \text{DN14}_{x,\lambda,\text{Hz},\text{TaV},\text{TaW},t,r} \\ & - (\alpha_{ea} \cdot \text{Bias}_{x,\lambda,\text{TdV},\text{TdW},\text{Hz},t} + \alpha_{ad} \cdot \text{Bias}_{x,\lambda,\text{TeV},\text{TeW},\text{Hz},t}) / (\alpha_{ad} + \alpha_{ea}) \\ & - \beta_{V,\text{Hz}} \cdot [\alpha_{ea} \cdot (\text{Tav} - \text{Tdv}) + \alpha_{ad} \cdot (\text{TeV} - \text{Tav})] / (\alpha_{ad} + \alpha_{ea}) \\ & - \beta_{W,\text{Hz}} \cdot [\alpha_{ea} \cdot (\text{Taw} - \text{Tdw}) + \alpha_{ad} \cdot (\text{TeW} - \text{Taw})] / (\alpha_{ad} + \alpha_{ea}) \end{aligned}$$

The  $\alpha$  coefficients in the VNIR equation are time-weighting coefficients. The two VNIR bias images are linearly interpolated in time to the time of the scene image. The variable  $t$  represents integration time, not clock time, so a new variable,  $t_{a1}$  indicates clock time. The value of  $t_{a1}$  is the mean value of encoded SCLK for that image specifically. It is derived from the instrument timetag value in the header of each image, calculated by the CRISM instrument clock, frequently updated by the spacecraft clock, and corrected using the partition number to be encoded SCLK instead of just SCLK. Calculations on a local computer may not have the SPICE information available to convert SCLK to encoded SCLK. One may use SCLK for this calculation as long as the partition number does not change. Just like for the temperatures,  $t_{a1}$  indicates timetag for the scene image,  $t_{d1}$  and  $t_{e1}$  the dark images,  $t_{b1}$  the bias images, and  $t_{c1}$  the calibration images.

$$\alpha_{ad} = t_{a1} - t_{d1} \text{ and } \alpha_{ea} = t_{e1} - t_{a1}$$

The VNIR bias images  $\text{Bias}_{x,\lambda,\text{TdV},\text{TdW},\text{Hz},t}$  and  $\text{Bias}_{x,\lambda,\text{TeV},\text{TeW},\text{Hz},t}$  are calculated from the VNIR bias EDRs by taking the mean DN value in each detector element across all the images in an EDR, with the two largest and two smallest DN values thrown out. The results are stored as level 4 calibration data records (CDRs) named CDR4#tttttttt\_BIrbeeewS\_v.IMG, where #=spacecraft SCLK partition for the beginning of time of validity of the data product, tttttttt=spacecraft time SCLK for the beginning of time of validity of the data product, r=frame rate, b=binning, eee=exposure time parameter, w=wavelength filter, s=0, S=detector (VNIR), and v=version number. The calibration software uses the partition # and the mean SCLK to calculate encoded SCLK for the bias measurement. It uses the SCLK given in the .TAB list file that goes with each frame of the EDR along with a partition # given in the .LBL file that goes with that EDR to calculate encoded SCLK for that EDR. It then uses the CDR4 file with the value of encoded SCLK that is closest to the value of encoded SCLK for the scene measurement. A description of the calculation of  $\text{Bias}_{x,\lambda,\text{TdV},\text{TdW},\text{Hz},t}$  and  $\text{Bias}_{x,\lambda,\text{TeV},\text{TeW},\text{Hz},t}$  is given in section 3.2.

The VNIR coefficients  $\beta_{V,HZ}$  are given in CDR6 # 0000000000\_DB\_n\_v.TAB, and the VNIR coefficients  $\beta_{W,HZ}$  are given in CDR6 # 0000000000\_EB\_n\_v.TAB. The VNIR temperature correction is with respect to the temperatures  $T_{dV}$ ,  $T_{eV}$  of the VNIR detector and  $T_{dW}$ ,  $T_{eW}$  of the VNIR focal plane electronics board during the before and after darks respectively.

The above description of the bias correction applies to the scene images, which have temperatures  $T_{aI}$ ,  $T_{aJ}$  and  $T_{aV}$ ,  $T_{aW}$ . The bias correction is also applied to dark images for the IR, and the formula is the same except  $T_{aI}$ ,  $T_{aJ}$  are replaced by  $T_{dI}$ ,  $T_{dJ}$ . It is also applied to the calibration images for both IR and VNIR, and likewise  $T_{aI}$ ,  $T_{aJ}$  are replaced by  $T_{cI}$ ,  $T_{cJ}$  and  $T_{aV}$ ,  $T_{aW}$  by  $T_{cV}$ ,  $T_{cW}$ .

## 2.4 Remove detector quadrant electronics ghost

Next, electronics ghosts are removed from the data. There are two types of ghosts, each at the percent level, that add to the measured DN but do not represent real signal.

The first type of electronics ghost is a weak, negative image of any one of the four 160-column wide quadrants in each other quadrant.



Weak electronics ghost negative images of the quadrant 4 signal in each other quadrant.

Each quadrant produces the same ghost image in all 4 quadrants. We include the self-ghosting because it makes the subsequent nonlinearity correction smaller. For VNIR, the ghost is a nonlinear function of the signal. For IR, the ghost is a linear function of the signal, but with a nonzero intercept when extrapolated to zero signal indicating that the ghost would be nonlinear at small signal levels if we had data there. For VNIR or IR, the ghost has the same function  $G(DN)$  for all 4 quadrants whether one changes the quadrant in which the source is located or the quadrant in which the ghost appears.

To remove the detector quadrant ghost, we subtract the ghost calculated from the signal in each of the 4 quadrants from each pixel. The quadrant the pixel itself is in is included, so the self-ghosting is subtracted.

$$DN14^b_{x,\lambda,TaV,HZ,t,r} = DN14^a_{x,\lambda,TaV,HZ,t,r} - \sum_{n=0}^{n=3} Gv(DN14^a_{x0+n\delta,\lambda,TaV,HZ,t,r})$$

for VNIR and

$$DN14^b_{x,\lambda,TaI,Ta2,Hz,t,r} = DN14^a_{x,\lambda,TaI,Ta2,Hz,t,r} - \sum_{n=0}^{n=3} G_l(DN14^a_{x_0+n\delta,\lambda,TaI,Ta2,Hz,t,r})$$

for IR, where  $\delta$  = the width of a quadrant (160 for full resolution images), and  $x_0 = x$  modulo  $\delta$ , the position in the first quadrant corresponding to the position of  $x$  in the current quadrant.  $G()$  is the ghost function, which is different for VNIR and IR but does not depend on frame rate or any other parameter. The coefficients in the ghost function  $G()$  are given in a level 6 CDR named: CDR6 # 000000000 GH n v.TAB.

The above functions define the ghost removal function  $H()$ , so that

$$DN14^b_{x,\lambda,TaV,Hz,t,r} = H(DN14^a_{x,\lambda,TaV,Hz,t,r}) \text{ for VNIR and}$$

$$DN14^b_{x,\lambda,TaI,Ta2,Hz,t,r} = H(DN14^a_{x,\lambda,TaI,Ta2,Hz,t,r}) \text{ for IR.}$$

Treatment of pixels flagged with 65535 in ghost removal correction:

These pixels are passed on to the next step in the calibration algorithm with no processing. For the right hand side of the equation above,  $DN14^a_{x_0+n\delta,\lambda,TaI,Ta2,Hz,t,r}$  is set equal to zero, so these pixels have zero contribution.

## 2.5 Masked pixel (dark column) subtract for VNIR

After the temperature corrections were implemented, it was determined that there was a frame-to-frame noise in the bias that generated horizontal lines in the VNIR image. This noise could not be modeled. The only way to eliminate it was to subtract the median of a set of detector pixels covered by a physical mask and therefore completely unilluminated, even by scattered light. The median is taken over a set of columns  $x_1 \dots x_n$  along the edge of the detector, and over all detector wavelengths  $\lambda_1 \dots \lambda_s$ .

VNIR:

$$DN14^{bb}_{x,\lambda,TaV,Hz,t,r} = DN14^b_{x,\lambda,TaV,Hz,t,r} - \text{median}_{x,\lambda}(DN14^b_{x_1 \dots x_n, \lambda_0 \dots \lambda_s, TaV, TaW, Hz, t, r})$$

The columns used for dark column subtraction for a given pixel binning b and wavelength table w are specified in the DM level 4 CDR CDR410000000000\_DM0b000w0S\_v.IMG.

The dark column subtract makes some of the corrections in Section 2.3 redundant. The corrections for dependence of the bias on temperature of the detector and temperature of the focal plane electronics apply equally to every pixel in the detector, so they are canceled out in the masked pixel correction step.

## 2.6 Apply a priori bad pixel mask to all images

The a priori bad pixel mask uses the bias, sphere, and background flight calibration images to calculate pixels that are potentially saturated in the scene or sphere image, dead, or excessively noisy in the scene or sphere image. These pixels are replaced by linear spatial interpolation from neighboring good pixels at the same wavelength.

The a priori bad pixel mask for each scene image is calculated entirely from calibration images and scene brightness models. In addition, at the end of the calibration an ex post facto bad pixel mask is calculated from the calibrated scene radiance image and applied to it. See section **Error! Reference source not found.**

1. Noisy pixels. For each detector element (“pixel” for the current discussion, but this is a column and wavelength bin on the detector, *\*not\** a spatial pixel on Mars which has multiple wavelengths), we take the standard deviation of the DN value in multiple nominally identical images, with the largest two and smallest two DN values thrown out. If that standard deviation is greater than 15 DN, the pixel is “bad”. This is calculated for each pixel within each EDR for all bias EDRs (multiple integration times for IR) including the sphere bias EDRs, and for all IR background EDRs, including those for the sphere EDRs. If a pixel is bad in even one of these EDRs, it is included in the bad pixel mask. Note the “bad pixel bias” EDRs are *\*not\** used to calculate noisy pixels.
2. Dead pixels. Bias and background subtract are applied to sphere calibration images, and any pixel that is <5% (this criterion is given in the VL CDR CDR6\_1\_0000000000\_VL\_n\_0.TAB) of the median of its wavelength band is deemed “dead” and added to the bad pixel mask.
3. Potentially saturated pixels. The AS CDR CDR6\_1\_0000000000\_AS\_n\_0.TAB contains a model of the maximum DN level expected from any scene image, and the same for any sphere calibration image. This was derived from models of the scene radiance, sphere radiance, and instrument responsivity, allowing for the integration times used in the different types of images. For sphere and scene, bias and dark current (for VNIR, dark current is assumed to be zero) calculated from the “bad pixel bias” EDRs is added to the AS CDR value. If the result exceeds 93% of the saturation value of the detector (the 93% criterion and the saturation values are given in the VL CDR), then that pixel is declared bad and added to the bad pixel mask. In practice, almost all of the saturated pixels in the image are identified as potentially saturated pixels and replaced.

#### Binning:

Noisy pixels are usually calculated from images with the same spatial binning as the scene. In cases where the noisy pixels are calculated from higher spatial resolution images (sphere biases, for example), the binned pixel is bad if any of the individual pixels are bad (“OR binning”). When dead pixels are binned, the binned pixel is bad only if all the individual pixels are bad (“AND binning”). Potentially saturated pixels are always calculated at the full spatial resolution of 640 columns. They are always OR binned. This is why a special “bad pixel bias” EDR or set of EDRs is defined, to ensure the potentially saturated pixels are always calculated at full resolution. The binning done in the CRISM electronics is at the digital level, and the binned pixel will have an inaccurate DN value if any of the sub-pixels are saturated. A detail: The “binning” done in the CRISM electronics is averaging, not summing.

The bad pixel masks are stored as images for each frame rate in the files named CDR4#tttttttt\_BPrbeewsn\_v.IMG. The file CDR6\_#\_0000000000\_PD\_n\_v.TAB contains a list of the bad pixel mask image CDR4 filenames. The bad pixel mask CDR for a scene image contains bad pixels for the ex post facto bad pixel correction as well as the a priori bad pixel

correction.

In addition to the BP CDR written for the scene image, BP CDRs are also written for the bias, sphere, and background images that are written to the BI, SP, and BK CDRs respectively. They can be distinguished by the spacecraft clock value tttttttt in the filename. The value put in the BP CDR filename is the spacecraft clock value at the time the bias, sphere, or background EDR was taken. For the IR bias, there are several EDRs, and we use the midpoint of the EDRs for the spacecraft clock value. The bias BP CDRs flag only the noisy pixels for the given bias EDRs. The sphere BP CDRs flag the noisy, dead, and potentially saturated (for that sphere image, not for the scene) pixels for a given SP CDR. The BP CDRs written for the IR background images include all the a priori bad pixels for the scene image, except if there are noisy pixels in one background image that are not in the other, they will be in only one of the background BK CDRs. The set of pixels that are bad pixels in one or the other of the two BP CDRs for the background images that go with a scene gives the full set of a priori bad pixels applied to that scene. Note this includes scene bias and scene background noisy pixels, dead pixels, and potentially saturated scene pixels. It does not include noisy and potentially saturated sphere pixels, which have been corrected in the sphere image, and the corrected values have been used to calibrate the scene image. If one wants to look at just the a priori bad pixel mask for the IR, one must use the background BP CDRs. The BP CDR for the scene itself also contains many bad pixels from the IR ex post facto bad pixel correction, described in section **Error! Reference source not found..**

The a priori bad pixel mask is applied to an image by replacing each bad pixel with the average of the two pixels in adjacent columns (spatial pixels) in the same row (wavelength pixel). If two or more pixels in the same row and adjacent columns are bad, they are replaced using a linear interpolation of the two nearest good pixels in that row. The bad pixel mask is applied after bias subtraction and detector ghost removal. Pixels with value 65535 are not replaced.

Special cases:

1. When the bad pixel is the first or last column of the scene mask, so that the nearest neighbor on one side is not a scene pixel, the bad pixel will be replaced by the neighboring pixel in the adjacent column that is part of the scene, and the neighboring pixel not part of the scene will not be used. If two or more pixels in the same row and adjacent columns are bad, including the first or last column, they will be replaced by the nearest good pixel in that row.
2. When the bad pixel is in the stray light mask, it will not be used. If all of the stray light pixels in a given row are bad, then they are replaced by a linear interpolation of the two pixels in adjacent rows in the same column. If two or more stray light pixels in adjacent rows are bad, they will be replaced using a linear interpolation of the two nearest good pixels in that column. See section **Error! Reference source not found..**

In the above rules, a “good” pixel is one not in the bad pixel mask and also with a value not equal to 65535.

The stray light mask defines columns close enough to the edge of the detector to be outside the image of the spectrometer entrance slit but far enough away from the edges of the detector to be unmasked. They sample any stray light that is uniform in character. The stray light pixels are defined as columns  $x_1 \dots x_n$  and the values are as follows: 8-27, 4-13, 2-4, and 1 for the IR detector with 1x, 2x, 5x, and 10x binning respectively. For VNIR, there are stray light columns on both sides of the detector: 12-23 and 627-639 for 1x binning, 6-11 and 314-319 for 2x binning, 3 and 126-127 for 5x binning, and 1 and 63 for 10x binning. The values are given in a level 4 calibration data record (CDR) named CDR4100000000000\_DM0b000w0n\_v.IMG, where b=binning, w=wavelength filter, n=detector, and v=version number.

Applying the calculations described in the calculation above is defined as  $B()$ , the bad pixel removal function, so we have

$$DN14^c_{x,\lambda,TaV,TaI,Ta2,Hz,t,r} = B_{x,\lambda,Hz}( DN14^{bb}_{x,\lambda,TaV,TaI,Ta2,Hz,t,r} )$$

The bad pixel mask is not applied to bias images written to the BI CDRs, because it is calculated from the bias images and applied after the bias subtraction. However, the sphere bad pixel mask, including noisy, dead, and saturated pixels, is applied to the sphere calibration images before the SP CDR is written. Likewise, the IR background bad pixel mask, including almost all the scene bad pixels, is applied to the background image before the BK CDR is written.

Each RDR generated from an EDR will have ancillary information that includes the name of the bad pixel mask CDR4 file used as part of the generation of that RDR, so users who wish to reject the bad pixels entirely have the information to do so. All of the bad pixels are flagged by this method. However, the calibration algorithm will replace the bad pixels with interpolated values, not reject them.

## 2.7 Flag saturated pixels

Saturated pixels do not represent accurate data values, so we intended to flag them by replacing them with the value 65535. The saturated pixels are processed up to the level of the detector electronics ghost, because it is more accurate to apply the saturated value to the ghost correction than to apply zero. In practice, almost all the saturated pixels are identified in the last section as potentially saturated pixels and interpolated across, and those are not identified as saturated in this step and replaced by a value of 65535.

The saturated pixel removal function replaces  $DN14^c_{x,\lambda,TaV,Hz,t,r}$  with the value 65535 if  $DN14^c_{x,\lambda,TaV,Hz,t,r} > DN14^c_{maxV,x,Hz}$  for VNIR, and replaces  $DN14^c_{x,\lambda,TaI,Ta2,Hz,t,r}$  with the value 65535 if  $DN14^c_{x,\lambda,TaI,Ta2,Hz,t,r} > DN14^c_{maxI,x,Hz}$  for IR. The values  $DN14^c_{maxV,x,Hz}$  and  $DN14^c_{maxI,x,Hz}$  are given in the level 6 CDR named CDR6\_1\_000000000\_VL\_n\_v.TAB, where n=detector and v=version number. There are different values for different detector quadrants and frame rates, but the values are close for a given detector.

The function  $S()$  is defined as the function that flags the saturated pixels as described above.

$$DN14^d_{x,\lambda,TaI,Ta2,Hz,t,r} = S(DN14^c_{x,\lambda,TaV,TaI,Ta2,Hz,t,r})$$

Any pixels flagged with 65535 are not processed by any subsequent step in the calibration algorithm, but just passed on to the next step unchanged. An exception is that the ex post facto bad pixel correction does replace them, and in practice nearly all the 65535 values do get replaced. See Section **Error! Reference source not found..**

## 2.8 Detector average nonlinearity correction

We use an empirical model of the detector nonlinearity to correct 14-bit DNs to a signal related linearly to the sum of contributions from dark current, thermal background, scattered light, and scene imaged through the slit. This is a correction for nonlinearity in the responsivity of the instrument. The source of this nonlinearity is in the detector electronics, as part of the conversion of electrons to DN. We correct for the fact that conversion efficiency of electrons to DN increases with DN. The value of DN is converted back to what it would be in an idealized case with a constant number of electrons per DN. In detector level testing it was found that, on average, conversion efficiency varies nearly linearly with the logarithm of bias-corrected DN, and that the relationship differs slightly between frame rates. This gives the following model.

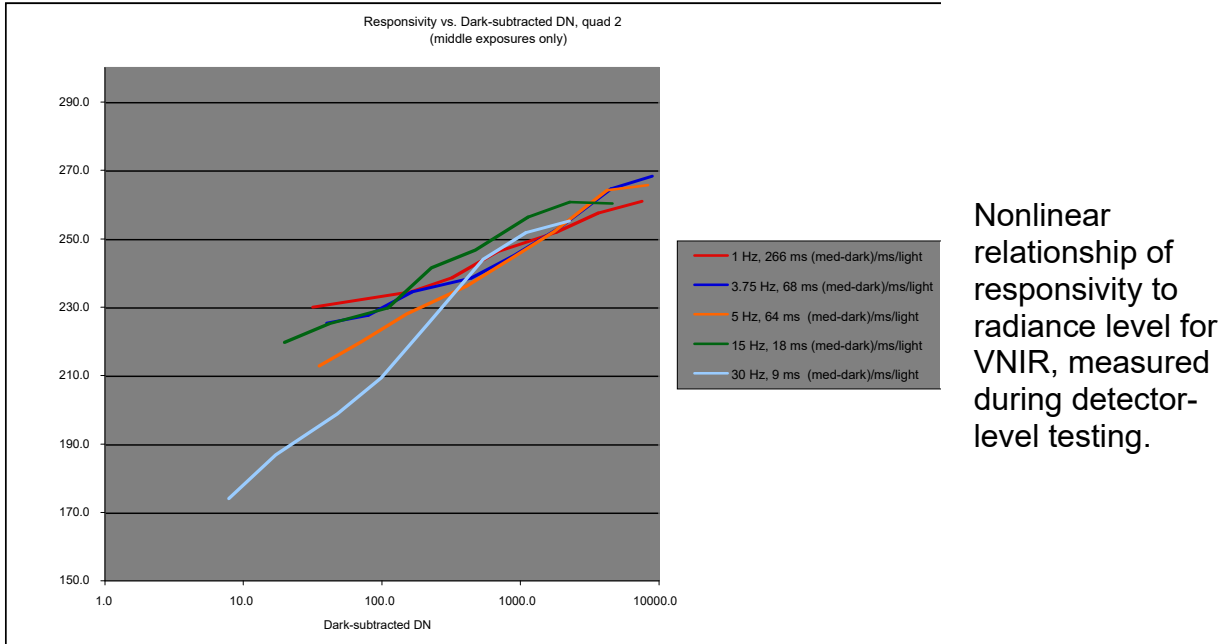
$$Eff = DN / (Rate \cdot t) = \varepsilon \cdot \log(DN) + \phi$$

where  $Eff$  is the detector conversion efficiency (DN/electrons) and  $Rate$  is the total rate of production of electrons, including source photons, background photons, and detector dark current but not including detector bias. The function  $\log()$  is the natural or base-e logarithm. We calculate  $\varepsilon$  and  $\phi$  from  $DN_{crs}$ , from images taken during spacecraft cruise before arrival at Mars. We used the spectrometer focal plane lamps as sources. We used different exposure times ( $t$ ), and different lamp currents to give different electron production rates ( $Rate$ ). The exposure times were known to high accuracy, and by comparing image DN for different exposure times and lamp currents, we were able to determine the relative value of ( $Rate$ ) for each lamp current. Then, we used a linear fit to  $y=\varepsilon \cdot x + \phi$  with  $y=DN_{crs}/(Rate \cdot t)$  and  $x=\log(DN_{crs})$  to give the nonlinearity parameters  $\varepsilon$  and  $\phi$ .

The parameters  $\varepsilon$  and  $\phi$  are calculated as averages over the whole detector and applied to the DN level on a pixel by pixel basis. Typically, we use benchtop detector data and  $DN_{gnd}$  is an average over a region with constant filter performance and constant illumination to sample constant DN. We can also use  $DN_{gnd}$  from data taken with the detector in the instrument, in which case it is generally an average over a row or a few rows to sample fairly constant DN. We assume that variations in the nonlinearity parameters from pixel to pixel within a row are small enough to be addressed in the flat field correction, as long as the flat field DN is roughly similar to the scene DN.

Note the calibration pipeline software does have the ability to assign different values of  $\varepsilon$  and  $\phi$  for each pixel. For  $\phi$ , this is equivalent to the standard flat field, which scales the image for each

pixel. For  $\varepsilon$ , the flat field FF CDR has a second layer that includes values of  $\varepsilon$  that may be chosen independently for each pixel. As of 1/28/2009, the second layer of the FF CDR is all zeroes, and the only nonlinearity correction uses the same  $\varepsilon$  over the whole image. The flat field correction is described in more detail in Section [Error! Reference source not found..](#)



Then, we use the values of  $\varepsilon$  and  $\phi$  from the fit to convert our flight DN back to an idealized DN which would result from a linear response. That linearized DN is proportional to  $(\text{Rad} \cdot t)$ , so we solve for  $(\text{Rad} \cdot t)$  in the model and our correction equation becomes

$$\text{DN14}^g_{x,\lambda,\text{TaI},\text{Ta2},\text{TaV},\text{Hz},t,r} = F_{\text{Hz}}(\text{DN14}^e_{x,\lambda,\text{TaI},\text{Ta2},\text{TaV},\text{Hz},t,r})$$

$$F_{\text{Hz}}(\text{DN14}^e_{x,\lambda,\text{TaI},\text{Ta2},\text{TaV},\text{Hz},t,r}) = \text{DN14}^e_{x,\lambda,\text{TaI},\text{Ta2},\text{TaV},\text{Hz},t,r} / (\varepsilon_{\text{Hz}} \cdot \log(\text{DN14}^e_{x,\lambda,\text{TaI},\text{Ta2},\text{TaV},\text{Hz},t,r}) + \phi_{\text{Hz}})$$

where  $\text{DN14}^f_{x,\lambda,\text{TaI},\text{Ta2},\text{TaV},\text{Hz},t,r}$  is the linearized DN for our actual flight data. The function  $\log()$  is the natural or base-e logarithm. As shown,  $\varepsilon$  and  $\phi$  are a function of frame rate. They are proportional to  $(\text{Rate} \cdot t)$  but there's an arbitrary scaling factor. We scale them so that  $F(1000)=1$ . The coefficients  $\varepsilon$  and  $\phi$  are given in a level 6 CDR named `CDR6_#_0000000000_LC_n_v.TAB` where  $n=\text{sensor ID}$  and  $v=\text{version number}$ .

We use an empirical model of the detector nonlinearity to correct 14-bit DNs to a signal related linearly to the sum of contributions from dark current, thermal background, scattered light, and scene imaged through the slit. This is a correction for nonlinearity in the responsivity of the instrument. The source of this nonlinearity is in the detector electronics, as part of the conversion of electrons to DN. We correct for the fact that conversion efficiency of electrons to DN increases with DN. The value of DN is converted back to what it would be in an idealized case with a constant number of electrons per DN. In detector level testing it was found that, on average, conversion efficiency varies nearly linearly with the logarithm of bias-corrected DN,

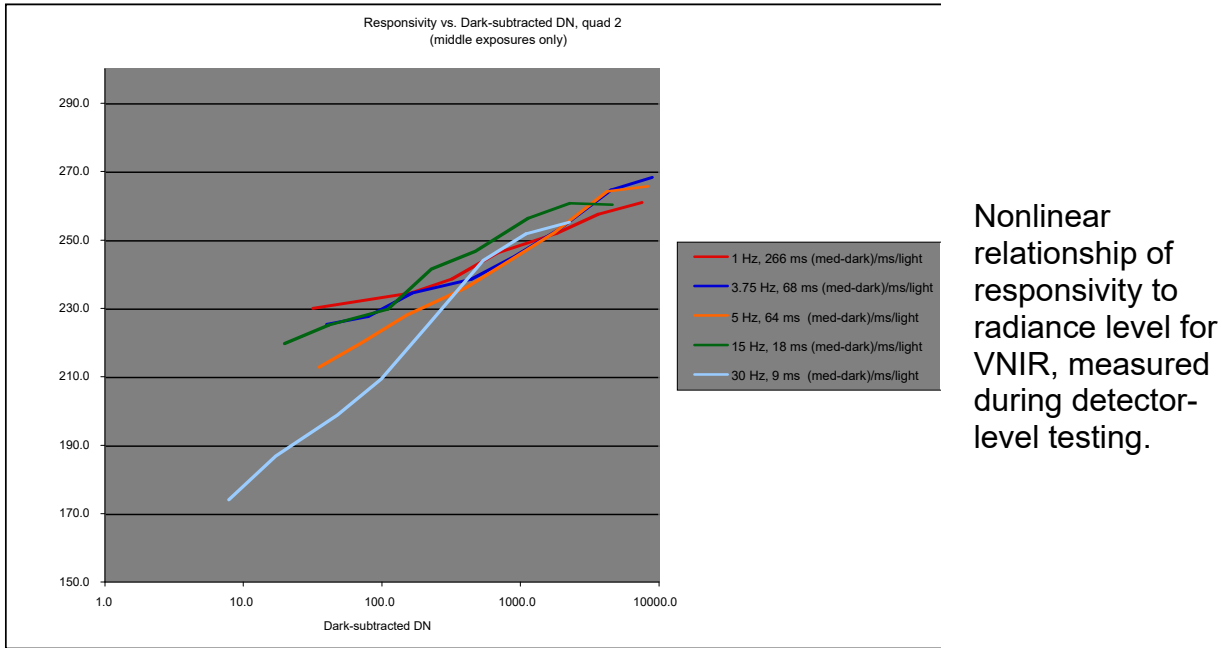
and that the relationship differs slightly between frame rates. This gives the following model.

$$\text{Eff} = \text{DN} / (\text{Rate} \cdot t) = \varepsilon \cdot \log(\text{DN}) + \phi$$

where Eff is the detector conversion efficiency (DN/electrons) and Rate is the total rate of production of electrons, including source photons, background photons, and detector dark current but not including detector bias. The function log() is the natural or base-e logarithm. We calculate  $\varepsilon$  and  $\phi$  from  $\text{DN}_{\text{crs}}$ , from images taken during spacecraft cruise before arrival at Mars. We used the spectrometer focal plane lamps as sources. We used different exposure times ( $t$ ), and different lamp currents to give different electron production rates (Rate). The exposure times were known to high accuracy, and by comparing image DN for different exposure times and lamp currents, we were able to determine the relative value of (Rate) for each lamp current. Then, we used a linear fit to  $y=\varepsilon \cdot x + \phi$  with  $y=\text{DN}_{\text{crs}}/(\text{Rate} \cdot t)$  and  $x=\log(\text{DN}_{\text{crs}})$  to give the nonlinearity parameters  $\varepsilon$  and  $\phi$ .

The parameters  $\varepsilon$  and  $\phi$  are calculated as averages over the whole detector and applied to the DN level on a pixel by pixel basis. Typically, we use benchtop detector data and  $\text{DN}_{\text{gnd}}$  is an average over a region with constant filter performance and constant illumination to sample constant DN. We can also use  $\text{DN}_{\text{gnd}}$  from data taken with the detector in the instrument, in which case it is generally an average over a row or a few rows to sample fairly constant DN. We assume that variations in the nonlinearity parameters from pixel to pixel within a row are small enough to be addressed in the flat field correction, as long as the flat field DN is roughly similar to the scene DN.

Note the calibration pipeline software does have the ability to assign different values of  $\varepsilon$  and  $\phi$  for each pixel. For  $\phi$ , this is equivalent to the standard flat field, which scales the image for each pixel. For  $\varepsilon$ , the flat field FF CDR has a second layer that includes values of  $\varepsilon$  that may be chosen independently for each pixel. As of 1/28/2009, the second layer of the FF CDR is all zeroes, and the only nonlinearity correction uses the same  $\varepsilon$  over the whole image. The flat field correction is described in more detail in Section **Error! Reference source not found..**



Then, we use the values of  $\varepsilon$  and  $\phi$  from the fit to convert our flight DN back to an idealized DN which would result from a linear response. That linearized DN is proportional to  $(\text{Rad} \cdot t)$ , so we solve for  $(\text{Rad} \cdot t)$  in the model and our correction equation becomes

$$\text{DN14}^g_{x,\lambda,\text{TaI},\text{Ta2},\text{TaV},\text{Hz},t,r} = F_{\text{Hz}}(\text{DN14}^e_{x,\lambda,\text{TaI},\text{Ta2},\text{TaV},\text{Hz},t,r})$$

$$F_{\text{Hz}}(\text{DN14}^e_{x,\lambda,\text{TaI},\text{Ta2},\text{TaV},\text{Hz},t,r}) = \text{DN14}^e_{x,\lambda,\text{TaI},\text{Ta2},\text{TaV},\text{Hz},t,r} / (\varepsilon_{\text{Hz}} \cdot \log(\text{DN14}^e_{x,\lambda,\text{TaI},\text{Ta2},\text{TaV},\text{Hz},t,r}) + \phi_{\text{Hz}})$$

where  $\text{DN14}^f_{x,\lambda,\text{TaI},\text{Ta2},\text{TaV},\text{Hz},t,r}$  is the linearized DN for our actual flight data. The function  $\log()$  is the natural or base-e logarithm. As shown,  $\varepsilon$  and  $\phi$  are a function of frame rate. They are proportional to  $(\text{Rate} \cdot t)$  but there's an arbitrary scaling factor. We scale them so that  $F(1000)=1$ . The coefficients  $\varepsilon$  and  $\phi$  are given in a level 6 CDR named `CDR6_#_0000000000_LC_n_v.TAB` where n=sensor ID and v=version number.

## 2.9 Divide by integration time to get counts/second

$$\text{RT14}^g_{x,\lambda,\text{TaI},\text{Ta2},\text{TaV},\text{Hz},r} = \text{DN14}^g_{x,\lambda,\text{TaI},\text{Ta2},\text{TaV},\text{Hz},t,r} / t$$

The nomenclature RT denotes rate instead of DN for data number, and the integration time is omitted to indicate that the images are nominally independent of integration time, but the rest of the subscripts are kept the same. We use t in milliseconds, so the units of RT are counts/ms.

## 2.10 Background subtraction

The IR detector has dark current and is sensitive to IR background from the walls of the

spectrometer. Now that the DN are bias-subtracted and linearized, this background must be subtracted before the scene images may be calibrated. The VNIR detector has no sensitivity to IR glow from the walls of the spectrometer, and at the  $-60^{\circ}$  C operating temperature there is no significant dark current, so no background subtraction is necessary for the VNIR channel.

The background is most strongly influenced by changes in the temperature of the IR detector. A spectrometer housing temperature only  $0.02^{\circ}$  C different from the data being corrected, at relatively warm housing temperatures near  $-78^{\circ}$  C, may result in a background at the longest IR wavelengths that is different by the noise-equivalent radiance. Originally, we had planned to interpolate the dark measurements using the measured spectrometer housing temperatures, but we do not expect the temperature sensors to be accurate enough. Therefore, the dark measurements are interpolated based on the time each was taken and the time of the image being background corrected. The value of  $t_{a1}$  is the mean value of encoded SCLK for that image specifically. It is derived from the instrument timetag value in the header of each image, calculated by the CRISM instrument clock, frequently updated by the spacecraft clock, and corrected using the partition number to be encoded SCLK instead of just SCLK. Calculations on a local computer may not have the SPICE information available to convert SCLK to encoded SCLK. One may use SCLK for this calculation as long as the partition number does not change. Just like for the temperatures,  $t_{a1}$  indicates timetag for the scene image,  $t_{d1}$  and  $t_{e1}$  the dark images,  $t_{b1}$  the bias images, and  $t_{c1}$  the calibration images.

The equation for background subtraction is

$$RT14^h_{x,\lambda,TaI,Ta2,Hz,r} = RT14^g_{x,\lambda,TaI,Ta2,Hz,t_{a1},r} - Bkgd_{x,\lambda,TdI,TeI,Td2,Te2,Hz,t_{a1},t_{d1},t_{e1}}$$

with

$$\begin{aligned} Bkgd_{x,\lambda,TdI,TeI,Td2,Te2,Hz,t_{a1},t_{d1},t_{e1}} &= [ 1 / ( t_{e1} - t_{d1} ) ] \cdot \\ &[ RTD14^g_{x,\lambda,TdI,Td2,Hz,t_{d1}} \cdot ( t_{e1} - t_{a1} ) + RTD14^g_{x,\lambda,TeI,Te2,Hz,t_{e1}} \cdot ( t_{a1} - t_{d1} ) ] \end{aligned}$$

$$\text{and } RTD14^g_{x,\lambda,TdI,Td2,Hz,t_{d1}} = DND14^g_{x,\lambda,TdI,Td2,Hz,t_d} / t_d$$

for IR. The term  $Bkgd_{x,\lambda,TdI,TeI,Td2,Te2,Hz,t_{a1},t_{d1},t_{e1}}$  is simply an average of the dark measurements taken before and after the given scene measurement, weighted by the inverse of the time difference between each dark measurement and the given scene measurement.

The term  $RTD14^g_{x,\lambda,TdI,Td2,Hz,t_{d1}}$  is simply the 14-bit DN/second for the dark measurement taken before the measurement being background-subtracted, the superscript g indicating that it has gone through the same set of corrections as the measurement being background-subtracted. The variable  $t_d$  is the integration time for that particular dark measurement.

The images  $DND14^g_{x,\lambda,TdI,Td2,Hz,t_d}$  are stored as level 4 calibration data records (CDRs) named  $CDR4\#tttttttt\_BKrbreeewsl\_v.IMG$ , where # = spacecraft time SCLK partition at the beginning of validity of the CDR, tttttttt = spacecraft time SCLK at the beginning of validity of the CDR, r = frame rate, b = binning, eee = exposure time parameter, w = wavelength filter, s = 0, L = detector (IR), and v = version number. The integration time  $t_d$ , used to calculate  $RTD14^g_{x,\lambda,TdI,Td2,Hz,t_d}$  from

$DND14^g_{x,\lambda,TdI,Td2,Hz,td}$ , may be calculated from the integration time parameter in the label file CDR4#tttttttt\_BKrbreeewsL\_v.LBL that goes with the .IMG file containing the  $DND14^g_{x,\lambda,TdI,Td2,Hz,td}$  images.

For VNIR, there's no background correction, so it's just

$$RT14^h_{x,\lambda,TaV,Hz,r} = RT14^g_{x,\lambda,TaV,Hz,r}$$

## 2.11 Masked pixel subtract for IR and scattered light correction for VNIR

Masked pixel (dark column) subtract for IR:

After the temperature corrections were implemented, it was determined that there was a frame-to-frame noise in the bias that generated horizontal lines in the IR image. This noise could not be modeled. The only way to eliminate it was to subtract the median of a set of detector pixels covered by a physical mask and therefore completely unilluminated, even by scattered light. The median is taken over a set of columns  $x_1 \dots x_n$  along the edge of the detector, and over all detector wavelengths  $\lambda_1 \dots \lambda_s$ .

$$RT14^i_{x,\lambda,TaI,Ta2,Hz,t,r} = RT14^h_{x,\lambda,TaI,Ta2,Hz,r} - \text{median}_{x,\lambda} ( RT14^h_{x_1 \dots x_n, \lambda_1 \dots \lambda_s, TaI, Ta2, Hz, t, r} )$$

The columns used for dark column subtraction for a given pixel binning b and wavelength table w are specified in the DM level 4 CDR CDR410000000000\_DM0b000w0L\_v.IMG.

The dark column subtract makes some of the corrections in Section 2.3 redundant. The corrections for dependence of the bias on temperature of the detector and temperature of the focal plane electronics apply equally to every pixel in the detector, so they are canceled out in the masked pixel correction step.

Scattered light correction for VNIR:

CRISM has two known significant sources of optical stray light that must be removed during the correction of spectrally dispersed light, that is, an integrating sphere measurement to a responsivity correction or a Mars scene to radiance:

- Scatter from optical elements in the spectrometer scatters light in the spatial direction x and the wavelength direction  $\lambda$ . This is measured directly by the unmasked pixels to the side of the slit image. The contribution to scattered light resembles glare and is not in focus. This scattered light is stronger at shorter wavelengths, and an explicit correction is made only for VNIR. For IR, a small correction is included implicitly in the radiance calibration SS CDR.
- Second order light (source wavelength 1/2) leaks through zone 3 of the order sorting filter at  $\lambda=2760\text{-}3960$  nm, and an apparent optical ghost with source wavelength near  $\lambda/1.8$  occurs in a narrow range of  $\lambda$  near 2400 nm. The optical ghost is small, and it has not

been detected in flight data, only in laboratory data. It is not corrected. The second order light occurs only in the IR, and an explicit correction is made.

The scattered light pixels are columns close enough to the edge of the detector to be outside the image of the spectrometer entrance slit but far enough away from the edges of the detector to be unmasked. They sample any stray light that is uniform in character. The stray light pixels are defined as columns  $x_1 \dots x_n$  and the values are as follows: 8-27, 4-13, 2-4, and 1 for the IR detector with 1x, 2x, 5x, and 10x binning respectively. Note the IR stray light pixels are not used in the calibration algorithm. For VNIR, there were originally stray light columns on both sides of the detector, but only one side is used: 630-639 for 1x binning, 315-319 for 2x binning, 126-127 for 5x binning, and 63 for 10x binning. The VNIR stray light pixels are used in the calibration algorithm. These values are given in a level 4 calibration data record (CDR) named CDR4#0000000000\_DM**rbeewsn\_v.IMG**, where #=spacecraft time SCLK partition at the beginning of validity of the CDR, tttttttt=spacecraft time, r=frame rate, b=binning, eee=exposure time parameter, w=wavelength filter s=0, n=detector, and v=version number.

The scattered light is corrected for a VNIR pixel by estimating the scattered light from the other pixels in the same frame (note a frame is column x wavelength for a single line of the Mars image) and subtracting that estimated scattered light.

There are several possible straightforward methods to estimate the VNIR scattered light:

1. Simply take an average value in the stray light pixels for each wavelength band in a frame and subtract it from the pixel in every column for that wavelength band in that frame. This technique would be accurate in theory if the scattered light were perfectly uniform with radiance independent of angle, like a Lambertian surface. In this case the stray light pixels would accurately monitor the same amount of scattered light as the pixels in the image at each wavelength. However, in practice this method is inaccurate because scattered light is peaked with scattering angle. The function varies but usually is close to an inverse power of the scattering angle, often the inverse square of the scattering angle. This causes two problems with just subtracting the stray light pixel.
  - a. The scene is not uniform with column number, and pixels with other bright pixels nearby have more scattered light than pixels with only dim pixels nearby. One scattered light value for a wavelength bin can't cover all the columns.
  - b. The scattered light pixels are on the edge of the detector and so they only get scattered light from one side, while scene pixels near the center of the detector get scattered light from both sides. In practice, for a uniformly bright scene, all scene pixels except those very close to the edge of the detector have scattered light of more than twice that recorded by the stray light pixels. Whether it's 2x, 2.5x, or 3x depends on how many stray light pixels are included in the average. The stray light pixels further away from the illuminated scene and closer to the edge of the detector have lower signal and a larger factor must be used if they are included.
2. The VNIR bands go down to very short wavelength, where the already dim direct signal is further reduced by a cut-on order sorting filter, leaving only the scattered light coming from longer wavelengths. The nominal wavelength of VNIR band 0 for CRISM multispectral mapping images (band 2 for hyperspectral images) is 378 nm. The short-

wavelength CRISM VNIR order sorting filter is made of Schott glass GG375, with nominal cut-on longward of 375 nm. For each CRISM frame, one can simply take the multispectral band 0 value (or the mean of bands 1-3 for hyperspectral images) and subtract it from all the pixels in that frame in the same column. This method samples the variation in stray light with column number. However, it suffers from the following problems.

- a. The stray light varies with wavelength, because the image brightness varies with wavelength and the stray light is locally peaked. Therefore, the scattered light sampled by multispectral band 0 is generally smaller overall than the scattered light in the rest of the frame.
  - b. Different parts of the scene can have considerably different spectra. For example, dust and rocks are reddish and ice is white. For frames with some columns of ice and some columns of rock, even the relative values of the scattered light in different columns of multispectral band 0 don't accurately measure the relative values of the scattered light in different columns of the longer wavelengths.
3. Except for the very edges of the detector, the source of the scattered light in a frame is well sampled by the frame itself, because the scattered light is locally peaked. One could simply model the scattered light by convolving each single VNIR CRISM frame with a scattering function, derived from lab data, representing the approximately inverse theta squared dependence of the scattered light for large scattering angle theta. The scattering function would have an approximately inverse lambda squared dependence on the source wavelength. Because the CRISM dichroic beamsplitter is an important source of scattered light and it's tilted, the scattering function may be anamorphic (have a different scaling in the spatial direction and wavelength direction). The scattering function would be smoothed and capped at small values of theta corresponding to just a few pixels away from the pixel being corrected, because the purpose of the correction is to correct scattered light, not alter the point spread function of the instrument. This method is accurate in theory, and does not require the scattered light pixels. However, we were concerned about the following possible problems.
    - a. If the scattering function is not accurate, artifacts might be generated in the scene images. For example, if the scattered light is overcorrected at smaller angles and undercorrected at larger angles, one might see a dark and then bright band next to a bright/dark boundary in a scene. Note that such an artifact would be introduced only in the cross-track direction in a Mars image, because the correction is applied independently to each detector frame, corresponding to a single line in the Mars image.
    - b. This method uses all the pixels in a given frame to calculate one pixel, so it is more computationally intensive than other calculations in the calibration algorithm.

The production scattered light subtraction algorithm incorporates elements of method 3, but we did not try the straightforward and naïve method 3 as described above. It might be interesting to do a trial with method 3 to see if the VNIR scattered light subtraction algorithm could be simplified, but the existing method, although complicated, works very well.

We started with method 1, simple subtraction of the stray light pixel. Then, discovering the

scattered light was undersubtracted, we scaled it by a factor of 2. Then, it became clear the subtraction was inaccurate for nonuniform scenes, and we scaled the value in the stray light pixel for each band with the signal in multispectral band 0 (bands 1-3 for hyperspectral) relative to the stray light pixel in multispectral band 0.

This hybrid version of methods 1 and 2 was not working for scenes that had both rock and ice and it didn't account well for spectral smile, so for longer wavelength bands the scattered light function for each band was further scaled to a convolution of an empirical scattering function, optimized to minimize artifacts in nonuniform Mars scenes, with the brightness of the pixels in the columns of that band (approximating the brightness of the source of scattered light). This differs from method 3 in that it's just a one-dimensional convolution, limited to the pixels in a single band, rather than using the pixels in the entire frame. Although multispectral band 0 was still explicitly in the algorithm, for the longer wavelength bands the scaling effectively replaced it with the convolution of the band being corrected with the one-dimensional scattering function.

The resulting method was fairly effective, but in scenes that had ice near the stray light pixels, the spectrum of the scattered light subtraction was the spectrum of the ice, which was not appropriate for the rock areas of scenes with mixed ice and rock. Therefore, the stray light pixels were corrected by dividing by the mean of scene pixels near the edge where the stray light pixels were located. This resulted in realistic VNIR spectra of both rock and ice, even in mixed ice-rock scenes, and the spectra were insensitive to whether there was rock or ice near the stray light pixel. Obvious artifacts were dramatically reduced from uncorrected spectra.

The VNIR scattered light algorithm explicitly uses the following data:

- A. The scattered light pixels in each band
- B. Multispectral band 0 (bands 1-3 for hyperspectral)
- C. The scene pixels in each band convolved with a one-dimensional scattering function
- D. Scene pixels near the edge of the detector close to the scattered light pixel in each band

The exact parameters of the algorithm were determined by much empirical optimization on CRISM target mode and mapping mode scenes, but there was not much analysis of the meaning of layering the different corrections on top of each other. The algorithm as implemented is effectively method 2 scaled with wavelength by method 1 at the short wavelengths, and it is my feeling (D. Humm, 12/23/2008) that it is effectively method 3 at the long wavelengths, except it uses a 1-dimensional scattering function instead of the actual 2-dimensional scattering function. At the long wavelengths, the scattered light pixel wavelength dependence is effectively canceled out by ratioing it to the average of nearby scene pixels, and the multispectral band 0 spatial function is effectively canceled out by scaling it to the convolved scene pixels in the band being corrected. Although the relative wavelength and spatial dependence of methods 1 and 2 are canceled out, they still contribute an overall scaling factor to the calculated scattered light.

The equation for VNIR scattered light correction is different for short and long wavelengths. Note the brackets  $\langle \rangle$  in the equations below all refer to taking a simple mean over some range of columns.

For detector rows 185-215 (roughly,  $\lambda < 563$  nm)

$$RT14^i_{x,\lambda,TaV,TaI,Ta2,Hz,r} = RT14^h_{x,\lambda,TaV,TaI,Ta2,Hz,r} - \{ \langle RT14^h_{xa...xb,\lambda,TaV,TaI,Ta2,Hz,r} \rangle \cdot SW^h_{x,TaV,TaI,Ta2,Hz}$$

}

where

$$SW_{x,TaV,TaI,Ta2,Hz}^h = RT14_{x,\lambda,0,TaV,TaI,Ta2,Hz,r}^h / \langle RT14_{xa...xb,\lambda,0,TaV,TaI,Ta2,Hz,r}^h \rangle$$

with  $\lambda_0$  corresponding to detector row 187 (roughly  $\lambda = 378$  nm) and  $x_a...x_b$  the stray light columns (from  $a=630$  to  $b=639$  for 1x binning,  $a=315$  to  $b=319$  for 2x binning,  $a=126$  to  $b=127$  for 5x binning, and  $a=b=63$  for 10x binning, given in the DM CDR), and the brackets {} represent a 15-point downtrack moving mean for each column and wavelength, with the two highest and two lowest points discarded. The moving mean with points discarded is used to ensure that the stray light correction doesn't inject noise from the stray light pixels into the image. Note that for hyperspectral images, a mean of the stray light columns in detector rows 186, 187, and 188 is taken instead of just row 187.

This is the hybrid of methods 1 and 2, taking the scattered light function from a short-wavelength row and scaling it to the value of the scattered light pixel in the row being corrected.

For detector rows 216-291 (roughly,  $\lambda > 563$  nm)

$$RT14_{x,\lambda,TaV,TaI,Ta2,Hz,r}^i = RT14_{x,\lambda,TaV,TaI,Ta2,Hz,r}^h - \{ \langle RT14_{xa...xb,\lambda,TaV,TaI,Ta2,Hz,r}^h \rangle \cdot CS_{x,\lambda,TaV,TaI,Ta2,Hz}^h \}$$

where

$$CS_{x,\lambda,TaV,TaI,Ta2,Hz}^h = SW_{x,TaV,TaI,Ta2,Hz}^h \cdot ( CB_{x,\lambda,TaV,TaI,Ta2,Hz,r}^h / CB_{x,\lambda,0,TaV,TaI,Ta2,Hz,r}^h ) \cdot ( \langle RT14_{xc...xd,\lambda,0,TaV,TaI,Ta2,Hz,r}^h \rangle / \langle RT14_{xc...xd,\lambda,TaV,TaI,Ta2,Hz,r}^h \rangle )$$

and

$$CB_{x,\lambda,TaV,TaI,Ta2,Hz,r}^h = \sum_k RT14_{xk,\lambda,TaV,TaI,Ta2,Hz,r}^h \cdot B_x / ( 1 + ( (x-x_k) / 10 )^2 )$$

with

$$B_x = 1 / ( \sum_k 1 / ( 1 + ( (x-x_k) \cdot binning / 10 )^2 ) )$$

$CB_{x,\lambda,TaV,TaI,Ta2,Hz,r}^h$  is just the convolution of a single band in a single frame with the function  $1 / ( 1 + ( (x-x_k) \cdot binning / 10 )^2 )$ , and  $B_x$  is the normalization factor for that function. The columns  $x_c...x_d$  are the scene full-resolution columns  $c=540$  to  $d=619$  (columns  $c=270$  to  $d=309$  for 2x binning,  $c=108$  to  $d=123$  for 5x, and  $c=54$  to  $d=61$  for 10x) near the stray light pixels, and  $[ (x-x_k) \cdot binning ]$  is the number of columns from  $x_k$  to  $x$  in full-resolution, unbinned pixel units. The symbol  $\sum_k$  indicates a sum over scene columns only, not including the extra stray light and dark columns at the edge of the detector. Note the normalization factor  $B_x$  depends on  $x$  because it depends on how close  $x$  is to the edge of the scene. The brackets {} represent a 15-point downtrack moving mean for each column and wavelength, with the two highest and two lowest points discarded.

This is the more complex correction that attempts to mimic method 3 without having to use all the detector rows of a frame to correct just one row. The factor  $( CB_{x,\lambda,TaV,TaI,Ta2,Hz,r}^h / CB_{x,\lambda,0,TaV,TaI,Ta2,Hz,r}^h )$  changes the relative value of the scattered light subtraction from the  $SW_{x,TaV,TaI,Ta2,Hz,r}^h$  value valid at short wavelengths to the  $CB_{x,\lambda,TaV,TaI,Ta2,Hz,r}^h$  value valid at long wavelengths. The factor  $( \langle RT14_{xc...xd,\lambda,0,TaV,TaI,Ta2,Hz,r}^h \rangle / \langle RT14_{xc...xd,\lambda,TaV,TaI,Ta2,Hz,r}^h \rangle )$  then divides out the wavelength dependence of the stray light pixel, using the scene pixels near the stray light pixel as a proxy for the stray light pixel. The resulting relative spatial and spectral function for scattered light subtraction at long wavelengths pretty much all derives from  $CB_{x,\lambda,TaV,TaI,Ta2,Hz,r}^{hh}$ , and the  $\langle RT14_{xa...xb,\lambda,TaV,TaI,Ta2,Hz,r}^{hh} \rangle \cdot SW_{x,TaV,TaI,Ta2,Hz,r}^{hh}$  factor used at

short wavelengths only affects the overall scale of the correction at long wavelengths.

A special case:

Multispectral images with spacecraft clock SCLK<850327000 (transition orbit and earlier) were taken with a different wavelength table, and those images do not have detector row 187. In that case,

$$SW_{x,TaV,TaI,Ta2,Hz}^h = SW_x^h$$

where  $SW_x^h$  gives the ratio of response of detector row 187 to response of the mean of the stray light pixels in detector row 187 for a uniform scene.  $SW_x^h$  is read from the level 4 calibration data record (CDR) named CDR4100000000000\_SCr000wsS\_v.IMG, where r=frame rate, b=binning, w=wavelength filter s=0, and v=version number. For detector rows 216-291, the formula for scattered light subtraction is unchanged. One just substitutes the new value of  $SW_{x,TaV,TaI,Ta2,Hz}^h$ . This algorithm isn't very sensitive to  $SW_{x,TaV,TaI,Ta2,Hz}^h$  anyway, except for overall normalization. For detector rows 185-215, the algorithm changes to one similar to that used at longer wavelengths.

For multispectral images with SCLK<85032700, detector rows 185-216 (roughly,  $\lambda < 563$  nm), the scattered light subtraction formula is

$$RT14^h_{x,\lambda,TaV,TaI,Ta2,Hz,r} = RT14^h_{x,\lambda,TaV,TaI,Ta2,Hz,r} - \{ <RT14^h_{xa...xb,\lambda,TaV,TaI,Ta2,Hz,r}> \cdot CS_{x,TaV,TaI,Ta2,Hz}^h \}$$

where

$$CS_{x,TaV,TaI,Ta2,Hz}^h = SW_{x,TaV,TaI,Ta2,Hz}^h \cdot ( CB_{x,\lambda_1,TaV,TaI,Ta2,Hz,r}^h / CB_{x,\lambda_0,TaV,TaI,Ta2,Hz,r}^h ) \\ \cdot ( <RT14^h_{xc...xd,\lambda_0,TaV,TaI,Ta2,Hz,r}> / <RT14^h_{xc...xd,\lambda_1,TaV,TaI,Ta2,Hz,r}> )$$

This is the same as used at longer wavelengths, except CS is no longer a function of wavelength  $\lambda$ , because CB and RT14 are evaluated at wavelength band  $\lambda_1$  instead of  $\lambda$ . Wavelength band  $\lambda_1$  is defined as the shortest wavelength (smallest detector row number) greater than or equal to detector row 216, the first detector row that uses the long wavelength scattered light subtraction formula. This is the wavelength where the short and long wavelength scattered light subtraction methods match most closely, so it's the best place to estimate the value of the short wavelength scattered light when we are missing detector row 187. Typically, detector row 221 (approx 599 nm) is the shortest multispectral wavelength matching this criterion. The brackets {} represent a 15-point downtrack moving mean for each column and wavelength, with the two highest and two lowest points discarded.

The fact that the above procedure works, with CS independent of wavelength at shorter wavelengths and a function of wavelength at longer wavelengths gives a window into why there are two different wavelength regions of scattered light behavior for the VNIR. The scattered light function is peaked and the source is much brighter at longer wavelengths. At short wavelengths, the spatial shape of the scattered light function is relatively independent of wavelength because the scattered light is mostly coming from the slowly varying tails of functions that are peaked at long wavelengths. At long wavelengths, the spatial shape of the scattered light function changes with wavelength because the scattered light is mostly coming from nearby wavelengths and one is close to the peak of the scattered light function. This tends to bring out changes in the spatial shape of scattered light due to scene nonuniformity and spectral smile.

If a pixel in one of the scattered light columns has the value 65535, is in the bad pixel mask, or is identified as one of the cosmic ray pixels, that pixel is not used. If all the scattered light columns in a given row are bad, the scattered light column value is filled in by linear interpolation of the nearest good rows.

## 2.12 Subtraction of second-order stray light

The CRISM IR channel has considerable second order light (source wavelength  $\lambda/2$ ) from the grating at  $\lambda=2760\text{-}3960$  nm. This stray light is sampled by detector pixels inside the focal plane at the source wavelengths for a given frame of  $(x,\lambda)$ , so it is subtracted just by defining a matrix containing the row number of the source of second order light for each detector row that contains scattered light, and another matrix defining the ratio of second order stray light signal to source signal. That ratio is measured using a monochromator in ground calibration. Interpolated values are used for columns not illuminated in that test. The second order light in a single pixel should come from at most two pixels near  $\lambda/2$ , but to be safe we define 6 row numbers which might all contribute to the stray light for a given pixel. We assume the second order light is translated directly along the columns of the detector, which is not exactly correct (there is some keystone which moves the second order light slightly from the source column) but should be good enough for stray light subtraction. The row number images  $y_{x,\lambda,n,Hz}$  with  $n=1\text{-}6$  give the detector row numbers of the 6 rows that are second order light sources for each detector pixel. The coefficient images  $\kappa_{x,\lambda,n,Hz}$  with  $n=1\text{-}6$  give the fraction of the direct signal from detector pixel  $(x,y_{x,\lambda,n,Hz})$  contributed to detector pixel  $(x,\lambda)$ . Then, the stray light is subtracted by the formula

$$RT14^i_{x,\lambda,TaI,Ta2,Hz,r} = RT14^i_{x,\lambda,TaI,Ta2,Hz,r} - \sum_{n=1}^{n=6} \kappa_{x,\lambda,n,Hz} \cdot RT14^i_{x,\lambda'=yn,Hz,TaI,Ta2,Hz,r}$$

for the IR. For the VNIR, this correction is not necessary, and the formula is just

$$RT14^i_{x,\lambda,TaV,Hz,r} = RT14^i_{x,\lambda,TaV,Hz,r}$$

The calculation of the  $y$  images is to uses only the closest wavelengths shorter and longer than at  $\lambda/2$ , calculated from the production WA CDRs. Detector rows 332-355 (wavelengths approximately 1744-1592 nm) are excluded as source rows because the zone 1/zone 2 order sorting filter boundary causes them to be inaccurately sampled. Note that for wavelengths in hyperspectral images outside this range (3184-3488 nm for the pixels being corrected), the wavelengths are densely sampled near  $\lambda/2$ . For the multispectral images and the hyperspectral images 3184-3488 nm, the wavelengths may be sparsely sampled near  $\lambda/2$ , and the correction will not be as accurate.

The  $\kappa$  values are derived from laboratory monochromator data on the second-order light contamination. The coefficient values are weighted to apply linear interpolation in wavelength between the detector rows with closest wavelength shorter and longer than  $\lambda/2$ , as given in the  $y$  images, to an effective value at  $\lambda/2$ .

These images are stored as level 4 calibration data records (CDRs) named

CDR4#0000000000\_LLrbeewsn\_v.IMG, where r=frame rate, b=binning, eee=exposure time parameter, w=wavelength filter, s=1 or 2 depending on whether side 1 or 2 lamps are used, n=detector, and v=version number. The LL CDRs have the 6 y images and the 6 κ images interleaved, starting with the n=1 y image, then the n=1 κ image, then the n=2 y image, etc.

If any pixels in the sum  $\sum_{n=1}^{n=4} \kappa_{x,\lambda,n,Hz} \cdot RT14^i_{x,\lambda'=yx\lambda,nHz,Ta1,Ta2,Hz,r}$  have the value 65535.0, they are treated as being zero for the purposes of this calculation.

## 2.13 Correction of instrument responsivity for detector temperature

Responsivity as a function of wavelength results from three effects:

- The instrument design including telescope design, efficiency of optical elements, and quantum efficiency of the detectors.
- Variations in detector responsivity as a function of detector temperature. The main effects are a shift in the long wavelength edge for the VNIR detector, and a movement in the interference fringes that appear on the long wavelength end of the IR detector.
- Accumulation of absorbing contaminants on optical surface. The major expected contaminant is water ice on the detector.

CRISM's responsivity is tracked in flight using the internal integrating sphere, run under closed loop control, using either bulb. This provides a field- and aperture-filling source with stable radiance. The current plan is to take sphere calibration measurements with one lamp within a few minutes of every scene measurement, and take calibration measurements with the other lamp once a month to check the first lamp. The sphere calibration may also be checked with images from Deimos when available. The calibration is not expected to be a function of integration time or frame rate, and all of the sphere calibration images are taken at 1 Hz.

The instrument responsivity is the ratio of the DN from the in-flight sphere data, corrected for bias, background, nonlinearity, stray light etc. in the same way as scene data, to the sphere radiance, measured on the ground and corrected to a value appropriate to the in-flight sphere data. The calculation of instrument responsivity at the time and temperatures of the in-flight sphere radiometric calibration is described in Section 3.5. The responsivity in DN/ms/(W/(m<sup>2</sup> micrometer sr)) is  $RSP^i_{x,\lambda,TcV,Tc1,Tc2}$ .

To apply that responsivity to a scene image to calculate radiance at the instrument aperture, we must first correct it for the instrument temperatures in effect during the scene measurement. The algorithm includes corrections for the detector temperatures  $T_{av}$  and  $T_{al}$ . It is possible the spectrometer temperature  $T_{a2}$  could also affect the responsivity by shifting the beamsplitter reflectivity and transmission in wavelength. In Section 3.4, this is discussed regarding the radiometric calibration itself, and we believe we will be taking radiometric calibration data close enough in time to the scene data that this effect will be the same in both. In other words,  $T_{a2}=T_{c2}$  to the accuracy required by the beamsplitter effect.

As of 12/30/2008, the responsivity correction for detector temperature is not applied either for VNIR or IR images. In both cases, the calibration software does the calculation, but the correction is zero.

The equation to correct the responsivity for detector temperature is

$$RSP^k_{x,\lambda,TaV,Ta2} = RSP^j_{x,\lambda,TcV,Tc2} \cdot (\mu_{x,\lambda} + v_{x,\lambda} \cdot TaV + \pi_{x,\lambda} \cdot TaV^2) / (\mu_{x,\lambda} + v_{x,\lambda} \cdot TcV + \pi_{x,\lambda} \cdot TcV^2)$$

for VNIR, where  $(\mu_{x,\lambda} + v_{x,\lambda} \cdot TaV + \pi_{x,\lambda} \cdot TaV^2)$  is a model of relative responsivity at each element  $x,\lambda$  as a function of detector temperature  $TaV$ . The quadratic functions are sufficiently accurate over the range of temperatures expected, about 2° C for the VNIR detector. If the temperature ranges are larger, they could be replaced with more descriptive functions, which would probably be  $(1+\tanh())$  for the VNIR.

The coefficient matrices  $\mu_{x,\lambda}$ ,  $v_{x,\lambda}$ , and  $\pi_{x,\lambda}$  are stored as a level 4 calibration data record (CDR) named CDR4#0000000000\_TDrbeewS\_v.IMG, where r=frame rate=0, b=binning=0, eee=exposure time parameter, w=wavelength filter, s=0, S=VNIR detector, and v=version number. Note that as of 12/30/2008,  $\mu_{x,\lambda}=1$ ,  $v_{x,\lambda}=0$ , and  $\pi_{x,\lambda}=0$  in the TD CDR, so no correction is applied.

For IR, instead of explicitly temperature correcting a single responsivity measurement, we calculate the responsivity twice using two flight sphere calibration measurements, one dayside and one nightside. We then linearly interpolate in IR detector temperature between those two responsivity images to get the temperature-corrected IR responsivity. For IR

$$RSP^k_{x,\lambda,TaI,Ta2} = (RSP^j_{x,\lambda,TcI,Tc2} \cdot (TaI - TfI) + RSP^j_{x,\lambda,TfI,Tf2} \cdot (TcI - TaI)) / (TcI - TfI)$$

where  $T_{cI}$  and  $T_{fI}$  are the IR detector temperatures for the dayside and nightside sphere calibrations respectively. IR detector temperature 2 is the sensor specified in the software. As of 12/30/2008, the “dayside” and “nightside” sphere calibration measurements specified in the calibration pipeline are always the same sphere image, generally the one closest in time to the scene image, so the detector temperature interpolation is not applied.

As of 12/30/2008, the responsivity correction for detector temperature is not applied for either VNIR or IR images. In both cases, the calibration software does the calculation, but the correction is zero. For the VNIR, the relevant values in the TD CDR were zero. It was determined that the correction was small and the values obtained from ground calibration not highly accurate, so we decided not to apply the correction. For IR, two sphere calibrations are specified in the software, but the tables generated always use just the single sphere calibration closest in time twice, so the interpolation with detector temperature does not get applied. It is possible the use of two sphere calibrations as described below might reduce Fabry-Perot fringing at long wavelengths of the detector, but we were concerned about introducing additional noise by using the second sphere calibration.

## 2.14 Apply binning and detector masks to responsivity

This step is trivial, because we do not expect binning to affect the responsivity. For pixels defined as “scene” pixels in the detector mask CDR, the responsivity of a binned pixel is just the mean of the responsivity of the detector elements in that bin.

Pixels not defined as “scene” pixels in the detector mask CDR have their values replaced by 65535 at this point. This includes dark and scattered light pixels. The number of columns in the responsivity image after this step is 640/binning, where binning is 1, 2, 5, or 10. At this point, we also apply the wavelength table to the responsivity, by simply selecting out the responsivity values at each wavelength present in the table and throwing away the rest. The number of rows in the responsivity image after this step is just the number of active rows in the wavelength table.

The binned responsivity is called  $RSP^l_{x,\lambda,TaV,TaI,Ta2,Hz}$ .

The detector masks are given in level 4 calibration data records (CDRs) named CDR4#0000000000\_DMrbbeewsn\_v.IMG, where r=frame rate, b=binning, eee=0, w=wavelength filter, s=0, n=detector, and v=version number. Each detector mask consists of an image of 8-bit integers, with the individual bits set equal to 1 for different masks. Bits 0,1,2,3,4,5,6,7 represent no data, scene, dark, dark/scatter transition, scattered light, scatter/scene transition, scene/dark transition, and row 0 respectively. For example, when bit 1 is 1, the pixel is a scene pixel, and when bit 1 is 0, the pixel is not a scene pixel.

The wavelength tables are implicit in the detector masks, because scene pixels in rows that are used have bit 1 set equal to 1 while all pixels in rows that are not used have bit 0 set equal to 1. However, the wavelength tables are also given in the level 6 CDR named CDR6\_0000000000\_WV\_n\_v.TAB, where n=sensor ID and v=version number. In these tables, a 1 indicates the row is used, and a 0 indicates the row is not used.

## 2.15 Calculate scene radiance at instrument aperture and divide by flat field

Again this is trivial now that we have gone through all the correction steps. The spectral radiance  $RD^m_{x,\lambda,r}$  is just the count rate divided by the instrument responsivity and the flat field  $FF_{x,\lambda}$ . The flat field is just the image of an external flat field with the scene pixels in each row normalized to average to 1.

$$RD^m_{x,\lambda,r} = RT^j_{x,\lambda,TaV,TaI,Ta2,Hz,r} / ( FF_{x,\lambda,Hz} \cdot RSP^l_{x,\lambda,TaV,TaI,Ta2,Hz} )$$

$$FF_{x,\lambda,Hz} = FL_{x,\lambda,Hz} + EP_{x,\lambda,Hz} \cdot \log( RT^j_{x,\lambda,TaV,TaI,Ta2,Hz,r} / RSP^l_{x,\lambda,TaV,TaI,Ta2,Hz} )$$

The units of  $RD^m_{x,\lambda,r}$  are W/(m<sup>2</sup> micrometer sr). As of 1/28/2009,  $EP_{x,\lambda,Hz}$  is zero, so it is a straight flat field with no allowance for pixel-dependent nonlinearity.

The flat field  $FL_{x,\lambda,Hz}$  is given in layer 0 of the flight level 4 calibration data records (CDRs) named CDR4#ttttttt\_NUrbeeewsd\_v.IMG, where #=spacecraft time SCLK partition at the

beginning of validity of the CDR, tttttttt=spacecraft time SCLK at the beginning of validity of the CDR, r=frame rate, b=binning, eee=exposure time parameter, w=wavelength filter, s=sphere lamp used to calibrate the flat field scenes (see section 3.3), d=detector, and v=version number. Unlike the rest of the flight CDR4s, which are generated automatically by the pipeline software, the NU CDR is generated periodically by the science team, based on averages of images of a featureless area of Mars. The IR flat fields are set equal to 1 in some bands, where the interaction of sharp atmospheric features with instrument smile makes the flat-fielding unreliable. The generation of the NU CDRs is described in section 3.3.

The pixel-dependent nonlinearity parameter  $EP_{x,\lambda,HZ}$  is given in layer 1 of the NU CDRs. This allows one to apply a different linearizing function for different pixels, using the same form of the nonlinearity as applied to the entire detector using average values of the nonlinearity parameters in Section **Error! Reference source not found.**. Instead of pixel-dependent nonlinearity, one could equally well call this a brightness-dependent flat field. The function  $\log()$  is the natural or base-e logarithm.

As of 1/28/2009,  $EP_{x,\lambda,HZ}$  is always zero in all the NU CDRs, so the pixel-dependent nonlinearity correction is not applied.

## 2.16 Calculate scene radiance at instrument aperture and divide by flat field

VNIR images generally have no bad pixels except for a single dead detector pixel in the full-resolution, hyperspectral mode.

IR image cubes, on the other hand, have many noisy pixels. Some detector pixels are always noisy, some are noisy for a time encompassing several image cubes, and some are noisy for a time period within an image cube. It's useful to assign bad detector pixels from the bias images (generally taken within a week of the scene) to filter out pixels that are saturated or always noisy, and bad pixels from the dark images (taken within 5 minutes of a scene) to filter out pixels that are noisy for several minutes. However, pixels that become noisy after the first dark calibration image is taken and before the start of the second dark calibration image aren't captured by this "a priori" bad pixel mask. Also, the "a priori" mask throws out the brightest two and dimmest two values when it calculates standard deviations on nominally identical images. A pixel has to be \*really\* noisy to be included in the "a priori" mask.

The result is that the IR image cubes still have many noisy pixels even after the "a priori" bad pixel mask is applied. The images benefit greatly from identification of bad pixels using the processed image itself, and interpolation over those bad pixels. This is an "ex post facto" bad pixel removal, because it uses only the scene image cube itself to identify bad pixels, which are then interpolated over in the scene image cube. The "a priori" bad pixel algorithm used only calibration images to identify bad pixels, which are then interpolated over in the scene image cube.

The ex post facto bad pixel map is calculated entirely from a single frame equal to the mean of all the lines in the image cube. A frame has spatial columns as the x coordinate and wavelength bands as the y coordinate. For this purpose, the content of the image cube in the spacecraft

downtrack direction is averaged out. Now, construct a “filtered mean frame” by filtering each wavelength band of that frame with a moving 7-element median in the spatial (i.e. crosstrack or column) direction. The 7-element median is used for full resolution images. For half-resolution images, we use a 5-element median. We use a 3-element median for 5x and 10x binned images. Now, define the “difference frame” as the difference of the mean frame and the filtered mean frame. For each wavelength band of the difference frame, calculate the standard deviation over the entire crosstrack scene. If the absolute value of a pixel of the difference frame is greater than 2.4 times the standard deviation for that pixel’s band, then that pixel is “ex post facto” bad. Bad pixels are replaced by linear interpolation from nearest neighbor columns just like for the “a priori” bad pixel map, unless they have the value 65535. The BP CDR for the scene includes all the “a priori” bad pixels and all the “ex post facto” bad pixels. See section **Error! Reference source not found..**

The bad pixels have now been replaced by interpolation. There is an additional step which replaces all bad pixels specified in the BP CDR with the average of the two pixels to either side in the cross-track direction (same line, same band), or just the value of the pixel on one side if the other side has the value 65535. If both the neighboring pixels are 65535, then it averages the closest 6 non-65535 pixels that are in the same image line and same band, and replaces the existing value of the pixel with that value. If all 6 are 65535 or the pixel is not bad, then the pixel value is not changed. Unlike the interpolation above and in section 2.6, and every other step of the calibration, this step does replace pixels that have been marked with the value 65535.

In addition, pixels from the edge of the detector (“non-scene” pixels) do not correctly represent the scene and are replaced with the value 65535 in this last step. The function  $M_{x,\lambda,HZ}()$  applies the IR ex post facto bad pixel correction described above, and also replaces the non-scene pixels with 65535.

$$RD^n_{x,\lambda,r} = M_{x,\lambda,HZ}( RD^m_{x,\lambda,r} )$$

The detector masks are given in level 4 calibration data records (CDRs) named CDR4#0000000000\_DM**r**beeewsn\_v.IMG, where r=frame rate, b=binning, eee=0, w=wavelength filter, s=0, n=detector, and v=version number. Each detector mask consists of an image of 8-bit integers, with the individual bits set equal to 1 for different masks. Bits 0,1,2,3,4,5,6,7 represent no data, scene, dark, dark/scatter transition, scattered light, scatter/scene transition, scene/dark transition, and row 0 respectively. For example, when bit 1 is 1, the pixel is a scene pixel, and when bit 1 is 0, the pixel is not a scene pixel.

The radiance  $RD^n_{x,\lambda,r}$  for each scene image is saved in a targeted radiance data record (TRDR) named CCC#####\_XX\_SCmmmn\_TRRv.TAB, where CCC describes the observation (target mode, multispectral survey or multispectral windows mode, etc.), ##### is the observation ID in hex, XX is the counter within the observation, mmm is the macro ID, n is the detector number 1 or 2, and v is the software version number.

TRDRs are saved in both target mode and mapping mode. The use of the word “targeted” in TRDR has nothing to do with target mode versus mapping mode. Rather, “targeted” in this application is synonymous with “scene”.

In addition to the scene radiance for every image, the TRDR also contains a smaller cube with summary products. The summary products are designed to isolate surface and atmospheric spectral features of scientific interest. Typically, they are formulae based on ratios of radiances in defined wavelength channels, but sometimes they are just the radiance of a given channel. Generally, the atmospheric summary products are calculated directly from the radiance  $RD_{x,\lambda,r}^n$ , while the surface summary products are calculated from radiances with further atmospheric corrections applied. The summary parameters are beyond the scope of this report, which deals only with generating calibrated radiance images.

The science team will monitor the TRDR files for saturated pixels and adjust the choice of integration time or bad pixel algorithm as necessary. As of 12/30/2008, no adjustments have been necessary.

## **2.17 Measurement uncertainties due to nonrepeatability**

Four sources of nonrepeatability contribute to uncertainty in  $RD_{x,\lambda,r}^n$ .

**(1)** Shot noise, from photon-counting statistics in the signal, is given as

$$\text{sqrt}( \text{DN14}_{x,\lambda,\text{TaI,Ta2,TaV,Hz,t,r}}^g \cdot \text{gain} ) / \text{gain}$$

where gain is approximately  $80\text{e}^-/\text{DN}$  for each detector.

**(2)** Dark noise, which contains both read noise, shot noise due to dark current and thermal background, and effects of any systematic detector noise. This is calculated with each set of dark data

$$\text{Noise}_{x,\lambda,\text{Hz}} = \sigma( \text{DND14}_{m=0 \dots m_{\text{tot}},x,\lambda,\text{TdI,Td2,Hz,t,r}} )$$

The  $\text{Noise}_{x,\lambda,\text{Hz}}$  read noise images are stored as a level 4 calibration data record (CDR) named CDR4#0000000000\_UBrbeewsn\_v.IMG, where r=frame rate=0, b=binning=0, eee=exposure time parameter, w=wavelength filter, n=detector, and v=version number. A time ordered list of these files is also maintained as a level 6 CDR, named CDR6\_#\_0000000000\_UD\_n\_v.TAB, where n=sensor ID and v=version number.

**(3)** Variations in throughput of the optics due to differences in the exact position of the shutter and what fraction of the beam of light it occludes. This would be the variations in sphere radiance after the shutter mirror correction has been made as described in section 3.4

**(4)** Variations in the sphere radiance each time the sphere is measured, as a function of any inaccuracy in the closed loop control system. Again, this is after the corrections for sphere temperature and shutter mirror position described in section 3.4 are made.

Note that all of the errors in the list above are either random errors or some other form of

nonrepeatability. Currently, the uncertainty tables do not include any allowance for systematic error such as errors in the calibration of the reference source used on the ground or aging of the sphere lamps over the course of the mission.

Another error term that would be important for zone 3 of the IR spectrometer is error due to subtraction of the 2<sup>nd</sup> order stray light. This would include a random term due to noise in the scene data at the source wavelength, and a systematic term accounting for errors in the ground measurement of the stray light matrix.

## 2.18 Processing from radiance to I/F

The I/F is the ratio of the radiance observed from a surface to that of a perfect white Lambertian surface illuminated by the same light but at normal incidence. The formula is

$$IF_{x,\lambda} = \pi \cdot RD_{x,\lambda,r}^n / ( SF_{x,\lambda} / r^2 )$$

The solar flux  $SF_{x,\lambda}$  is solar spectral irradiance as seen by a normally illuminated surface 1 AU from the Sun.  $SF_{x,\lambda}$  is evaluated at the wavelengths corresponding to the CRISM spectral calibration and convolved to the CRISM spectral profile functions. The variable  $r$  is the distance of Mars from the Sun in AU for that particular observation.

The array  $SF_{x,\lambda}$  is stored as a level 4 calibration data record (CDR) named CDR4#ttttttt\_SFrbeewsn\_v.IMG, where #=spacecraft time SCLK partition at the beginning of validity of the CDR, tttttttt=spacecraft time for start of applicability of the file, r=frame rate, b=binning, eee=exposure time parameter, w=wavelength filter, s=lamp=0, n=detector, and v=version number.

The I/F will have a dependence on incident (illumination) angle and emission (reflection) angle. Incidence and emission angles relative to a model of the Martian surface are given in a derived data record (DDR) file that is associated with each TRDR file. The name of the DDR file is CCC#####\_XX\_SCmmmn\_DDRv.TAB, where CCC describes the observation (target mode, multispectral survey or multispectral windows mode, etc.), ##### is the observation ID in hex, XX is the counter within the observation, mmm is the macro ID, n is the detector number 1 or 2, and v is the software version number. The variable r is the value of the keyword SOLAR\_DISTANCE in the label file CCC#####\_XX\_SCmmmn\_DDRv.LBL that accompanies each DDR file and describes its contents.

Interpretation of I/F. In optics, we often use BRDF, the ratio of the observed radiance from a surface area to the irradiance incident on that surface area. The quantity  $I/F = BRDF \cdot \pi \cdot \cos\theta$ , where  $\theta$  is the angle of incidence of the light from the Sun on the surface of Mars. The BRDF of a perfect Lambertian surface is a constant  $1/\pi$ , which gives the factor of  $\pi$  at  $\theta=0$ . The factor of  $\cos\theta$  comes from the fact that the solar flux is the energy per unit area per unit time incident on a normally illuminated surface, while the irradiance is the energy per unit area per unit time incident on the actual surface given the incidence angle of the light coming from the Sun. We prefer to leave in the dependence on  $\cos\theta$  rather than dividing it out because  $\theta$  depends on the

local topography of the surface, so the user may decide to use different values depending on the preferred model of the local topography. The factor of  $\pi$  makes I/F more intuitive in terms of energy absorbed and reflected. If the surface has some absorption but its reflections are diffuse with a Lambertian distribution, then the value of I/F for normal incidence light at a given wavelength is just the total reflectivity, the total light energy reflected at that wavelength divided by the total light energy incident at that wavelength.

### 3. ADDITIONAL MINI-PIPELINES FOR GENERATING CALIBRATION TABLES FROM FLIGHT CALIBRATION DATA

#### 3.1 Calculation of IR bias images

Bias is the DN level extrapolated to zero exposure time, in image form, taken at a particular frame rate. This represents an electronics bias added to the measured signal, to prevent near-zero DNs from going negative (and being clipped) due to superimposed noise. In detector-level testing it was found that bias has a nearly fixed pattern pixel to pixel, but that its magnitude varies weakly with temperature and strongly with frame rate.

In flight, bias for the IR detector is derived from a dedicated calibration, performed periodically, in which, at each frame rate, a burst of 12 images is taken with the shutter closed at each of several short exposure times. These data are taken at IR detector temperature  $T_{bI}$ . After making a correction for a step in the bias that is a function of integration time parameter, the DN values are fit linearly on a pixel-by-pixel basis and the exposure time=0 y-intercept image is used as the bias estimate.

Processing of the bias image cubes  $DNB_{n,x,\lambda,TbI,TbJ,Tb2,Hz,t}$  before bias  $Bias_{x,\lambda,TbI,TbJ,Hz}$  is calculated. See sections 2.2 and **Error! Reference source not found.** for details.

$DNB_{m,x,\lambda,TbI,TbJ,Tb2,Hz,t}$  is raw DN after fast lossless compression is undone. The subscript m runs from 0 to 11 and represents image number within a burst of identical images.

Lossy compression will never be used on bias measurements, so there is no 8-bit to 12-bit conversion.

$$\begin{aligned} DNB12_{m,x,\lambda,TbI,TbJ,Tb2,Hz,t} &= DNB_{m,x,\lambda,TbI,TbJ,Tb2,Hz,t} \\ DNB14_{m,x,\lambda,TbI,TbJ,Tb2,Hz,t} &= \text{Offset}_{\lambda} + \text{Gain}_{\lambda} \cdot DNB12_{m,x,\lambda,TbI,TbJ,Tb2,Hz,t} \\ DNB14^a_{x,\lambda,TbI,TbJ,Tb2,Hz,t} &= \text{mean}_{2,2}( DNB14_{m,x,\lambda,TbI,TbJ,Tb2,Hz,t} ) \end{aligned}$$

The function  $\text{mean}_{2,2}()$  is the per-pixel mean of the 12 bias frames with the two highest and two lowest values thrown out for each pixel. This removes cosmic rays and reduces noise.

At a single frame rate, each pixel of the set of bias images at different integration rates are fit to the following equation.

$$DNB14^a_{x,\lambda,TbI,TbJ,Tb2,Hz,t} = c0_{x,\lambda,TbI,TbJ,Hz} + c1_{x,\lambda,TbI,Tb2,Hz} \cdot t - a0_I \cdot Hv(\text{row}_{\lambda}+1-(502/480)) \cdot (480-$$

$\text{integ}(t))$

Note that  $c_0$  corresponds to the bias for that frame rate, and  $c_1 \cdot t$  corresponds to the background signal for that frame rate. The third term is a step function resulting from details of the readout of the image in the electronics. It is entirely predetermined. The constant  $a_0$  is determined from ground calibration data,  $Hv()$  is the Heaviside function, and  $\text{integ}(t)$  is the integration parameter. The value of  $t$  in ms is calculated from the integration time parameter  $\text{integ}$  using the formula  $t = 1000 \cdot (502 - \text{floor}((502/480) \cdot (480-\text{integ}))) / (502 \cdot \text{rate})$ , where  $\text{floor}()$  is a function that creates an integer from a real number by rounding down.

To calculate  $c_0$  and  $c_1$ , DNB is corrected for the third term and a linear fit is performed for each pixel. The fit is  $y=mx+b$ , where  $y = \text{DNB14}_{x,\lambda,T_{bI},T_{bJ},T_{b2},\text{Hz},t} + a_{0I} \cdot Hv(\text{row}_\lambda+1-(502/480) \cdot (480-\text{integ}(t)))$ ,  $m = c_1$ ,  $x = t$ , and  $b = c_0$ . Then,

$$\text{Bias}_{x,\lambda,T_{bI},T_{bJ},\text{Hz}} = B_{x,\lambda,\text{Hz}} (c_0_{x,\lambda,T_{bI},T_{bJ},\text{Hz}})$$

The function  $B()$  is the bad pixel removal algorithm (see section **Error! Reference source not found.**). Bias frames  $\text{Bias}_{x,\lambda,T_{bI},T_{bJ},\text{Hz}}$  are stored as level 4 calibration data records (CDRs) named  $\text{CDR4}\#tttttttt\_BIrbeewsl_v.IMG$ , where # = spacecraft time SCLK partition at the beginning of validity of the CDR, tttttttt = spacecraft time SCLK at the beginning of validity of the CDR, r = frame rate, b = binning, eee = exposure time parameter, w = wavelength filter, s = 0, L = detector (IR), and v = version number. The tttttttt = spacecraft time SCLK at the beginning of validity of the CDR tells the software which bias measurement to use for a given scene measurement. The calibration software uses the CDR4 file with the largest value of tttttttt that is smaller than the value of SCLK for the scene measurement.

The constants  $a_{0I}$  for IR and  $a_{0V}$  for VNIR are calculated from ground calibration data and given in the level 6 CDR named  $\text{CDR6\_}\#0000000000\_BS_n_v.TAB$ , where # = spacecraft time SCLK partition at the beginning time of validity of the CDR, 0000000000 = spacecraft time SCLK at the beginning time of validity of the CDR, n = detector, and v = version number.

### 3.2 Mini-pipeline for IR background and VNIR bias images (darks)

Shutter-closed image cubes (darks) are taken with every scene and calibration measurement to subtract instrumental background. They are taken at the same set of frame rates, integration times, wavelength tables, and binning as the associated scene or calibration measurement. For the VNIR, there is no dark current or IR thermal background and this represents just detector bias, the DN level at zero integration time. For the IR, the bias is subtracted separately so that the nonlinearity correction may be applied before the dark current and IR thermal background subtraction. The shutter-closed images are then used in the IR background subtraction step.

Pipeline for VNIR darks:

$DND_{m,x,\lambda,T_{dV},\text{Hz},t}$  is raw DN after fast lossless compression is undone. The subscript m represents line number within a burst of identical frames. The subscript d on the temperatures indicates

temperatures for the dark image taken before the scene image. The pipeline is exactly the same for the dark image taken after the scene image, which is given the subscript e in the main pipeline.

Lossy compression will never be used on dark measurements, so there is no 8-bit to 12-bit conversion.

$$\begin{aligned} \text{DND12}_{m,x,\lambda,TdV,TdW,Hz,t} &= \text{DND}_{m,x,\lambda,TdV,TdW,Hz,t} \\ \text{DND14}_{m,x,\lambda,TdV,TdW,Hz,t} &= \text{Offset}_\lambda + \text{Gain}_\lambda \cdot \text{DND12}_{m,x,\lambda,TdV,TdW,Hz,t} \\ \text{Bias}_{x,\lambda,TdV,TdW,Hz,t} &= \text{mean}_{2,2}(\text{B}_{x,\lambda,Hz}(\text{DND14}_{m,x,\lambda,TdV,TdW,Hz,t})) \end{aligned}$$

VNIR bias frames will be have to be binned in ground processing for use with scene images that are EPFs and have 10x binning at 3.75 Hz.

The function B() is the bad pixel removal algorithm (see section **Error! Reference source not found.**), and DND14 is the 14-bit DN for the dark images. The frames within the burst are averaged, throwing out the two as part of the cosmic ray removal algorithm, so the subscript m disappears at that point. The dark image taken before has VNIR detector temperature  $T_{dv}$ , and the dark image taken after has VNIR detector temperature  $T_{ev}$ .

The VNIR bias images  $\text{Bias}_{x,\lambda,TdV,TdW,Hz,t}$  are stored as level 4 calibration data records (CDRs) named CDR4#tttttttt\_BIrbeeewS\_v.IMG, where # = spacecraft time SCLK partition at the beginning of validity of the CDR, tttttttt = spacecraft time SCLK at the beginning of validity of the CDR, r = frame rate, b = binning, eee = exposure time parameter, w = wavelength filter, s = 0, S = detector (VNIR), and v = version number. The calibration software uses the CDR4 file with the largest value of tttttttt that is smaller than the value of SCLK for the scene measurement.

Pipeline for IR darks:

$\text{DND}_{m,x,\lambda,TdI,TdJ,Td2,Hz,t}$  is raw DN after fast lossless compression is undone. The subscript m represents frame number within a burst of identical frames. The subscript d on the temperatures indicates temperatures for the dark image taken before the scene image. The pipeline is exactly the same for the dark image taken after the scene image, which is given the subscript e in the main pipeline.

Lossy compression will never be used on dark measurements, so there is no 8-bit to 12-bit conversion.

$$\begin{aligned} \text{DND12}_{m,x,\lambda,TdI,TdJ,Td2,Hz,t} &= \text{DND}_{m,x,\lambda,TdI,TdJ,Td2,Hz,t} \\ \text{DND14}_{m,x,\lambda,TdI,TdJ,Td2,Hz,t} &= \text{Offset}_\lambda + \text{Gain}_\lambda \cdot \text{DND12}_{m,x,\lambda,TdI,TdJ,Td2,Hz,t} \\ \text{DND14}^a_{m,x,\lambda,TdI,Td2,Hz,t} &= \text{DND14}_{m,x,\lambda,TdI,TdJ,Td2,Hz,t} - \text{Bias}_{x,\lambda,TbI,TbJ,Hz} \\ &\quad + a0_I \cdot Hv(\text{row}_\lambda + 1 - (502/480) \cdot (480 - \text{integ}(t))) - \beta_{I,HZ} \cdot (T_{dI} - T_{bI}) - \beta_{J,HZ} \cdot (T_{dJ} - T_{bJ}) \\ \text{DND14}^b_{m,x,\lambda,TdI,Td2,Hz,t} &= \text{DND14}^a_{m,x,\lambda,TdI,Td2,Hz,t} - \sum_{n=0}^{n=3} G_I(\text{DND14}^a_{m,x,0+n\delta,\lambda,TdI,Td2,Hz,t}) \\ \text{DND14}^c_{m,x,\lambda,TdI,Td2,Hz,t} &= \\ &S(\text{DND14}^{bb}_{m,x,\lambda,TdI,Td2,Hz,t}, \text{DND14}^a_{m,x,\lambda,TdI,Td2,Hz,t}, \text{DND}_{m,x,\lambda,TdI,TdJ,Td2,Hz,t}) \end{aligned}$$

$$\begin{aligned} \text{DND14}^d_{m,x,\lambda,TdI,Td2,Hz,t} &= B_{x,\lambda,Hz}(\text{DND14}^c_{m,x,\lambda,TdI,Td2,Hz,t}) \\ \text{DND14}^e_{x,\lambda,TdI,Td2,Hz,t} &= \text{mean}_{2,2}(\text{DND14}^d_{m,x,\lambda,TdI,Td2,Hz,t}) \\ \text{DND14}^g_{x,\lambda,TdI,Td2,Hz,t} &= \text{DND14}^e_{x,\lambda,TdI,Td2,Hz,t} / (\epsilon_{Hz} \cdot \log(\text{DND14}^e_{x,\lambda,TdI,Td2,Hz,t}) + \phi_{Hz}) \\ \text{RTD14}^g_{x,\lambda,TdI,Td2,Hz,t} &= \text{DND14}^g_{x,\lambda,TdI,Td2,Hz,t} / t \end{aligned}$$

IR darks will have to be binned in ground processing for use with scene images that are EPFs and have 10x binning at a given frame rate 3.75 Hz.

The steps above follow the steps of correcting the scene images up to the point of the IR background subtraction. Those steps are described in sections **2.2-Error! Reference source not found..**

Background images  $\text{RTD14}^g_{x,\lambda,TdI,Td2,Hz,t}$  are stored in units of counts/millisecond as level 4 calibration data records (CDRs) named  $\text{CDR4}\#tttttttt\_BKrbbeewsl\_v.\text{IMG}$ , where # = spacecraft time SCLK partition at the beginning of validity of the CDR, tttttttt = spacecraft time SCLK at the beginning of validity of the CDR, r = frame rate, b = binning, eee = exposure time parameter, w = wavelength filter, s = 0, L = detector (IR), and v = version number. The integration time t, used to calculate  $\text{RTD14}^g_{x,\lambda,TdI,Td2,Hz,t}$  from  $\text{DND14}^g_{x,\lambda,TdI,Td2,Hz,t}$ , may be calculated from the integration time parameter in the label file  $\text{CDR4}\#tttttttt\_BKrbbeewsl\_v.\text{LBL}$  that goes with the .IMG file containing the  $\text{DND14}^g_{x,\lambda,TdI,Td2,Hz,t}$  images.

The IR background rate  $\text{RTD14}^g_{x,\lambda,TdI,Td2,Hz,t}$  is an input to section **Error! Reference source not found.** of the main pipeline, where the dark images are interpolated to the time of the scene or calibration measurement.

### 3.3 Generation of the flat fields

The flat field  $\text{FF}_{x,\lambda,Hz}$  is just an average of many images of a featureless region of Mars, with the scene pixels in each row normalized so they average to 1. The EDRs are sent through the entire calibration pipeline to make radiance images, and then averaged. A slight correction has to be made to the averaged images to account for the fact that the featureless scene spectral radiance varies with wavelength and the spectrometer has smile. Then, each row is normalized so that the scene pixels in that row average to 1.

Some of the IR flat field bands are set equal to 1. These are wavelengths near sharp atmospheric features, where the interaction between sharp spectral feature and instrument smile makes the flat field inaccurate.

The flat field  $\text{FF}_{x,\lambda,Hz}$  is given in layer 0 of the flight level 4 calibration data records (CDRs) named  $\text{CDR4}\#tttttttt\_NUrbeewsd\_v.\text{IMG}$ , where # = spacecraft time SCLK partition at the beginning of validity of the CDR, tttttttt = spacecraft time SCLK at the beginning of validity of the CDR, r = frame rate, b = binning, eee = exposure time parameter, w = wavelength filter, s = 0, d = detector, and v = version number. Unlike the rest of the flight CDR4s, which are generated automatically by the pipeline software, the NU CDR is generated by hand. It is based on the median of several hundred images of a featureless area of Mars.

### **3.4 Calculating sphere radiance including sphere temperature and shutter mirror position**

The sphere radiance was measured in ground calibration with respect to known external sources. The most useful ones were a Spectralon plate illuminated by a NIST standard lamp and a cavity radiation source imaged through a collimator. The sphere radiance measured on the ground is then corrected to a value appropriate for a given calibration source measurement in flight. There are two corrections currently planned:

1. A correction for the temperature of the integrating sphere in flight. The current in the sphere is controlled by a silicon photodiode through a closed loop. The long-wavelength edge of the sensitivity of that photodiode is temperature-dependent, which causes the lamp current and sphere output to be temperature-dependent. From the ground calibration data, we have images taken at different sphere temperatures and we can estimate this effect. This also corrects for variations in the thermal emission of the sphere, which may have a small effect at long wavelengths. In addition, the temperature of the beamsplitter tracks the temperature of the optical bench to some extent, and the temperature of the optical bench tracks the temperature of the integrating sphere. As an unintended side effect, the correction of the sphere radiance for the integrating sphere temperature will also give a partial correction for any dependence of the instrument response on the beamsplitter temperature.
2. A correction for the exact angle of the shutter mirror for the sphere measurement in flight. The shadow of the mask at the boundary of the VNIR order-sorting filter is compared between the flight measurement and the ground measurement, and a correction is made to the ground radiance to give the radiance expected for that flight measurement. This correction changes every time the shutter mirror is moved.

It is possible that other effects such as the temperature of the focal plane board controlling the sphere lamp have an effect on sphere radiance, but as of this writing (10/19/2005) we have not yet investigated the repeatability of the sphere images with changes in the temperature of the focal plane boards.

First, the calculation of sphere radiance at the temperature of the flight sphere images.

The ground measured sphere radiance as a function of temperature is found in level 4 calibration data record CDR4#tttttttt\_SSrbeewsn\_v.IMG, where #=spacecraft time SCLK partition at the beginning of validity of the CDR, tttttttt=spacecraft time, r=frame rate=0, b=binning, eee=exposure time parameter, w=wavelength filter, s=1 or 2 depending on whether side 1 (IRFPE-controlled, cross-slit) or 2 (VNIRFPE-controlled, along-slit) lamp is used, n=detector, and v=version number. It consists of 3 images that are polynomial coefficients for the sphere radiance at each pixel as a function of temperature in degrees C. The sphere radiance is

$$\theta_{s,x,\lambda} + \sigma_{s,x,\lambda} \cdot T_{c3} + \tau_{s,x,\lambda} \cdot T_{c3}^2$$

The units of sphere radiance are W/(m<sup>2</sup> micrometer sr). Note: As of 12/30/2008, we are using values  $\theta=1$ ,  $\sigma=0$ , and  $\tau=0$ , so the correction is not explicitly applied.

Second, the correction of the sphere radiance for shutter mirror position nonrepeatability.

Rows 223-247 of the VNIR sphere images have DN levels sensitive to the shutter mirror position because they are on the edges of the VNIR filter zone boundary mask, and the shadow of the mask moves with the shutter mirror. The mirror parameter MP<sub>s</sub>, a single value for each set of calibration images taken without moving the shutter mirror, measures the microscopic difference between the shutter mirror angle for the flight radiance calibration and the ground radiance calibration. A different definition of MP<sub>s</sub> is used for s=1 (IRFPE controlled, cross-slit lamp) and s=2 (VNIRFPE-controlled, along-slit lamp).

$$MP_1 = \frac{\sum RTS14^j_{s=1,x=0\dots639,\lambda=232\dots234,Tc3} / RGSB^j_{s=1,Tc3} - \sum RTS14^j_{s=1,x=0\dots639,\lambda=223\dots225,Tc3} / RGSA^j_{s=1,Tc3}}{RGSA^j_{s=1,Tc3}}$$

$$MP_2 = \frac{\sum RTS14^j_{s=2,x=0\dots639,\lambda=235\dots237,Tc3} / RGSB^j_{s=2,Tc3} - \sum RTS14^j_{s=2,x=0\dots639,\lambda=245\dots247,Tc3} / RGSA^j_{s=2,Tc3}}{RGSA^j_{s=2,Tc3}}$$

with

$$RGSB^j_{s=1,Tc3} = \frac{\sum_{x=0\dots639,\lambda=232\dots234} RGS14^j_{s=1,x,\lambda,TgV,Tg3} \cdot (\theta_{s=1,x,\lambda} + \sigma_{s=1,x,\lambda} \cdot T_{c3} + \tau_{s=1,x,\lambda} \cdot T_{c3}^2)}{(\theta_{s=1,x,\lambda} + \sigma_{s=1,x,\lambda} \cdot T_{g3} + \tau_{s=1,x,\lambda} \cdot T_{g3}^2)}$$

$$RGSA^j_{s=1,Tc3} = \frac{\sum_{x=0\dots639,\lambda=223\dots225} RGS14^j_{s=1,x,\lambda,TgV,Tg3} \cdot (\theta_{s=1,x,\lambda} + \sigma_{s=1,x,\lambda} \cdot T_{c3} + \tau_{s=1,x,\lambda} \cdot T_{c3}^2)}{(\theta_{s=1,x,\lambda} + \sigma_{s=1,x,\lambda} \cdot T_{g3} + \tau_{s=1,x,\lambda} \cdot T_{g3}^2)}$$

$$RGSB^j_{s=2,Tc3} = \frac{\sum_{x=0\dots639,\lambda=235\dots237} RGS14^j_{s=2,x,\lambda,TgV,Tg3} \cdot (\theta_{s=2,x,\lambda} + \sigma_{s=2,x,\lambda} \cdot T_{c3} + \tau_{s=2,x,\lambda} \cdot T_{c3}^2)}{(\theta_{s=2,x,\lambda} + \sigma_{s=2,x,\lambda} \cdot T_{g3} + \tau_{s=2,x,\lambda} \cdot T_{g3}^2)}$$

$$RGSA^j_{s=2,Tc3} = \frac{\sum_{x=0\dots639,\lambda=245\dots247} RGS14^j_{s=2,x,\lambda,TgV,Tg3} \cdot (\theta_{s=2,x,\lambda} + \sigma_{s=2,x,\lambda} \cdot T_{c3} + \tau_{s=2,x,\lambda} \cdot T_{c3}^2)}{(\theta_{s=2,x,\lambda} + \sigma_{s=2,x,\lambda} \cdot T_{g3} + \tau_{s=2,x,\lambda} \cdot T_{g3}^2)}$$

RTS14 is count rate observed with the onboard sphere as a source, and RGSA, RGSB are the total count rates from sample rows in a given column of the ground data from which the sphere radiance CDR is derived, corrected from T<sub>g3</sub>, the integrating sphere temperature for the ground calibration, to T<sub>c3</sub>, the integrating sphere temperature for the flight calibration. Rows 223-247 of the VNIR have responsivity insensitive to detector temperature, so RTS14, RGSA, and RGSB are not functions of T<sub>cV</sub> or T<sub>gV</sub>. RTS14<sup>j</sup> and RGS14<sup>j</sup> have the full set of corrections for bias, detector ghosts, bad pixel and cosmic ray removal, detector nonlinearity, background subtraction, and stray light subtraction. A detailed description of these corrections is given in section 3.5, and also in the main data pipeline in sections 2.2 to **Error! Reference source not found..**

RGS14<sup>j</sup><sub>s,x, $\lambda$ ,TgV,Tg3</sub> is the count rate for the sphere radiance measurement made during the ground calibration. It is given in the level 4 calibration data record CDR4#tttttttt\_SHrbeewsn\_v.IMG described at the end of this chapter. The integration time t for the reference measurement may be calculated from the integration time parameter for the reference measurement, which is given in

the label file CDR4#ttttttttt\_SHrbeewsn\_v.LBL. The integrating sphere temperature  $T_{g3}$  for the ground measurement is also given in the label file CDR4#ttttttttt\_SHrbeewsn\_v.LBL.

The movement of the shutter mirror causes the signal to increase in one set of rows and decrease in the other. Subtracting the ratios in the two sets of rows makes the parameter  $MP_s$  insensitive to small changes in the brightness of the sphere lamps.  $MP_s$  is derived from just the VNIR image, but it is used to correct both VNIR and IR images.

The formula for sphere radiance  $SR_{s,x,\lambda,Tc3}$  including the shutter mirror nonrepeatability correction simply comes from the assumption that the correction is linearly dependent on the shutter movement parameter  $MP_s$ . This should be a good assumption if the correction is small, and in ground data it appears to be 5% or less so far.

$$SR_{s,x,\lambda,Tc3} = (\theta_{s,x,\lambda} + \sigma_{s,x,\lambda} \cdot T_{c3} + \tau_{s,x,\lambda} \cdot T_{c3}^2) / (1 + MP_s \cdot SC_{s,x,\lambda})$$

The shutter correction  $SC_{s,x,\lambda}$  image is derived by taking ratios of images, subtracting 1, and dividing by the value of  $MP_s$  for each image ratio. This may be done with ground or flight images, and the correction is proven valid by the fact that the correction image thus derived is pretty much the same for all image pairs for which the shutter mirror has moved enough that the correction is significant. In practice,  $SC_{s,x,\lambda}$  is an average of values calculated from multiple ground images. Note: the images ratioed to calculate  $SC_{s,x,\lambda}$  as part of the analysis of the ground calibration data not only have all the data pipeline corrections from sections 2.2 to **Error! Reference source not found.**, but also are corrected for the detector temperature as described in section **Error! Reference source not found.**, a later step. This is just a detail of how the relevant ground CDR4 is generated, and it does not affect the flight data pipeline.

$MP_s$  itself will depend on which sphere lamp is used, but the correction for shutter mirror position should be the same for either sphere lamp if the mirror is not moved between one sphere lamp measurement and the other.

The shutter correction image  $SC_{s,x,\lambda}$  is kept in layer 1 of the level 4 calibration data record CDR4#ttttttttt\_SHrbeewsn\_v.IMG, where #=spacecraft time SCLK partition at the beginning of validity of the CDR, tttttttt=spacecraft time, r=frame rate=0, b=binning=0, eee=exposure time parameter, w=wavelength filter=0, s=1 or 2 depending on whether side 1 (IRFPE-controlled, cross-slit) or 2 (VNIRFPE-controlled, along-slit) lamp is used, n=detector, and v=version number. The image  $RGS14^j_{s,x,\lambda,TgV,Tg3,t}$  is kept in layer 0 of the level 4 calibration data record CDR4#ttttttttt\_SHrbeewsn\_v.IMG, where #=spacecraft time SCLK partition at the beginning of validity of the CDR, tttttttt=spacecraft time, r=frame rate=0, b=binning=0, eee=exposure time parameter, w=wavelength filter=0, s=1 or 2 depending on whether side 1 (IRFPE-controlled, cross-slit) or 2 (VNIRFPE-controlled, along-slit) lamp is used, n=detector, and v=version number. The image  $RGS14^j_{s,x,\lambda,TgV,Tg3,t}$  is simply the count rate in DN/millisecond for the VNIR ground sphere radiance measurement, converted to 14-bits and with all corrections applied that are applied to the  $RT^j$  flight data except the division by integration time  $t$  is not applied. The count rate from the VNIR ground sphere radiance measurement is necessary in order to calculate the shutter movement parameter  $MP_s$  from the flight VNIR calibration image. That calculation also requires the sphere temperature  $T_{g3}$  for the ground sphere radiance

measurement.  $T_{g3}$  is listed in the label file CDR4#tttttttt\_SHrbeewsn\_v.LBL. The integration time parameter is listed in the label file CDR4#tttttttt\_SHrbeewsn\_v.LBL, and the integration time  $t$  may be calculated from the integration time parameter.

### 3.5 Calculation of instrument responsivity from sphere radiance

Responsivity as a function of wavelength results from three effects:

- The instrument design including telescope design, optical efficiency, and detector performance.
- Variations in detector responsivity as a function of detector temperature. The main effects are a shift in the long wavelength edge for the VNIR detector, and a movement in the interference fringes that appear on the long wavelength end of the IR detector.
- Accumulation of absorbing contaminants on optical surface. The major expected contaminant is water ice on the detector.

CRISM's responsivity is tracked in flight using the internal integrating sphere, run under closed loop control, using either bulb. This provides a field- and aperture-filling source with stable radiance. The current plan is to take sphere calibration measurements with one lamp within a few minutes of every scene measurement, and take calibration measurements with the other lamp once a month to check the first lamp. The sphere calibration may also be checked with images from Diemos when available.

The calculation of sphere radiance  $SR_{s,x,\lambda,Tc3}$  is described in Section 3.4, including the correction for shutter mirror position.

The pipeline processing for the onboard integrating sphere images before they are used to calculate the responsivity.

$DNS_{m,s,x,\lambda,TcV,TcI,Tc2,Tc3,t}$  is raw DN after fast lossless compression is undone. The subscript  $m$  represents image number within a burst of identical images. The subscript  $s$  represents choice of sphere lamp, 1 or 2. The subscript  $c$  on the temperatures indicates temperatures for the calibration images. Note the sphere radiance depends on the sphere temperature  $Tc3$ , so there's an implicit dependence of  $DNS$  on  $Tc3$  that is shown. Also, all sphere images are taken at 1 Hz with no binning and the largest wavelength tables, so the Hz subscript is omitted. The results are binned and the wavelength tables applied in section **Error! Reference source not found.** of the main pipeline.

Lossy compression will never be used on sphere measurements, so there is no 8-bit to 12-bit conversion.

$$DNS12_{m,s,x,\lambda,TcV,TcW,TcI,TcJ,Tc2,Tc3,t} = DNS_{m,s,x,\lambda,TcV,TcW,TcI,TcJ,Tc2,Tc3,t}$$

$$DNS14_{m,s,x,\lambda,TcV,TcW,TcI,TcJ,Tc2,Tc3,t} = Offset_{\lambda} + Gain_{\lambda} \cdot DNS12_{m,s,Lx,\lambda,TcV,TcW,TcI,TcJ,Tc2,Tc3,t}$$

$\text{DNS14}^{\text{a}}_{\text{m}, \text{s}, \lambda, \text{TcI}, \text{Tc2}, \text{Tc3}, \text{t}} = \text{DNS14}_{\text{m}, \text{s}, \lambda, \text{TcI}, \text{TcJ}, \text{Tc2}, \text{Tc3}, \text{t}} - \text{Bias}_{\text{x}, \lambda, \text{TbI}, \text{TbJ}, \text{Hz}=1}$   
 $+ a_{0\text{I}} \cdot \text{Hv}(\text{row}_\lambda + 1 - (502/480)) \cdot (480\text{-integ}(\text{t})) - \beta_{\text{I}, \text{Hz}=1} \cdot (\text{TcI} - \text{TbI}) - \beta_{\text{J}, \text{Hz}=1} \cdot (\text{TcJ} - \text{TbJ})$   
 $\text{DNS14}^{\text{a}}_{\text{m}, \text{s}, \lambda, \text{TcV}, \text{t}} = \text{DNS14}_{\text{m}, \text{s}, \lambda, \text{TcV}, \text{TeW}, \text{t}} - (\alpha_{\text{ec}} \cdot \text{Bias}_{\text{x}, \lambda, \text{TdV}, \text{TdW}, \text{t}} + \alpha_{\text{cd}} \cdot \text{Bias}_{\text{x}, \lambda, \text{TeV}, \text{TeW}, \text{t}}) / (\alpha_{\text{cd}} + \alpha_{\text{ec}})$   
 $- \beta_{\text{V}, \text{Hz}=1} \cdot [\alpha_{\text{ec}} \cdot (\text{TcV} - \text{TdV}) + \alpha_{\text{cd}} \cdot (\text{TeV} - \text{TcV})] / (\alpha_{\text{cd}} + \alpha_{\text{ec}})$   
 $- \beta_{\text{W}, \text{Hz}=1} \cdot [\alpha_{\text{ec}} \cdot (\text{TeW} - \text{TdW}) + \alpha_{\text{cd}} \cdot (\text{TeV} - \text{TeW})] / (\alpha_{\text{cd}} + \alpha_{\text{ec}})$   
 $\text{DNS14}^{\text{b}}_{\text{m}, \text{s}, \lambda, \text{TcV}, \text{t}} = \text{DNS14}^{\text{a}}_{\text{m}, \text{s}, \lambda, \text{TcV}, \text{t}} - \sum_{n=0}^{n=3} \text{Gv}(\text{DNS14}^{\text{a}}_{\text{m}, \text{s}, \lambda, \text{x0+n}\bullet\delta, \text{TcV}, \text{t}}) \text{ for VNIR and}$   
 $\text{DNS14}^{\text{b}}_{\text{m}, \text{s}, \lambda, \text{TcI}, \text{Tc2}, \text{Tc3}, \text{t}} = \text{DNS14}^{\text{a}}_{\text{m}, \text{s}, \lambda, \text{TcI}, \text{Tc2}, \text{Tc3}, \text{t}} - \sum_{n=0}^{n=3} \text{Gi}(\text{DNS14}^{\text{a}}_{\text{m}, \text{s}, \lambda, \text{x0+n}\bullet\delta, \text{TcI}, \text{Tc2}, \text{Tc3}, \text{t}}) \text{ for IR}$   
 $\text{DNS14}^{\text{bb}}_{\text{x}, \lambda, \text{TaV}, \text{Hz}, \text{t}, \text{r}} = \text{DNS14}^{\text{b}}_{\text{x}, \lambda, \text{TaV}, \text{Hz}, \text{t}, \text{r}} - \text{median}_{\text{x}, \lambda}(\text{DNS14}^{\text{b}}_{\text{x1...xn}, \lambda, \text{TaV}, \text{Hz}, \text{t}, \text{r}}) \text{ for VNIR}$   
and  
 $\text{DNS14}^{\text{c}}_{\text{m}, \text{x}, \lambda, \text{TcV}, \text{TcI}, \text{Tc2}, \text{Tc3}, \text{t}} =$   
 $S(\text{DNS14}^{\text{bb}}_{\text{m}, \text{x}, \lambda, \text{TcV}, \text{TcI}, \text{Tc2}, \text{Tc3}, \text{t}}, \text{DNS14}^{\text{a}}_{\text{m}, \text{x}, \lambda, \text{TcV}, \text{TcI}, \text{Tc2}, \text{Tc3}, \text{t}}, \text{DNS}_{\text{m}, \text{x}, \lambda, \text{TcV}, \text{TeW}, \text{TcI}, \text{TcJ}, \text{Tc2}, \text{Tc3}, \text{t}})$   
 $\text{DNS14}^{\text{d}}_{\text{m}, \text{s}, \lambda, \text{TcV}, \text{TcI}, \text{Tc2}, \text{Tc3}, \text{t}} = \text{B}_{\text{x}, \lambda, \text{Hz}}(\text{DNS14}^{\text{c}}_{\text{m}, \text{s}, \lambda, \text{TcV}, \text{TcI}, \text{Tc2}, \text{Tc3}, \text{t}})$   
 $\text{DNS14}^{\text{e}}_{\text{s}, \lambda, \text{TcV}, \text{TcI}, \text{Tc2}, \text{Tc3}, \text{t}} = \text{mean}_{2,2}(\text{DNS14}^{\text{d}}_{\text{m}, \text{s}, \lambda, \text{TcV}, \text{TcI}, \text{Tc2}, \text{Tc3}, \text{t}})$   
 $\text{DNS14}^{\text{g}}_{\text{s}, \lambda, \text{TcI}, \text{Tc2}, \text{Tc3}, \text{Taf}, \text{t}} = \text{DNS14}^{\text{e}}_{\text{s}, \lambda, \text{TcI}, \text{Tc2}, \text{Tc3}, \text{TcV}, \text{t}} / (\epsilon_{\text{Hz}} \cdot \log(\text{DNS14}^{\text{e}}_{\text{s}, \lambda, \text{TcI}, \text{Tc2}, \text{Tc3}, \text{TcV}, \text{t}}) + \phi_{\text{Hz}})$   
 $\text{RTS14}^{\text{g}}_{\text{s}, \lambda, \text{TcI}, \text{Tc2}, \text{Tc3}, \text{TeV}} = \text{DNS14}^{\text{g}}_{\text{s}, \lambda, \text{TcI}, \text{Tc2}, \text{Tc3}, \text{TeV}, \text{t}} / \text{t}$   
 $\text{RTS14}^{\text{h}}_{\text{s}, \lambda, \text{TcV}, \text{Tc3}} = \text{RTS14}^{\text{g}}_{\text{s}, \lambda, \text{TcV}, \text{Tc3}} \text{ for VNIR and}$   
 $\text{RTS14}^{\text{h}}_{\text{s}, \lambda, \text{TcI}, \text{Tc2}, \text{Tc3}} = \text{RTS14}^{\text{g}}_{\text{s}, \lambda, \text{TcI}, \text{Tc2}, \text{Tc3}, \text{ta1}} - \text{Bkgd}_{\text{x}, \lambda, \text{TdI}, \text{TeI}, \text{Td2}, \text{Te2}, \text{ta1}, \text{td1}, \text{te1}} \text{ for IR}$   
 $\text{RTS14}^{\text{i}}_{\text{x}, \lambda, \text{TaI}, \text{Ta2}, \text{Hz}, \text{t}, \text{r}} = \text{RTS14}^{\text{h}}_{\text{x}, \lambda, \text{TaI}, \text{Ta2}, \text{Hz}, \text{t}, \text{r}} - \text{median}_{\text{x}, \lambda}(\text{RTS14}^{\text{h}}_{\text{x1...xn}, \lambda, \text{TaI}, \text{Ta2}, \text{Hz}, \text{t}, \text{r}}) \text{ for IR}$   
 $\text{RTS14}^{\text{i}}_{\text{s}, \lambda, \text{TcV}, \text{TcI}, \text{Tc2}, \text{Tc3}, \text{Hz}} = \text{RTS14}^{\text{h}}_{\text{s}, \lambda, \text{TcV}, \text{TcI}, \text{Tc2}, \text{Tc3}} - <\text{RTS14}^{\text{h}}_{\text{x1...xn}, \lambda, \text{TaV}, \text{TaI}, \text{Ta2}, \text{Hz}}> \cdot$   
 $\text{SW}_{\text{x}, \text{TaV}, \text{TaI}, \text{Ta2}, \text{Hz}} \text{ for } \lambda < 563 \text{ nm}, - <\text{RTS14}^{\text{h}}_{\text{x1...xn}, \lambda, \text{TaV}, \text{TaI}, \text{Ta2}, \text{Hz}}> \cdot \text{CS}_{\text{x}, \lambda, \text{TaV}, \text{TaI}, \text{Ta2}, \text{Hz}} \text{ for } \lambda > 563 \text{ nm}$   
for VNIR and  
 $\text{RTS14}^{\text{j}}_{\text{s}, \lambda, \text{TcV}, \text{TcI}, \text{Tc2}, \text{Tc3}, \text{Hz}} = \text{RTS14}^{\text{i}}_{\text{s}, \lambda, \text{TcV}, \text{TcI}, \text{Tc2}, \text{Tc3}} - \sum_{n=1}^{n=6} \kappa_{\text{x}, \lambda, \text{n}, \text{Hz}} \cdot \text{RTS14}^{\text{i}}_{\text{x}, \lambda, \text{n}, \text{Hz}}$   
for IR.

The steps above follow the steps of correcting the scene images up to the point of the subtraction of second-order stray light. Those steps are described in sections 2.2 to **Error! Reference source not found..**

For VNIR detector rows 185-215, the sphere is too dim to be used to calibrate the images, and the SS CDR values in those rows are just instrument responsivity calculated from the laboratory calibration.

The sphere count rate images  $\text{RTS14}^{\text{j}}_{\text{s}, \lambda, \text{TcI}, \text{Tc2}, \text{Tc3}}$  are written to level 4 calibration data records (CDRs) named  $\text{CDR4}#\text{tttttttt\_SPrbeewsn_v.IMG}$ , where # = spacecraft time SCLK partition at the beginning of validity of the CDR, tttttttt = spacecraft time SCLK at the beginning of validity of the CDR, r = frame rate, b = binning, eee = exposure time parameter, w = wavelength filter, s = 0, n = detector, and v = version number.

The calculation of responsivity  $\text{RSP}^{\text{j}}_{\text{x}, \lambda, \text{TcI}, \text{Tc2}}$  is then very simple. It's just counts/radiance.

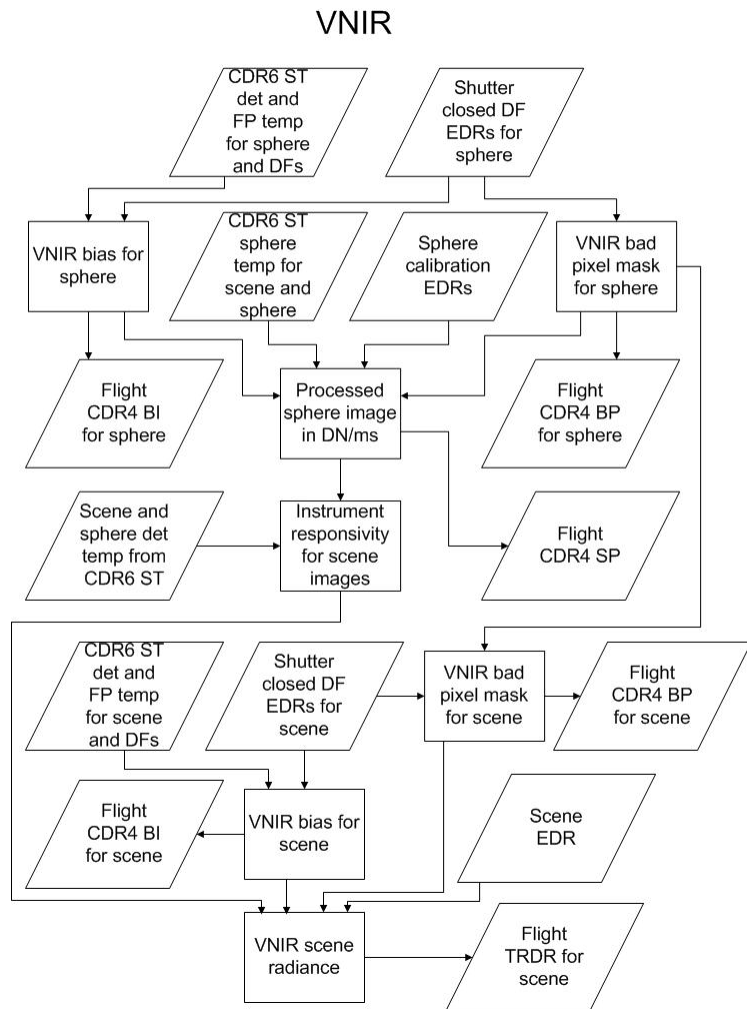
$$\text{RSP}^{\text{j}}_{\text{x}, \lambda, \text{TcI}, \text{Tc2}} = \text{RTS14}^{\text{j}}_{\text{s}, \lambda, \text{TcV}, \text{TcI}, \text{Tc2}, \text{Tc3}} / \text{SR}_{\text{s}, \lambda, \text{Tc3}}$$

The corrections to the responsivity for detector temperature are made in the main data pipeline in

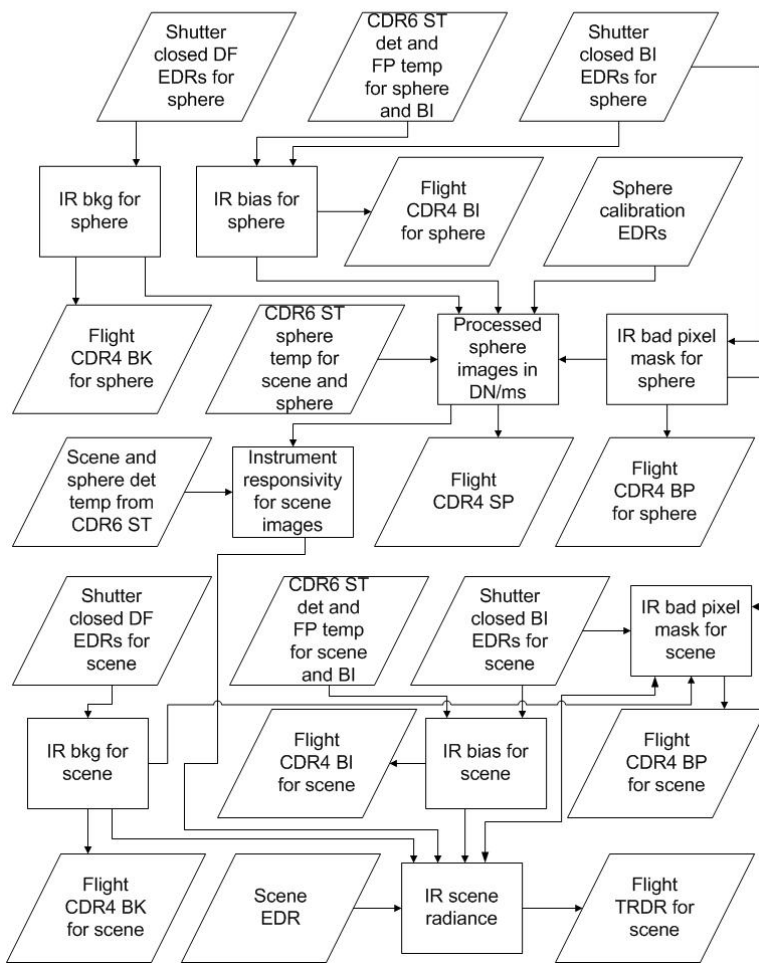
section **Error! Reference source not found.**. The responsivity is not saved as a calibration data record. It is calculated each time from the flight sphere images and the ground sphere radiance. Normally, the responsivity is calculated using data from the primary sphere lamp, which is s=2 (the VNIRFPE-controlled, cross-slit lamp) as of 10/28/2005. Measurements with the secondary lamp are taken during monthly engineering checkouts. The responsivity should be the same calculated with either lamp, and this is a useful in-flight check on the accuracy of the onboard calibration system. The units of responsivity are DN/ms/(W/(m<sup>2</sup> micrometer sr)).

## 4. IMPLEMENTATION IN PIPE

### 4.1 Data flow of flight calibration and scene EDRs to flight CDR4s and TRDRs



## IR



## **4.2 Logic for choosing specific flight calibration EDRs to use with a given scene EDR**

The ATF table is a special CDR used to list the calibration EDRs to be used to calibrate each scene EDR. It is located in the crism\_pds\_archive/edr/CDR/yyyy\_doy/ATF directory of the PDS archive. The first column of the ATF table lists every scene EDR with START\_TIME in that day. The remaining columns of each row list the calibration EDRs to use for the scene EDR given in the first column of that row. The ATF table consists only of EDRs that have actually been received. These are the ones used in calibration. There is a similar BTF table that gives the calibration EDRs that were planned for use with each scene EDR. The BTF table is generated for comparison with the ATF table, in case some of the calibration EDRs are not downlinked and the algorithm was forced to use a substitute.

### **VNIR**

There are 2 types of calibration EDRs to be searched for, the shutter-closed DFs (for VNIR these are for the bias calculation) and the sphere calibration SP EDRs. The SP EDRs have their own DFs for calculating the bias for sphere measurements.

Note that any downlinked EDRs with a “UN” macro descriptor in the filename should be rejected as calibration EDRs. This will filter out any problem EDRs caused when the instrument occasionally reverts back to default state 2 frames before the end of a mapping mode observation.

- I. Logic for determining desired calibration EDRs from predicted EDRs in initial observation tracking table for a given measurement (BTF table)
  - a. Shutter closed DF EDRs for bias for scene or sphere EDR
    - i. Select latest (in encoded SCLK) DF EDR that is earlier than the scene or sphere EDR and has the same frame rate, exposure, and binning as the scene or sphere EDR, and acceptable wavelength filter for the scene or sphere EDR
    - ii. Select earliest (in encoded SCLK) DF EDR that is later than the scene or sphere EDR and has the same frame rate, exposure, and binning as the scene or sphere EDR, and acceptable wavelength filter for the scene or sphere EDR
    - iii. Definition of “acceptable wavelength filter for the scene or sphere EDR”
      1. Filter 0 DF is acceptable for filters 0, 1, 2, and 3 SP or SC
      2. Filter 1 DF is acceptable for filter 1 SP or SC
      3. Filter 2 DF is acceptable for filters 1, 2, and 3 SP or SC
      4. Filter 3 DF is acceptable for filters 1 and 3 SP or SC
  - b. Sphere calibration SP SC EDR for radiometric calibration
    - i. Select closest (in encoded SCLK) SP EDR that has acceptable binning and wavelength filter to go with the scene EDR
    - ii. Select shutter closed DF EDRs to go with the SP EDR by following (a) above
    - iii. Definition of “acceptable binning to go with the scene EDR”

1. For 10x binning scene EDR, any binning is OK for the SP EDR
  2. For 5x binning scene EDR, 1x or 5x are OK for the SP EDR
  3. For 2x binning scene EDR, 1x or 2x are OK for the SP EDR
  4. For 1x binning scene EDR, 1x is OK for the SP EDR
- c. Shutter closed DF EDR for bad pixel mask
- i. Select closest (in encoded SCLK) DF EDR with 1x binning, 1Hz frame rate, integ time parameter 425, and hyperspectral wavelength filter
- II. Logic for determining calibration EDRs to use from the list of valid downlinked calibration EDRs (ATF table), and what to do if some of them are invalid
- a. Shutter closed DF EDRs for bias for scene or sphere EDR
    - i. Select latest (in encoded SCLK) existing valid DF EDR that is earlier than the scene or sphere EDR and has the same frame rate, exposure, and binning as the scene or sphere EDR, and acceptable wavelength filter for the scene or sphere EDR
    - ii. Select earliest (in encoded SCLK) existing valid DF EDR that is later than the scene or sphere EDR and has the same frame rate, exposure, and binning as the scene or sphere EDR, and acceptable wavelength filter for the scene or sphere EDR
    - iii. If unexpected DF EDRs are selected
      1. If the early DF EDR is more than 6 hours earlier than the scene EDR, do not select that EDR but instead select the late DF EDR twice
      2. If the late DF EDR is more than 6 hours later than the scene EDR, do not select that EDR but instead select the early DF EDR twice
      3. If both DF EDRs differ from the scene EDR by more than 6 hours, select the one that is closest in time to the scene EDR twice
      4. If either of the DF EDRs selected is different from that predicted in the early observation tracking table (note this part of the logic is implemented by the C++ program, while the rest is implemented in PIPE)
        - a. For scene measurements, set the flag in the data quality indicator in the TRDR but otherwise continue normally
        - b. For DF EDRs to be used with SP EDRs, declare that SP EDR invalid, do not generate an SP flight CDR4 from that SP EDR, and go back to PIPE to get another SP EDR
    - b. Sphere calibration SP EDR for radiometric calibration
      - i. For VNIR, detector temperature effect on responsivity is forward modeled, so we use only one SP EDR
      - ii. Select closest (in encoded SCLK) SP EDR that has acceptable binning and wavelength filter to go with the scene EDR
      - iii. Select shutter closed DF EDRs to go with the SP EDR by following (a) above
      - iv. If unexpected SP EDRs are selected
        1. There is no time limit on whether SP EDRs are acceptable, just use the closest in time of the valid ones.

2. If the SP EDR selected is different from that predicted in the early observation tracking table, set the flag in the data quality indicator in the TRDR but otherwise continue normally (note this part of the logic is implemented by the C++ program, while the rest is implemented in PIPE)
- c. Shutter closed DF EDR for bad pixel mask
  - i. Select closest (in encoded SCLK) DF EDR with 1x binning, 1 Hz frame rate, integ time parameter 425, and hyperspectral wavelength filter

## IR

There are 3 types of calibration EDRs to be searched for, the shutter-closed DFs (for IR these are used for background subtraction), the shutter-closed BIs (for IR these are used for bias subtraction), and the sphere calibration SP EDRs. The SP EDRs have their own DF EDRs for calculating the background for sphere measurements.

Note that any downlinked EDRs with a “UN” macro descriptor in the filename should be rejected as calibration EDRs. This will filter out any problem EDRs caused when the instrument occasionally reverts back to default state 2 frames before the end of a mapping mode observation.

- I. Logic for determining desired calibration EDRs from predicted EDRs in initial observation tracking table for a given measurement (BTF table)
  - a. Shutter closed DF EDRs for background for scene or sphere EDR
    - ii. Select latest (in encoded SCLK) DF EDR that is earlier than the scene or sphere EDR and has the same frame rate and binning as the scene or sphere EDR, and acceptable wavelength filter for the scene or sphere EDR
    - iii. Select earliest (in encoded SCLK) DF EDR that is later than the scene or sphere EDR and has the same frame rate and binning as the scene or sphere EDR, and acceptable wavelength filter for the scene or sphere EDR
  - b. Shutter closed BI EDRs for bias for scene or sphere EDR
    - iv. Find closest (in encoded SCLK) set of BI EDRs and select all EDRs from that set that have the same frame rate and binning as the scene or sphere measurement regardless of exposure, and acceptable wavelength filter for the scene or sphere EDR
  - c. Sphere calibration SP EDRs for radiometric calibration
    - i. Select closest (in encoded SCLK) nightside SP EDR that has acceptable binning and wavelength filter, and frame rate to go with the scene EDR (note as of 12/30/2008, nightside or dayside is acceptable)
    - ii. Definition of “acceptable frame rate to go with the scene EDR”
      1. 1 Hz SP is acceptable for 1 Hz or 3.75 Hz SC
      2. 3.75 Hz SP is acceptable for 1 Hz or 3.75 Hz SC
      3. 15 Hz SP is acceptable for 15 Hz SC
      4. 30 Hz SP is acceptable for 30 Hz SC
      5. Note 1 Hz SC only occurs for FLAT macro, but 1 Hz SP will be fairly common

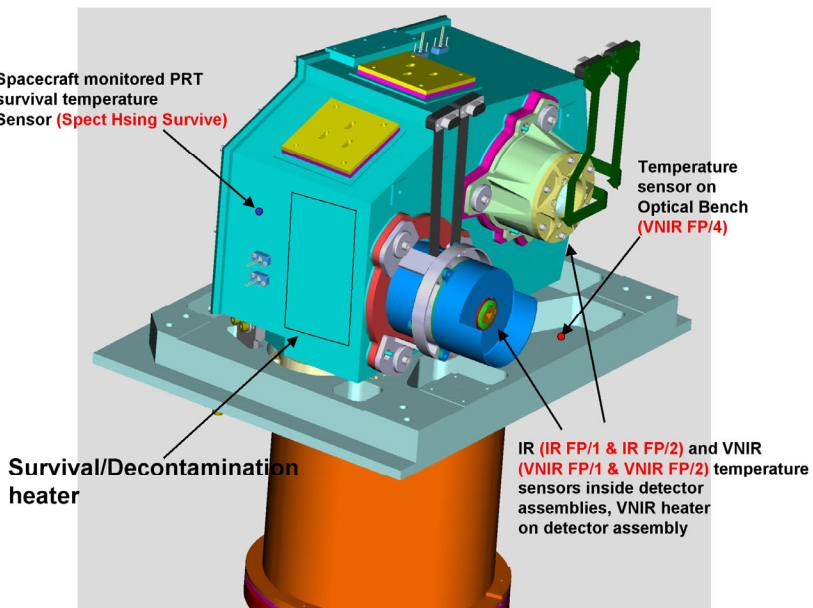
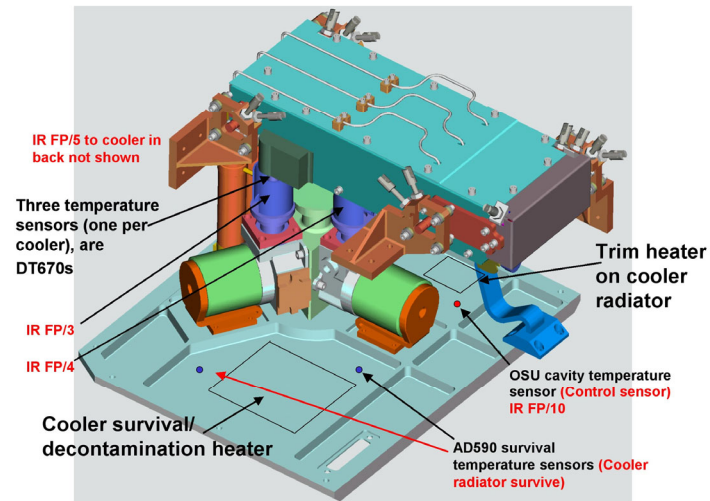
- iii. Select closest (in encoded SCLK) dayside SP EDR that has acceptable binning, wavelength filter, and frame rate to go with the scene EDR (note as of 12/30/2008, it finds the same sphere as i, nightside or dayside)
    - iv. If either SP EDR differs from the scene EDR by more than 24 hours, replace the errant SP EDR by a dummy EDR name to force the C++ program to set the data quality flag in the TRDR no matter what SP EDR it actually ends up using
    - v. Select the VNIR SP EDRs taken at the same time as the IR SP EDRs to do the shutter mirror position correction. Select shutter closed DF EDRs to go with each sphere EDR by following (a) above
    - vi. Select shutter closed BI EDRs to go with each sphere EDR by following (b) above
  - d. Shutter closed BI EDRs for bad pixel mask
    - i. Select closest (in encoded SCLK) set of BI EDRs with 1x binning and hyperspectral wavelength filter
- II. Logic for determining calibration EDRs to use from the list of valid downlinked calibration EDRs (ATF table), and what to do if some of them are invalid
- a. Shutter closed DF EDRs for background for scene or sphere EDR
    - ii. Find latest (in encoded SCLK) existing valid DF EDR that is earlier than the scene or sphere EDR and has the same frame rate and binning as the scene or sphere EDR, and acceptable wavelength filter for the scene or sphere EDR
    - i. Find earliest (in encoded SCLK) existing valid DF EDR that is later than the scene or sphere EDR and has the same frame rate and binning as the scene or sphere EDR, and acceptable wavelength filter for the scene or sphere EDR
    - ii. If unexpected DF EDRs are selected
      1. If the early DF EDR is more than 6 hours earlier than the scene EDR, do not select that EDR but instead select the late DF EDR twice
      2. If the late DF EDR is more than 6 hours earlier than the scene EDR, do not select that EDR but instead select the early DF EDR twice
      3. If both DF EDRs differ from the scene EDR by more than 6 hours, select the one that is closest in time to the scene EDR twice
      4. If either of the DF EDRs selected is different from that predicted in the early observation tracking table (note this part of the logic is implemented by the C++ program, while the rest is implemented in PIPE)
        - a. For scene measurements, set the flag in the data quality indicator in the TRDR but otherwise continue normally
        - b. For DF EDRs to be used with SP EDRs, declare that SP EDR invalid, do not generate an SP flight CDR4 from that SP EDR, and go back to PIPE to get another SP EDR
    - b. Shutter closed BI EDRs for bias for scene or sphere EDR

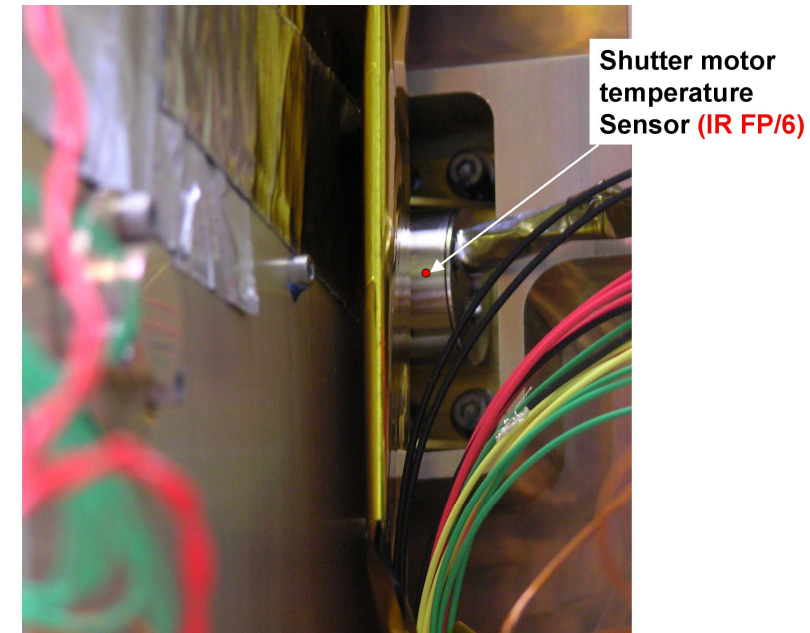
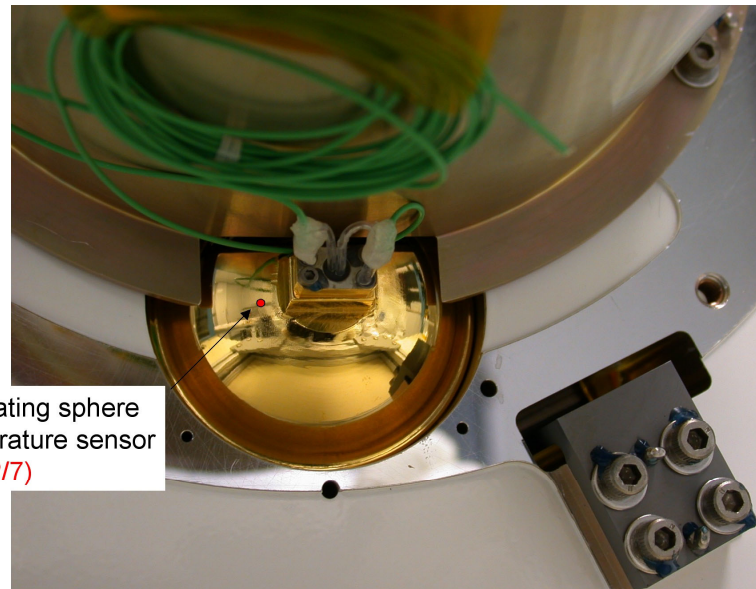
- i. Find closest (in encoded SCLK) set of BI EDRs and choose all EDRs from that set that have the same frame rate and binning as the scene or sphere measurement regardless of exposure, and acceptable wavelength filter for the scene or sphere EDR
- ii. If unexpected BI EDRs are selected (note this part of the logic is implemented by the C++ program, while the rest is implemented in PIPE)
  - 1. There is no time limit on whether BI EDRs are acceptable, just use the closest in time of the valid ones
  - 2. If the BI EDR selected is different from that predicted in the early observation tracking table, set the flag in the data quality indicator in the TRDR but otherwise continue normally
  - 3. For BI EDRs to be used with SP EDRs, declare that SP EDR invalid, do not generate an SP flight CDR4 from that SP EDR, and go back to PIPE to get another SP EDR
- c. Sphere calibration SP EDRs for radiometric calibration
  - i. Select closest (in encoded SCLK) nightside SP EDR that has acceptable binning, wavelength filter, and frame rate to go with the scene EDR (note as of 12/30/2008, nightside or dayside is acceptable)
  - ii. Select closest (in encoded SCLK) dayside SP EDR that has acceptable binning, wavelength filter, and frame rate to go with the scene EDR (note as of 12/30/2008, it finds the same sphere as i, nightside or dayside)
  - iii. Ensure the IR detector temperature for the scene EDR does not fall too far outside the range of the dayside and nightside SP EDRs
    - 1. Let T, Td, and Tn be the median IR detector temperatures for the frames of each of the scene, dayside SP, and nightside SP EDRs respectively
    - 2. If  $Td \leq Tn$ , replace the dayside SP EDR with the one closest (in encoded SCLK) to the scene EDR with  $Td > Tn$
    - 3. If  $(T - Td) > 0.5 * (Td - Tn)$ , replace the currently selected dayside SP EDR with the one closest (in encoded SCLK) to the scene EDR with  $(T - Td) < 0.5 * (Td - Tn)$
    - 4. If  $(Tn - T) > 0.5 * (Td - Tn)$ , replace the nightside SP EDR with the one closest (in encoded SCLK) to the scene EDR with  $(Tn - T) < 0.5 * (Td - Tn)$
  - iv. Select the VNIR SP EDRs taken at the same time as the IR SP EDRs to do the shutter mirror position correction
  - v. Find shutter closed DF EDRs to go with each sphere EDR by following (a) above
  - vi. Find shutter closed BI EDRs to go with each sphere EDR by following (b) above
  - vii. If unexpected SP EDRs are selected
    - 1. If either SP EDR differs from the scene EDR by more than 24 hours, generate an error and ask for human intervention to select the proper pair of SP EDRs to use in generating the TRDR for the given scene EDR

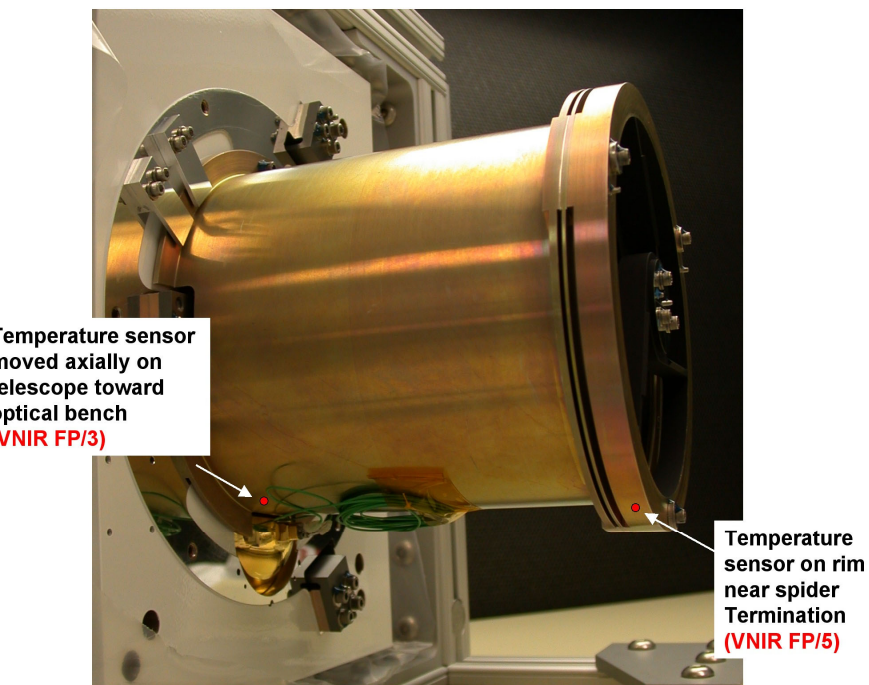
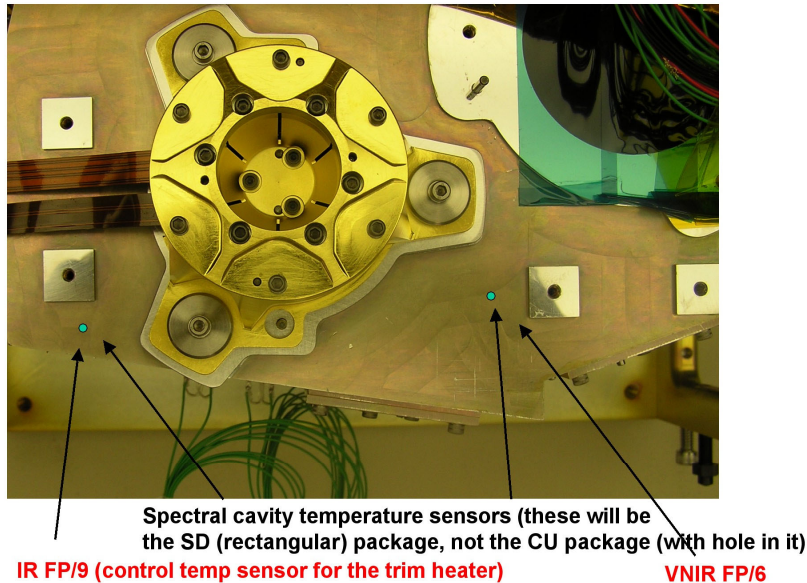
2. If either of the SP EDRs selected is different from that predicted in the early observation tracking table, set the flag in the data quality indicator in the TRDR but otherwise continue normally (note this part of the logic is implemented by the C++ program, while the rest is implemented in PIPE)
  - e. Shutter closed BI EDRs for bad pixel mask
    - i. Select closest (in encoded SCLK) set of BI EDRs with 1x binning and hyperspectral wavelength filter

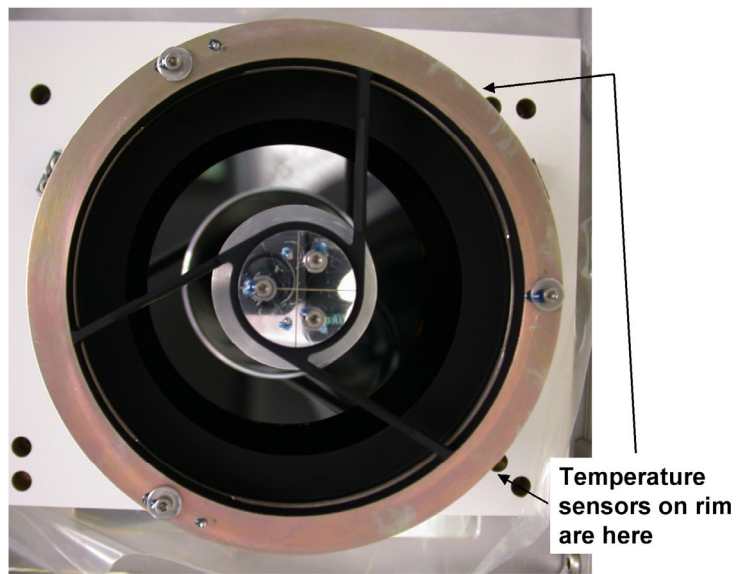
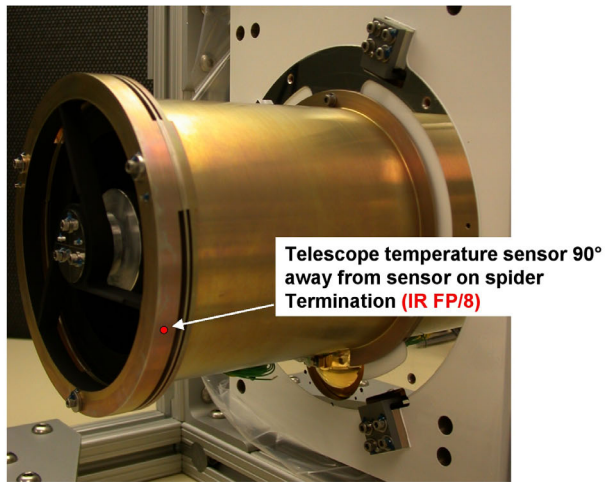
## APPENDIX M. TEMPERATURE SENSOR AND HEATER LOCATIONS

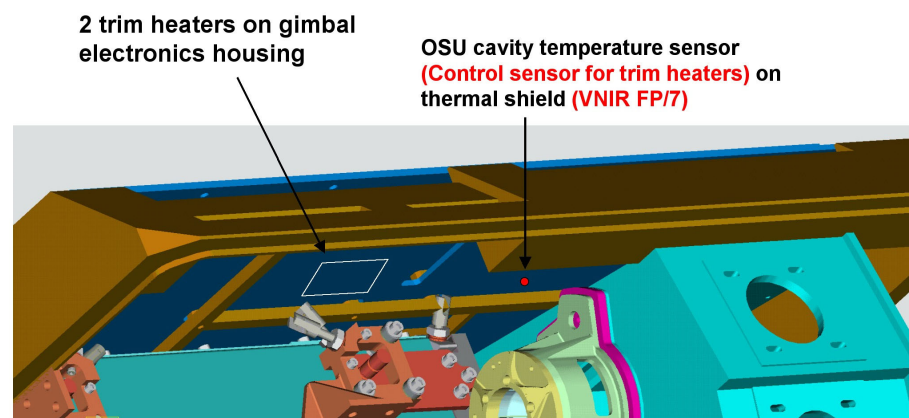
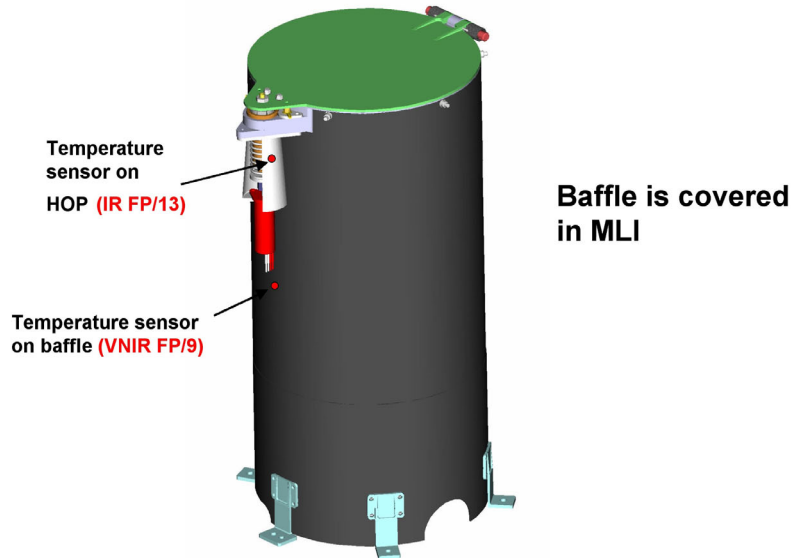
Locations of the reported temperatures, as well as locations of heaters whose current is reported in housekeeping, are shown in the following graphics



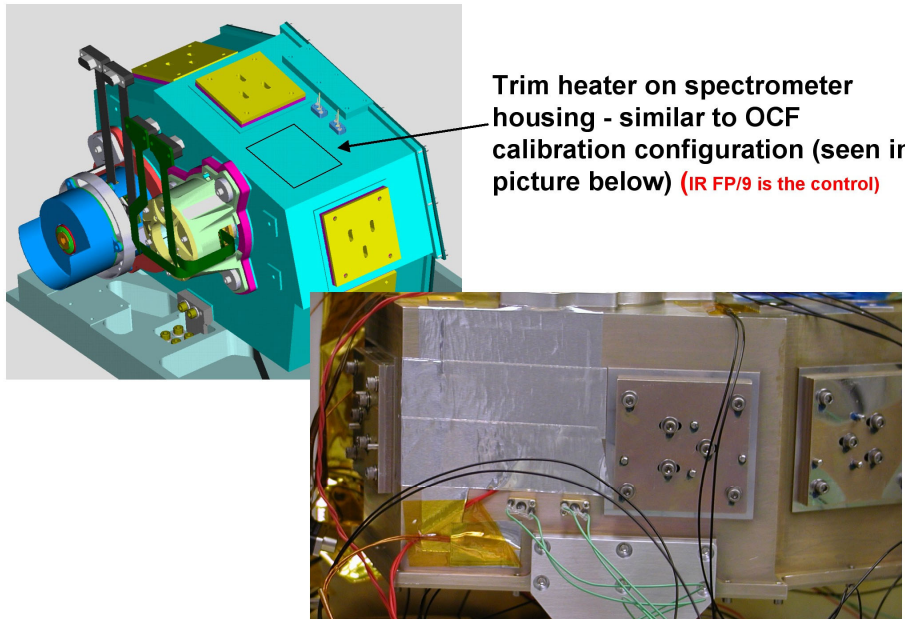




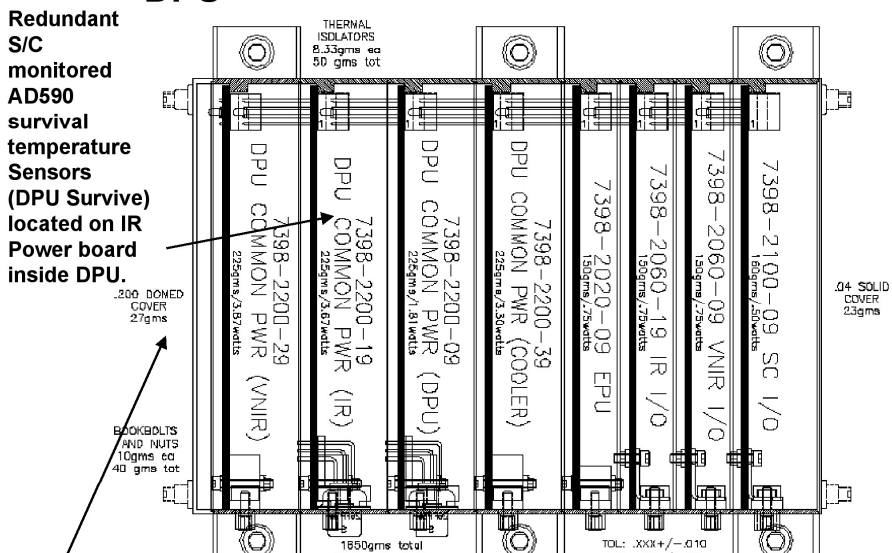




**IR (IR FP/11) and VNIR (VNIR FP/8) FPU board temperature sensors on boards**



## DPU



**Redundant DPU Survive Heater location is on end cover**

## APPENDIX N. DESCRIPTION OF TRR3 FILTERING

CRISM Hyperspectral Data Filter

PDS Data Product SIS Appendix - 02/02/2011

F. Seelos

CRISM version 3 TRDR (TRR3) I/F full and half resolution hyperspectral data products (observations classes FRT, HRS, HRL, FRS, ATO, ATU; e.g.

FRT0000C202\_07\_IF165L\_TRR3.IMG shown in Figure N-8) have been processed with a custom filtering procedure prior to PDS delivery (Figure N-1) [1,2]. The corresponding PDS delivered radiance on sensor spectral data products (e.g. FRT0000C202\_07\_RA165L\_TRR3.IMG) have not been filtered, allowing for the recovery of unmodified reflectance spectra (Figure N-2). Over the course of the Mars Reconnaissance Orbiter (MRO) mission, CRISM has operated with an IR detector temperature between ~107 K and ~127 K. IR observations acquired at higher detector temperatures exhibit an increase in systematic and stochastic noise (e.g. Figure N-2, Figure N-4). The primary systematic noise component in both CRISM IR and VNIR data appears as along track column-oriented striping due in part to artifacts in ground calibration files applied to inflight integrating sphere image cubes. This is addressed by the Ratio Shift Correction (RSC) - a scene-dependent multiplicative correction frame developed through the serial evaluation of channel-specific inter-column ratio statistics. The dominant CRISM IR stochastic noise components appear as isolated positive or negatives data spikes or as column-oriented groups of pixels with erroneous values. The spikes are thought to originate from the delayed response of specific detector elements to high time frequency changes in brightness as the slit moves across a contrasty scene on Mars. The column-oriented features come from transient elevated values of detector dark current either in the science data or the accompanying calibrations. Non-systematic noise in IR data is identified and corrected through the application of an Iterative Kernel Filter (IKF), which employs a formal statistical outlier test as the iteration control and recursion termination criterion. This allows the filtering procedure to make a statistically supported distinction between high frequency (spatial/spectral) signal and high frequency noise based on the information content of a given multidimensional data kernel. To illustrate the end-to-end hyperspectral filtering process each data processing procedure shown in Figure 1 is briefly described with the corresponding resulting data products shown in Figures N-2 through N-9.

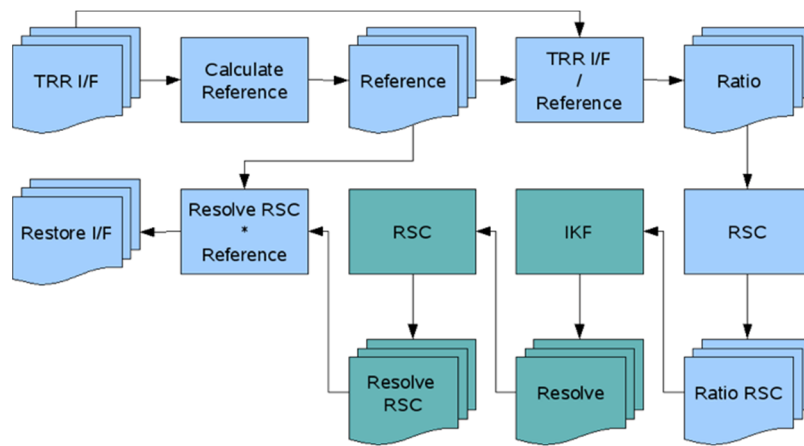


*Figure N-1: CRISM hyperspectral data filter processing flow chart. Boxes represent data processing steps; Stacks represent CRISM image cubes. All procedures and intermediate products are employed in the filtering of IR data. The elements shown in green are bypassed by the VNIR filtering process.*

**Data Processing Overview** – The CRISM hyperspectral data filtering process takes as input a three dimensional ( $x, t, \lambda$ ) CRISM VNIR or IR I/F full or half resolution hyperspectral image cube (Figure N-1: TRR I/F) and generates a filtered version of the input data (Restore I/F) with the same dimensions – there is a 1:1 correspondence between a given input and output pixel ( $x_0, t_0, \lambda_0$ ). The two main data filtering procedures – RSC and IKF – are optimally performed on continuum-normalized spectral data, so the initial data processing steps are the calculation of a reference image cube (Calculate Reference) and the subsequent calculation of a ratio image cube using the reference image cube as the denominator (TRR I/F / Reference). In this reference-normalized ratio space, the filtering procedures to be applied depend on the wavelength range of the input image cube. CRISM VNIR data does not exhibit the non-systematic or stochastic noise the IKF procedure is designed to address, so only a single application of the RSC procedure is required. The noise structure in CRISM IR data is more complex, and requires the use of the RSC procedure as a pre- and post- processing step relative to the application of the IKF procedure. The image cube resulting from the ratio space data processing (VNIR: Ratio RSC; IR: Resolve RSC) is then recombined with the previously calculated reference cube (Resolve RSC \* Reference) to transform the data back to I/F. The image cubes used are described further below.

**TRR I/F** - PDS deliverable radiance on sensor image cube (e.g. FRT0000C202\_07\_RA165L\_TRR3.IMG) transformed to I/F (Figure N-2).

**Reference Cube** - The reference cube is a low spectral frequency / high spatial frequency representation of the input image cube (Figure N-3). The spectrum for each spatial pixel is processed with a series of boxcar filter and tuned implementations of the RSC procedure to produce a 'pristine' reference spectrum for each pixel. Any residual noise in the reference cube will be propagated into the final result.

**Ratio Cube** - The reference cube is used to normalize the input image cube to produce a ratio cube (Figure N-4). High frequency real spatial variability in spectral radiance is normalized out of the ratio, while high frequency spectral variability (signal and noise) is retained. All subsequent data processing occurs in ratio space or a space resulting from further transformations of the ratio cube.

**Ratio Shift Correction (RSC)** - The RSC procedure is applied to the normalized spectral data as both a pre-processing (Figure N-5) and post-processing (Figure N-7) step relative to the application of the IKF procedure for IR data, or as the dominant filtering process for VNIR data. Within a given spectral band, a spatial column corresponds to a single detector element. The Ratio Shift Correction characterizes residual bias of each detector element through the evaluation of inter-column (or cross-track shifted) ratio statistics relative to an appropriate cross track model. Modifying the complexity of the underlying cross track model allows the RSC procedure to address high frequency column striping (Figure N-4 to Figure N-5) or low frequency banding (Figure N-6 to Figure N-7), while retaining real scene cross-track variability.

**Iterative Kernel Filter (IKF)** - The IKF procedure is a kernel based filtering algorithm that models the information content of a given three dimensional ( $x, t, \lambda$ ) normalized data kernel as a multidimensional polynomial. The model residuals are treated as a sample set and examined for outliers using the Grubbs test. If an outlier is detected, the corresponding pixel is removed from

consideration and the kernel model is iterated. Model iteration is terminated when no further outliers are detected. The filtered value for the target pixel at the center of the input kernel is then given by a proximity weighted model of the kernel elements that were not marked as outliers. The confidence level threshold for the Grubbs test is conservative so the filter retains some marginal noise (Figure N-6) rather than erroneously removing real spectral structure.

**Restore I/F** - The result of the ratio space data processing (Figure N-7) is multiplied by the reference cube (Figure 3) to transform the filtered data back to I/F (Figure N-8). Figure N-9 shows the effect of the CRISM hyperspectral filtering process on the example image cube.

### References -

- [1] Seelos F. P., Parente M., Clark T., Morgan F., Barnouin O. S., McGovern A., Murchie S. L, and Taylor H. (2009) American Geophysical Union, Fall Meeting, P23A-1234.
- [2] F. P. Seelos, S. L. Murchie, D. C. Humm, O. S. Barnouin, F. Morgan, H. W. Taylor, and C. Hash (2011) 42<sup>nd</sup> Lunar and Planetary Science Conference, 1438.

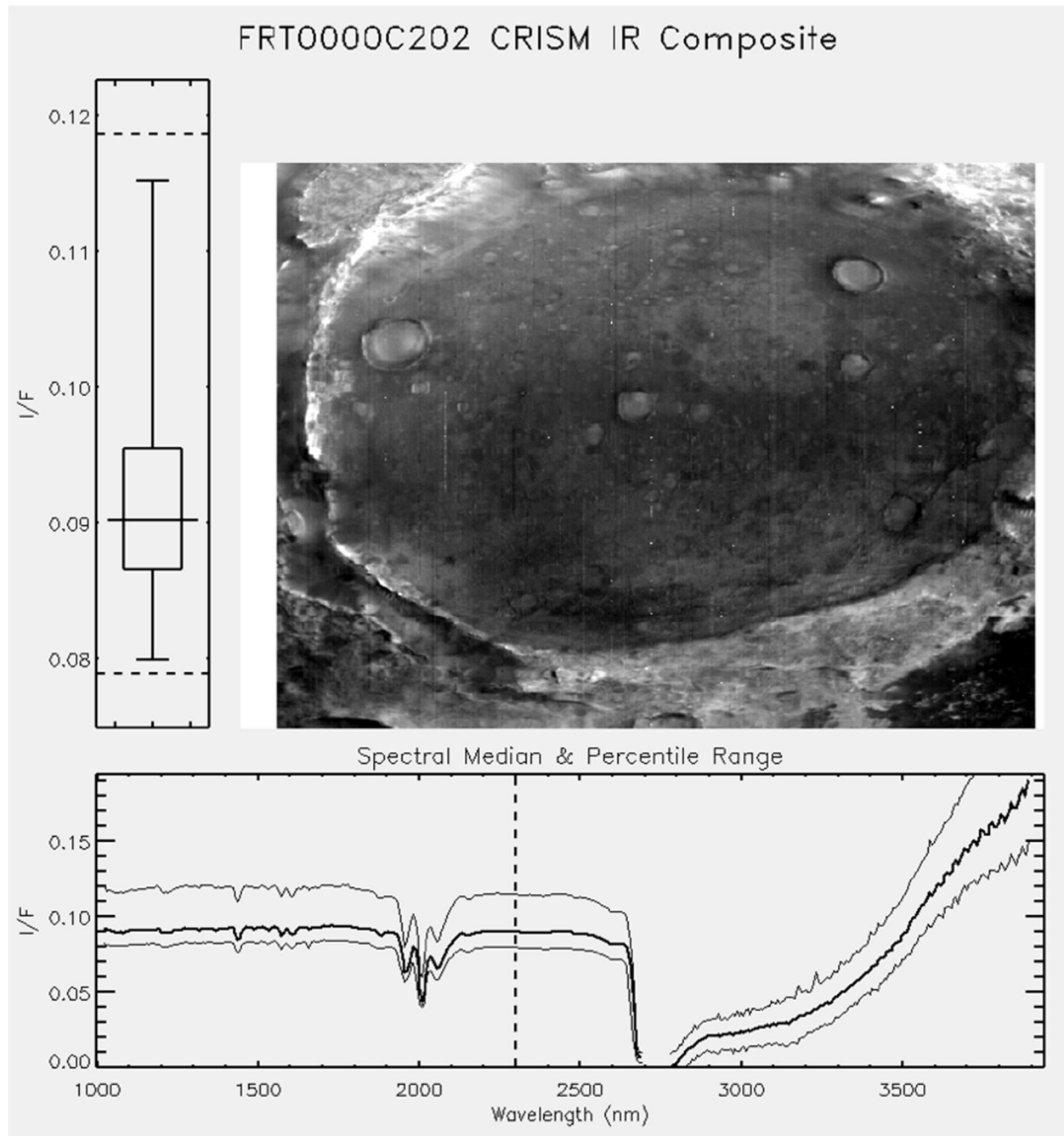


*Figure N-2: Three panel composite view of FRT0000C202 segment 0x07 (central scan) input I/F IR image cube. The corresponding radiance image has been delivered to the PDS as FRT0000C202\_07\_RA165L\_TRR3.IMG Observation FRT0000C202 was acquired with an IR detector temperature of ~120.8 K. The systematic and stochastic noise components to be addressed by the filtering procedure are evident as bright pixels and vertical lines. The composite plot consists of: 1) Band 240 (~2300 nm) ground plane ( $x,t$ ) image with a 1% linear stretch; 2) Boxplot showing the data distribution and stretch limits for the displayed band; 3) Median spectrum and [1,99]% envelope for the input image cube.*

### FRT0000C202 CRISM IR Composite

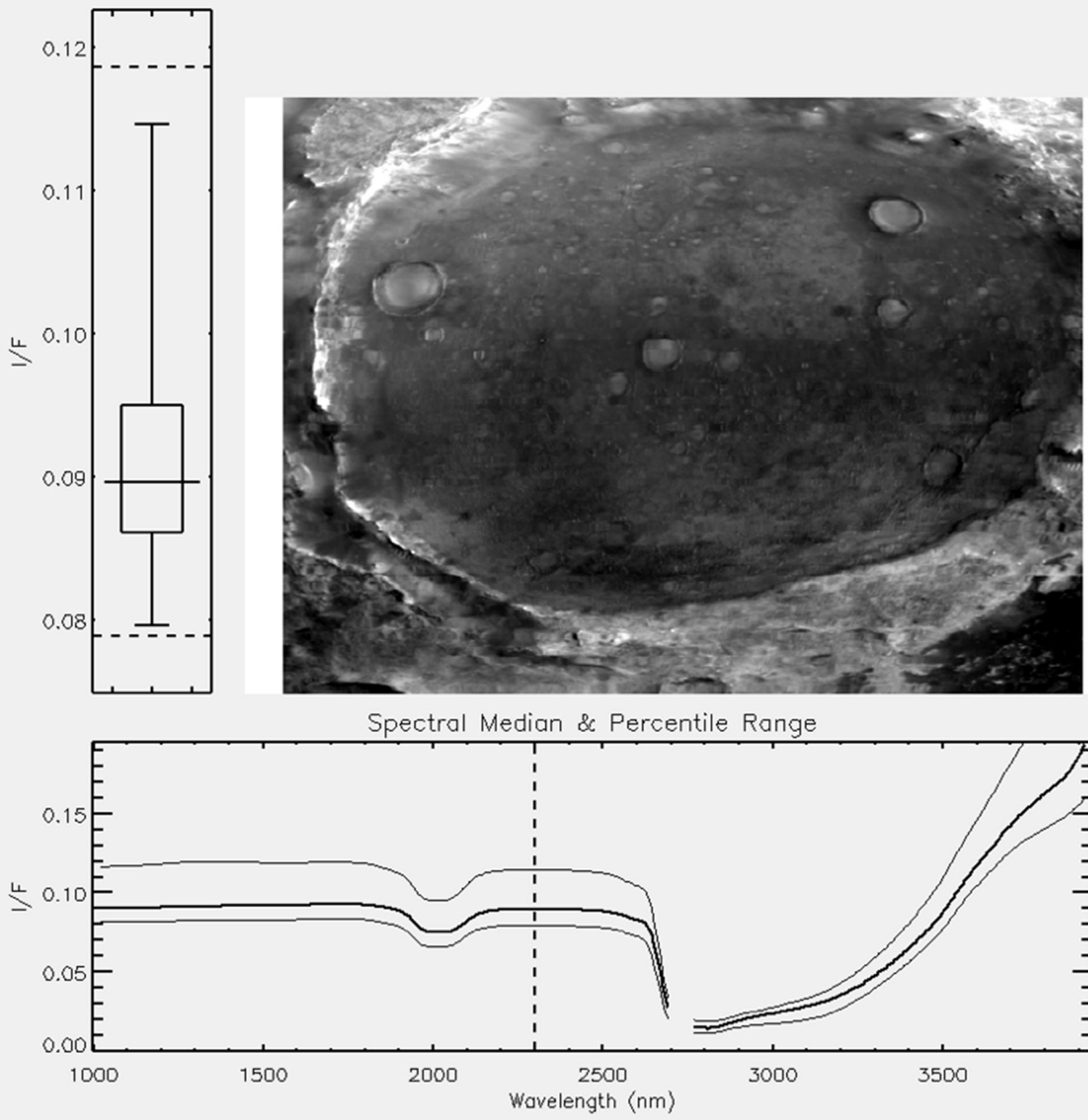
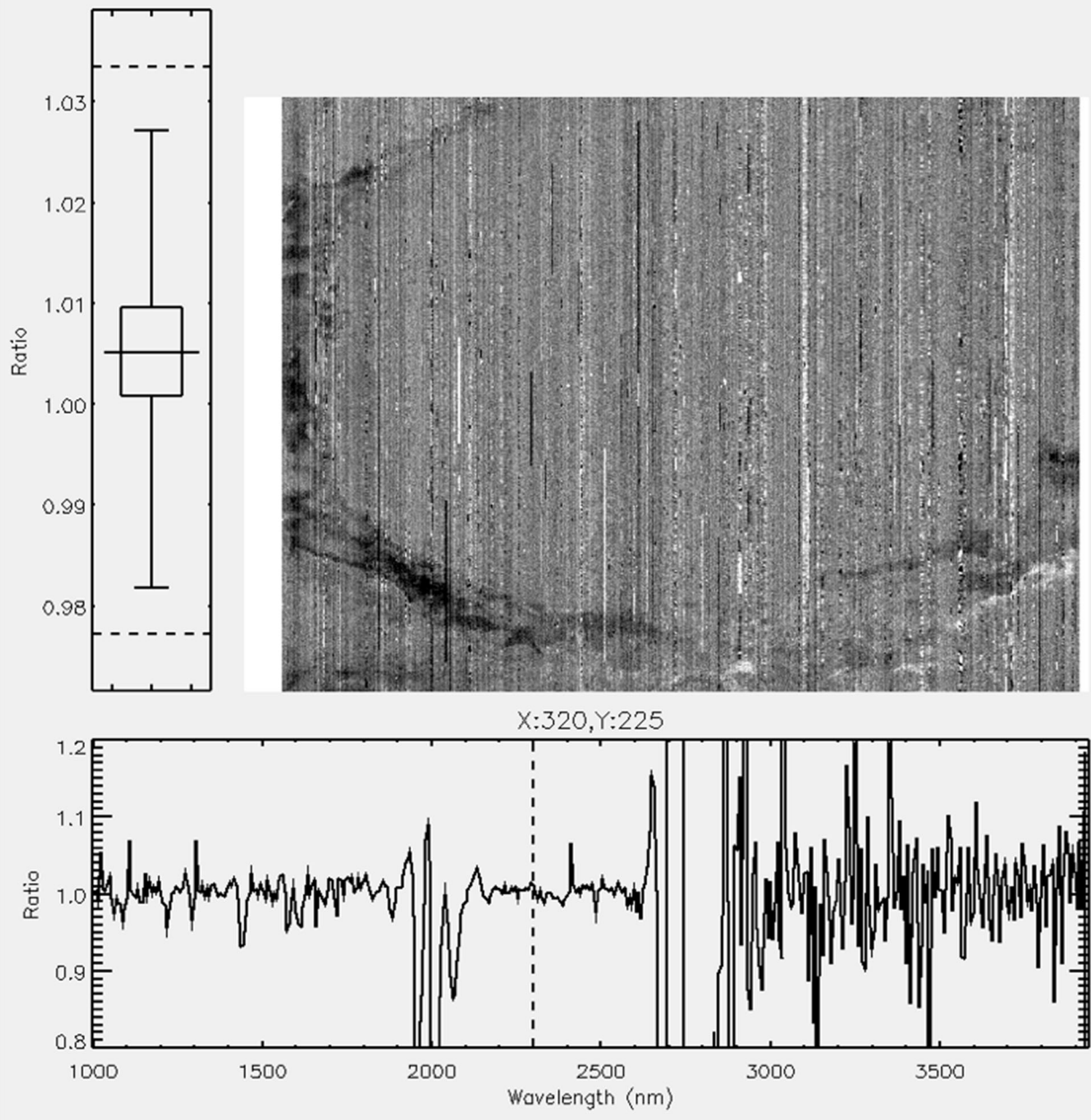


Figure N-3: FRT0000C202 reference cube. High frequency spatial information is retained while high frequency spectral information is discarded.

### FRT0000C202 CRISM IR Composite



*Figure N-4: FRT0000C202 ratio cube. Spatial pixel scale variability due to low-spectral frequency continuum variation is retained by the reference cube (Figure 3) but normalized out of the ratio cube. The ratio cube contains both high frequency noise and high frequency signal components. The spectral plot corresponds to the center pixel in the scene.*

### FRT0000C202 CRISM IR Composite

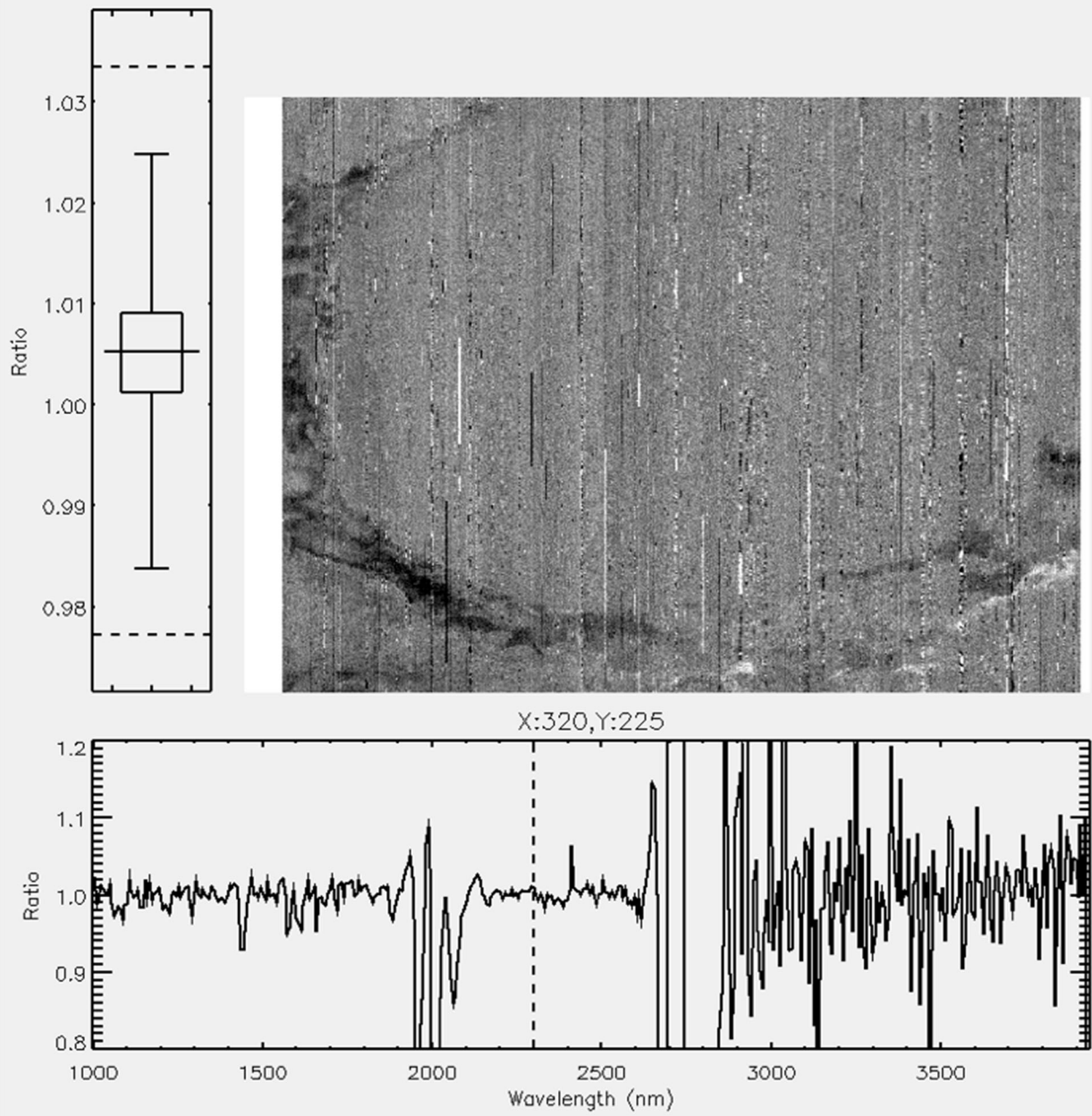


Figure N-5: FRT0000C202 ratio RSC cube. Systematic column-to-column (along track) bias has been mitigated.

### FRT0000C202 CRISM IR Composite

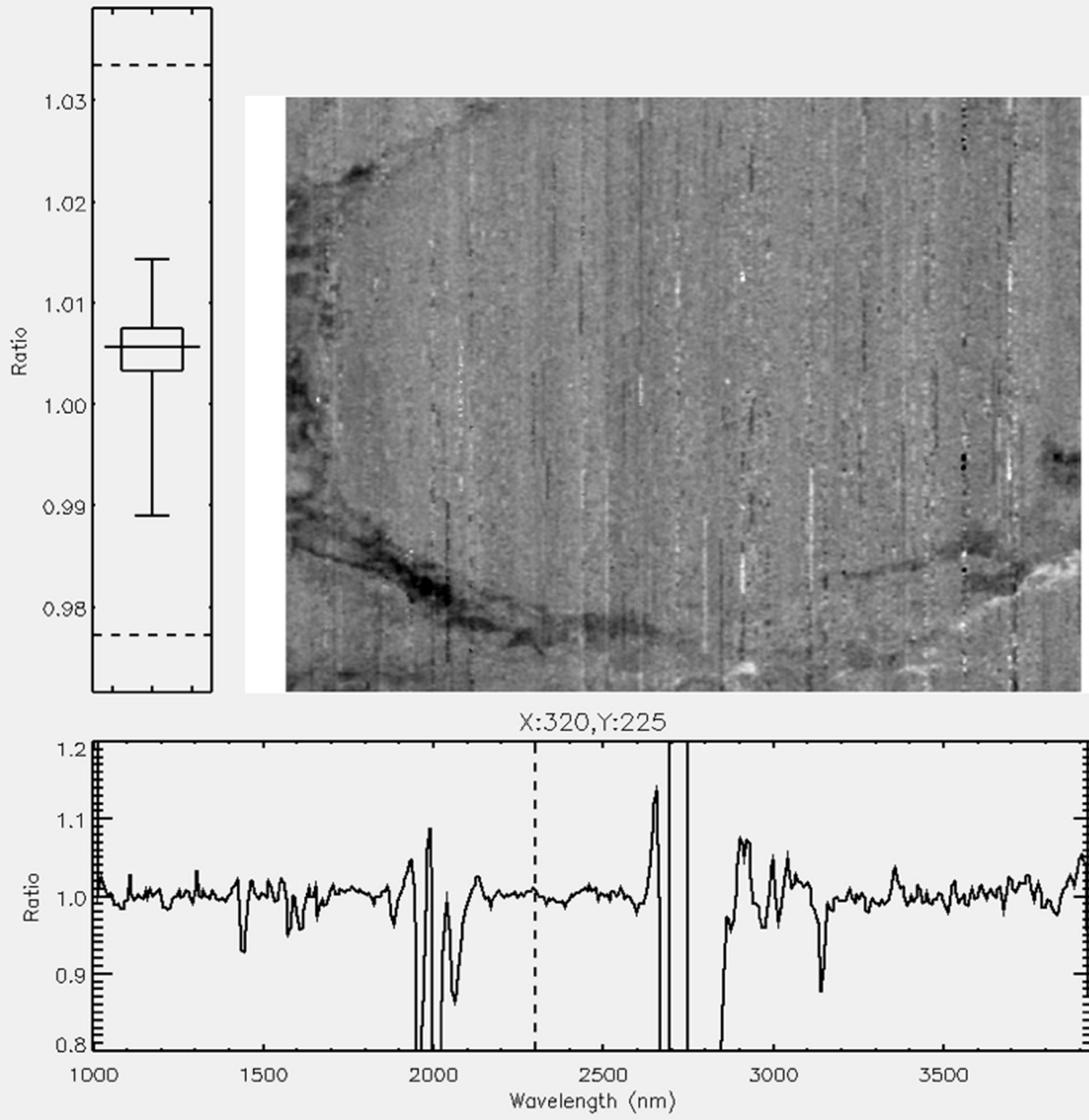


Figure N-6: FRT0000C202 resolve cube. Stochastic noise components have been highly reduced while real high frequency spatial/spectral variability has been retained.

### FRT0000C202 CRISM IR Composite

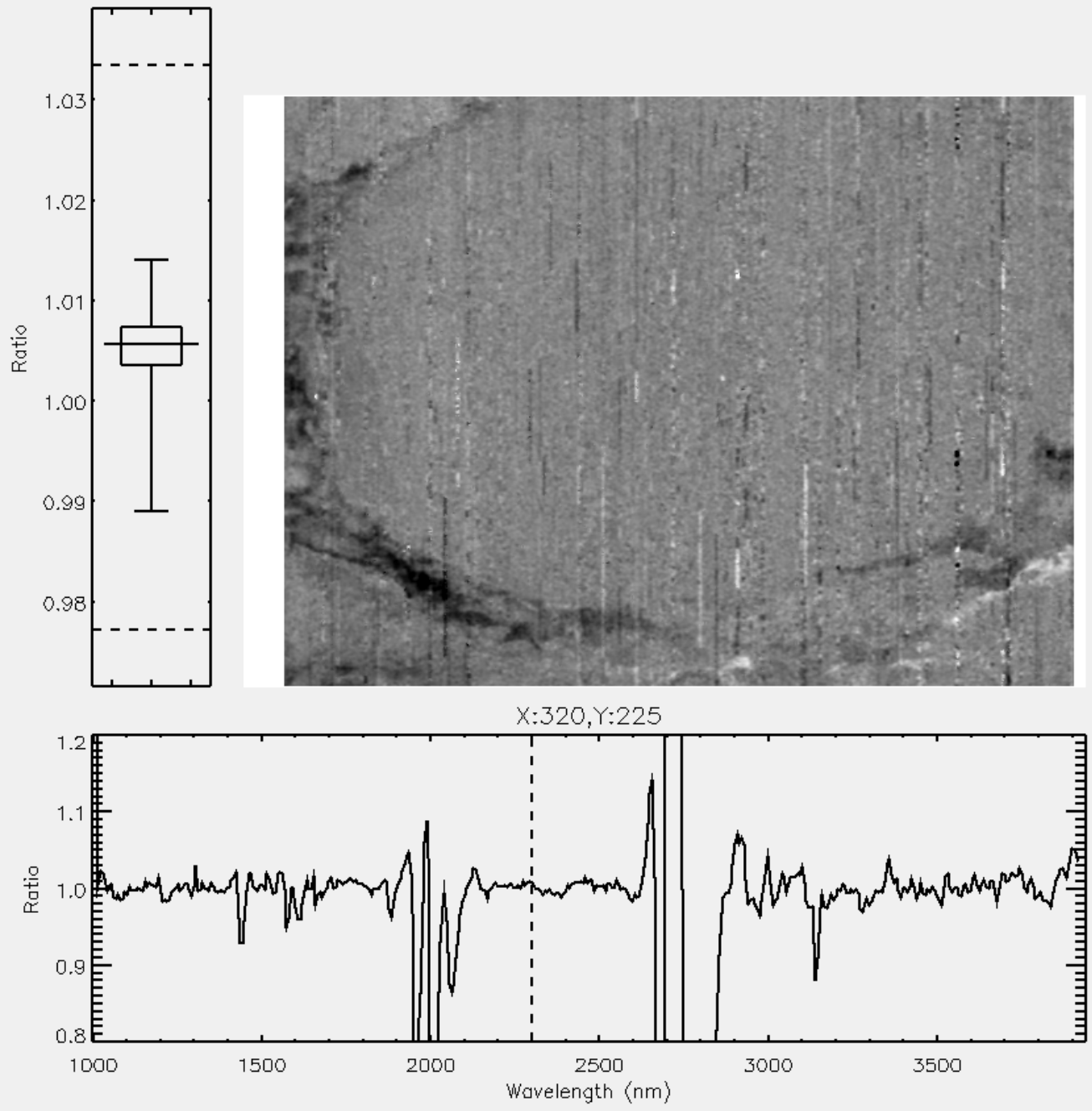


Figure N-7: RFRT0000C202 resolve RSC cube. Systematic along track banding has been mitigated.

### FRT0000C202 CRISM IR Composite

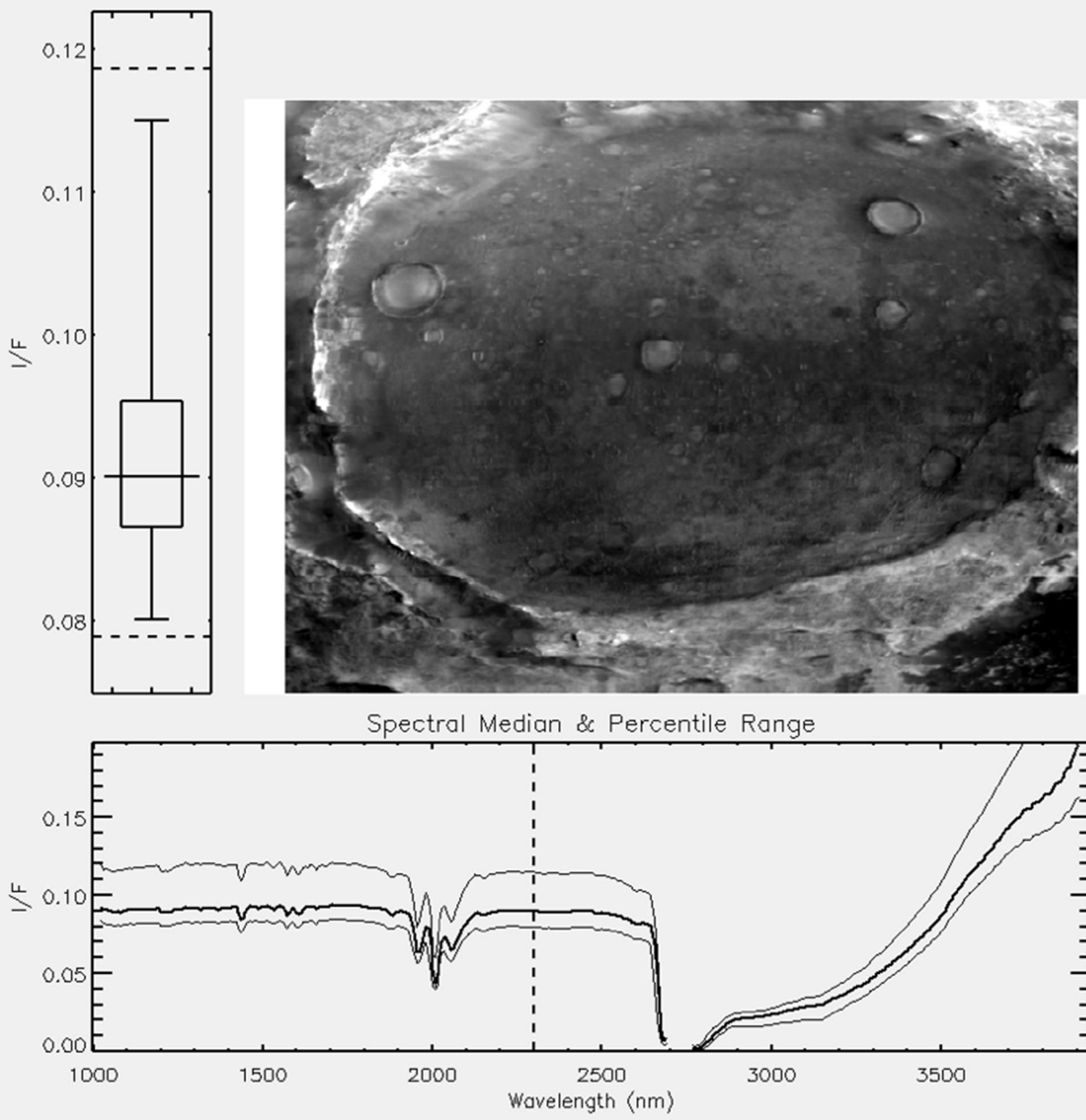


Figure N-8: FRT0000C202 restore cube – delivered to the PDS as FRT0000C202\_07\_IF165L\_TRR3.IMG. Compare the ground plane image, median spectrum and spectral percentile envelope, and data distribution boxplot to Figure 2.

### FRT0000C202 CRISM IR Composite

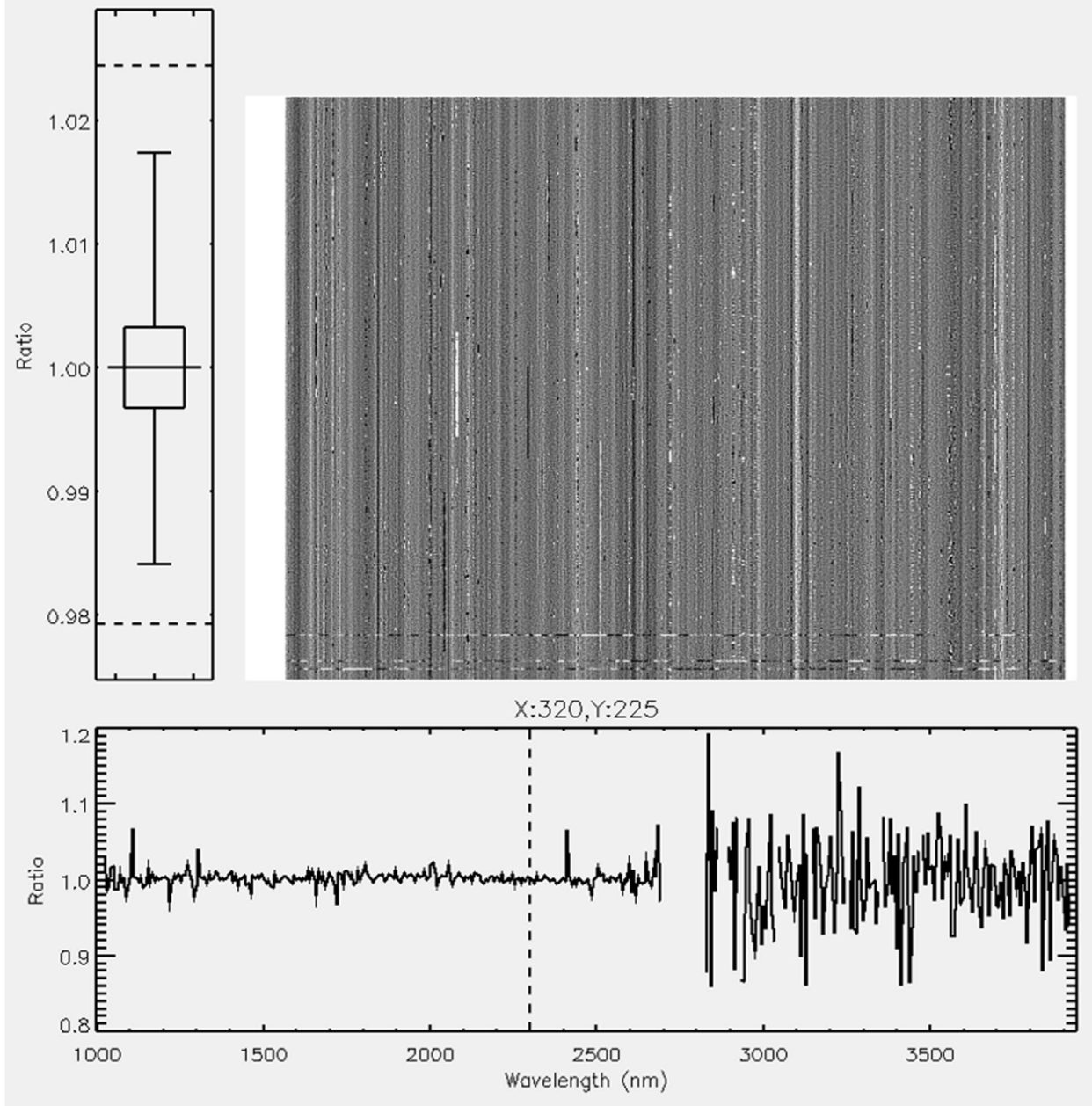


Figure N-9: FRT0000C202 input / output ratio cube showing the effect of the data filtering procedure. Note that the single pixel input/output ratio spectrum and band 240 ratio data are centered on unity.

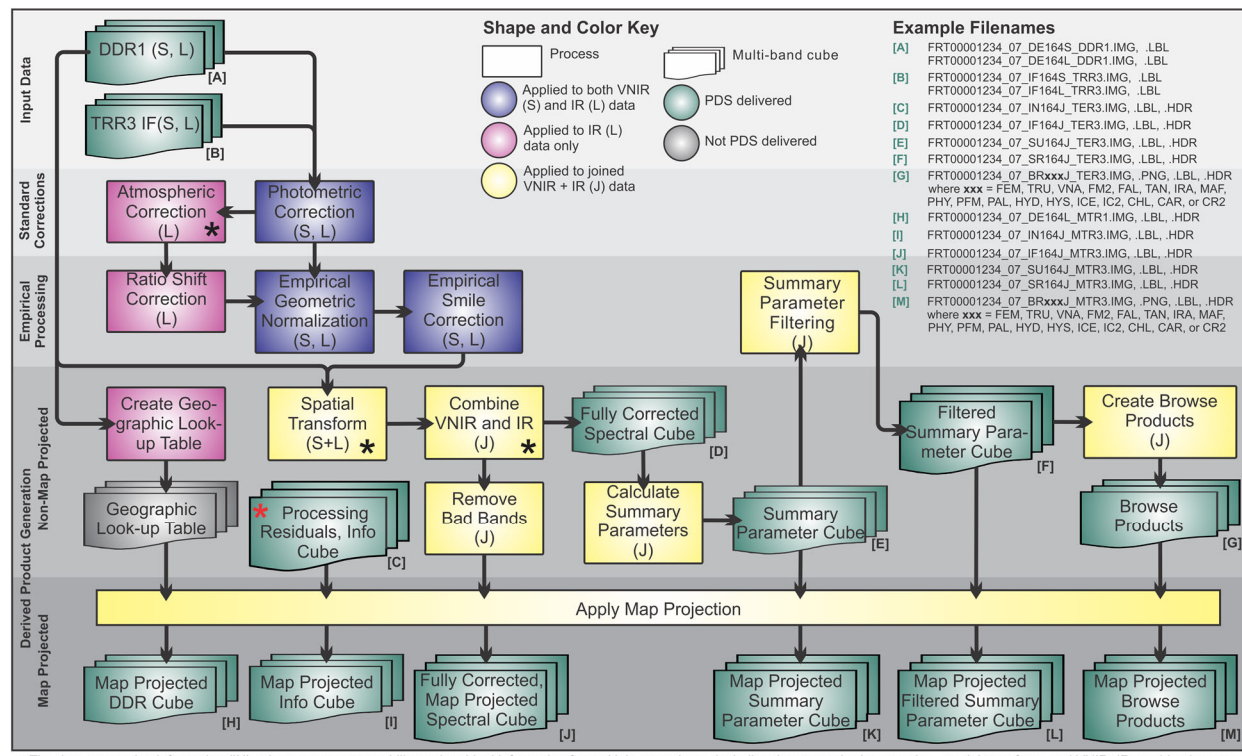
## **APPENDIX O. DESCRIPTION AND USAGE OF ADRS**

N/A

## APPENDIX P1. TER/MTRDR Data Processing and Product Description

### 0. Orientation – CRISM Hyperspectral Targeted Observation Structure

A CRISM hyperspectral targeted observation is composed of one central scan that is acquired at either 1x (full resolution) or 2x (half resolution) cross-track binning at relatively small gimbal angles ( $\sim[-30.0^\circ, 30.0^\circ]$ ) and accompanying 10x binned Emission Phase Function (EPF) scans that are acquired at larger gimbal angles ( $\sim[-60^\circ, -30^\circ], \sim[30^\circ, 60^\circ]$ ). The central scan typically has a counter within observation value (or segment ID) of 0x07, but this can vary in anomalous circumstances. The majority of the TER/MTRDR data processing pertains to the central scan, though the EPFs are critical to the Empirical Geometric Normalization (EGN) procedure (P1-4). The central scan results in a three dimensional hyperspectral image cube with dimensions  $[x,t,\lambda]$  where individual  $[x,\lambda]$  frames are accumulated over time  $[t]$ . A given element in the image cube can be indexed as  $[x_i, t_j, \lambda_k]$  where  $0 \leq i \leq (ns - 1)$ ,  $0 \leq j \leq (nl - 1)$ ,  $0 \leq k \leq (nb - 1)$ , and  $ns$ ,  $nl$ , and  $nb$  are the number of samples, lines, and bands. Overall flow of the processing is repeated below from Figure 2-9a. Visualizations of the TER/MTRDR data processing procedures as applied to each targeted observation are included in the PDS EXTRAS directory. These visualizations are described in detail in Appendix P2.



### 1. PHT – Lambertian Photometric Correction

The TER/MTRDR data processing pipeline photometric correction uses a Lambert assumption:

$$IOF_1 = IOF_0 / \cos(\theta) \text{ where } IOF_0 \text{ is the observed spectral reflectance (I/F), } IOF_1 \text{ is photometrically corrected spectral reflectance, and } \theta \text{ is the angle of incidence.}$$

The photometric correction is calculated for each spatial pixel  $[x_i, t_j]$  and is applied uniformly to all spectral channels  $[\lambda]$ . The spatial pixel specific incidence angle information is derived from the 'INA at areoid' band (incidence angle with respect to the Mars areoid) in the CRISM DDR (Derived Data Record) associated with the targeted observation and segment under consideration. The DDR INA information is calculated with respect to the MOLA (Mars Orbiter Laser Altimeter) areoid, which is reported as a degree and order 50 spherical harmonic expansion [Smith *et al.*, 1999] and stored in the PDS (Planetary Data System) as a 16 pixel/degree gridded data product. CRISM targeted observations spatially oversample the gridded areoid data ( $\sim 20/40$  m/pxl vs.  $\sim 3.7$  km/pxl), which results in non-physical spatial discretization in the DDR incidence and emission angle bands. To prevent the propagation of this sampling effect into the TER/MTRDR data products the INA data are fit by a low-order two-dimensional polynomial in CRISM sensor space and the polynomial model is used as the incidence angle information source in the spatial pixel specific photometric correction.

The reference polynomial model has the form:

$\theta_{model} = c_0 + c_1 x + c_2 x^2 + c_3 t + c_4 t^2$  where  $x$  is the CRISM sample index,  $t$  is the CRISM line index, and the model coefficients  $c_0, c_1, \dots, c_4$  minimize  $\sum_{i,j} (\theta_{INA_{x_i,t_j}} - \theta_{model_{x_i,t_j}})^2$  where  $\theta_{INA}$  and  $\theta_{model}$  are the DDR INA and model incidence angle bands.

The spatial/spectral impact of the PHT correction in the TER/MTRDR processing of a given targeted observation can be assessed by comparing

[Class Type][Target ID]\_[Sensor]\_COMPOSITE\_01.PNG and

[Class Type][Target ID]\_[Sensor]\_COMPOSITE\_02.PNG in the PDS EXTRAS directory. The variation in incidence angle across a CRISM targeted observation central scan is generally very small so the PHT correction does not differ greatly from a scalar multiplicative change in scale. The PHT correction is applied to all segments of a targeted observation to maintain radiometric consistency across the central scan and EPFs for downstream data processing.

## 2. ATM – Modified 'Volcano Scan' Atmospheric Correction

The volcano scan atmospheric correction uses empirically derived Mars atmospheric transmission spectra to correct CRISM IR (L-detector) spectral reflectance data for atmospheric gas absorptions (due primarily to CO<sub>2</sub>, H<sub>2</sub>O, and CO) [Langevin *et al.*, 2005; McGuire *et al.*, 2009; Morgan *et al.*, 2011]. There are no significant atmospheric gas absorptions over the CRISM VNIR wavelength range, so this correction is not applied to VNIR (S-detector) data. Detector column-specific reference atmospheric transmission spectra ( $[x_i, \lambda]$  to accommodate spectral smile) are derived from a suite of push-broom hyperspectral Flat Field Calibration (FFC) scans over Olympus Mons and are matched to a given targeted observation to minimize high frequency residual spectral structure due to sub-nm wavelength calibration variability across the wavelengths affected by the 2000 nm CO<sub>2</sub> absorption (1947 – 2066 nm). The depth of the 2000 nm CO<sub>2</sub> absorption is determined for the spectrum of each spatial pixel  $[x_i, t_j]$  in the image cube under consideration, the selected reference transmission spectrum is scaled to match according to the Beer-Lambert Law, and the resulting model transmission spectrum is ratioed out of the I/F data. The TER/MTRDR pipeline implementation of the volcano also includes a CRISM-specific volcano scan patch (included in the CRISM Analysis Toolkit v7.1+ available at the PDS Geosciences Node) that is applied after the initial correction to reduce the influence of varying

path length and pressure broadening in the derivation of the reference transmission spectra.

The spectral impact of the ATM correction on the IR data for a given targeted observation in the TER/MTRDR processing flow is illustrated by comparing [Class Type][Target ID]\_L\_COMPOSITE\_02.PNG and [Class Type][Target ID]\_L\_COMPOSITE\_03.PNG in the PDS EXTRAS directory. The wavelength bands selected for the RGB composite visualization are by design not greatly influenced by atmospheric gas absorptions, so the effect of the ATM correction is most evident in the scene median and percentile envelope spectral plots. The ATM correction is applied to all segments of a targeted observation to maintain radiometric consistency across the central scan and EPFs for downstream data processing.

### **3. RSC – Ratio Shift Correction (Empirical Flat Field / Along-Track 'Destriping')**

The Ratio Shift Correction (RSC) is a spatial column-oriented ‘destriping’ procedure applied after the correction for atmospheric gas absorptions (ATM) to mitigate the reintroduction of column stripe residuals  $[x_i, t, \lambda_j]$  that arise due to differences in detector element nonuniformity between the acquisition of the selected reference Olympus Mons scan and the acquisition of the targeted observation under consideration. The RSC procedure was initially developed as a component of the TRR3 (targeted reduced data record calibration version 3) hyperspectral data filtering procedure [Seelos *et al.*, 2009] and seeks to isolate and mitigate systematic calibration residuals traceable to individual detector elements  $[x_i, \lambda_j]$ . The detector column and wavelength specific nature of the ATM correction can result in similarly structured residuals. The RSC procedure is a band-independent operation that gathers adjacent inter-column ratio statistics from continuum-normalized spectral data and constructs a cross-track multiplicative aggregate profile from robust estimates (median values) of the inter-column ratios. The ratio of the cross-track aggregate profile to a low-order Legendre polynomial (typically  $l = 5$ ,  $m = 0$ ) model profile fit results in a correction profile  $[x]$  for the subject band  $[\lambda]$ , and the accumulation of correction profiles with wavelength results in a correction frame  $[x, \lambda]$ . This correction frame is applied to all frames  $[t]$  in the continuum normalized spectral cube, and the data are then transformed back to I/F. The accumulation of the cross-track aggregate profile is subject to memory (history) effects, so the inter-column ratio statistics are collected with both a +1 and -1 column shift, and the profile accumulation is conducted in both cross-track directions ( $+x$ ,  $-x$ ). The average of the four resulting correction profiles is forwarded into the correction frame. The reference Legendre polynomial profile is determined using a least absolute deviation figure of merit which reduces the influence of spurious inter-column ratio median samples on the model profile fit.

Visualizations of the information content of an IR hyperspectral targeted observation central scan image cube before and after application of the RSC procedure are provided by

[Class Type][Target ID]\_L\_COMPOSITE\_03.PNG and [Class Type][Target ID]\_L\_COMPOSITE\_04.PNG in the PDS EXTRAS directory. The magnitude of the RSC result is commonly much smaller than the dynamic range of a targeted observation central scan so the effect of the RSC procedure is not always evident when comparing the 3-panel visualizations. In the TER/MTRDR data processing flow this correction is applied to the central scan but not the corresponding EPFs which do not provide adequate sampling statistics.

#### 4. EGN – Empirical Geometric Normalization

CRISM hyperspectral targeted (gimbaled) observation data exhibit geometric effects traceable to the requisite continuously varying observation geometry (gimbal motion). The EGN procedure is designed to characterize the geometric dependencies of spectral radiance across all segments of a CRISM targeted observation (the central scan and any associated EPFs), isolate the spectral continuum variability attributable to the gimbal motion, and transform the central scan to a synthetic idealized (zero gimbal angle or push-broom) acquisition geometry. Note that this procedure effectively normalizes the effects of observing geometry to the minimum emergence angle (more-or-less equivalent to the MRO spacecraft roll off nadir) during the central scan.

For this correction the CRISM spectral data are binned as a function of two geometric variables – the cosine of the emission angle [ $\cos(e)$ ] which is proportional to the atmospheric path length under a plane-parallel simplifying assumption, and the phase angle [ $g$ ] which is a strong discriminator for atmospheric aerosol scattering. With the (generally minimal) incidence angle variability across the observation structure accommodated by the PHT correction, the [ $\cos(e)$ ,  $g$ ] sampling also captures variability due to surface photometry. The data are binned in one degree increments in phase angle [ $g$ ] and an equivalent sampling frequency in emission angle cosine (90 bins over the interval [0,1]).

The spatial pixel specific geometric data are taken from the 'EMA at areoid' (emission angle with respect to the Mars areoid) and 'Phase angle' bands in the DDRs associated with the targeted observation under consideration. An abstract polynomial model of the form:

$IOF_{model} = c_0 + c_1 \cos(e) + c_2 \cos(e)^2 + c_3 g + c_4 g^2$  is fit to the sampled data so that the coefficients  $c_0, c_1, \dots, c_4$  minimize  $\sum_n (IOF_{data_n} - IOF_{model_n})^2$  where  $1 \leq n \leq N$  for the  $N$  binned data points. The sampled spectral data for each wavelength are modeled independently, but the high channel-to-channel correlation in hyperspectral data allows the model parameters for band  $\lambda_k$  to be used to seed the optimization for band  $(\lambda_k + 1)$ .

The model parameters for each spectral channel are used to calculate a central scan spatial pixel specific forward model using the EMA and Phase angle bands from the associated central scan DDR as the independent variables. The accumulation of forward model bands with wavelength produces a forward model spectral cube that encompasses the geometric dependent variation across the central scan. The objective of the EGN procedure is to transform the I/F data to a synthetic idealized observation geometry, rather than a geometry-dependent continuum removed space, so the forward model spectral cube is scaled by the forward model spectrum at a reference [ $\cos(e)$ ,  $g$ ] geometry that corresponds to the center of the cross-track field of view [ $x$ ] within the frame [ $t_j$ ] that includes the minimum sampled emission angle. As a result the correction cube is unity at all wavelengths at the reference geometry and a relative multiplicative correction at all other geometric coordinates.

In high spectral contrast scenes (e.g. observations of polar layered deposit scarps), particularly those with spatially organized disparate spectral classes (e.g. regolith to ice transition across the central scan), the empirical geometric modeling can be unduly influenced by surface spectral variability leading to the incorporation of interpretable spectral structure in the correction cube.

To ensure that that resulting correction cube tracks the spectral continuum and maintains channel-to-channel continuity the correction cube is spectrally stabilized. The stabilization takes the form of a low-order Legendre polynomial least absolute deviation figure of merit model fit as a function of wavelength, weighted by the reference forward model spectrum. The resulting correction cube is approximately unity at all wavelengths at the reference geometry, and a multiplicative correction at all other geometric coordinates.

The spatial/spectral impact of the EGN procedure in the TER/MTRDR processing of a given targeted observation can be assessed by comparing

[Class Type][Target ID]\_S\_COMPOSITE\_02.PNG and

[Class Type][Target ID]\_S\_COMPOSITE\_05.PNG for VNIR (S-detector) data and

[Class Type][Target ID]\_L\_COMPOSITE\_04.PNG and

[Class Type][Target ID]\_L\_COMPOSITE\_05.PNG for IR (L-detector) data in the PDS EXTRAS directory. Snapshots of the geometric modeling at the foundation of the EGN procedure are shown in the series of model fit plots

[Class Type][Target ID]\_[Sensor]\_EGN\_FIT\_[Number].PNG, and EGN along-track correction profiles are presented in [Class Type][Target ID]\_[Sensor]\_EGN\_PRO.PNG.

## 5. ESC – Empirical Smile Correction

CRISM data exhibit spatial/spectral structure traceable to spectral smile – an optical artifact where the wavelength calibration shifts as a function of cross-track spatial position [ $x_i$ ]. Spectral smile effects are most evident where the observed spectral reflectance is changing rapidly with wavelength (steep spectral slopes) and a small change in the center wavelength of the bandpass can result in a relatively large change in the measured signal. The most notable examples are the steep spectral slopes from 450–750 nm and within the composite CO<sub>2</sub> absorption from 1850–2150 nm. In addition to spectral slope effects, the CRISM radiometric calibration exhibits a small residual related to spectral smile that appears as a wavelength-dependent cross-track gradient. These effects are addressed by the Empirical Smile Correction (ESC) which uses the WA-CDR (detector center wavelength sampling map) and SW-CDR (detector sweet-spot wavelength vector) for the targeted observation under consideration to transform data acquired across the detector to the reference (SW-CDR) center wavelength sampling vector.

The primary ESC procedure uses the detector wavelength map to construct an intra-channel wavelength sampling histogram for each spectral channel that delineates the cross-track spatial columns that fall into each wavelength bin. The bin size is 0.125 nm for full resolution data (FRT) and 0.250 nm for half resolution data (HRL, HRS). Continuum normalized spectral data are binned according to the histogram map and the resulting data points are modeled as a linear function of wavelength. Each binned data point is weighted in the linear fit by the corresponding histogram count and the inverse of the binned sample set dispersion. A forward model is calculated for the detector wavelength map cross-track profile for each spectral channel, and the reference wavelength for each channel is used to calculate a reference model value. Each channel-specific forward model is then normalized to the appropriate reference, the resulting correction frame [ $x, \lambda$ ] is applied to all frames [t] in continuum normalized spectral cube, and the result is transformed back to I/F.

Spectral smile related effects in CRISM IR (L-detector) data are primarily due to spectral slope, so spectral interpolation to the reference wavelength sampling vector is performed prior to the application of the empirical correction procedure. Spectral smile effects in CRISM VNIR (S-detector) data are generally consistent with a minor radiometric residual, so the empirical correction procedure is applied directly.

The spatial/spectral impact of the primary ESC procedure in the TER/MTRDR processing of a given targeted observation can be assessed by comparing

[Class Type][Target ID]\_[Sensor]\_COMPOSITE\_05.PNG and

[Class Type][Target ID]\_[Sensor]\_COMPOSITE\_06.PNG in the PDS EXTRAS directory.

Snapshots of the intra-band wavelength dependency modeling at the foundation of the ESC procedure are shown in the series of model fit plots

[Class Type][Target ID]\_[Sensor]\_ESC\_FIT\_[Number].PNG, and ESC cross-track correction profiles are presented in [Class Type][Target ID]\_[Sensor]\_ESC\_PRO.PNG.

## 6. XFM - VNIR → IR Sensor Space Transform (Geometric Reconciliation)

The CRISM VNIR and IR optical designs were individually optimized. As a result a given location in the field of view is sampled differently and mapped to different coordinates on the two detectors. The VNIR/IR sensor space transform uses the known ground location of every VNIR and IR spatial pixel to construct a spatial transformation that maps VNIR data into the IR sensor space. This transformation allows for the concatenation of VNIR and IR spectral information and the generation of full spectral range IR sensor space (TER) and map projected (MTR) data products. The spatial transformation of the VNIR data is conducted as a nearest neighbor resampling to avoid spectral averaging. After the corrected and transformed VNIR data and corrected IR data are concatenated in the IR sensor space, an image mask is generated that sets all the spectral channels in any spatial pixels that do not have both VNIR and IR data to the CRISM NAN value (65535.0). This results in the TER IF data product – a fully corrected, full spectral range image cube.

## 7. INF – TER/MTRDR Data Processing Pipeline Information Maps

Spatial pixel specific performance and traceability information for the ATM and XFM procedures is stored in the processing information (IN) data product. Spectral discontinuity at the ~1000 nm VNIR/IR interface can be inherited from the source TRR3 I/F data, arise as a byproduct of the TER/MTRDR data processing pipeline which operates on the VNIR (S-detector) and IR (L-detector) data independently prior to the spatial reconciliation and spectral concatenation, and/or as a result of the nearest neighbor mapping of the VNIR data into the IR sensor space. A spectral discontinuity residuals map (which can be influenced by all of the above factors) and spatial sampling residual map (which traces specifically to the VNIR/IR spatial transform) are both provided in the TER IN data product (VNIR/IR Spectral Continuity Residual and VNIR/IR Spatial Gradient Residual). The most common ATM correction residual is a high spectral frequency oscillation across the wavelengths affected by the ~2000 nm CO<sub>2</sub> absorption ultimately traceable to small variations in the wavelength calibration between the observation being corrected and the best matching reference atmospheric transmission frame. The IN product includes a parameterization of this spectral shift artifact (ATM Correction Spectral Shift

Artifact). The remaining IN product bands provide full spatial traceability to the source VNIR and IR TRR data products (VNIR Sample, VNIR Line, IR Sample, IR Line), a measure of the magnitude of the VNIR/IR sampling discrepancy (VNIR/IR Ground Sampling Offset), and a mask band which indicates which IR sensor space spatial pixels have both VNIR and IR spectra (VNIR/IR Mask).

## 8. SUM – Spectral Summary Parameters

The CRISM spectral summary parameter library has been revised to take full advantage of the hyperspectral sampling in CRISM targeted observation data and augmented to span the diverse mineralogy identified and/or reported in CRISM data [Viviano-Beck *et al.*, 2014]. The revised library is used to generate a suite of 56 parameterizations of the spectral structure in the TER and MTRDR IF data products (Table 3-12). The hyperspectral implementation of each summary parameter generally takes the form of sampling multiple adjacent spectral channels for a given reference wavelength used in the band math calculation for a given parameter, and integrating the data in the sampling kernel as appropriate to reduce the influence of spectral noise in the parameter result. The dimension and handling of the spectral sampling ‘boxcar’ varies depending on the nature of the spectral feature being parameterized. Narrow spectral features (e.g. BD1435 – CO<sub>2</sub> ice) use few channels to characterize the center and shoulders in the calculation of the relative band depth, while parameters that are chiefly directed at the spectral continuum level at a given wavelength (e.g. R1330 – proxy for IR albedo) use a large boxcar and a spectral median to arrive at the parameterization result. The summary parameter calculation results in the TER SU data product image cube.

## 9. SRE – Refined Spectral Summary Parameters

The hyperspectral data filtering procedure put in place as part of the CRISM v3 radiometric calibration (Appendix N) and the hyperspectral implementation of the parameter calculations in the revised spectral summary parameter library are effective at mitigating and suppressing spectral noise. However, the majority of the parameter calculations seek to accentuate small spectral variations so spectral noise residuals can still be propagated into the summary parameters – particularly from IR (L-detector) data acquired later in the mission at elevated detector operating temperatures. This has the potential to compromise data visualizations based on the summary products and derivative browse products. To maximize the scientific utility of the visualization products a custom noise remediation procedure is applied to the majority of the summary parameters. This procedure has some heritage in the CRISM hyperspectral data filtering procedure implemented in version 3 of the CRISM calibration pipeline, but has been modified to operate on individual parameter bands, rather than hyperspectral I/F data. The filtering procedure identifies spurious pixels using a statistical outlier test applied to an iterative sampling kernel. Pixels that are flagged as outliers are subsequently interpolated from neighboring non-spurious data elements. The parameter filtering procedure results in the TER SR data product image cube.

## 10. BRS – Browse Products

Browse products are a series of up to 18 8-bit scaled RGB color composites that display 3-band combinations of thematically related summary products (section 3.11). They provide a high-level visualization of the information content in the source spectral image cube. The suite of CRISM browse products was augmented in 2014 to span the diverse mineralogy reported in the CRISM data set, and to provide better discrimination between spectrally similar phases [Viviano-Beck *et al.*, 2014]. The utility of a browse product visualization is dependent on the quality of the constituent summary parameter bands and the stretch limits applied in scaling the parameter bands from 32-bit (floating point) to 8-bit (byte). Parameters that are measures of the spectral continuum at a given wavelength (e.g. R770, R1330) and those that encode spectral ratio or slope information (e.g. ISLOPE1, IRR2) are stretched according to the scene statistics. Parameters that are seeking to quantify the presence and magnitude of a particular spectral feature (i.e., those with the embedded character strings BD, INDEX, and MIN) are scaled using a stretch that is calculated from the scene statistics but constrained by both the range of physically meaningful parameter calculations and cumulative statistics representative of the parameter variability for the entire data set. The stretch floor is set by the expected minimum meaningful value for a featureless spectrum according to the underlying band math calculation (e.g. band depth (BD) parameters are designed to return zero for a featureless spectrum), and the stretch ceiling is set by the scene statistics, subject to a minimum reasonable ceiling value. This value is based on cumulative statistics for each parameter band across a TER sample set encompassing ~5% of all targeted observations. This parameter stretching protocol prevents saturation in scenes where the parameter values are in the tail of the global distribution (when the stretch ceiling is set by scene statistics), and prevents scenes that lack the spectral structure a given parameter is designed to isolate from presenting spectral noise as a meaningful detection (when the stretch ceiling is set by cumulative statistics). Scaling information for each band is stored in the associated PDS label. Each resulting browse product is stored as both a 3-band raw binary file (.IMG) and a Portable Network Graphics file (.PNG) with an alpha transparency channel corresponding to the non-scene spatial pixels. The generation of the TER BR product suite marks the end of the TER/MTRDR data processing pipeline sensor space data processing.

## 11. Spectral Bad Bands

A canonical set of spectral ‘bad bands’ has been identified through the evaluation of a set of prototype TER IF data products and includes spectral channels with questionable radiometry identified in the TRDR\_DS.CAT catalog file, as well as those that are subject to large uncertainties in the MTRDR data processing pipeline. The TER/MTRDR ‘bad bands’ list is stored in the TER WV table, and applied to the TER IF spectral data prior to map projection so the ‘bad bands’ are not forwarded into the MTR IF data product.

## 12. Calculate Map-Projection Transformation

All of the TER data products are in the IR (L-detector) sensor space established by the source targeted observation. This allows for the calculation of a single map-projection spatial transformation that will map the data from the IR sensor space to the map projected space. The MTRDR data processing pipeline makes use of the ESRI Projection Engine (PE) available through the ENVI APIs (ENVI version 4.7+) in the generation of a Geographic Lookup Table (GLT) that encodes this transformation. The map projection transformation is generated in

accordance with MRO project standards and is detailed in the MTR\_MAP.CAT catalog file.

### 13. Map-Projection

The GLT is applied to each TER data product to produce a paired MTR data product. The ‘bad bands’ identified in the TER WV table are removed from the TER IF image cube prior to map projection, so there are fewer spectral channels in the MTR IF spectral product as compared to the TER IF spectral product. A map projected version of the source targeted observation IR (L-detector) DDR is also included in the MTR data product suite.

### 14. References

- Langevin, Y., F. Poulet, J.-P. Bibring, and B. Gondet (2005), Sulfates in the North Polar Region of Mars Detected by OMEGA/Mars Express, *Science*, 307(5715), 1584–1586, doi:10.1126/science.1109091.
- McGuire, P. C. et al. (2009), An improvement to the volcano-scan algorithm for atmospheric correction of CRISM and OMEGA spectral data, *Planet. Space Sci.*, 57(7), 809–815, doi:10.1016/j.pss.2009.03.007.
- Morgan, F., J. F. Mustard, S. M. Wiseman, F. P. Seelos, S. L. Murchie, P. C. McGuire, and CRISM Team (2011), Improved Algorithm for CRISM Volcano Scan Atmospheric Correction, in *Lunar and Planetary Institute Science Conference Abstracts*, vol. 42, p. 2453.
- Seelos, F. P., M. Parente, T. Clark, F. Morgan, O. S. Barnouin-Jha, A. McGovern, S. L. Murchie, and H. Taylor (2009), CRISM Hyperspectral Data Filtering with Application to MSL Landing Site Selection, *AGU Fall Meet. Abstr.*, 23, 1234.
- Smith, D. E., W. L. Sjogren, G. L. Tyler, G. Balmino, F. G. Lemoine, and A. S. Konopliv (1999), The Gravity Field of Mars: Results from Mars Global Surveyor, *Science*, 286(5437), 94–97, doi:10.1126/science.286.5437.94.
- Viviano-Beck, C. E. et al. (2014), Revised CRISM Spectral Parameters and Summary Products Based on the Currently Detected Mineral Diversity on Mars, *J. Geophys. Res. Planets*, doi:2014JE004627.

## APPENDIX P2. TER/MTRDR EXTRAS Documentation

The Targeted Empirical Record (TER) EXTRAS directory contains a series of data processing visualizations for each CRISM hyperspectral targeted observation that has been processed through the Map-Projected Targeted Reduced Data Record (MTRDR) pipeline. These visualizations collectively depict the geometric structure of the source TRR3 I/F spectral data, illustrate the spatial and spectral impact of the TER/MTRDR data processing procedures (Figure 2-9a), and provide snapshots of the underlying modeling behavior of the empirical data processing. Detailed descriptions of the TER/MTRDR data processing procedures are provided in Appendix P1. The MTRDR EXTRAS directory contains one visualization for each processed observation that illustrates the spatial/spectral information content of the primary MTRDR I/F data product. Every TER/MTRDR data product set that is released to the PDS has been reviewed and approved by members of the CRISM Science Operations Center (SOC). The information generated by this release review process is included in a Microsoft Excel format spreadsheet that is stored in the top level TER/MTRDR EXTRAS directories.

All TER/MTRDR EXTRAS visualizations are Portable Network Graphics (PNG) format files. The TER detector specific systematic data processing visualizations have file names with the form [Class Type][Target ID]\_[Sensor]\_[Name].PNG where [Class Type] is a three letter observation type code (e.g. FRT, HRL, HRS), [Target ID] is an eight character hexadecimal observation identifier, [Sensor] is a single character indicating the VNIR (S-detector) or IR (L-detector) wavelength range, and [Name] indicates the plot contents.

### TRR3 I/F Observation Geometry:

Three CRISM targeted observation geometry plots are color coded within a single file with the inbound EPF branch in blue, the central scan in green, and the outbound EPF branch in red. The geometric visualization plots are only generated for CRISM VNIR (S-detector) data as the observation geometry is consistent across the entire CRISM spectral range and a reference VNIR spectral band is sufficient to illustrate the geometric dependency.

[Class Type][Target ID]\_S\_PHA\_EMI.PNG – Cartesian plot showing phase angle ( $\text{g}$ ) vs. emission angle ( $\text{e}$ ). The incidence angle is plotted in black at [ $\text{g} = \text{i}$ ,  $\text{e} = \text{i}$ ] for completeness.

[Class Type][Target ID]\_S\_EMI\_AZI.PNG – Polar plot showing emission angle ( $\text{e}$ ) vs. azimuth angle ( $\psi$ ). The  $360^\circ$  azimuth space has been folded about the principal plane ( $\psi = 0^\circ$ ;  $\psi = 180^\circ$ ) to reduce redundancy. In this coordinate system the sub-solar azimuth is  $\psi = 180^\circ$  and the zero phase point lies along  $\psi = 0^\circ$ . The incidence angle is plotted in black at [ $\text{e} = \text{i}$ ,  $\psi = 90^\circ + \text{i}$ ] for completeness.

[Class Type][Target ID]\_S\_REF\_EMD.PNG – Cartesian plot showing I/F for a reference VNIR wavelength (~770 nm) vs. signed (directional) emission angle ( $\text{e}$ ) with the inbound branch plotted at negative emission angles.

### MTRDR processing 3-panel composites:

A three panel display is generated for each significant processing step in the TER/MTRDR pipeline allowing the spatial/spectral impact to be visualized and evaluated. Each display

includes a false color RGB composite with a 0.5% linear stretch on each band, a spectral plot with the scene median and 5%-95% spectral envelope (dashed lines indicate RGB band wavelengths), and distribution boxplots for the three bands in the RGB composite (dashed lines indicate RGB band stretch limits). The composite visualizations are numbered 01-06, but 03 and 04 only apply to IR (L-detector data).

[Class Type][Target ID]\_[Sensor]\_COMPOSITE\_01.PNG – CRISM TRR3 I/F (MTRDR data processing input – P1.0).

[Class Type][Target ID]\_[Sensor]\_COMPOSITE\_02.PNG – Lambertian photometric correction (PHT – P1.1). The incidence angle does not vary significantly over the duration of a CRISM targeted observation so this is most evident as a change in scale. The plot scales are held constant for composites 02-06 for ease of comparison.

[Class Type][Target ID]\_L\_COMPOSITE\_03.PNG – Volcano scan atmospheric correction (ATM – P1.2). Spectral structure resulting from atmospheric gas absorption is mitigated.

[Class Type][Target ID]\_L\_COMPOSITE\_04.PNG – Ratio Shift Correction (RSC – P1.3). Applied after the ATM correction to address spatially structured correction residuals.

[Class Type][Target ID]\_[Sensor]\_COMPOSITE\_05.PNG – Empirical Geometric Normalization (EGN – P1.4). Geometric dependencies that manifest as wavelength dependent along-track gradients are mitigated.

[Class Type][Target ID]\_[Sensor]\_COMPOSITE\_06.PNG – Empirical Smile Correction (ESC – P1.5). Spectral smile related spectral sampling (L-detector) and radiometric residuals (S-detector; L-detector) are mitigated.

### **Empirical procedure modeling plots:**

The TER/MTRDR empirical processing procedures (Empirical Geometric Normalization (EGN) and Empirical Smile Correction (ESC)) address spatial/spectral variability as a function of known observation properties (geometry and wavelength sampling). The series of modeling plots are snapshots of the processes that underpin the empirical procedures showing the sampled data and model fits for the spectral channels that compose the RGB composites in the 3-panel displays. The reference band ordering is inherited from the CRISM TRR3 I/F data and is reversed for the IR (L-detector) relative to the VNIR (S-detector).

[Class Type][Target ID]\_[Sensor]\_EGN\_FIT\_00.PNG – I/F vs.  $\cos(e)$  for IR red (band 205) / VNIR blue (band 12).

[Class Type][Target ID]\_[Sensor]\_EGN\_FIT\_01.PNG – I/F vs.  $g$  for IR red (band 205) / VNIR blue (band 12).

[Class Type][Target ID]\_[Sensor]\_EGN\_FIT\_02.PNG – I/F vs.  $\cos(e)$  for IR green (band 360) / VNIR green (band 25).

[Class Type][Target ID]\_[Sensor]\_EGN\_FIT\_03.PNG – I/F vs.  $g$  for IR green (band 360) /

VNIR green (band 25).

[Class Type][Target ID]\_[Sensor]\_EGN\_FIT\_04.PNG – I/F vs.  $\cos(e)$  for IR blue (band 425) / VNIR red (band 36).

[Class Type][Target ID]\_[Sensor]\_EGN\_FIT\_05.PNG – I/F vs.  $g$  for IR blue (band 425) / VNIR red (band 36).

[Class Type][Target ID]\_[Sensor]\_ESC\_FIT\_00.PNG – Normalized I/F vs. center wavelength for IR red (band 205) / VNIR blue (band 12).

[Class Type][Target ID]\_[Sensor]\_ESC\_FIT\_01.PNG – Normalized I/F vs. center wavelength for IR green (band 360) / VNIR green (band 25).

[Class Type][Target ID]\_[Sensor]\_ESC\_FIT\_02.PNG – Normalized I/F vs. center wavelength for IR blue (band 425) / VNIR red (band 36).

### **Empirical procedure profile plots:**

The empirical corrections (EGN and ESC) are both constructed relative to reference independent variable coordinates representative of idealized observing circumstances – a nadir push-broom observation geometry for EGN and uniform spectral sampling for ESC. The EGN geometric reference is set to the  $[\cos(e), g]$  geometry at the middle of the CRISM FOV (cross-track) in the frame that includes the minimum sampled emission angle. The ESC wavelength reference is taken from the SW-CDR (sweet-spot wavelength vector) for the observation under consideration. Since the empirical corrections are relative and operate orthogonally in the CRISM sensor space (EGN – along track; ESC – cross track) it is instructive to evaluate profiles taken through I:O ratio cubes in the direction of greatest influence. Each of the empirical correction profile plots show three traces corresponding to the spectral channels that compose the RGB composites in the 3-panel displays.

[Class Type][Target ID]\_[Sensor]\_EGN\_PRO.PNG – Along-track slice through the cross-track center of the EGN I:O ratio cube.

[Class Type][Target ID]\_[Sensor]\_ESC\_PRO.PNG – Cross-track slice through the along-track center of the ESC I:O ratio cube.

### **Empirical procedure input and output comparison:**

The aggregate impact of the TER/MTRDR empirical processing (EGN and ESC) is illustrated in four visualizations.

[Class Type][Target ID]\_[Sensor]\_EGN\_ESC\_DST.PNG – Comparison of the data distributions before and after the empirical processing in the three spectral channels that compose the RGB composites in the 3-panel displays.

[Class Type][Target ID]\_[Sensor]\_EGN\_ESC\_GRD.PNG – The base image is equivalent to the

sensor space TRU (VNIR RGB natural color) or FAL (IR RGB false color) browse products as well as the RGB composite in the final 3-panel display. The nine evenly distributed plot symbols indicate the spatial locations detailed in the companion empirical processing I:O comparison spectral plots (IOS and IOR).

[Class Type][Target ID]\_[Sensor]\_EGN\_ESC\_IOS.PNG – EGN and ESC aggregate input (gray) and output (black) spectra for the spatial locations indicated in the companion scene visualization (GRD).

[Class Type][Target ID]\_[Sensor]\_EGN\_ESC\_IOR.PNG – EGN and ESC aggregate input to output spectral ratios for the spatial locations indicated in the companion scene visualization (GRD). Low spectral frequency variation is generally attributable to the EGN procedures and high spectral frequency variation to the ESC procedure.

#### **MTRDR processing resultant spectral product visualizations:**

The two main spectral data products that result from the TER/MTRDR data processing pipeline are a fully corrected full spectral range image cube in the CRISM IR (L-detector) sensor space ([Class Type][Target ID]\_[Counter]\_IF[Macro]J\_TER3.IMG) and the corresponding map projected data product with spectral bands known to be radiometrically questionable or inconsistently processed through the MTRDR pipeline removed from the image cube ([Class Type][Target ID]\_[Counter]\_IF[Macro]J\_MTR3.IMG). Three-panel displays for both of these image cubes provide an overview of the information content and have a file name form inherited directly from the source TRR3 I/F data products:

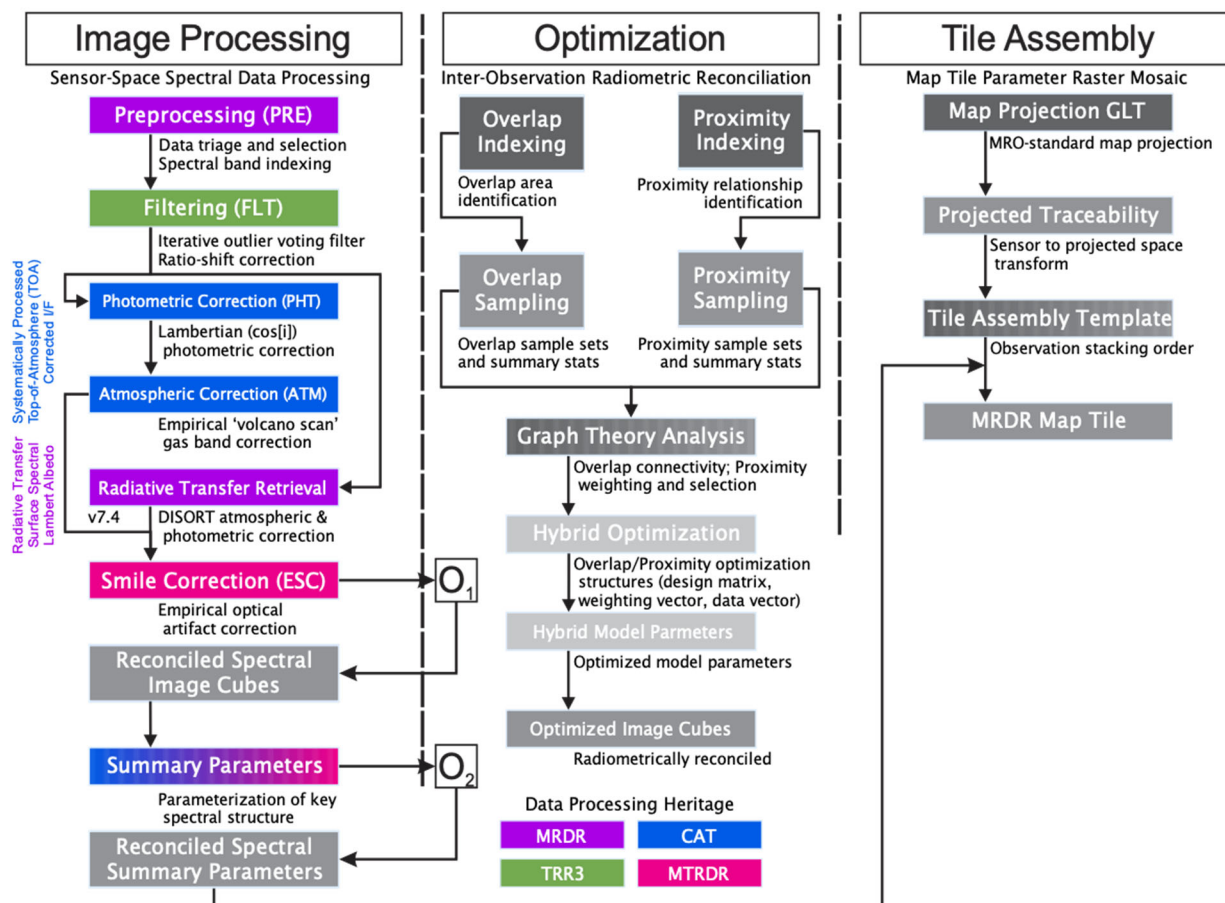
[Class Type][Target ID]\_[Counter]\_IF[macro]J\_TER3\_Composite.PNG – 3-panel display for the Targeted Empirical Record (TER) spectral product.

[Class Type][Target ID]\_[Counter]\_IF[macro]J\_MTR3\_Composite.PNG – 3-panel display for the Map-projected Targeted Record (MTR – short for MTRDR) spectral product.

## APPENDIX P3. MRDR Data Processing and Product Description

### 0. Orientation – CRISM VNIR+IR Mapping Strip Structure

A CRISM VNIR+IR mapping observation is composed of a series of one or more 180-second acquisitions of nadir-pointed mapping data acquired at 10x binning. There are two classes of such data, 72/73 selected channels called Multispectral Survey (MSP), and 262 channels called Hyperspectral Survey (HSP). Both include the same core set of 72 selected VNIR+IR channels with meaningful measurements of the surface and atmosphere, and 1 nominally UV VNIR channel that measures only scattered light and is used as part of the radiometric calibration process as described in Appendix M. For the purpose of MRDR construction, the 72 channels of calibrated I/F data are extracted from a parent TRDR of either class. A single input strip is a three dimensional hyperspectral image cube with dimensions  $[x,t,\lambda]$  where individual  $[x,\lambda]$  frames are accumulated over time  $[t]$ . The dimension  $\lambda$  is built from discrete, non-adjacent VNIR or IR detector rows. A given element in the image cube can be indexed as  $[x_i,t_j,\lambda_k]$  where  $0 \leq i \leq (ns - 1)$ ,  $0 \leq j \leq (nl - 1)$ ,  $0 \leq k \leq (nb - 1)$ , and  $ns$ ,  $nl$ , and  $nb$  are the number of samples, lines, and bands. Augmentations to the processing for version 4 MRDRs are repeated below from Figure 2-9b. Processing in versions 1 and 3 is shown in Figure 2-9.



## 1. Pre-processing

Pre-processing of input strips calibrated to I/F consists of three major downselections of the input data.

First, only data acquired with an IR detector temperature of  $\leq 127.5\text{K}$  are included. This is determined using the calibrated value of IR\_DETECTOR\_TEMP1 from the label on the multiband image.

Second, only data from time periods when atmospheric dust opacity  $\tau_{\text{dust}} < 1.0$  (scaled to CRISM wavelengths) are included. This is determined from time periods when that range was consistently exceeded in historical record of dust opacity retrievals, and rejecting data acquired during those time periods. The opacities used are from multiannual climatology of airborne dust from Martian year 24 to 35 using observations of the Martian atmosphere from April 1999 to February 2021 made by the Thermal Emission Spectrometer (TES) aboard Mars Global Surveyor, the Thermal Emission Imaging System (THEMIS) aboard Mars Odyssey, and the Mars Climate Sounder (MCS) aboard Mars Reconnaissance Orbiter (MRO), from Montabone et al. [2015, 2020]. These are accessible at [http://www-mars.lmd.jussieu.fr/mars/dust\\_climatology/](http://www-mars.lmd.jussieu.fr/mars/dust_climatology/). The scaling factor in dust opacity from thermal IR to CRISM wavelengths is 2.0.

Third, all input data are reformatted as 72-channel I/F by deleting the detector rows in dimension  $\lambda$  that are outside of the core VNIR+IR 72-channel set.

## 2. Filtering (beginning with v4)

The subsetted 72-channel I/F mapping strips are then filtered for stochastic and systematic noise in two steps, respectively. The first step to remediate stochastic noise is a simplified version of the Iterative Kernel Filter used for noise remediation in the I/F version of TRR3's. The second step to remediate systematic noise is the Ratio Shift Correction also applied during that filtering.

The Iterative Kernel Filter (IKF) procedure as applied to multispectral data is a kernel based filtering algorithm that models the information content of a given two dimensional (x,t) normalized data kernel as a multidimensional polynomial. The model residuals are treated as a sample set and examined for outliers using the Grubbs test. If an outlier is detected, the corresponding pixel is removed from consideration and the kernel model is iterated. Model iteration is terminated when no further outliers are detected. The filtered value for the target pixel at the center of the input kernel is then given by a proximity weighted model of the kernel elements that were not marked as outliers. The confidence level threshold for the Grubbs test is conservative so the filter retains some marginal noise. The IKF is applied primarily to IR data.

The Ratio Shift Correction (RSC) procedure as applied to multispectral data is the primary filtering process for VNIR data. Within a given spectral band, a spatial column corresponds to a single detector element. The Ratio Shift Correction characterizes residual bias of each detector element through the evaluation of inter-column (or cross-track shifted) ratio statistics relative to a cross track model. Modifying the complexity of the underlying cross track model allows the RSC procedure to address high frequency column striping or low frequency banding while retaining real scene cross-track variability.

### **3. Two alternative paths for correction of atmospheric and photometric effects (second path only applies to v4)**

(3.1) Mapping data acquired prior to May 2012 fall within the time range of acquisition of CRISM EPF data, from which retrievals provide a record of atmospheric dust opacity sampled at CRISM's wavelength sampling and resolution as a function of latitude, longitude, Ls, and Mars year (stored in the ADR-CL; section 3.9). MRO MARCI data provide retrievals of atmospheric water-ice opacity also as a function of latitude, longitude, Ls, and Mars year (also stored in the ADR-CL). Where these opacities are present, using the procedures described by McGuire et al. [2013] and shown in Figs. 2-9 and 2-9b, a full radiative transfer model is used to correct I/F to a standard reference photometric geometry with atmospheric contributions to I/F normalized. Rather than calculations being repeated for each pixel with minor inter-pixel differences, calculations are done using DISORT for the range of expected variables and stored as look-up tables in ADRs for discrete values, and the corrections are interpolated to the specific conditions of each element in the I/F image cube  $[x, t, \lambda]$ .

Information on latitude, longitude, Ls, and altitude are extracted from the header of the TRDR containing the I/F data and the companion DDR. These data are used to extrapolate to the best estimate of the atmospheric opacities from the ADR-CL. Then the photometric angles, altitude, Ls, and wavelength plus the opacities extracted from the ADR-CL are used to interpolate wavelength-by-wavelength to correction from I/F to Lambert albedo at  $i=30^\circ$ ,  $e=0^\circ$ ,  $g=30^\circ$ ,  $\tau_{dust}=0.2$ , and  $\tau_{ice}=0.0$  with no absorptions due to atmospheric gases. The Lambert albedo becomes the basis to which mapping strips acquired after May 2012 (when EPFs were no longer acquired) are corrected.

(3.2a) For mapping data acquired after May 2012, a two-step (2a, 2b) correction is used that does normalize out atmospheric gas absorptions and correct for photometric effects, but does not attempt to correct for aerosol effects. This processing closely follows that applied to TERs and MTRDRs (Appendix P1). The first step is the volcano scan atmospheric correction uses empirically derived Mars atmospheric transmission spectra to correct CRISM IR (L-detector) spectral reflectance data for atmospheric gas absorptions (due primarily to CO<sub>2</sub>, H<sub>2</sub>O, and CO) [Langevin et al., 2005; McGuire et al., 2009; Morgan et al., 2011]. There are no significant atmospheric gas absorptions over the CRISM VNIR wavelength range, so this correction is not applied to VNIR (S-detector) data. Detector column-specific reference atmospheric transmission spectra ( $[x_i, \lambda]$  to accommodate spectral smile) are derived from a suite of push-broom hyperspectral Flat Field Calibration (FFC) scans over Olympus Mons and are matched to a given targeted observation to minimize high frequency residual spectral structure due to sub-nm wavelength calibration variability across the wavelengths affected by the 2000 nm CO<sub>2</sub> absorption (1947 – 2066 nm). The depth of the 2000 nm CO<sub>2</sub> absorption is determined for the spectrum of each spatial pixel  $[x_i, t_j]$  in the image cube under consideration, the selected reference transmission spectrum is scaled to match according to the Beer-Lambert Law, and the resulting model transmission spectrum is ratioed out of the I/F data. The MRDR pipeline implementation of the volcano also includes a CRISM-specific volcano scan patch (included in the CRISM Analysis Toolkit v7.1+ available at the PDS Geosciences Node) that is applied after the initial correction to reduce the influence of varying path length and pressure broadening in the derivation of the reference transmission spectra.

(3.2b) The second step for data corrected using the volcano scan is application of a photometric correction using a Lambert assumption:

$IOF_1 = IOF_0 / \cos(\theta)$  where  $IOF_0$  is the observed spectral reflectance (I/F),  $IOF_1$  is photometrically corrected spectral reflectance, and  $\theta$  is the angle of incidence.

The photometric correction is calculated for each spatial pixel  $[x_i, t_j]$  and is applied uniformly to all spectral channels  $[\lambda]$ . The spatial pixel specific incidence angle information is derived from the 'INA at areoid' band (incidence angle with respect to the Mars areoid) in the CRISM DDR (Derived Data Record) associated with the targeted observation and segment under consideration.

#### **4. Empirical Smile Correction (beginning with v4)**

CRISM data exhibit spatial/spectral structure traceable to spectral smile – an optical artifact where the wavelength calibration shifts as a function of cross-track spatial position  $[x_i]$ . Spectral smile effects are most evident where the observed spectral reflectance is changing rapidly with wavelength (steep spectral slopes) and a small change in the center wavelength of the bandpass can result in a relatively large change in the measured signal. The most notable examples are the steep spectral slopes from 450–750 nm and within the composite CO<sub>2</sub> absorption from 1850–2150 nm. In addition to spectral slope effects, the CRISM radiometric calibration exhibits a small residual related to spectral smile that appears as a wavelength-dependent cross-track gradient. These effects are addressed by the Empirical Smile Correction (ESC) which uses the WA-CDR (detector center wavelength sampling map) and SW-CDR (detector sweet-spot wavelength vector) for the strip under consideration to transform data acquired across the detector to the reference (SW-CDR) center wavelength sampling vector.

The primary ESC procedure uses the detector wavelength map to construct an intra-channel wavelength sampling histogram for each spectral channel that delineates the cross-track spatial columns that fall into each wavelength bin. Each binned data point is weighted in the linear fit by the corresponding histogram count and the inverse of the binned sample set dispersion. A forward model is calculated for the detector wavelength map cross-track profile for each spectral channel, and the reference wavelength for each channel is used to calculate a reference model value. Each channel-specific forward model is then normalized to the appropriate reference, the resulting correction frame  $[x, \lambda]$  is applied to all frames  $[t]$  in continuum normalized spectral cube, and the result is transformed back to I/F.

#### **6. Reconciliation of Inter-strip Residuals in Corrected I/F and Lambert Albedo (beginning with v4)**

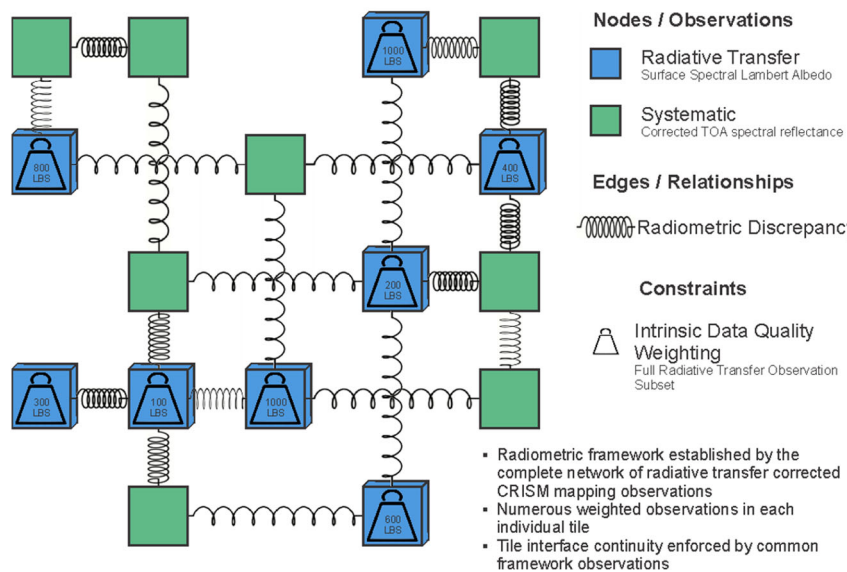
At this stage of processing there are significant residual differences in I/F between overlapping strips of mapping data due to several effects: systematic errors in radiometric calibration between strips; inaccuracy in the assumption of a wavelength-independent Lambert photometric function; for strips processed to Lambert albedo, differences between the modeled and actual atmospheric dust and ice opacities; for strips processed using the volcano scan correction, the presence of atmospheric dust and ice opacities different than the target values of  $\tau_{dust}=0.2$ , and  $\tau_{ice}=0.0$ ; and differences between the actual and modeled values of H<sub>2</sub>O vapor and CO due to seasonal or meteorological variations. The calibration residuals are only somewhat notable in I/F, but the

magnitudes are in family with real spectral variations for many of the mineralogical spectral indices represented as summary products.

To remediate these interstrip differences, an optimization procedure is performed in which derived values of surface reflectance are corrected to the values in the closest to ideal data among the mapping strips, using the millions of overlap and proximity relations among the approximately 83,000 strips of VNIR+IR data in the map. The optimization procedure is shown schematically in the diagram below. Prior to optimization, the millions of areas of intersection and close proximity are identified. The differences between each such pair of strips is analyzed using graph theory, and the best-fit gain and offset describing the differences are recorded. Of course, each such solution will have some systematic error.

In the optimization procedure, overall error is minimized (and the data set is optimized) by applying the gains and offsets in a weighted fashion, anchoring the output values to that part of the data which is closest to ideal. Those “anchor” strips have the following attributes: low IR detector temperature, as close as possible to the minimum value used in flight; low solar incidence angles; low  $\tau_{\text{dust}}$  in the data as acquired as recorded in the Montabone et al. data; and the atmospheric corrections were performed using the ADRs (traceable to DISORT; blue in the diagram below). The mapping strips with such attributes have large weights as represented by the dumbbells. The relative weighting among competing overlaps in correcting an individual strip is represented by the springs below, with the “higher spring constants” representing large overlaps or closer adjacencies and smaller radiometric discrepancies.

Note that only mapping strips corrected to  $\tau_{\text{dust}}=0.2$  and  $\tau_{\text{ice}}=0.0$  using DISORT-traceable ADRs populate the anchor strips. Provided that there are overlaps with such strips, the strips corrected with the volcano scan approach effectively have their dust and ice opacities normalized to the values in the overlapping ADR-corrected strips. Thus the correction to Lambert albedo is propagated among all strips. The resulting processed data populate the MRRAL multiband image.



## **7. Spectral Summary Products (revised for v4)**

The revised CRISM spectral summary parameter library has been augmented to span the diverse mineralogy identified and/or reported in CRISM data [Viviano-Beck et al., 2014; Applicable Document 12]. The library is used to generate a suite of 56 parameterizations of the spectral structure in the MRDR I/F and Lambert albedo data products (MRRIF and MRRAL respectively; Table 3-12). The summary product calculation results in the MRRSU data product image cube. Note that unlike summary products for TERs and MTRDRs, which are evaluated hyperspectrally at wavelengths specified in the summary product formulas, MRDR summary products are evaluated at the detector row closest to the specified wavelengths. Thus the values resulting from the calculation are different for MRDRs. The parameters specified as “surface” in Table 3-12 are evaluated using the MRRAL multiband image; the parameters specified as “atmosphere” in Table 3-12, if present, are evaluated using the MRRIF multiband image (v1).

## **8. Reconciliation of Inter-strip Residuals in “Surface” Summary Products (beginning with v4)**

Even after reconciliation of inter-strip residuals in reflectance data, very small wavelength-dependent strip-to-strip residuals remain. These result in small strip-to-strip residuals in “surface” summary products which in principle capture stable surface spectral reflectance properties. To remediate the residuals, the optimization procedure is applied a second time to “surface” summary products (1-51 in Table 3-12), using the same weights and relative weightings as applied earlier to strips corrected to Lambert albedo using ADRs or corrected I/F using the volcano scan correction and photometric normalization using a Lambertian function.

## **9. VNIR to IR Sensor Space Transform (v4)**

The VNIR and IR component strips of mapping data are in slightly different sensor spaces established by the instrument optics and detector layout. This difference is accommodated by the calculation and application of a VNIRtoIR sensor space transformation. The VNIR and IR DDR per-pixel latitude and longitude information is used to construct a nearest-neighbor transform, where each IR spatial scene pixel is assigned the nearest-neighbor VNIR spatial scene pixel. This transformation carries the VNIR data into the IR sensor space, and ensures that all populated pixels in the downstream assembled tile have full spectral range information (VNIR + IR).

## **10. Map-Projection; Tile Traceability Template (v4)**

The VNIR to IR sensor space transformation also allows both the IR sensor space data and transformed VNIR sensor space data to be propagated into the map projected tile space using the IR DDR per-pixel latitude and longitude information. The map projection of the IR and VNIR traceability data makes use of the ESRI Projection Engine (PE) available through the ENVI APIs (ENVI version 4.7+) in the generation of a Geographic Lookup Table (GLT) for each observation that encodes this transformation. The map projection is generated in accordance with MRO project standards and is detailed in the MRR\_MAP.CAT catalog file. After map projection, the VNIR and IR traceability information is assembled into a map tile virtual mosaic which informs the downstream tile assembly. In the v1 and v3 tile production process the individual data products were map projected directly, rather than through a traceability tile template.

## **11. Stacking and Tiling**

The tiling scheme for MRDRs is described in section 3.5.2 and shown in Figure 2-10. Groups of map tiles are processed one Mars chart at a time as described in the CRISM Data Archive SIS (Applicable Document 5, section 3.2.7 and Table 3-12). For v4, the traceability tile constituent observations are ordered so that the strips acquired under the highest atmospheric optical depth (Montabone et al.) are placed first, and strips are then placed in order of decreasing optical depth with the strips acquired under the clearest atmospheric conditions “on top”. The ordered traceability tile governs the assembly of all the corresponding tile data products which ensures stacking order and per-pixel data source consistency. In the v1 and v3 tile production process, the constituent observation are ordered by solar incidence angle rather than atmospheric opacity, and the data product tiles were assembled directly from the constituent map projected data products, rather than through a traceability template. Up to five map projected multiband images are generated: (a) uncorrected I/F which [MRRIF file], (b) Lambert albedo [MRRAL file], (c) summary products [MRRRSU file], (d) data from the VNIR and IR DDRs corresponding to the data strips that are part of the I/F file [MRRDE], and (e) data from the VNIR and IR DDRs corresponding to the data strips that are part of the Lambert albedo file [MRRDE].

## **12. Browse Products (revised for v4)**

Browse products are a series of up to 18 8-bit scaled RGB color composites that display 3-band combinations of thematically related summary products (section 3.11). They provide a high-level visualization of the information content in the source spectral image cube. The suite of CRISM browse products was augmented in 2014 to span the diverse mineralogy reported in the CRISM data set, and to provide better discrimination between spectrally similar phases [Viviano-Beck *et al.*, 2014]. The utility of a browse product visualization is dependent on the quality of the constituent summary parameter bands and the stretch limits applied in scaling the parameter bands from 32-bit (floating point) to 8-bit (byte). Parameters that are measures of the spectral continuum at a given wavelength (e.g. R770, R1330) and those that encode spectral ratio or slope information (e.g. ISLOPE1, IRR2) are stretched according to the scene statistics. Parameters that are seeking to quantify the presence and magnitude of a particular spectral feature (i.e., those with the embedded character strings BD, INDEX, and MIN) are scaled using a stretch that is calculated from the tile statistics, but constrained by both the range of physically meaningful parameter calculations and cumulative statistics representative of the parameter variability for the entire data set. The stretch floor is set by the expected minimum meaningful value for a featureless spectrum according to the underlying band math calculation (e.g. band depth (BD) parameters are designed to return zero for a featureless spectrum), and the stretch ceiling is set by the scene statistics, subject to a minimum reasonable ceiling value. This value is based on cumulative statistics for each parameter band across a sample of all MRDRs. This parameter stretching protocol prevents saturation in scenes where the parameter values are in the tail of the global distribution (when the stretch ceiling is set by scene statistics), and prevents scenes that lack the spectral structure a given parameter is designed to isolate from presenting spectral noise as a meaningful detection (when the stretch ceiling is set by cumulative statistics). Scaling information for each band is stored in the associated PDS label. Each resulting browse product is stored as both a 3-band raw binary file (.IMG) and a Portable Network Graphics file (.PNG) with an alpha transparency channel corresponding to the non-scene spatial pixels. The generation of the browse product suite marks the end of the MRDR data processing pipeline.

### **13. Differences by Version**

V1 MRDRs were built using TRR1 mapping strips, and a preliminary version of the radiometric transfer corrections stored in ADRs. All five multiband images are present, and the MRRSU files use older formulations of summary products. MRRAL and MRRSU files retain uncorrected interstrip residuals; MRRSU files suffer from unfiltered stochastic noise. MRRIF files are available to create custom products using derived information in the MRRDE file and CAT.

V3 MRDRs were built using TRR3 mapping strips. The MRRIF and MRRDE multiband images are present, representing coverage from 2012. MRRIF files can be used to create custom products using derived information in the MRRDE file and CAT. MRRAL, MRRDL, and MRRSU files are not present.

V4 MRDRs are built using TRR3 mapping strips, and the refined version of the radiometric transfer corrections stored in ADRs. All reflectance data are corrected to Lambert albedo using the optimization procedures described above, and the MRRSU files use current formulations of summary products. In MRRAL and MRRSU files interstrip residuals and stochastic noise are minimized using the IKF filter and optimization. The MRRDL files provide observing conditions and traceability to source observations. MRRIF and MRRDE files are not present.

### References:

- Langevin, Y., F. Poulet, J.-P. Bibring, and B. Gondet (2005), Sulfates in the North Polar Region of Mars Detected by OMEGA/Mars Express, *Science*, 307(5715), 1584–1586, doi:10.1126/science.1109091.
- McGuire, P.C., et al. (2013) Mapping Minerals on Mars with CRISM: Atmospheric and Photometric Correction for MRDR Map Tiles, Version 2, and Comparison to OMEGA. 44th Lunar and Planetary Science Conference, abstract #1581.pdf
- McGuire, P. C. et al. (2009), An improvement to the volcano-scan algorithm for atmospheric correction of CRISM and OMEGA spectral data, *Planet. Space Sci.*, 57(7), 809–815, doi:10.1016/j.pss.2009.03.007.
- Montabone, L., et al. (2015) Eight-year Climatology of Dust Optical Depth on Mars. *Icarus* 251, pp. 65-95, doi: <https://doi.org/10.1016/j.icarus.2014.12.034>
- Montabone, L., et al. (2020) Martian Year 34 Column Dust Climatology from Mars Climate Sounder Observations: Reconstructed Maps and Model Simulations. *J. Geophys. Res. - Planets*, <https://doi.org/10.1029/2019JE006111>
- Morgan, F., J. F. Mustard, S. M. Wiseman, F. P. Seelos, S. L. Murchie, P. C. McGuire, and CRISM Team (2011), Improved Algorithm for CRISM Volcano Scan Atmospheric Correction, in Lunar and Planetary Institute Science Conference Abstracts, vol. 42, p. 2453.
- Seelos, F. P., M. Parente, T. Clark, F. Morgan, O. S. Barnouin-Jha, A. McGovern, S. L. Murchie, and H. Taylor (2009), CRISM Hyperspectral Data Filtering with Application to MSL Landing Site Selection, AGU Fall Meet. Abstr., 23, 1234.
- Viviano-Beck, C. E. et al. (2014), Revised CRISM Spectral Parameters and Summary Products Based on the Currently Detected Mineral Diversity on Mars, *J. Geophys. Res. Planets*, doi:2014JE004627.